



**DETERMINATION OF  
RESILIENT MODULUS VALUES  
FOR TYPICAL PLASTIC SOILS  
IN WISCONSIN**

SPR # 0092-08-12

---

**Hani H. Titi, Ph.D., P.E.  
Ryan English, M.S.**

**University of Wisconsin - Milwaukee  
Department of Civil Engineering and Mechanics  
September 2011**

Wisconsin Highway Research Program Project ID 0092-08-12

**Determination of Resilient Modulus Values  
for Typical Plastic Soils in Wisconsin**

Final Report

Hani H. Titi, Ph.D., P.E., M.ASCE  
Associate Professor

Ryan English, M.S.  
Former Graduate Research/Teaching Assistant

Department of Civil Engineering and Mechanics  
University of Wisconsin – Milwaukee  
3200 N. Cramer St.  
Milwaukee, WI 53211

Submitted to  
Wisconsin Highway Research Program  
The Wisconsin Department of Transportation  
September 2011

## Technical Report Documentation Page

1. Report No. WHRP 11-04	2. Government Accession No	3. Recipient's Catalog No	
4. Title and Subtitle Determination of Resilient Modulus Values for Typical Plastic Soils in Wisconsin		5. Report Date September 2011	6. Performing Organization Code Wisconsin Highway Research Program
7. Authors Hani H. Titi and Ryan English		8. Performing Organization Report No.	
9. Performing Organization Name and Address Department of Civil Engineering and Mechanics University of Wisconsin-Milwaukee 3200 N. Cramer St. Milwaukee, WI 53211		10. Work Unit No. (TRAIS)	11. Contract or Grant No. WisDOT SPR# 0092-08-12
12. Sponsoring Agency Name and Address Wisconsin Department of Transportation Division of Business Services Research Coordination Section 4802 Sheboygan Ave. Rm 104 Madison, WI 53707		13. Type of Report and Period Covered Final Report, 2008-2011	14. Sponsoring Agency Code
15. Supplementary Notes			
<p>16. Abstract</p> <p>. The objectives of this research are to establish a resilient modulus test results database and to develop correlations for estimating the resilient modulus of Wisconsin fine-grained soils from basic soil properties. A laboratory testing program was conducted on representative Wisconsin fine-grained soils to evaluate their physical and compaction properties. The resilient modulus of the investigated soils was determined from the repeated load triaxial (RLT) test following the AASHTO T307 procedure. The laboratory testing program produced a high-quality and consistent test results database.</p> <p>The resilient modulus constitutive equation of the mechanistic-empirical pavement design was selected to estimate the resilient modulus of Wisconsin fine-grained soils. Material parameters (<math>k_i</math>) of the constitutive equation were evaluated from RLT test results. Then, statistical analysis was performed to develop correlations between basic soil properties and constitutive model parameters (<math>k_i</math>). Comparisons of resilient modulus values obtained from RLT test and values estimated from the resilient modulus constitutive equations showed that both results are in agreement. The correlations developed in this study were able to estimate the resilient modulus of the compacted subgrade soils with reasonable accuracy. The proposed material parameters correlations could be used to estimate the resilient modulus of Wisconsin fine-grained soils as level II input parameters. Statistical analysis on the test results also provided resilient modulus values for the investigated soil types, which can be used as Level III input parameters.</p>			
17. Key Words Resilient modulus, fine-grained soils, Wisconsin fine-grained soils.		18. Distribution Statement  No restriction. This document is available to the public through the National Technical Information Service 5285 Port Royal Road Springfield VA 22161	
19. Security Classif.(of this report) Unclassified	19. Security Classif. (of this page) Unclassified	20. No. of Pages 193	21. Price

## **DISCLAIMER**

This research was funded through the Wisconsin Highway Research Program by the Wisconsin Department of Transportation and the Federal Highway Administration under Project 0092-08-12. The contents of this report reflect the views of the authors who are responsible for the facts and accuracy of the data presented herein. The contents do not necessarily reflect the official views of the Wisconsin Department of Transportation or the Federal Highway Administration at the time of publication.

This document is disseminated under the sponsorship of the Department of Transportation in the interest of information exchange. The United States Government assumes no liability for its contents or use thereof. This report does not constitute a standard, specification or regulation.

The United States Government does not endorse products or manufacturers. Trade and manufacturers' names appear in this report only because they are considered essential to the object of the document.

## ABSTRACT

The objectives of this research are to establish a resilient modulus test results database and to develop correlations for estimating the resilient modulus of Wisconsin fine-grained soils from basic soil properties. A laboratory testing program was conducted on representative Wisconsin fine-grained soils to evaluate their physical and compaction properties. The resilient modulus of the investigated soils was determined from the repeated load triaxial (RLT) test following the AASHTO T307 procedure. The laboratory testing program produced a high-quality and consistent test results database.

The resilient modulus constitutive equation of the mechanistic-empirical pavement design was selected to estimate the resilient modulus of Wisconsin fine-grained soils. Material parameters ( $k_i$ ) of the constitutive equation were evaluated from RLT test results. Then, statistical analysis was performed to develop correlations between basic soil properties and constitutive model parameters ( $k_i$ ). Comparisons of resilient modulus values obtained from RLT test and values estimated from the resilient modulus constitutive equations showed that both results are in agreement. The correlations developed in this study were able to estimate the resilient modulus of the compacted subgrade soils with reasonable accuracy. The proposed material parameters correlations could be used to estimate the resilient modulus of Wisconsin fine-grained soils as level II input parameters. Statistical analysis on the test results also provided resilient modulus values for the investigated soil types, which can be used as Level III input parameters.

## TABLE OF CONTENTS

<b>Chapter 1: Introduction</b>	<b>1</b>
1.1 Problem Statement	3
1.2 Objectives	5
1.3 Scope	6
1.4 Organization of Report	6
<b>Chapter 2: Background</b>	<b>7</b>
2.1 Determination of Resilient Modulus	7
2.2 AASHTO T307	8
2.3 Repeated Load Triaxial Test System	10
2.4 Resilient Modulus Models	12
2.5 Resilient Modulus Correlations	14
2.6 Soil Distribution in Wisconsin	19
<b>Chapter 3: Research Methodology</b>	<b>22</b>
3.1 Investigated Soils	22
3.2 Laboratory Testing Program	24
3.2.1 Physical Properties and Compaction Characteristics	24
3.2.2 Repeated Load Triaxial Test	25
<b>Chapter 4: Test Results and Discussion</b>	<b>32</b>
4.1 Physical Properties and Compaction Characteristics	32
4.2 Resilient Modulus	44
4.3 Statistical Analysis	57
4.3.1 Evaluation of the Resilient Modulus Model Parameters	57
4.3.2 Correlations of Model Parameters with Soil Properties	59
4.3.3 Statistical Analysis Results	68

<b>Chapter 5: Conclusions and Recommendations</b>	<b>91</b>
<b>References</b>	<b>94</b>
<b>Appendix A: Figures of Compaction and Grain Size Analysis</b>	<b>A-1</b>
<b>Appendix B: Figures of Resilient Modulus Data</b>	<b>B-1</b>
<b>Appendix C: Figures of Resilient Modulus Data and Statistical Model</b>	<b>C-1</b>

## LIST OF FIGURES

Figure 2.1	Loading waveform according to AASHTO T307	9
Figure 2.2	Repeated load triaxial test setup and INSTRON 8802	11
Figure 2.3	Predicted versus measured resilient modulus of Wisconsin soils (Titi et al. 2006)	15
Figure 2.4	Wisconsin soil regions (Madison and Gundlach 1993)	21
Figure 3.1	Investigated soil locations across Wisconsin	23
Figure 3.2	Sample preparation and sample compaction according to AASHTO T307	27
Figure 3.3	Target unit weights and moisture contents under which soil specimens were prepared	28
Figure 3.4	Assembly of the triaxial cell and placement on the load frame for repeated load triaxial test	29
Figure 3.5	Computer software controlling the repeated load triaxial test	31
Figure 4.1	Grain size distribution of all investigated soils	38
Figure 4.2	Grain size distribution curve for soil Lincoln-1	42
Figure 4.3	Moisture – unit weight relationship for soil Lincoln-1	42
Figure 4.4	Results of repeated load triaxial test for soil Lincoln-1 target compaction values of $\gamma_d = 17.8 \text{ kN/m}^3$ and $w = 13.3 \%$	48
Figure 4.5	Results of repeated load triaxial test for soil Lincoln-1 target compaction values of $\gamma_d = 18.1 \text{ kN/m}^3$ and $w = 8.0 \%$	50
Figure 4.6	Results of repeated load triaxial test for soil Lincoln-1 target compaction values of $\gamma_{dmax} = 19.0 \text{ kN/m}^3$ and $w_{opt} = 11.0 \%$	52
Figure 4.7	Results of repeated load triaxial test for soil Lincoln-1 target compaction values of $\gamma_d = 18.1 \text{ kN/m}^3$ and $w = 14.5 \%$	54
Figure 4.8	Results of repeated load triaxial test for soil Lincoln-1 target compaction values of $\gamma_d = 17.8 \text{ kN/m}^3$ and $w = 15.3 \%$	56
Figure 4.9	Normal probability plot of $k_I$	60

Figure 4.10	Lack of normal distribution plot of $k_2$	61
Figure 4.11	Lack of normal distribution plot of $k_3$	61
Figure 4.12	Normal probability plot for transformed $k_2$ values	62
Figure 4.13	Normal probability plot for transformed $k_3$ values	63
Figure 4.14	Residual Plot for $k_1$	64
Figure 4.15	Residual Plot for $\log k_1$	64
Figure 4.16	Residual Plot for $(k_3)^{1/3}$	64
Figure 4.17	Comparison of model parameter $k_1$ for the values estimated from repeated load triaxial test results and $k_1$ estimated from soil properties	72
Figure 4.18	Comparison of model parameter $k_2$ for the values estimated from repeated load triaxial test results and $k_2$ estimated from soil properties	73
Figure 4.19	Comparison of model parameter $k_3$ for the values estimated from repeated load triaxial test results and $k_3$ estimated from soil properties	73
Figure 4.20	Predicted versus measured resilient modulus of compacted fine-grained soils	75
Figure 4.21	Predicted versus measured resilient modulus of compacted A-4 fine-grained soils	77
Figure 4.22	Predicted versus measured resilient modulus of compacted A-6 fine-grained soils	79
Figure 4.23	Predicted versus measured resilient modulus of compacted A-7 fine-grained soils	81
Figure 4.24	Predicted versus measured resilient modulus of compacted A-7-6 fine-grained soils	83

## LIST OF TABLES

Table 2.1	Testing sequence for subgrade soil (type II material)	10
Table 2.2	Regression equations from Titi et al (2006)	17
Table 2.3	Model parameters determined from multiple linear regression analysis	18
Table 3.1	Investigated soils location by county and soil sample ID that will be referenced in this report	24
Table 3.2	Standard test designations used for soil testing in this study	25
Table 4.1	Properties of investigated soils	33
Table 4.2	Grain size analysis properties of investigated soils	40
Table 4.3	Results for standard compaction tests on the investigated soils	43
Table 4.4	Results of repeated load triaxial test for soil Lincoln-1 compacted at 93% of $\gamma_{dmax}$ and dry of $w_{opt}$	47
Table 4.5	Results of repeated load triaxial test for soil Lincoln-1 compacted at 95% of $\gamma_{dmax}$ and dry of $w_{opt}$	49
Table 4.6	Results of repeated load triaxial test for soil Lincoln-1 compacted at $\gamma_{dmax}$ and dry of $w_{opt}$	51
Table 4.7	Results of repeated load triaxial test for soil Lincoln-1 compacted at 95% of $\gamma_{dmax}$ and wet of $w_{opt}$	53
Table 4.8	Results of repeated load triaxial test for soil Lincoln-1 compacted at 93% of $\gamma_{dmax}$ and wet of $w_{opt}$	55
Table 4.9	Statistical data for estimated model parameters $k_i$ from repeated load triaxial test results	59
Table 4.10	Correlation of model parameter $k_1$ to soil properties	69
Table 4.11	Correlation of model parameter $k_2$ to soil properties	70
Table 4.12	Correlation of model parameter $k_3$ to soil properties	71
Table 4.13	Results of the statistical analysis for the measured resilient modulus of all soils	85

Table 4.14	Results of the statistical analysis for the measured resilient modulus of A-4 soils	86
Table 4.15	Results of the statistical analysis for the measured resilient modulus of A-6 soils	87
Table 4.16	Results of the statistical analysis for the measured resilient modulus of A-7 soils	88
Table 4.17	Results of the statistical analysis for the measured resilient modulus of A-7-5 soils	89
Table 4.18	Results of the statistical analysis for the measured resilient modulus of A-7-6 soils	90

## **ACKNOWLEDGEMENTS**

This research project is financially supported by the Wisconsin Department of Transportation (WisDOT) through the Wisconsin Highway Research Program (WHRP).

The authors would like to acknowledge the help, support and guidance of Robert Arndorfer, WHRP Geotechnical TOC past Chair. The research team would like to thank Dan Reid, WisDOT, for his help and support in collecting soil samples for this research project.

The authors would like to acknowledge the support and comments provided by WHRP Geotechnical TOC Chair Jeff Horsfall and committee members. The help provided by Andrew Hanz, WHRP and Peg Lafky, WisDOT is appreciated.

The help and support of UW-Milwaukee graduate students Andrew Druckrey, Timothy Leonard, Emil Bautista, and Aaron Coenen during resilient modulus testing is greatly appreciated. The guidance and help provided by Dr. Habib Tabatabai, UW-Milwaukee, Dr. Ahmed Faheem, Bloom Companies and Dr. Chin-Wei Lee, UW-Milwaukee in the statistical analysis are greatly appreciated.

The authors would like to thank Michelle Schoenecker for the valuable review and comments on the final report.

## Chapter 1

### Introduction

The design and evaluation of pavement structures on base and subgrade soils requires a significant amount of supporting data such as traffic loading characteristics, base, subbase and subgrade material properties, environmental conditions, and construction procedures. Until recently, empirical correlations developed between field and laboratory material properties were used to obtain highway performance characteristics (Barksdale et al., 1990). These correlations do not satisfy the design and analysis requirements because they neglect all possible failure mechanisms in the field. Also, most of these methods, which use the California Bearing Ratio (CBR) and Soil Support Value (SSV), do not represent the conditions of a pavement subjected to repeated traffic loading. Recognizing this deficiency, the 1986 and the subsequent 1993 American Association of State Highway and Transportation Officials (AASHTO) design guides recommended the use of resilient modulus ( $M_r$ ) for characterizing base and subgrade soils and for designing flexible pavements. The resilient modulus accounts for soil deformation under repeated traffic loading with consideration of seasonal variations of moisture conditions. A major effort was undertaken by the National Cooperative Highway Research Program (NCHRP) to develop mechanistic-empirical pavement design procedures based on the existing technology, in which state-of-the-art models and databases are used. The NCHRP project 1-37A: “Development of the 2002 Guide for Design of New and Rehabilitated Pavement Structures” was completed and the final report and software were published in July 2004. The outcome of the NCHRP project 1-37A is the “Guide for Mechanistic-Empirical Design of New and Rehabilitated Pavement Structures,” which

has been subjected to extensive evaluation and review by state highway agencies across the country.

The mechanistic-empirical pavement design procedures described by Project 1-37A are based on the existing technology, in which state-of-the-art models and databases are used. Design input parameters are generally required in three major categories: (1) traffic; (2) material properties; and (3) environmental conditions. The mechanistic-empirical design identifies three levels of design input parameters in a hierarchy. This gives the pavement designer flexibility in achieving pavement design with available resources based on the significance of the project. The three levels of input parameters apply to traffic characterization, material properties, and environmental conditions, as described below:

Level 1: These design input parameters are the most accurate, with highest reliability and lowest level of uncertainty. They require the designer to conduct a laboratory/field testing program for the project considered in the design. This requires extensive effort and increases costs.

Level 2: When resources are not available to obtain the high-accuracy Level 1 input parameters, Level 2 inputs provide an intermediate level of accuracy for pavement design. Level 2 inputs can be obtained by developing correlations among different variables.

Level 3: These input parameters provide the highest level of uncertainty and the lowest level of accuracy. They are usually typical average values for the region. Level 3 inputs might be used in projects associated with minimal consequences of early failure such as low-volume roads.

## 1.1 Problem Statement

The Wisconsin Department of Transportation (WisDOT) uses the AASHTO 1972 Design Guide for flexible pavement design, in which the SSV is used to characterize subgrade soils; however, WisDOT is in the process of implementing mechanistic/empirical (M/E) procedures and methods for pavement design. One of the major factors in the M/E approach is the inclusion of the resilient modulus of the subgrade soils. WisDOT has not used resilient modulus values for past pavement designs, and, as a result, does not have sufficient data or experience to apply these values to Wisconsin soils. WisDOT also does not have the resources available to enter into project-specific testing.

Therefore, WisDOT initiated a research project through Wisconsin Highway Research Program (WHRP) to determine the resilient modulus values of selected Wisconsin subgrade soils. The research was awarded to the University of Wisconsin-Milwaukee under WHRP Project ID 0092-03-11. Titi et al. (2006) published the research results in the report, "Determination of Typical Resilient Modulus Values for Selected Soils in Wisconsin," which provided extensive data on resilient modulus values for 15 soils over a range of moisture and density conditions. The report also provided extensive data on a full range of more typical soil parameters for the selected soils. Using these parameters, Titi et al. (2006) then attempted to conduct analyses to determine if correlations could be found between certain parameters and the actual resilient modulus values. The analyses found that accurate correlations could not be found if the 15 soils were considered as a whole. This related back to the condition that the 15 soils covered a full range of textures and levels of plasticity. Titi et al. (2006) found that correlations could be developed if the

tested soils were divided into groups with similar properties. The analyses placed the tested soils into the following three groups.

- 1) Coarse-grained, non-plastic soils (<50%  $P_{200}$ , NP)
- 2) Coarse-grained, plastic soils (<50%  $P_{200}$ ,  $PI > 0$ )
- 3) Fine-grained soils (>50%  $P_{200}$ ,  $PI > 0$ )

However, in subdividing the 15 selected soils into the three groups above, the number of soils within each group became small. Employing extensive regression analyses, Titi et al. (2006) developed empirical formulas for each of the three soil groupings for the factors  $k_1$ ,  $k_2$ , and  $k_3$  necessary to calculate the estimated resilient modulus values.

Although the formulas were developed for soils within the boundaries of the defined groups, Titi et al. (2006) cautioned that applying the equations to materials with parameters beyond those of specific soils tested had not been validated.

WisDOT has conducted further analyses to test the validity of Titi et al. (2006) formulas over a wide range of conditions for each of the identified soil groups. It was found that for the coarse-grained, non-plastic soils (Group 1), the formulas gave reasonable results for the normal range of conditions anticipated for this group. However, when analyzing the coarse-grained, plastic soils (Group 2) and the fine-grained soils (Group 3), it was found that the predicted resilient modulus values became increasingly questionable as the formula/soil parameters increasingly varied from those of the specific soils tested in these groups. This is thought to relate directly back to the small number of soils available for testing and analyses within each of these groups. WisDOT concluded that while the

predictive formulas for Groups 2 and 3 are valid for the narrow range of the soils' conditions tested and analyzed, these formulas are not valid for the broader range of soil conditions typical for these groups. WisDOT also concluded that additional testing of a broader spectrum of soils was necessary to refine and improve the predictive formulas.

## **1.2 Objectives**

The objective of this research is to develop (and/or expand, improve) and validate a methodology for estimating the resilient modulus of various Wisconsin subgrade soils from basic soil properties (Level 2 input parameters in the mechanistic-empirical pavement design). To successfully accomplish this research, the following objectives will be met:

1. Conduct repeated load triaxial tests to determine the resilient modulus of Wisconsin fine-grained soils. These soils will also be subjected to different laboratory tests to obtain their physical and compaction properties. The obtained test results will augment and expand the test data conducted during Phase I of the resilient modulus research.
2. Develop/expand/modify resilient modulus correlations (models) proposed by Titi et al. (2006) between the resilient modulus constitutive model parameters ( $k_1$ ,  $k_2$ , and  $k_3$ ) and basic soil properties. The new correlations will be validated for a wide range of Wisconsin soils and conditions.

### **1.3 Scope**

The scope of this research is limited to investigating the resilient modulus of fine-grained soils obtained from various locations in Wisconsin. Resilient modulus is determined by repeated load triaxial tests following the AASHTO standard test T307: "Determining the Resilient Modulus of Soils and Aggregate Materials."

### **1.4 Organization of the Report**

There are five chapters in this report: Chapter 1 introduces the research problem statement, significance, objectives, and scope. Chapter 2 provides background information on determining subgrade soil resilient modulus, characterizing subgrade resilient modulus for mechanistic-empirical pavement design, subgrade resilient modulus models, and Wisconsin soils distributions and general characteristics/properties. Chapter 3 presents the research methodology used and describes the laboratory testing program on fine-grained Wisconsin soils. Chapter 4 discusses the results of the laboratory testing program, presents a critical evaluation and discussion of the research findings, and presents developed models to estimate the resilient modulus of Wisconsin fine-grained soils from basic soil properties. Finally, Chapter 5 presents the conclusions obtained from the testing program and recommendations for future work on characterizing the resilient modulus of Wisconsin fine-grained soils.

## Chapter 2

### Background

This chapter presents background information on the resilient modulus of subgrade soils, factors affecting resilient modulus, resilient modulus correlations, and resilient modulus models. The distributions of Wisconsin soils also are discussed.

#### 2.1 Determination of Resilient Modulus

The repeated load triaxial test is one of the laboratory tests used to determine the resilient modulus of soils. The test consists of applying a cyclic load on a cylindrical soil specimen under confining pressure and measuring the axial recoverable deformation.

Resilient modulus ( $M_r$ ) determined from the repeated load triaxial test is defined as the ratio of the repeated axial deviator stress ( $\sigma_d$ ) to the recoverable or resilient axial strain ( $\varepsilon_r$ ):

$$M_r = \frac{\sigma_d}{\varepsilon_r} \quad (2.1)$$

Determining resilient modulus using the repeated load triaxial test requires extensive investment in equipment and expertise, and the test is time-consuming. Several research studies (e.g., Titi et al. (2006), Ooi et al. (2004), and Yau and Von Quintus (2004)) were conducted to develop correlations between resilient modulus and fundamental soil properties such as moisture content, soil density, and plasticity characteristics. Such correlations were developed using regression analysis techniques. Some of these studies are specific to soils in certain geographical areas, and other studies used certain test

procedures and sampling.

The quality of the data to be used to develop resilient modulus correlations must be good. Carmichael and Stuart (1985) reported that many of the data used in previous regression studies were inadequate, with problems ranging from the lack of observations and variety of test procedures, to the lack of range in predictor values, colinearity, confounding of data and inconsistent sample sizes. Also, Karasahin et al. (1994) reported the use of multivariate nonlinear regression might not be acceptable for evaluating resilient modulus model parameters since it can be operator-sensitive.

## **2.2 AASHTO T307**

The repeated load triaxial test is specified for determining resilient modulus in AASHTO T307: “Standard Method of Test for Determining the Resilient Modulus of Soils and Aggregate Materials”

Sample preparation is done by using a static-force compactor. A split mold with pistons and rings was used to determine the lift thickness of the specimen. The sample is prepared with five equal lifts with a specified moist unit weight ( $\gamma_s$ ) and moisture content ( $w$ ).

AASHTO T307 requires a haversine-shaped loading waveform, which is shown in Figure 2.1. A load cycle is defined as 1 second with 0.1 second load duration and 0.9 second unloaded duration (contact load). The cycle is repeated 100 times per sequence and the test includes 15 sequences with changing deviator stress and confining pressure. Table 2.1 describes the loading sequences according to the AASHTO T307 test standard. Sequence zero is the conditioning stage of the specimen to seat the porous stones, caps,

and loading rod on the specimen. The conditioning stage gives the operator the chance to check the Linear Variable Differential Transducer's (LVDT's) balance and triaxial chamber alignment. If after 500 cycles the height of the specimen still decreases, the sequence should be carried out through the full 1000 cycles. AASHTO T307 specifies the load cell and LVDTs to be placed outside of the triaxial chamber. Test specimen is a cylindrical shape and to have a ratio of 1:2 for diameter-to-height. The confining fluid inside the triaxial chamber is air.

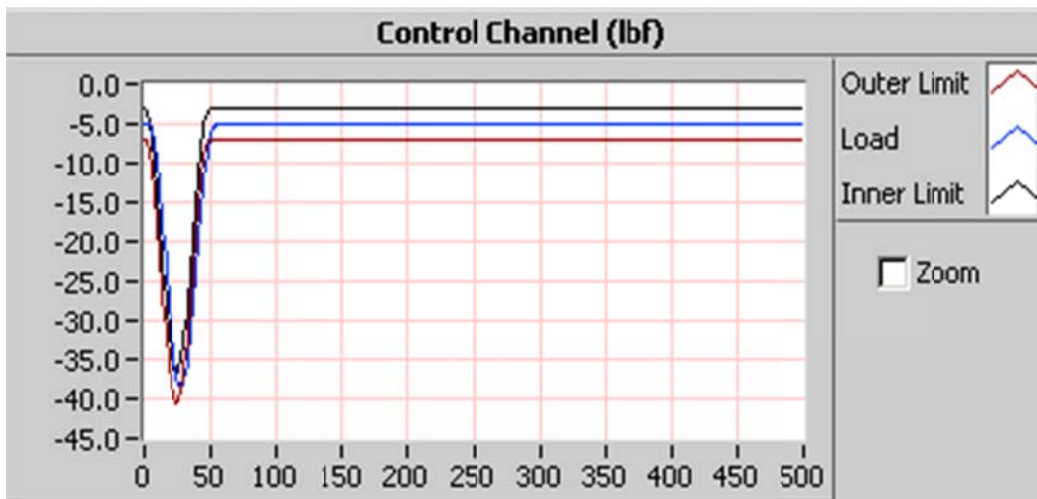


**Figure 2.1: Loading waveform according to AASHTO T307**

**Table 2.1: Testing sequence for subgrade soil (type II material)-AASHTO T307**

Sequence No.	Confining Pressure, $S_3$		Max. Axial Stress, $S_{max}$		Cyclic Stress $S_{cyclic}$		Constant Stress $0.1S_{max}$		No. of Load Applications
	kPa	psi	kPa	psi	kPa	psi	kPa	psi	
0	41.4	6	27.6	4	24.8	3.6	2.8	.4	500-1000
1	41.4	6	13.8	2	12.4	1.8	1.4	.2	100
2	41.4	6	27.6	4	24.8	3.6	2.8	.4	100
3	41.4	6	41.4	6	37.3	5.4	4.1	.6	100
4	41.4	6	55.2	8	49.7	7.2	5.5	.8	100
5	41.4	6	68.9	10	62.0	9.0	6.9	1.0	100
6	27.6	4	13.8	2	12.4	1.8	1.4	.2	100
7	27.6	4	27.6	4	24.8	3.6	2.8	.4	100
8	27.6	4	41.4	6	37.3	5.4	4.1	.6	100
9	27.6	4	55.2	8	49.7	7.2	5.5	.8	100
10	27.6	4	68.9	10	62.0	9.0	6.9	1.0	100
11	13.8	2	13.8	2	12.4	1.8	1.4	.2	100
12	13.8	2	27.6	4	24.8	3.6	2.8	.4	100
13	13.8	2	41.4	6	37.3	5.4	4.1	.6	100
14	13.8	2	55.2	8	49.7	7.2	5.5	.8	100
15	13.8	2	68.9	10	62.0	9.0	6.9	1.0	100

### 2.3 Repeated Load Triaxial Test System

The repeated load triaxial test was conducted at the University of Wisconsin-Milwaukee (UWM) using a state-of-the-art technology Instron FastTrack 8802 closed loop servo-hydraulic dynamic materials testing system. It has an 8800 Controller with four control channels of 19-bit resolution and data acquisition. A computer with FastTrack Console is

the main user interface. This is a fully digital-controlled system with an adaptive control that continuously updates PID terms at 1 kHz, which automatically compensates for specimen stiffness during repeated load testing. The loading frame capacity of the system is 56 kips with a series 3690 actuator that has a stroke of 150 mm (6 in.) and a load capacity of 250 kN (56 kip). The system has two dynamic load cells 5 kN and 1 kN for measuring the repeated applied load. The load cells include an integral accelerometer to remove the effect of dynamic loading on the load cell. Figure 2.2 shows the repeated load triaxial test set-up and load frame.



**Figure 2.2: Repeated load triaxial test set up and Instron 8802**

## 2.4 Resilient Modulus Models

Mathematical models are developed to estimate the value of resilient modulus for subgrade soils. The models should consider most of the factors that affect the resilient modulus. Parameter correlations are used to account for soil properties and different stress states (confining and deviator stress).

The bulk stress model formulated by Seed et al. (1967) describes the nonlinear stress-strain characteristic for granular soils:

$$M_r = k_1 P_a \left[ \frac{\theta}{P_a} \right]^{k_2} \quad (2.2)$$

Where  $\theta$  = is the bulk stress ( $\sigma_1 + \sigma_2 + \sigma_3$ ),  $k_1$ ,  $k_2$  are model parameters related by soil properties, and  $P_a$  is the atmospheric pressure. The bulk stress model does not accurately model the effect of the deviator stress or consider shear stress/strain. May and Witczak (1981) suggests the following equation, which evolved from the bulk stress model with adding the coefficient  $K_i$ :

$$M_r = K_i k_1 \theta^{k_2} \quad (2.3)$$

Where  $K_i$  is a function of pavement structure, test load, and developed shear strain.

Uzan (1985) describes that Equation 2.2 cannot be used to describe granular soils and produce a new model using three parameters; therefore, the Uzan model is used to determine resilient modulus using bulk and deviator stress, which considers the actual field stress state. The model defines the resilient modulus, as follows:

$$M_r = k_1 P_a \left( \frac{\theta}{P_a} \right)^{k_2} \left( \frac{\sigma_d}{P_a} \right)^{k_3} \quad (2.4)$$

The above model is normalized with atmospheric pressure;  $\theta$  and  $\sigma_d$  are the bulk and deviator stresses, respectively.

The model in Equation 2.4 was revised by Witczak and Uzan (1988) by replacing the bulk stress with octahedral shear stress:

$$M_r = k_1 P_a \left( \frac{\theta}{P_a} \right)^{k_2} \left( \frac{\tau_{oct}}{P_a} \right)^{k_3} \quad (2.5)$$

where  $\tau_{oct}$  is octahedral shear stress, and the model is normalized with atmospheric pressure ( $P_a$ ).

The most widely accepted resilient modulus constitutive equation is the general model developed by NCHRP project 1-28A and adopted by NCHRP project 1-37A for implementation in the mechanistic-empirical pavement design. The model can be used for all types of subgrade materials and is defined by:

$$M_r = k_1 P_a \left( \frac{\sigma_b}{P_a} \right)^{k_2} \left( \frac{\tau_{oct}}{P_a} + 1 \right)^{k_3} \quad (2.6)$$

Where,  $M_r$  is resilient modulus,  $P_a$  is atmospheric pressure (101.325 kPa),  $\sigma_b$  is bulk stress =  $\sigma_1 + \sigma_2 + \sigma_3$ ,  $\sigma_1$  is major principal stress,  $\sigma_2 = \sigma_3$  is intermediate principal stress in a repeated load triaxial test, which is the minor principal stress or confining pressure,  $\tau_{oct}$  is octahedral shear stress, and  $k_1$ ,  $k_2$  and  $k_3$  are material model parameters.

The octahedral shear stress is defined in general as:

$$\tau_{oct} = \frac{1}{3} \sqrt{(\sigma_1 - \sigma_2)^2 + (\sigma_1 - \sigma_3)^2 + (\sigma_2 - \sigma_3)^2} \quad (2.7)$$

In a triaxial stress space,  $\sigma_2 = \sigma_3$  and  $\sigma_1 - \sigma_3 = \sigma_d$ ; therefore the octahedral shear stress is reduced to:

$$\tau_{oct} = \frac{\sqrt{2}}{3}(\sigma_d) \quad (2.8)$$

## 2.5 Resilient Modulus Correlations

Titi et al. (2006) conducted a comprehensive resilient modulus investigation on selected Wisconsin soils. Initiated by WisDOT, this project aimed to develop correlations for estimating the resilient modulus of various Wisconsin subgrade soils from basic soil properties. A laboratory testing program was conducted on common subgrade soils to evaluate their physical and compaction properties. The resilient modulus of the investigated soils was determined from the repeated load triaxial test following the AASHTO T307 procedure. The laboratory testing program produced a high-quality and consistent test results database. These test results were assured through a repeatability study and by performing two tests on each soil specimen at the specified physical conditions.

Titi et al. (2006) selected the general resilient modulus constitutive equation given on Equation 2.6. A comprehensive statistical analysis was performed to develop correlations between basic soil properties and the resilient modulus model parameters  $k_1$ ,  $k_2$ , &  $k_3$ . The analysis did not yield good results when the whole test database was used; however, good results were obtained when fine-grained and coarse-grained soils were analyzed separately. The correlations developed in this study were able to estimate the resilient modulus of the compacted subgrade soils with reasonable accuracy, as shown in Figure 2.3. In order to inspect the performance of the models developed in this study,

they were compared with the models developed based on the Long Term Pavement Performance (LTPP) database. The LTPP models did not yield good results compared with the models proposed by this study, primarily due to differences in the test procedures, test equipment, sample preparation, and other conditions involved with development of both LTPP and the models of this study.

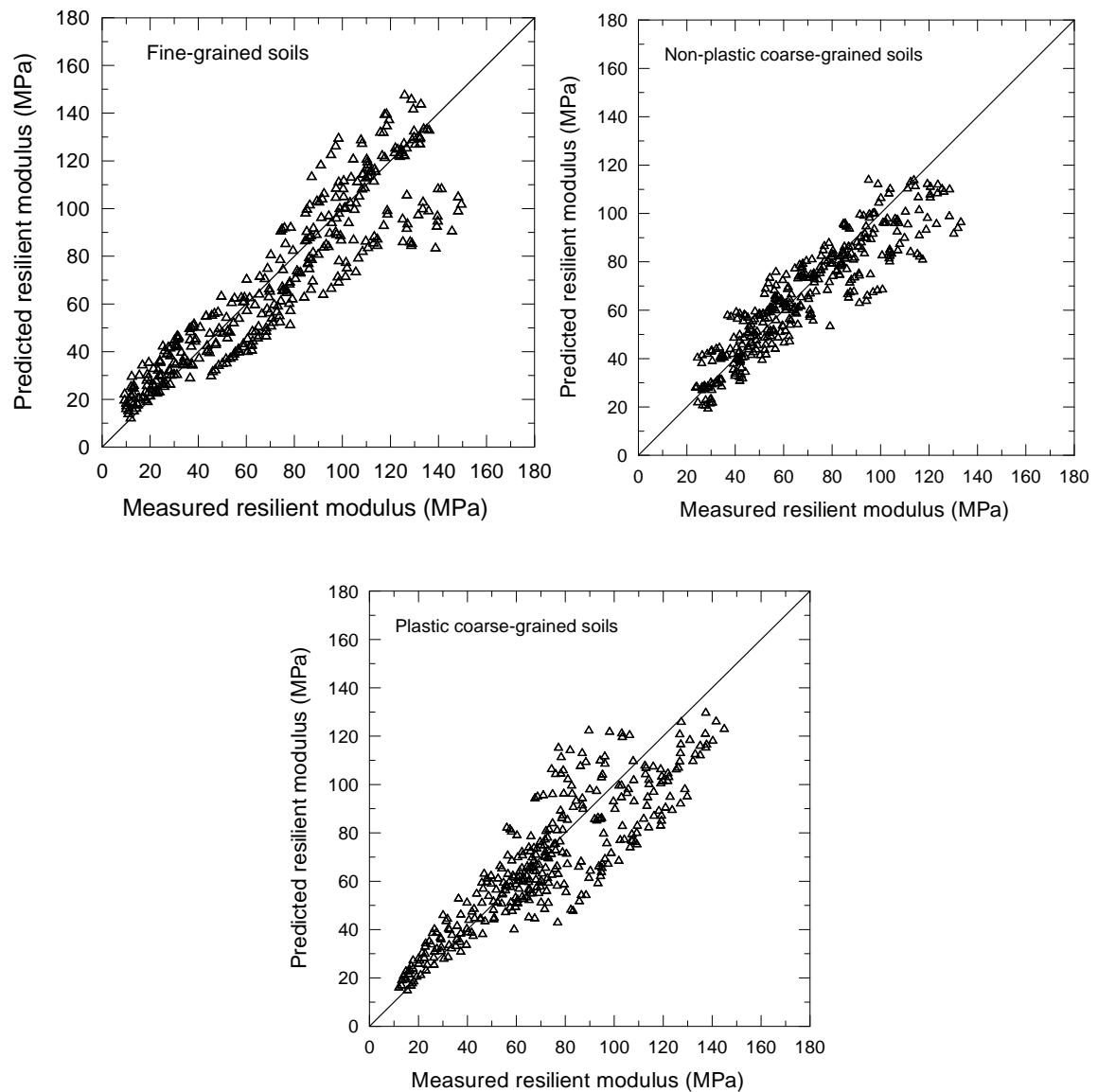


**Figure 2.3: Predicted versus measured resilient modulus of Wisconsin soils (Titi et al. 2006)**

The equations developed by Titi et al. (2006) that correlate resilient modulus model parameters ( $k_1$ ,  $k_2$ , &  $k_3$ ) with basic soil properties for fine-grained and coarse-grained soils can be used to estimate Level 2 resilient modulus input for the mechanistic-empirical pavement design. These equations (correlations) are based on statistical analysis of laboratory test results that were limited to the soil physical conditions specified. Table 2.2 describes all regression equations for the different types of soils. Estimation of resilient modulus of subgrade soils beyond these conditions was not validated.

Malla and Joshi (2006) performed a study to correlate resilient modulus values using LTPP data for subgrade soils. The study divided the subgrade soils into their own AASHTO classification (A-1-b, A-3, A-2-4, A-4, A-6, and A-7-6). The generalized constitutive model for estimating  $M_r$  (Equation 2.6) was used.

Multiple linear regression analysis was conducted on test results of all soil samples. Table 2.3 summarizes the model parameters from Malla and Joshi (2006) for soil type A-4, A-6, and A-7-6 which are considered fine-grained subgrade soils.

**Table 2.2: Regression equations from Titi et al. (2006)**

Soil Type	Regression Equations
Fine-grained	$k_1 = 404.166 + 42.933PI + 52.260\gamma_d - 987.353 \left( \frac{w}{w_{opt}} \right)$
	$k_2 = 0.25113 - 0.0292PI + 0.5573 \left( \frac{w}{w_{opt}} \right) \left( \frac{\gamma_d}{\gamma_{dmax}} \right)$
	$k_3 = -0.20772 + 0.23088PI + 0.00367\gamma_d - 5.4238 \left( \frac{w}{w_{opt}} \right)$
Coarse-grained (non-plastic)	$k_1 = 809.547 + 10.568P_{No.4} - 6.112P_{No.40} - 578.337 \left( \frac{w}{w_{opt}} \right) \left( \frac{\gamma_d}{\gamma_{dmax}} \right)$
	$k_2 = 0.5661 + 0.006711P_{No.40} - 0.02423P_{No.200} + 0.05849(w - w_{opt}) + 0.001242(w_{opt})(\gamma_{dmax})$
	$k_3 = -0.5079 - 0.041411P_{No.40} + 0.14820P_{No.200} - 0.1726(w - w_{opt}) - 0.01214(w_{opt})(\gamma_{dmax})$
Coarse-grained (plastic)	$k_1 = 8642.873 + 132.643P_{No.200} - 428.067(\%Silt) - 254.685PI + 197.230\gamma_d - 381.400 \left( \frac{w}{w_{opt}} \right)$
	$k_2 = 2.325 - 0.00853P_{No.200} + 0.02579LL - 0.06224PI - 1.73380 \left( \frac{\gamma_d}{\gamma_{dmax}} \right)$
	$k_3 = -32.5449 + 0.7691P_{No.200} - 1.1370(\%Silt) + 31.5542 \left( \frac{\gamma_d}{\gamma_{dmax}} \right) - 0.4128(w - w_{opt})$

where:  $P_{No.4}$  is percent passing sieve #4,  $P_{No.40}$  is percent passing sieve #40,  $P_{No.200}$  is percent passing sieve #200,  $\%Silt$  is the amount of silt in the soil,  $\%Clay$  is the amount of clay in the soil,  $LL$  is the liquid limit,  $PI$  is the plasticity index,  $w$  is the moisture content of the soil,  $w_{opt}$  is the optimum moisture content,  $\gamma_d$  is the dry unit weight, and  $\gamma_{dmax}$  is the maximum dry unit weight.

**Table 2.3: Model parameters determined from multiple linear regression analysis**

Soil Type	Regression Equation	R <sup>2</sup>	R <sup>2</sup> Adj
A-4 Case (1)	$\log k_1 = 5.74999 - 0.13693 * OMC - 0.79256 * MCR$ $- 0.00161 * MAXDD - 0.01092 * S1$ $+ 0.00591 * SN200 + 0.00774 * CLAY$	0.52	0.47
	$k_2 = -0.74402 + 0.03585 * MC + 0.0004803 * DD$ $+ 0.00641 * PL - 0.00839 * LL + 0.00484$ $* SN10 - 0.00477 * SN80 - 0.00994 * CLAY$	0.54	0.48
	$k_3 = 1.30193 - 0.02367 * MC - 0.02764 * OMC$ $- 0.0006325 * MAXDD + 0.00156 * SN10$ $+ 0.00253 * SILT$	0.30	0.24
A-6 Case (1)	$\log k_1 = 4.59815 - 0.12918 * MC - 0.00211 * MAXDD$ $+ 0.04246 * LL - 0.0150 * CSAND - 0.01746$ $* CLAY$	0.52	0.44
	$k_2 = -2.54229 + 0.00971 * MC + 0.00122 * MAXDD$ $+ 0.02703 * SN40 - 0.02122 * SN200$ $- 0.02393 * FSAND$	0.47	0.38
	$k_3 = 2.08649 - 0.05214 * MC + 0.0007171 * MAXDD$ $+ 0.02450 * LL - 0.01231 * S1 + 0.00493$ $* SN80 - 0.00922 * CLAY$	0.49	0.38
A-7-6 Case (1)	$\log k_1 = 6.54551 - 0.08119 * MC - 0.00202 * MAXDD -$ $0.00719 * PL - 0.01842 * SN200 - 0.06529 * CSAND$	0.79	0.72
	$k_2 = 9.78523 + 0.00743 * MC - 0.00018782 * DD$ $- 0.01787 * LL - 0.08598 * S1\_HALF$	0.45	0.30
	$k_3 = 3.38876 - 0.03515 * MC - 0.00121 * MAXDD$ $- 0.01073 * PL - 0.00711 * SN200$ $- 0.02667 * CSAND$	0.70	0.60

where: specimen moisture content (*MC*), optimum moisture content (*OMC*), moisture content ratio ( $MCR=MC/OMC$ ), maximum dry density (*MAXDD*), specimen dry density (*DD*), liquid limit (*LL*), plastic limit (*PL*), percent passing 1 ½" sieve (*S1\_HALF*), percent passing 1" sieve (*S1*), percent passing #10 sieve (*SN10*), percent passing #80 sieve (*SN80*), percent passing #200 sieve (*SN200*), percent coarse sand (*CSAND*, particles of size 2–0.42mm), percent fine sand (*FSAND*, particles of size 0.42–0.074mm), percent silt (*SILT*, particles of size 0.074-0.002mm), and percent clay (*CLAY*, particles of size 0.002mm).

Laboratory  $M_r$  values vs. the predicted  $M_r$  values for A-4 showed 59% of predicted  $M_r$

were within  $\pm 10\%$  of actual  $M_r$  values, and 88% of predicted values were within  $\pm 20\%$  of

actual  $M_r$  values. For the prediction of A-7-6 soils,  $k_2$  parameter produces negative numbers, therefore the  $M_r$  values could not be predicted.

NCHRP synthesis 382 summarizes resilient modulus correlation to soil properties produced by recent research studies.

## **2.6 Soil Distribution in Wisconsin**

Madison and Gundlach developed a map that shows the different soil regions of Wisconsin in 1993. The map is divided into five sections: 1) soils of northern and eastern Wisconsin; 2) soils of central Wisconsin; 3) soils of southwestern and western Wisconsin; 4) soils of southeastern Wisconsin; and 5) statewide soils. Within each of the divided sections, subgroups describe the specific soil found in the region. Figure 2.4 shows the map of Wisconsin with the regions labeled for the specific soil types.

### ***Soils of Northern and Eastern Wisconsin:***

Region E- Forested, red, sandy, loamy soils with uplands covered with loamy soils covering calcareous silt, and sandy soils found primarily in glacial lake beds.

Region Er- Forested, red loamy or clayey soils over dolomite bedrock or till with parts covering calcareous material in the uplands.

Region F- Forested, silty soils. On uplands soils formed silt over very dense, acid, loam till.

Region G- Forested, loamy soils. Antigo Silt Loam (Wisconsin state soil) that overlies sand and gravel.

Region H- Forested, sandy soils. Sand contains 15% to 35% gravel in northern outwash plains. Loamy materials over acid sand and gravel.

Region I- Forested, red, clayey or loamy soils. Silty materials overlie calcareous, red, clay till or lake deposits, which formed near Lake Michigan and larger lakes.

***Soils of Central Wisconsin:***

Region C- Forested, sandy soils. Loamy or sandy materials overlie limy till in uplands.

Region Cm- Prairie, sandy soils. Soil is dark deep sandy soils.

Region Fr- Forested, silty soils over igneous/metamorphic rock.

***Soils of Southwestern and Western Wisconsin:***

Region A- Forested, silty soils. On uplands are deep, silty soils, deep silty and clayey soils, and silty and clayey soils that overlie limestone bedrock.

Region Am- Prairie, silty Soils. Deep, silty soils cover uplands.

Region Dr- Forested soils over sandstone.

***Soils of Southeastern Wisconsin:***

Region B- Forested, silty soils. Loamy soils underlain by limy sand and gravel outwash, organic soils formed where plant materials accumulated in depressions.

Region Bm- Prairie, silty soils. Deep, silty loamy soils overlying limy till cover rolling uplands. Clayey soils over limy till are common near Milwaukee and Racine-Kenosha.

*Statewide:*

Region J- Streambottom and major wetland soils, occur in depressions and drainageways.

Extensive areas of organic soils are included in this region.

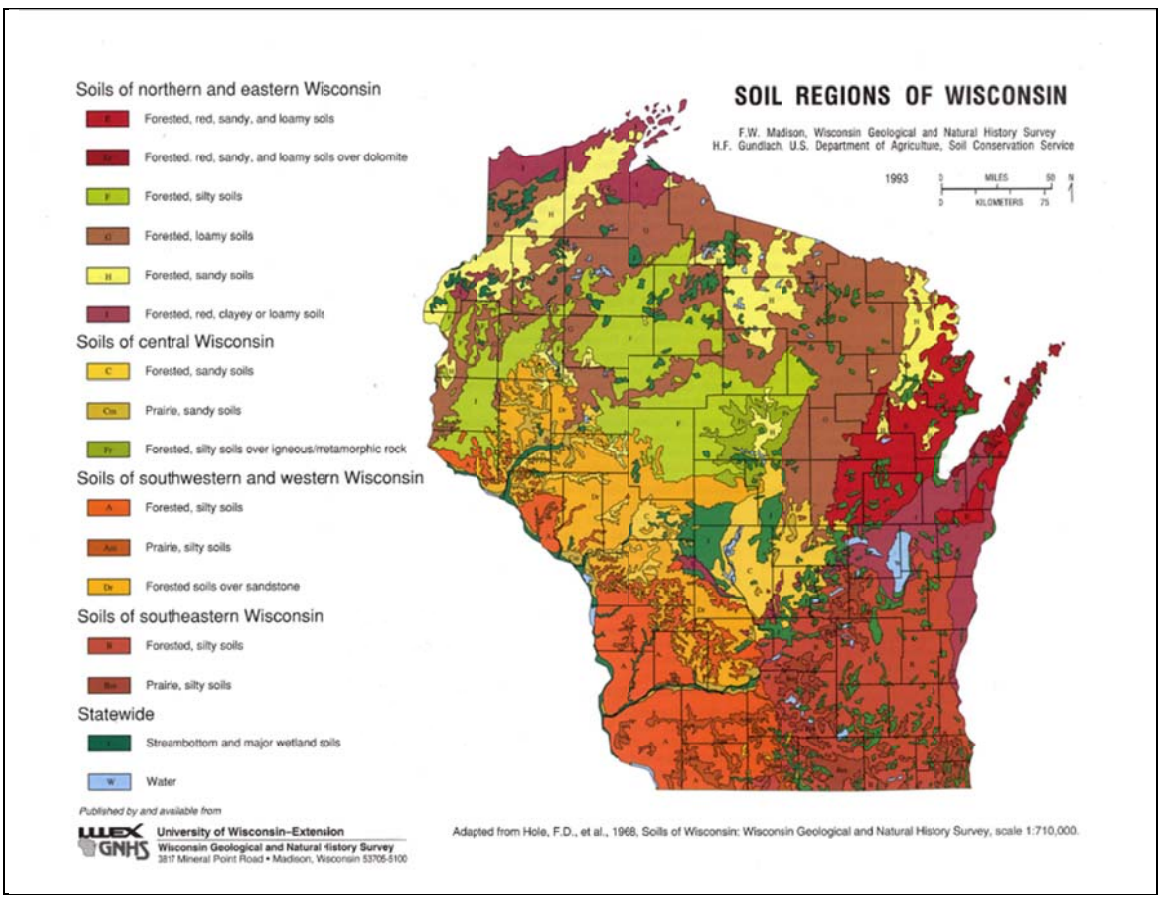


**Figure 2.4: Wisconsin soil regions (Madison and Gundlach, 1993)**

## **Chapter 3**

### **Research Methodology**

Chapter 3 discusses the research methodologies used in the laboratory testing program for the investigated soils. In this study, thirteen soil samples collected throughout the state of Wisconsin were investigated. American Society for Testing and Materials (ASTM) and American Association of State Highway and Transportation Officials (AASHTO) test standards were used for lab testing procedures. The repeated load triaxial test was conducted following the AASHTO T307 standard procedure.

#### **3.1 Investigated Soils**

Wisconsin fine-grained soils were collected and investigated for this study as disturbed soil samples. The soils were selected by WisDOT engineers and sampled by WisDOT engineers and UW-Milwaukee team. The samples, representing a wide range of fine-grained soils in Wisconsin, were analyzed in the soil lab at UW-Milwaukee. A map in Figure 3.1 shows the location of the collected soil samples across Wisconsin.

Table 3.1 describes the sample name and symbols used throughout this report and the county the soil is located in.

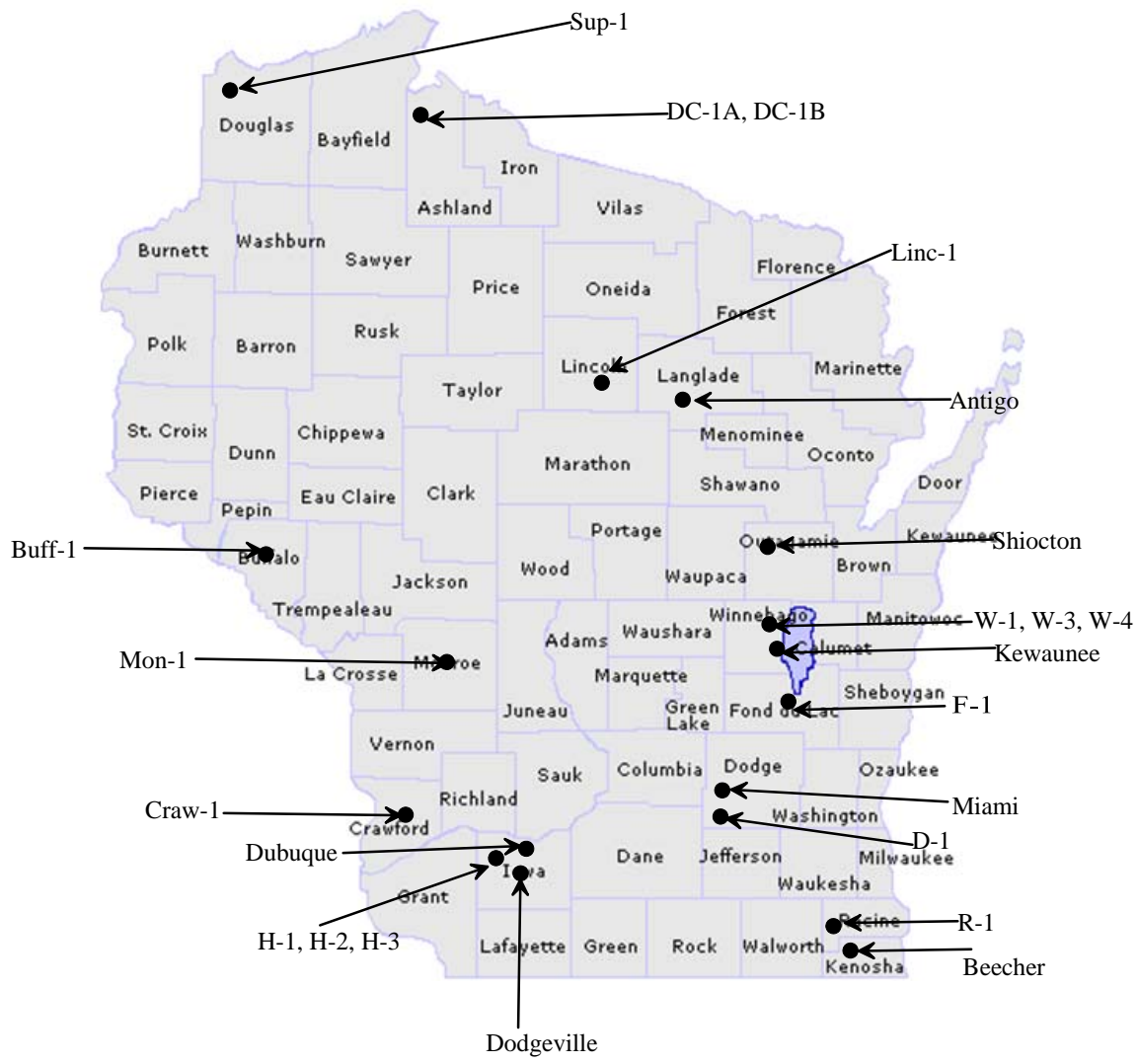


Figure 3.1: Investigated soil locations across Wisconsin

**Table 3.1: Investigated soils location by county and soil sample ID referenced in this report**

<b>Soil Name</b>	<b>Sample ID</b>	<b>County</b>
Fond du Lac-1	F-1	Fond du Lac
Dodge-1	D-1	Dodge
Highland-1	H-1	Iowa
Highland-2	H-2	Iowa
Highland-3	H-3	Iowa
Lincoln-1	Linc-1	Lincoln
Racine-1	R-1	Racine
Deer Creek-1A	DC-1A	Ashland
Deer Creek-1B	DC-1B	Ashland
Superior-1	Sup-1	Douglas
Winnebago-2	W-2	Winnebago
Winnebago-3	W-3	Winnebago
Winnebago-4	W-4	Winnebago
Crawford-1	Craw-1	Crawford
Monroe-1	Mon-1	Monroe
Buffalo-1	Buff-1	Buffalo

### **3.2 Laboratory Testing Program**

#### **3.2.1 Physical Properties and Compaction Characteristics**

The investigated soil samples were subjected to laboratory testing to determine the physical properties and moisture-unit weight relationship. The laboratory tests to determine physical properties were: 1) grain size distribution (hydrometer and sieve analysis); 2) Atterberg limits (liquid limit, *LL* and plastic limit, *PL*); and 3) specific gravity ( $G_s$ ). The Standard Proctor test procedure was used to determine the moisture-unit weight relationship for each soil.

The laboratory tests were conducted using ASTM and AASHTO test standards. Table 3.2 summarizes the test standards used for all testing and classification conducted in the lab. All tests were conducted under the same test procedure used by WisDOT.

Laboratory tests were conducted at least twice to ensure quality results and to reduce variability in soil properties. More than two tests were conducted when the results of the soil properties were not consistent.

**Table 3.2: Standard test designations used for soil testing in this study**

<b>Soil Property</b>	<b>Standard Test Designation</b>
Particle Size Analysis	AASHTO T88-00: Particle Size Analysis of Soils
Liquid Limits	AASHTO T89-02: Determining the Liquid Limit of Soils
Plastic Limit and Plasticity Index	AASHTO T90-00: Determining the Plastic Limit and Plasticity Index of Soils
Specific Gravity	AASHTO 100-03: Specific Gravity of Soils
Compaction	AASHTO T99-01: Moisture-Density Relations of Soils Using a 2.5kg (5.5lb) Rammer and a 305-mm (12-in.) Drop
ASTM Soil Classification (USCS)	ASTM D2487-93: Standard Classification of Soils for Engineering Purposes
AASHTO Soil Classification	AASHTO M 145-91 (2000): Classification of Soils and Soil-Aggregate Mixtures for Highway Construction Purposes
Repeated Load Triaxial Test	AASHTO T307-99 (2003): Determining the Resilient Modulus of Soils and Aggregate Materials

### **3.2.2 Repeated Load Triaxial Test**

The repeated load triaxial test was conducted to determine resilient modulus values according to AASHTO T307: “Determining the Resilient Modulus of Soils and

Aggregate Materials.” Soil samples were disturbed and recompacted according to AASHTO T307.

### ***Sample Preparation***

Recompacted soil specimens were prepared following the AASHTO T307 procedure. Soil samples were compacted in five lifts of equal height using static compaction. Fine-grained soils are classified as Type II material; therefore, a mold 2.8 inches in diameter by 5.6 inches in height was used to compact the specimens. Each lift was weighed to determine a uniform unit weight of the sample under static compaction. Figure 3.2 illustrates the compaction method used for sample preparation.

Soil samples were prepared and different combinations of unit weights and moisture contents were prepared using the standard proctor test results. The sample unit weights and moisture contents were determined by maximum dry unit weight ( $\gamma_{dmax}$ ) with optimum moisture content ( $w_{opt}$ ), 95% of  $\gamma_{dmax}$  with the corresponding dry moisture content, and corresponding wet moisture content, 93% of  $\gamma_{dmax}$  with the corresponding dry moisture content, and corresponding wet moisture content. For some of the soils, 97% or 98% of  $\gamma_{dmax}$  was used instead of 93%  $\gamma_{dmax}$  due to weak stiffness values. Figure 3.3 shows a graph of the different compaction values with corresponding moisture contents for a typical soil sample.



(a) 2.8inch diameter split mold



(b) Weighing soil lift for compaction



(c) Lubricating split mold



(d) Filling the mold



(e) Applying static compaction



(f) Jacking soil specimen

**Figure 3.2: Sample preparation and sample compaction according to AASHTO T307**

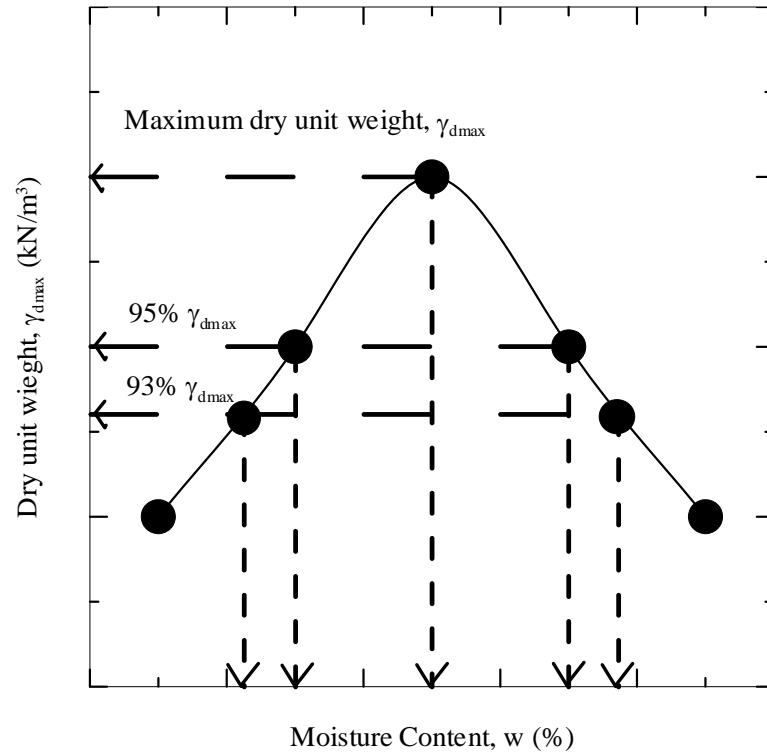


**Figure 3.3: Target unit weights and moisture contents under which soil specimens were prepared**

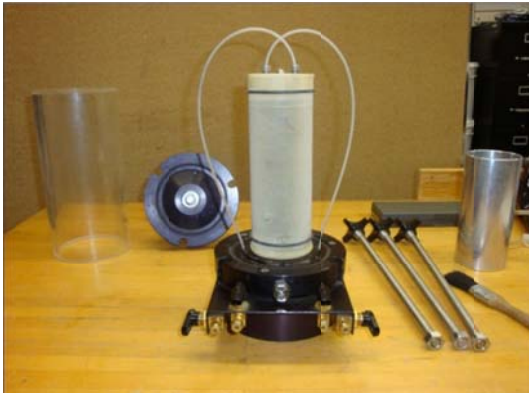
After compaction, the specimen is jacked out of the mold and set on the base of the triaxial cell. Porous stones and filter paper are placed on both ends of the specimen. A membrane is placed over the specimen and sealed with “O” rings to separate the confining pressure and specimen. All hoses are connected and the top of the cell is centered and assembled. Then, the triaxial cell is centered on the load frame and the LVDTs and load cell are placed into position and checked. Figure 3.4 illustrates the setup of the triaxial cell and mounting of the triaxial cell in the loading frame.



(a) Compacted specimen



(b) Housing specimen in a membrane



(c) Seating soil specimen on base



(d) Assembly of triaxial cell



(e) Mounting cell on load frame

**Figure 3.4: Assembly of the triaxial cell and placement on the load frame for repeated load triaxial test.**

### *Specimen Testing*

A Fast Track console is used to control the dynamic test system for initial calibration and positioning. A Laboratory Virtual Instrumentation Engineering Workbench (LabVIEW) program was developed to apply the cyclic sequences from AASHTO T307 test procedure. The computer controls all loads through the entire AASHTO T307 test. After the cell is placed on the load frame, confining pressure ( $\sigma_c$ ) is connected to the cell and manually adjusted throughout the test. Several photos of the computer software are shown in Figure 3.5.

In the conditioning stage, 500–1000 cycles were applied with a specified deviator stress ( $\sigma_d$ ) and confining pressure ( $\sigma_c$ ). The conditioning stage seats the specimen and eliminates any imperfect contacts between the platens and specimen. The LVDTs and triaxial cell can be adjusted during the conditioning stage if any part is out of level. After the conditioning stage is complete, the computer software follows the sequences listed in the AASHTO T307 test standard. Table 2.1 lists the different deviator stress and confining pressure for each sequence.

The computer software has quality control settings to determine if the LVDTs are out of balance and/or if the load function is not within its tolerable limits. Graphs are presented throughout the test, allowing the technician to observe any out-of-range loading or LVDT measurements. The computer program will prompt the user if the specimen exceeds 5% strain at any point throughout the test and determine a test termination. The servo-hydraulic test system is one of the most accurate systems to run cyclic testing, but the load is still monitored to ensure accurate test results.

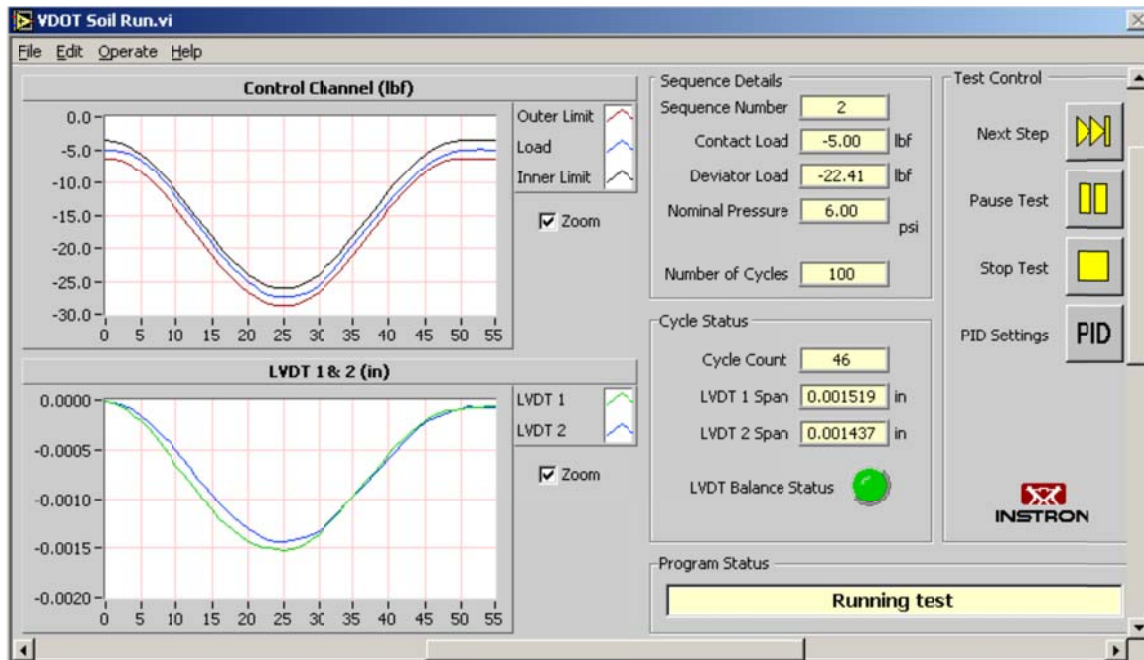
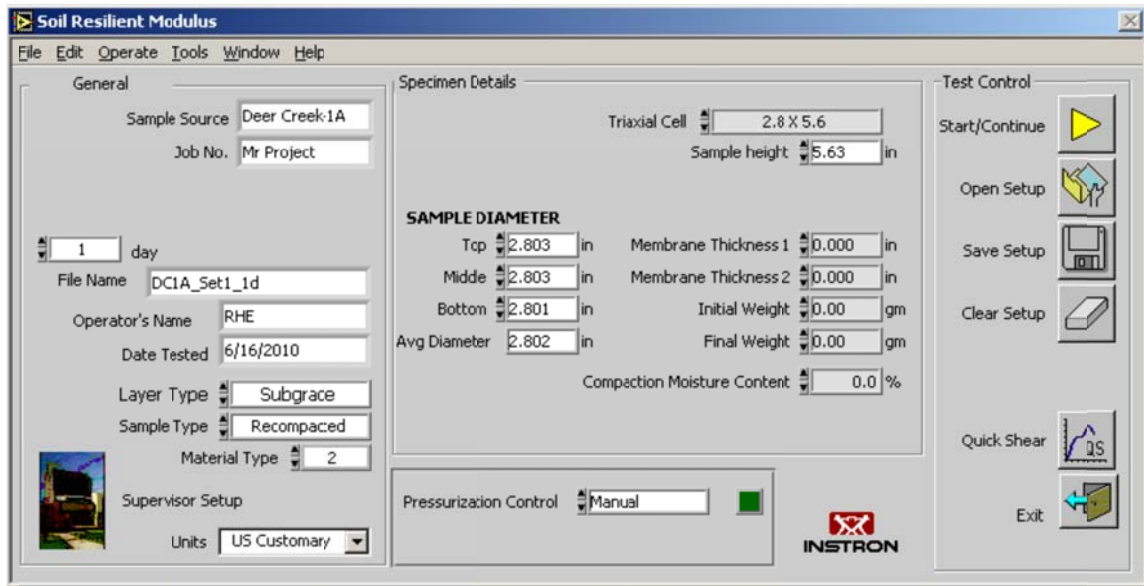


Figure 3.5: Computer software controlling the repeated load triaxial test

## Chapter 4

### Test Results and Discussion

Results of the laboratory testing program on Wisconsin fine grained subgrade soils are presented in this chapter. Physical properties, compaction characteristics, and resilient modulus of the investigated soils are summarized and discussed. Statistical analysis is conducted on the test results to develop models for estimating/predicting resilient modulus of Wisconsin fine-grained subgrade soils from basic soil properties.

#### 4.1 Physical Properties and Compaction Characteristics

Soil properties consist of particle size analysis (sieve and hydrometer); consistency limits (liquid limit, plastic limit, and plasticity index); specific gravity; maximum dry unit weight and optimum moisture content; soil classification using the USCS; and soil classification using the AASHTO method including group index (*GI*). Table 4.1 summarizes the test results on the investigated Wisconsin fine-grained subgrade soils as well as fine grained soils investigated in Phase I by Titi et al. (2006) . Two tests were conducted on each soil to ensure representative and reliable results are obtained.

Examination of Table 4.1 shows that all investigated soils are fine-grained soils with fines ranging between 41 and 98.1%. Plasticity index varies from 6 to 33.2%. These results indicate that the investigated soils cover a wide range of fine-grained soils and one could assume that these soils are representative of Wisconsin fine-grained soils. Figure 4.1 depicts the particle size distribution curves for the investigated Wisconsin fine-grained subgrade soils. Table 4.2 presents calculated parameters of grain size distribution

Table 4.1: Properties of investigated soils

Soil Name (Soil ID)	Test #	Passing Sieve #200 (%)	Liquid Limit LL (%)	Plastic Limit PL (%)	Plasticity Index PI (%)	Specific Gravity G <sub>s</sub>	Optimum Moisture Content W <sub>opt</sub> (%)	Maximum Dry Unit Weight		Soil Classification		
								γ <sub>dmax</sub> (kN/m <sup>3</sup> )	γ <sub>dmax</sub> (pcf)	USCS	Group Index (GI)	AASHTO
Fond du Lac- 1 (F-1)	1	92.0	54.5	32.0	23.0	2.77	20.5	16.3	103.8	MH Elastic Silt	26	A-7-5 Clayey Soil
	2	90.0	56.5	35.0	21.0	2.85	22.0	15.7	100.0	MH Elastic Silt	24	A-7-5 Clayey Soil
Deer Creek- 1A (DC-1A)	1	85.1	47.8	25.3	22.5	2.59	16.0	16.9	107.9	CL Lean Clay	21	A-7-6 Clayey Soil
	2	81.0	41.0	25.7	15.0	2.48	17.0	16.8	107.7	CL Lean Clay with Sand	13	A-7-6 Clayey Soil
Deer Creek- 1B (DC-1B)	1	75.8	43.7	24.4	19.3	2.62	16.0	17.3	110.0	CL Lean Clay with Sand	15	A-7-6 Clayey Soil
	2	85.0	42.0	25.5	16.5	2.38	17.0	16.9	108.0	CL Lean Clay	22	A-7-6 Clayey Soil
Superior-1 (Sup-1)	1	80.3	60.8	22.8	23.0	2.55	24.5	14.8	94.2	MH Elastic Silt with Sand	22	A-7-5 Clayey Soil
	2	89.0	66.0	36.4	30.0	2.73	24.5	14.8	94.2	MH Elastic Silt with Sand	33	A-7-5 Clayey Soil

Table 4.1 (cont.): Properties of investigated soils

Soil Name (Soil ID)	Test #	Passing Sieve #200 (%)	Liquid Limit LL (%)	Plastic Limit PL (%)	Plasticity Index PI (%)	Specific Gravity $G_s$	Optimum Moisture Content $w_{opt}$ (%)	Maximum Dry Unit Weight		Soil Classification		
								$\gamma_{dmax}$ (kN/m <sup>3</sup> )	$\gamma_{dmax}$ (pcf)	USCS	Group Index (GI)	AASHTO
Racine-1 (R-1)	1	90.4	37.3	23.3	14.0	2.60	16.6	17.3	109.9	CL Lean Clay	11	A-6 Clayey Soil
	2	81.0	33.5	22.1	11.4	2.52	15.3	17.6	112.2	CL Lean Clay with Sand	9	A-6 Clayey Soil
Highland-1 (H-1)	1	82.0	37.0	21.0	16.0	2.71	17.0	16.5	105.0	CL Lean Clay with Sand	13	A-6 Clayey Soil
	2	84.5	37.0	23.0	13.0	2.77	14.5	16.9	107.3	CL Lean Clay with Sand	11	A-6 Clayey Soil
Highland-2 (H-2)	1	78.7	36.0	24.0	12.0	2.70	15.0	17.3	110.0	CL Lean Clay with Sand	9	A-6 Clayey Soil
	2	85.2	38.0	24.0	14.0	2.84	14.0	17.4	111.0	CL Lean Clay	12	A-6 Clayey Soil
Highland-3 (H-3)	1	87.5	56.5	23.3	33.2	2.56	22.0	15.6	99.0	CH Fat Clay	32	A-7-6 Clayey Soil
	2	87.4	59.8	28.5	31.3	2.49	24.0	15.4	98.0	CH Fat Clay	24	A-7-6 Clayey Soil

Table 4.1 (cont.): Properties of investigated soils

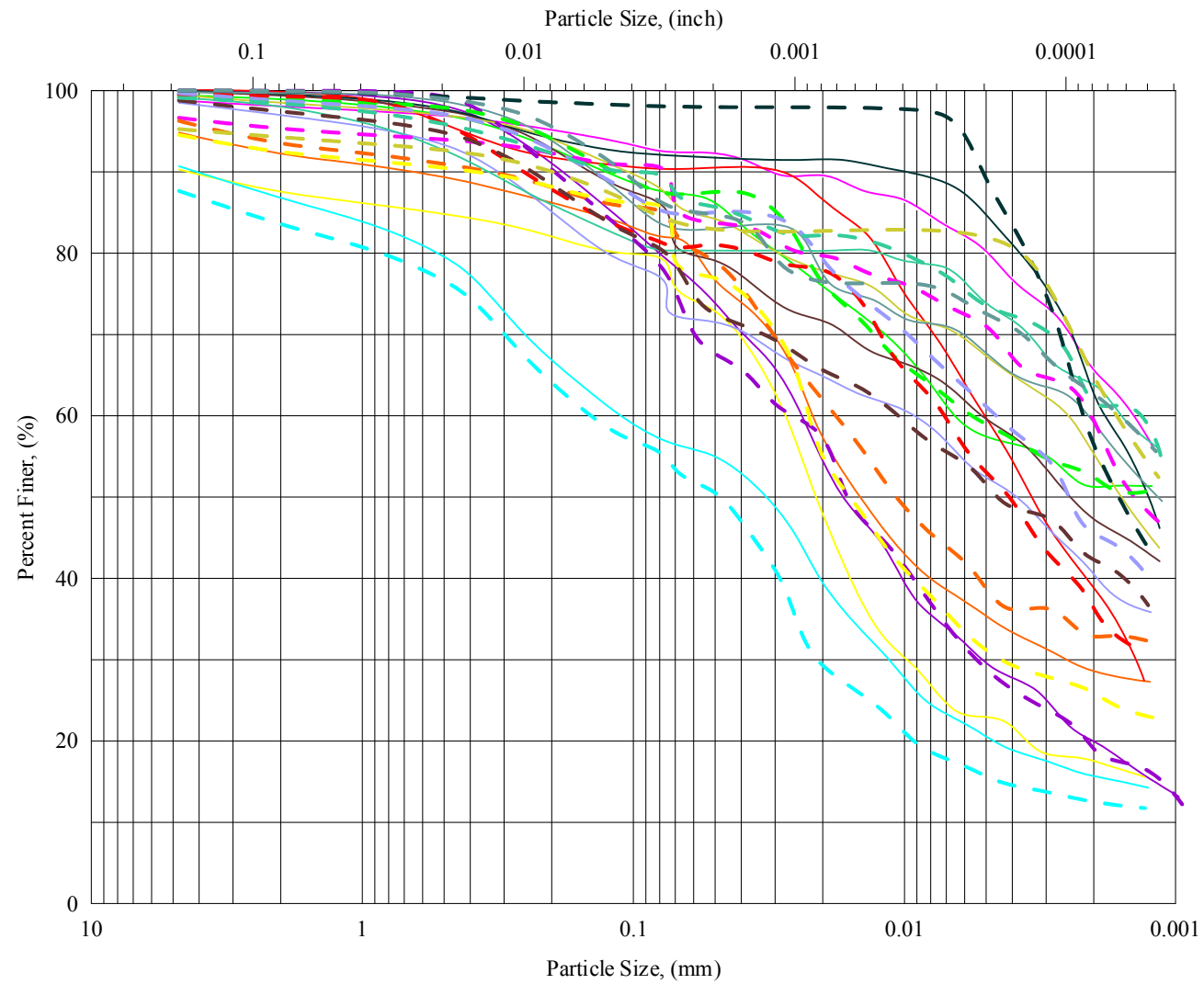
Soil Name (Soil ID)	Test #	Passing Sieve #200 (%)	Liquid Limit LL (%)	Plastic Limit PL (%)	Plasticity Index PI (%)	Specific Gravity $G_s$	Optimum Moisture Content $w_{opt}$ (%)	Maximum Dry Unit Weight		Soil Classification		
								$\gamma_{dmax}$ (kN/m <sup>3</sup> )	$\gamma_{dmax}$ (pcf)	USCS	Group Index (GI)	AASHTO
Winnebago-2 (W-2)	1	92.1	64.5	35.0	29.0	2.62	23.0	14.9	95.0	MH Elastic Silt	33	A-7-5 Clayey Soil
	2	98.1	62.0	36.0	26.0	2.58	26.0	14.8	94.3	MH Elastic Silt	33	A-7-5 Clayey Soil
Winnebago-3 (W-3)	1	87.2	41.5	26.8	14.8	2.82	22.0	16.0	101.5	ML Silt	14	A-7-6 Clayey Soil
	2	84.2	43.8	26.4	17.4	2.85	23.0	15.7	99.5	CL Lean Clay with Sand	23	A-7-6 Clayey Soil
Winnebago-4 (W-4)	1	83.3	60.5	29.3	31.0	2.69	21.0	15.7	100.0	CH Fat Clay with Sand	29	A-7-6 Clayey Soil
	2	85.9	60.5	27.3	33.0	2.58	NA	NA	NA	CH Fat Clay	32	A-7-6 Clayey Soil
Dodge-1 (D-1)	1	79.2	34.0	23.6	11.4	2.49	17.0	16.8	107.0	CL- Lean Clay with Sand	8	A-4 Silty Soil
	2	77.3	33.0	22.6	10.4	2.60	16.5	15.8	100.5	CL- Lean Clay with Sand	7	A-4 Silty Soil

Table 4.1 (cont.): Properties of investigated soils

Soil Name (Soil ID)	Test #	Passing Sieve #200 (%)	Liquid Limit LL (%)	Plastic Limit PL (%)	Plasticity Index PI (%)	Specific Gravity G <sub>s</sub>	Optimum Moisture Content w <sub>opt</sub> (%)	Maximum Dry Unit Weight		Soil Classification		
								γ <sub>dmax</sub> (kN/m <sup>3</sup> )	γ <sub>dmax</sub> (pcf)	USCS	Group Index (GI)	AASHTO
Lincoln-1 (Linc-1)	1	56.8	25.0	19.0	6.0	2.81	10.5	18.9	120.0	CL-ML Sandy Silty Clay with Gravel	1	A-4 Silty Soil
	2	54.7	25.0	18.0	7.0	2.76	10.0	19.2	122.0	CL-ML Sandy Silty Clay with Gravel	1	A-4 Silty Soil
Beecher, B, Kenosha County	1	48	29	17	12	2.67	13.9	18.3	116.5	SC Clayey Sand	3	A-6 Clayey Soil
Antigo, B, Langlade County	1	91	30	19	11	2.63	14.5	17.5	111.4	CL Lean Clay	9	A-6 Clayey Soil
Shiocton, C, Outagamie County	1	41	NP	NP	NP	2.69	11.2	15.9	101.3	SM Silty sand with gravel	0	A-4 Silty Soil
Dodgeville, B, Iowa County	1	97	37	25	12	2.55	18.8	16.1	102.5	CL Lean Clay	13	A-6 Clayey Soil
Miami, B, Dodge County	1	96	39	22	17	2.57	18.1	16.6	105.7	CL Lean Clay	18	A-6 Clayey Soil

Table 4.1 (cont.): Properties of investigated soils

Soil Name (Soil ID)	Test #	Passing Sieve #200 (%)	Liquid Limit LL (%)	Plastic Limit PL (%)	Plasticity Index PI (%)	Specific Gravity G <sub>s</sub>	Optimum Moisture Content w <sub>opt</sub> (%)	Maximum Dry Unit Weight		Soil Classification		
								γ <sub>dmax</sub> (kN/m <sup>3</sup> )	γ <sub>dmax</sub> (pcf)	USCS	Group Index (GI)	AASHTO
Kewaunee-2C Winnebago County	1	48	28	14	14	2.69	13.5	19.0	121.0	SC Clayey Sand	3	A-6 Clayey Soil
Dubuque, C, Iowa County	1	72	35	23	12	2.55	18.0	16.6	105.7	CL Lean Clay	8	A-6 Clayey Soil
Mon-1	1	64.0	23.0	16.0	7	2.71	14.7	17.6	112.0	CL-ML Silty Clay with Sand	2	A-4 Silty Soil
Craw-1	1	93.5	58	25	33	2.67	14.9	17.3	109.9	CH Fat Clay	35	A-7-6 Clayey Soil
Buff-1	1	91.6	34	26	8	2.67	16.9	17.2	109.4	ML Silt	8	A-4 Silty Soil



**Figure 4.1: Grain size distribution of all investigated soils**

such as the coefficient of uniformity and coefficient of curvature. Variables such as the effective size ( $D_{10}$ ) were calculated by extrapolation and may reflect approximate results. Thirteen fine-grained soils were investigated herein and only a representative soil will be presented and discussed below. Test results of all investigated soils are summarized in Appendix A.

### **Soil Lincoln (Linc-1)**

Test results indicated that the soil consists of 56.8 and 54.7% of fine materials (passing sieve #200) with a plasticity index values  $PI = 6$  and  $7$ , which was classified sandy silty clay with gravel (CL-ML) according to the USCS and silty soil (A-4) according to the AASHTO soil classification with a group index  $GI = 1$  and  $11$ . Figure 4.2 shows the particle size distribution curve for Linc-1 soil. The results of the Standard Proctor test are depicted in Figure 4.3. Results of test #1 showed that the maximum dry unit weight  $\gamma_{dmax} = 18.9 \text{ kN/m}^3$  and the optimum moisture content  $w_{opt.} = 10.5\%$ , while results of test #2 indicated that  $\gamma_{dmax} = 19.2 \text{ kN/m}^3$  and  $w_{opt.} = 10\%$ . The results of the compaction tests are considered consistent.

It was motioned earlier that two tests were conducted on each soil to ensure representative and reliable results are obtained. As shown in Table 4.1, levels of variation exist between the results of the two tests for each property. These variation levels are considered acceptable. The average values for test results were adopted for the purpose of preparing repeated load triaxial test specimens and for performing statistical analysis.

Table 4.3 presents the average values for maximum dry unit weight and optimum moisture content.

**Table 4.2: Grain size analysis properties of investigated soils**

Sample ID	Test	P <sub>200</sub> (%)	D <sub>10</sub> (mm)	D <sub>30</sub> (mm)	D <sub>60</sub> (mm)	C <sub>c</sub>	C <sub>u</sub>
Fond du Lac-1	1	92.5	0.00012	0.00032	0.0016	0.53	13.33
	2	90.0	0.0002	0.0005	0.002	0.06	1.00
Superior-1	1	80.3	0.000055	0.00021	0.0017	0.47	30.91
	2	89.0	0.000026	0.00014	0.0018	0.42	69.23
Deer Creek-1A	1	85.1	0.000064	0.00034	0.0052	0.35	81.25
	2	79.9	0.00013	0.00067	0.011	0.31	84.62
Deer Creek-1B	1	75.8	0.00018	0.00065	0.0091	0.26	50.56
	2	85.0	0.00019	0.0008	0.0047	0.72	24.74
Racine-1	1	90.4	0.00059	0.0015	0.0051	0.75	8.64
	2	81.0	0.00034	0.0013	0.0072	0.69	21.18
Highland-1	1	82.0	0.000027	0.0025	0.022	10.52	814.81
	2	84.5	0.0000092	0.00077	0.018	3.58	1956.52
Highland-2	1	78.7	0.00035	0.0098	0.028	9.80	80.00
	2	85.2	0.00015	0.0045	0.023	5.87	153.33
Highland-3	1	87.5	0.0000043	0.000073	0.0068	0.18	1581.40
	2	87.4	0.000018	0.00017	0.0058	0.28	322.22
Winnebago-2	1	92.1	0.00031	0.0006	0.0019	0.61	6.13
	2	98.0	0.00047	0.00082	0.0023	0.62	4.89
Winnebago-3	1	87.2	0.00023	0.00059	0.0027	0.56	11.74
	2	84.2	0.00021	0.00046	0.0017	0.59	8.10
Winnebago-4	1	83.3	0.0001	0.00034	0.0021	0.55	21.00
	2	85.9	0.000031	0.00016	0.0017	0.49	54.84
Dodge-1	1	79.2	0.00076	0.0055	0.025	1.59	32.89
	2	77.3	0.00075	0.0054	0.027	1.44	36.00
Lincoln-1	1	56.8	0.00043	0.012	0.12	2.79	279.07
	2	54.7	0.00075	0.022	0.15	4.30	200.00
Beecher, B	1	48	0.0000904	0.001	.0092	1.29	102
Antigo, B	1	91	0.0006	0.011	0.0303	6.66	50.5
Shioction, C	1	41	0.000125	0.0014	0.0033	4.32	47.6
Dodgeville, B	1	97	0.0006	0.016	0.0401	10.64	66.83
Miami, B	1	96	0.0001	0.0065	0.029	14.57	290

**Table 4.2 (cont): Grain size analysis properties of investigated soils**

<b>Sample ID</b>	<b>Test</b>	<b>P<sub>200</sub> (%)</b>	<b>D<sub>10</sub> (mm)</b>	<b>D<sub>30</sub> (mm)</b>	<b>D<sub>60</sub> (mm)</b>	<b>C<sub>c</sub></b>	<b>C<sub>u</sub></b>
Kewaunee – 2, C	1	48	0.0000888	0.001	0.0038	1.2	110.2
Dubuque, C	1	72	0.001	0.012	0.07	2.06	70
Craw-1	1	93.5	0.000058	0.000667	0.0109	0.704	187.9
Mon-1	1	63.9	0.0011	0.0185	0.075	4.15	68.18
Buff-1	1	91.6	0.000081	0.00093	0.0211	0.51	260.5

Some values were interpolated

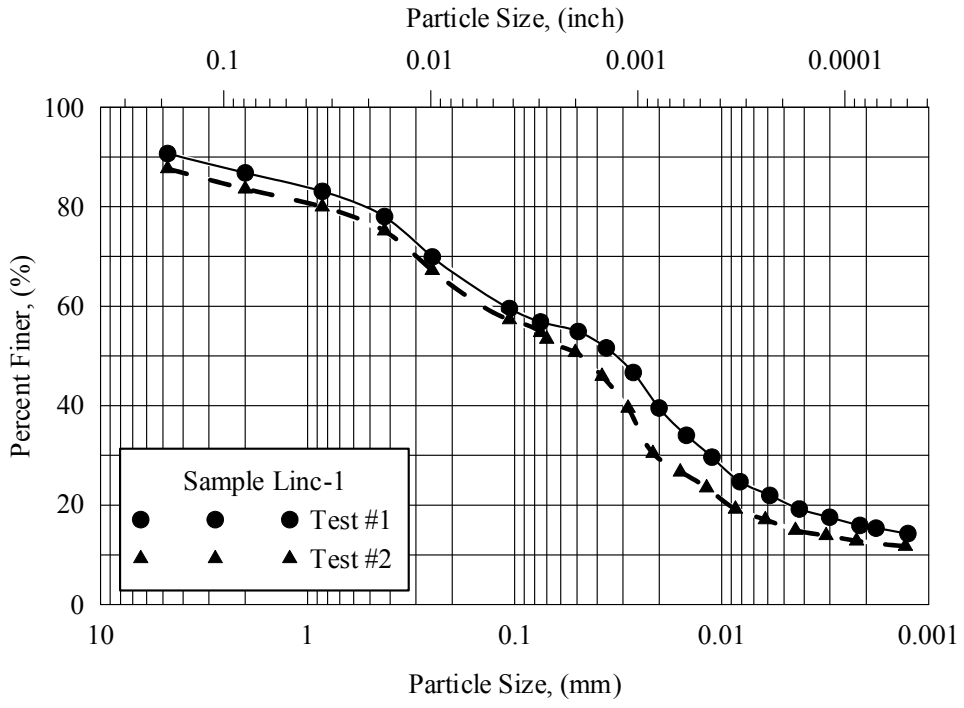


Figure 4.2: Grain size distribution curve for soil Lincoln-1

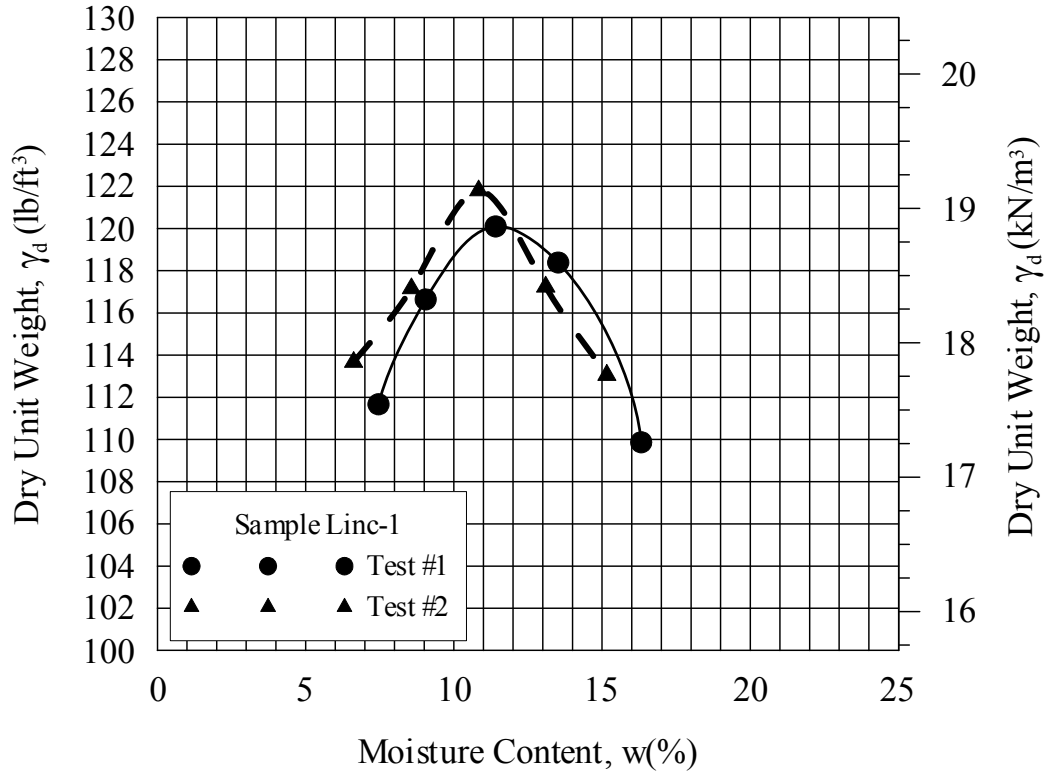


Figure 4.3: Moisture - unit weight relationship for soil Lincoln-1

**Table 4.3: Results for standard compaction tests on the investigated soils**

Sample ID	Test 1		Test 2		Average	
	$\gamma_{dmax}$ (kN/m <sup>3</sup> )	W <sub>opt</sub> (%)	$\gamma_{dmax}$ (kN/m <sup>3</sup> )	W <sub>opt</sub> (%)	$\gamma_{dmax}$ (kN/m <sup>3</sup> )	W <sub>opt</sub> (%)
Fond du Lac-1	16.3	20.5	15.7	22.0	16.0	21.0
Deer Creek-1A	16.9	16.0	16.8	17.0	16.8	18.0
Deer Creek-1B	17.3	16.0	16.9	17.0	17.1	17.6
Superior-1	14.8	24.5	14.8	24.5	14.8	24.8
Racine-1	17.3	16.6	17.6	15.3	17.4	17.0
Highland-1	16.5	17.0	16.9	14.5	16.8	16.0
Highland-2	17.3	15.0	17.4	14.0	17.3	15.0
Highland-3	15.6	22.0	15.4	24.0	15.4	22.5
Winnebago-2	14.9	23.0	14.8	26.0	14.8	24.8
Winnebago-3	16.0	22.0	15.7	23.0	15.8	21.8
Winnebago-4	15.7	21.0	NA	NA	15.7	21.0
Dodge-1	16.8	17	15.8	16.5	16.3	16.5
Lincoln-1	18.9	10.5	19.2	10.0	19.0	11.0
Antigo, B	17.5	14.5	17.5	14.5	17.5	14.5
Beecher, B	18.3	14.1	18.3	13.7	18.3	13.9
Shiocton, C	16.0	11.0	15.7	11.3	15.9	11.2
Dodgeville, B	15.9	19.6	16.2	18.0	16.1	18.8
Miami, B	16.5	18.4	16.7	17.8	16.6	18.1
Kewaunee-2, C	19.0	13.0	18.9	14.0	19.0	13.5
Dubuque, C	16.5	18.0	16.7	18.0	16.6	18.0
Mon-1	17.6	14.7	-	-	17.6	14.7
Craw-1	17.3	14.9	-	-	17.3	14.9
Buff-1	17.2	16.9	-	-	17.2	16.9

## 4.2 Resilient Modulus

Table 4.4 presents a typical summary of the repeated load triaxial test results. As an illustration, test results for Lincoln soil are discussed. As shown in Table 4.4, the repeated load triaxial test was conducted on soil specimens 1 and 2 compacted at  $0.93\gamma_{dmax}$  and moisture content  $w < w_{opt}$ . (dry of optimum side). Data presented in Table 4.4 consists of the mean resilient modulus values, standard deviation, and coefficient of variation for the 15 test sequences. Confining pressure and deviator stress at each test sequence are also given. The mean resilient modulus values, standard deviation and coefficient of variation are obtained from the last five load cycles of each test sequence. The coefficient of variation for the test results presented in Table 4.4 ranges between 0.06 and 0.52% for specimen #1 and from 0.04 to 0.39% for specimen #2. This indicates that each soil specimen showed consistent behavior during each test sequence.

Figure 4.4 shows the variation of the resilient modulus ( $M_r$ ) with deviator stress ( $\sigma_d$ ) at different confining pressures ( $\sigma_c$ ) for Lincoln soil. Inspection of Figure 4.4 indicates that the resilient modulus slightly decreases with the increase of the deviator stress under constant confining pressure. As an illustration, in Figure 4.4a for  $\sigma_c = 41.4$  kPa, the resilient modulus decreased from  $M_r = 117$  MPa at  $\sigma_d = 12.4$  kPa to  $M_r = 107$  MPa at  $\sigma_d = 61.8$  kPa for soil specimen #1. Moreover, the resilient modulus increases with the increase of confining pressure under constant deviator stress, which reflects a typical behavior.

Table 4.5 presents the results of the repeated load triaxial test which was conducted on soil specimens 1 and 2 compacted at  $0.95\gamma_{dmax}$  and moisture content  $w < w_{opt}$ . (dry of

optimum side). Figure 4.5 shows the variation of the resilient modulus of Lincoln soil (at  $0.95\gamma_{dmax}$  and at  $w < w_{opt}$ ) with deviator stress.

Table 4.6 presents the results of the repeated load triaxial test on Lincoln soil specimens compacted at maximum dry unit weight ( $\gamma_{dmax}$ ) and optimum moisture content ( $w_{opt}$ ).

Generally, the resilient modulus values of Table 4.6 are lower than the resilient modulus values of Table 4.5. Figure 4.6a shows the variation of the resilient modulus of Lincoln soil (at  $\gamma_{dmax}$  and at  $w_{opt}$ ) with deviator stress. For soil specimen #1, at confining pressure  $\sigma_c = 41.4$  kPa, the resilient modulus decreased from  $M_r = 94$  MPa at  $\sigma_d = 12.4$  kPa to  $M_r = 74$  MPa at  $\sigma_d = 61.5$  kPa. However, for Lincoln soil specimen #1 (at  $0.93\gamma_{dmax}$  at and  $w < w_{opt}$ ) for  $\sigma_c = 41.4$  kPa, the resilient modulus decreased from  $M_r = 117$  MPa at  $\sigma_d = 12.4$  kPa to  $M_r = 107$  MPa at  $\sigma_d = 61.8$  kPa for soil specimen #1, as shown in Figure 4.4a. Resilient modulus is influenced by moisture content and unit weight (density) of soil. In this case, with soil specimens at  $\gamma_{dmax}$  and at  $w_{opt}$  have greater unit weight and moisture content than specimens at  $0.93\gamma_{dmax}$  at and  $w < w_{opt}$ , the effect of moisture content on resilient modulus surpassed the influence of unit weight.

Table 4.7 presents the results of the repeated load triaxial test which was conducted on soil specimens 1 and 2 compacted at  $0.95\gamma_{dmax}$  and moisture content  $w > w_{opt}$ . (wet of optimum side). Figure 4.7 shows the variation of the resilient modulus of Lincoln soil (at  $0.95\gamma_{dmax}$  and at  $w > w_{opt}$ ) with deviator stress.

The results of the repeated load triaxial test on Lincoln soil specimens compacted at 93%  $\gamma_{dmax}$  and  $w > w_{opt}$  are summarized in Table 4.8. For soil specimen #1, at confining pressure  $\sigma_c = 41.4$  kPa, the resilient modulus decreased from  $M_r = 62$  MPa at  $\sigma_d = 12.3$  kPa to  $M_r = 45$  MPa at  $\sigma_d = 61.2$  kPa. Test results for Lincoln soil compacted at 93%

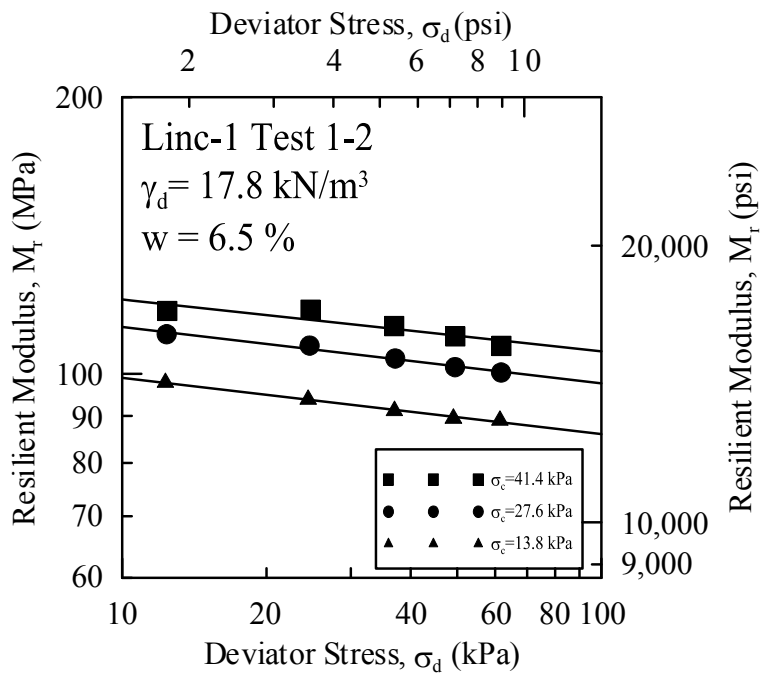
$\gamma_{dmax}$  and  $w > w_{opt}$  are depicted in Figure 4.8. Typical resilient modulus behavior in which  $M_r$  decreases with the increase in  $\sigma_d$  is observed. However, the rate of resilient modulus decrease is significant when compared with results depicted in Figures 4.6 and 4.8. It is clear that Lincoln soil specimens with higher moisture content and lower unit weight exhibited lower resilient modulus values when compared with other soil specimens that are compacted at lower moisture content under higher unit weight. The effect of increased moisture content of the soil on reducing the resilient modulus is significant. The results of repeated load triaxial test on the investigated soils are presented in Appendix B.

**Table 4.4: Results of repeated load triaxial test for soil Lincoln-1 compacted at 93% of  $\gamma_{dmax}$  and dry of  $w_{opt}$**

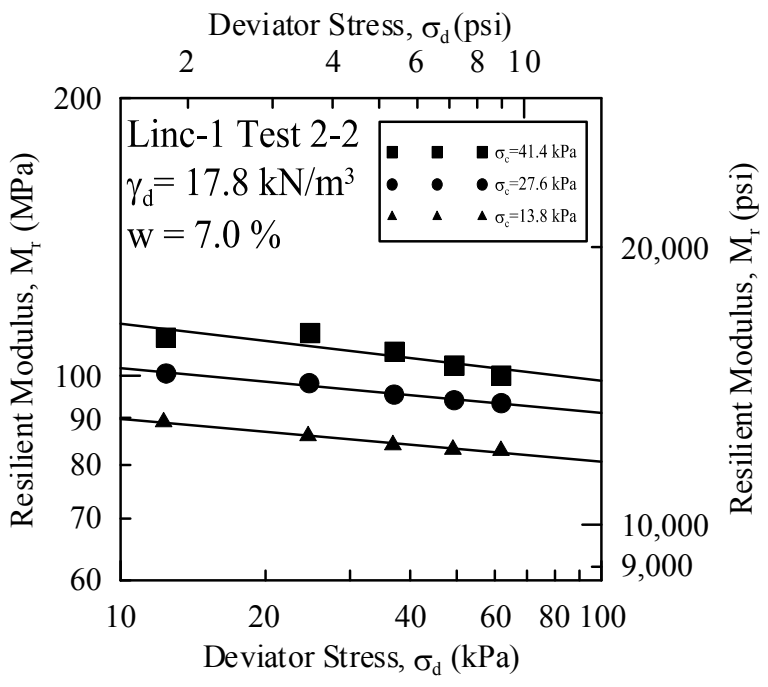
Test Sequence No.	Confining Stress $\sigma_c$ (kPa)	Deviator Stress $\sigma_d$ (kPa)	Linc-1 Set1 Dry2 93% $\gamma_{dmax}$ $M_r$ (MPa)			Deviator Stress $\sigma_d$ (kPa)	Linc-1 Set2 Dry2 93% $\gamma_{dmax}$ $M_r$ (MPa)		
			Mean	SD	CV (%)		Mean	SD	CV (%)
1	41.4	12.4	117	0.33	0.28	12.4	110	0.43	0.39
2	41.4	24.7	117	0.23	0.20	24.8	111	0.17	0.15
3	41.4	36.9	113	0.08	0.07	37.1	106	0.19	0.18
4	41.4	49.6	110	0.18	0.16	49.4	103	0.04	0.04
5	41.4	61.8	107	0.14	0.13	61.9	100	0.08	0.08
6	27.6	12.4	110	0.58	0.52	12.4	101	0.20	0.20
7	27.6	24.6	107	0.22	0.20	24.7	98	0.30	0.30
8	27.6	37.1	104	0.24	0.23	37.0	95	0.12	0.13
9	27.6	49.5	102	0.06	0.06	49.4	94	0.07	0.08
10	27.6	61.7	100	0.08	0.08	61.9	93	0.06	0.07
11	13.8	12.3	98	0.13	0.13	12.3	89	0.29	0.32
12	13.8	24.4	94	0.16	0.17	24.5	86	0.17	0.19
13	13.8	37.0	91	0.13	0.15	36.8	84	0.09	0.11
14	13.8	49.1	89	0.13	0.14	49.1	83	0.05	0.06
15	13.8	61.4	89	0.08	0.09	61.8	83	0.03	0.04

SD: Standard Deviation

CV: Coefficient of Variation



(a) Test on Linc1\_Set1\_2d



(b) Test on Linc1\_Set2\_2d

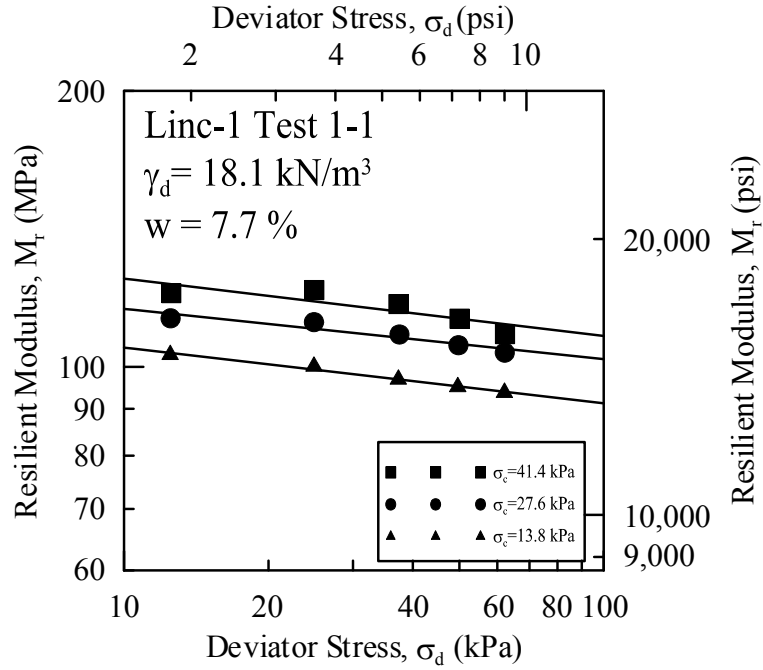
Figure 4.4: Results of repeated load triaxial test for soil Lincoln-1 target compaction values of  $\gamma_d = 17.8 \text{ kN/m}^3$  and  $w = 13.3 \%$

**Table 4.5: Results of repeated load triaxial test for soil Lincoln-1 compacted at 95% of  $\gamma_{dmax}$  and dry of  $w_{opt}$**

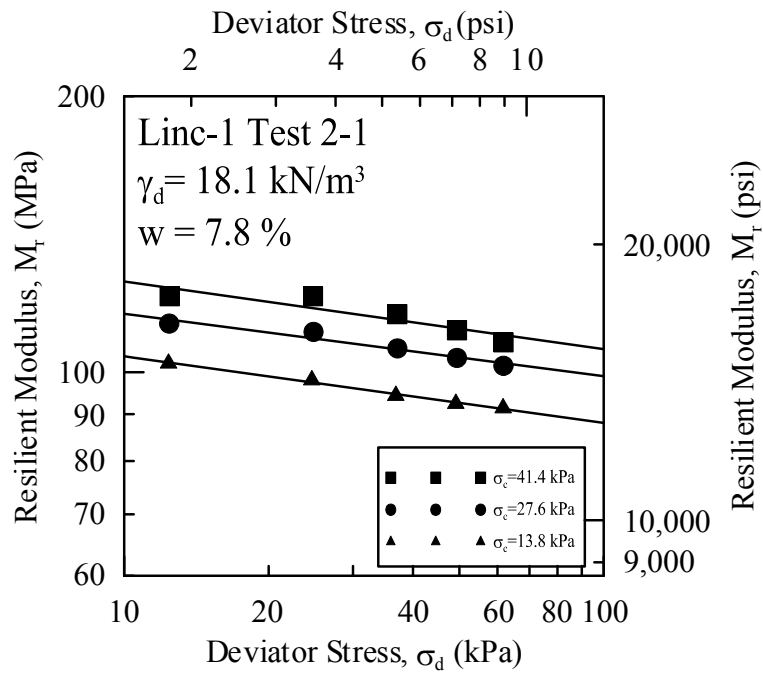
Test Sequence No.	Confining Stress $\sigma_c$ (kPa)	Deviator Stress $\sigma_d$ (kPa)	Linc-1 Set1 Dry1 95% $\gamma_{dmax}$ $M_r$ (MPa)			Deviator Stress $\sigma_d$ (kPa)	Linc-1 Set2 Dry1 95% $\gamma_{dmax}$ $M_r$ (MPa)		
			Mean	SD	CV (%)		Mean	SD	CV (%)
1	41.4	12.5	120	0.53	0.44	12.4	121	0.91	0.75
2	41.4	24.9	121	0.59	0.49	24.8	121	0.62	0.52
3	41.4	37.3	117	0.16	0.13	37.1	116	0.12	0.10
4	41.4	50.1	113	0.13	0.12	49.4	111	0.14	0.12
5	41.4	62.2	109	0.04	0.03	61.7	108	0.07	0.06
6	27.6	12.5	113	0.59	0.52	12.4	113	0.79	0.70
7	27.6	24.9	112	0.18	0.16	24.8	111	0.19	0.17
8	27.6	37.5	108	0.19	0.17	37.1	106	0.10	0.09
9	27.6	49.8	106	0.10	0.09	49.4	104	0.12	0.11
10	27.6	62.2	104	0.06	0.06	61.8	102	0.08	0.08
11	13.8	12.5	103	0.36	0.35	12.4	102	0.41	0.40
12	13.8	24.9	100	0.30	0.30	24.6	98	0.29	0.29
13	13.8	37.3	97	0.13	0.14	36.8	94	0.20	0.21
14	13.8	49.6	95	0.08	0.08	49.1	92	0.05	0.05
15	13.8	62.1	94	0.04	0.05	61.7	91	0.06	0.06

SD: Standard Deviation

CV: Coefficient of Variation



(a) Test on Linc1\_Set1\_1d



(b) Test on Linc1\_Set2\_1d

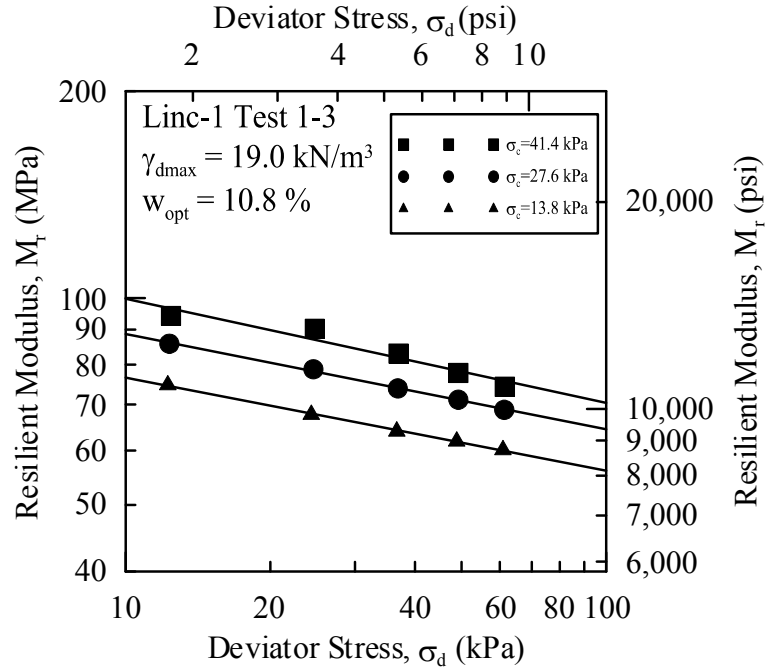
Figure 4.5: Results of repeated load triaxial test for soil Lincoln-1 target compaction values of  $\gamma_d = 18.1 \text{ kN/m}^3$  and  $w = 8.0 \%$

**Table 4.6: Results of repeated load triaxial test for soil Lincoln-1 compacted at  $\gamma_{dmax}$  and dry of  $w_{opt}$**

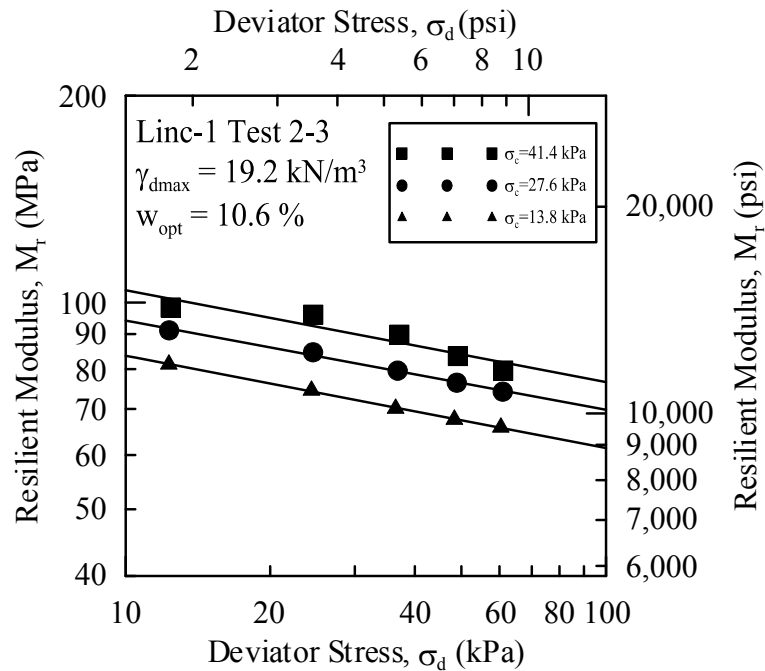
Test Sequence No.	Confining Stress $\sigma_c$ (kPa)	Deviator Stress $\sigma_d$ (kPa)	Linc-1 Set1 Opt3			Deviator Stress $\sigma_d$ (kPa)	Linc-1 Set2 Opt 3		
			$\gamma_{dmax}$ $M_r$ (MPa)				$\gamma_{dmax}$ $M_r$ (MPa)		
			Mean	SD	CV (%)		Mean	SD	CV (%)
1	41.4	12.4	94	0.49	0.52	12.4	98	0.28	0.29
2	41.4	24.7	90	0.16	0.18	24.6	96	0.19	0.19
3	41.4	37.0	83	0.06	0.07	37.1	90	0.13	0.15
4	41.4	49.2	78	0.08	0.10	49.1	84	0.07	0.09
5	41.4	61.5	74	0.03	0.03	61.1	80	0.05	0.06
6	27.6	12.3	86	0.28	0.33	12.3	91	0.14	0.16
7	27.6	24.6	79	0.21	0.26	24.5	85	0.14	0.16
8	27.6	36.8	74	0.04	0.06	36.8	80	0.09	0.11
9	27.6	49.2	71	0.05	0.07	48.9	76	0.10	0.13
10	27.6	61.3	69	0.01	0.02	61.0	74	0.01	0.02
11	13.8	12.2	75	0.26	0.35	12.3	81	0.48	0.59
12	13.8	24.3	68	0.06	0.09	24.4	74	0.16	0.22
13	13.8	36.6	64	0.04	0.05	36.5	70	0.06	0.09
14	13.8	48.8	62	0.04	0.06	48.3	68	0.07	0.10
15	13.8	60.9	60	0.02	0.03	60.4	66	0.07	0.11

SD: Standard Deviation

CV: Coefficient of Variation



(a) Test on Linc1\_Set1\_3o



(b) Test on Linc1\_Set2\_3o

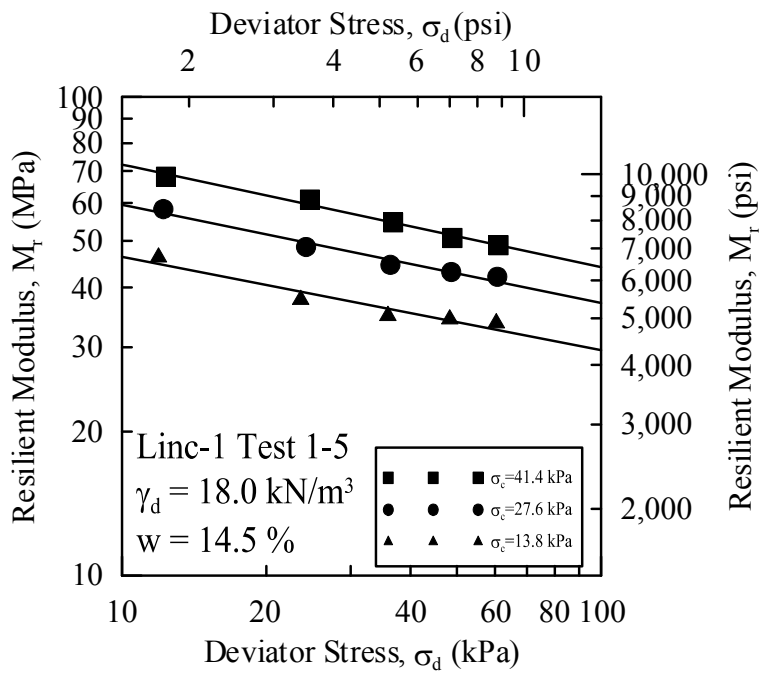
**Figure 4.6: Results of repeated load triaxial test for soil Lincoln-1 target compaction values of  $\gamma_{dmax} = 19.0 \text{ kN/m}^3$  and  $w_{opt} = 11.0 \%$**

**Table 4.7: Results of repeated load triaxial test for soil Lincoln-1 compacted at 95% of  $\gamma_{dmax}$  and wet of  $w_{opt}$**

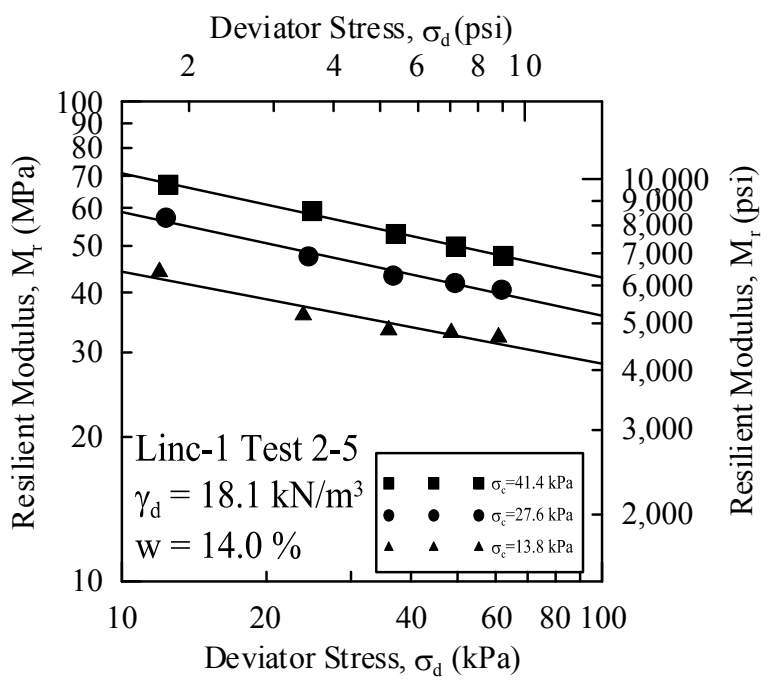
Test Sequence No.	Confining Stress $\sigma_c$ (kPa)	Deviator Stress $\sigma_d$ (kPa)	Linc-1 Set1 Wet5 95% $\gamma_{dmax}$ $M_r$ (MPa)			Deviator Stress $\sigma_d$ (kPa)	Linc-1 Set2 Wet5 95% $\gamma_{dmax}$ $M_r$ (MPa)		
			Mean	SD	CV (%)		Mean	SD	CV (%)
1	41.4	12.3	68	0.28	0.41	12.5	67	0.24	0.36
2	41.4	24.7	61	0.07	0.11	24.9	59	0.10	0.16
3	41.4	36.8	55	0.06	0.12	37.2	53	0.02	0.05
4	41.4	48.9	51	0.03	0.05	49.6	50	0.04	0.08
5	41.4	61.0	49	0.04	0.09	62.3	48	0.03	0.07
6	27.6	12.2	58	0.11	0.18	12.3	57	0.12	0.22
7	27.6	24.2	49	0.05	0.09	24.5	48	0.07	0.15
8	27.6	36.3	45	0.04	0.09	36.7	43	0.02	0.06
9	27.6	48.6	43	0.03	0.08	49.4	42	0.03	0.07
10	27.6	60.7	42	0.03	0.08	61.8	41	0.04	0.09
11	13.8	11.9	46	0.06	0.13	12.0	44	0.16	0.35
12	13.8	23.6	38	0.05	0.14	23.9	36	0.05	0.14
13	13.8	35.9	35	0.03	0.09	35.9	33	0.02	0.07
14	13.8	48.3	34	0.02	0.06	48.5	33	0.02	0.07
15	13.8	60.4	34	0.02	0.05	60.8	32	0.02	0.06

SD: Standard Deviation

CV: Coefficient of Variation



(a) Test on Linc1\_Set1\_5w



(b) Test on Linc1\_Set2\_5w

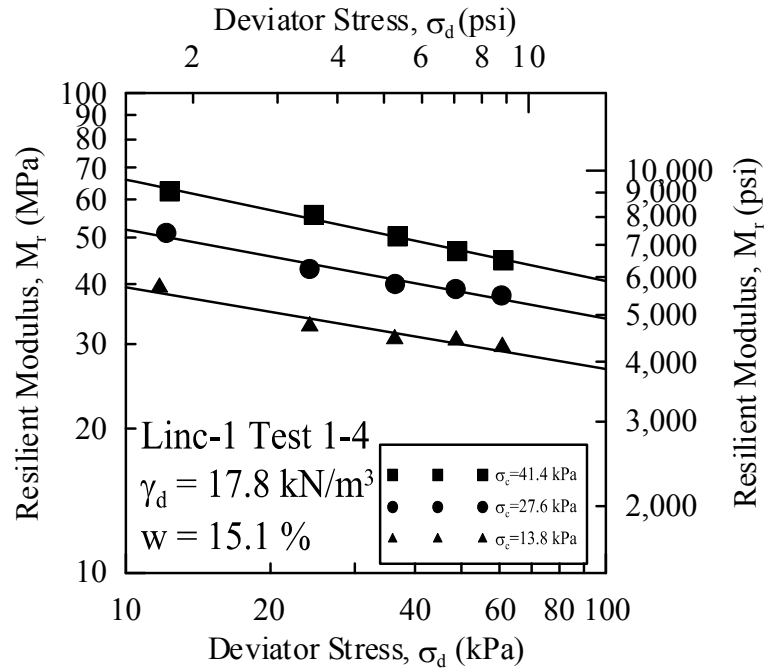
Figure 4.7: Results of repeated load triaxial test for soil Lincoln-1 target compaction values of  $\gamma_d = 18.1 \text{ kN/m}^3$  and  $w = 14.5 \%$

**Table 4.8: Results of repeated load triaxial test for soil Lincoln-1 compacted at 93% of  $\gamma_{dmax}$  and wet of  $w_{opt}$**

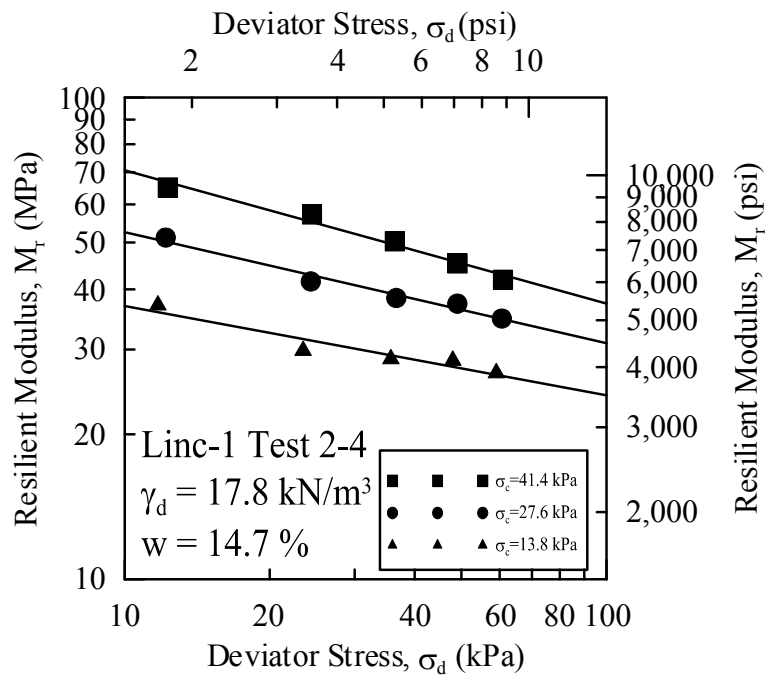
Test Sequence No.	Confining Stress $\sigma_c$ (kPa)	Deviator Stress $\sigma_d$ (kPa)	Linc-1 Set1 Wet4 93% $\gamma_{dmax}$ $M_r$ (MPa)			Deviator Stress $\sigma_d$ (kPa)	Linc-1 Set2 Wet4 93% $\gamma_{dmax}$ $M_r$ (MPa)		
			Mean	SD	CV (%)		Mean	SD	CV (%)
1	41.4	12.3	62	0.27	0.43	12.3	65	0.17	0.26
2	41.4	24.6	56	0.09	0.16	24.5	57	0.08	0.14
3	41.4	36.8	50	0.05	0.09	36.4	50	0.05	0.10
4	41.4	49.0	47	0.06	0.12	49.1	45	0.07	0.15
5	41.4	61.2	45	0.02	0.04	61.0	42	0.02	0.06
6	27.6	12.1	51	0.11	0.21	12.2	51	0.16	0.30
7	27.6	24.1	43	0.06	0.14	24.3	42	0.02	0.05
8	27.6	36.4	40	0.03	0.06	36.6	38	0.03	0.08
9	27.6	48.6	39	0.03	0.07	49.0	37	0.01	0.03
10	27.6	60.6	38	0.03	0.07	60.6	35	0.02	0.06
11	13.8	11.7	39	0.16	0.40	11.7	37	0.03	0.08
12	13.8	24.1	33	0.05	0.17	23.4	30	0.05	0.18
13	13.8	36.3	31	0.03	0.10	35.7	29	0.04	0.15
14	13.8	48.7	31	0.02	0.06	48.0	28	0.02	0.06
15	13.8	60.8	30	0.01	0.05	59.1	27	0.02	0.09

SD: Standard Deviation

CV: Coefficient of Variation



(a) Test on Linc1\_Set1\_4w



(b) Test on Linc1\_Set2\_4w

Figure 4.8: Results of repeated load triaxial test for soil Lincoln-1 target compaction values of  $\gamma_d = 17.8 \text{ kN/m}^3$  and  $w = 15.3 \%$

### 4.3 Statistical Analysis

Results obtained from laboratory testing program on the investigated Wisconsin fine-grained soils were used to develop correlations for predicting the resilient modulus model parameters using the resilient modulus constitutive equation selected by NCHRP Project 1-37A for the mechanistic-empirical pavement design. Repeated load triaxial tests were conducted, on average, ten times on each soil type at five different moisture content levels and three dry unit weight levels (i.e. 93%  $\gamma_{dmax}$ , 95%  $\gamma_{dmax}$  and  $\gamma_{dmax}$ ).

#### 4.3.1 Evaluation of the Resilient Modulus Model Parameters

The general resilient modulus model developed through NCHRP project 1-28A was selected for implementation in the AASHTO Guide for the Design of New and Rehabilitated Pavement Structures. The general resilient modulus model can be used for fine-grained soils and is given by :

$$M_r = k_1 P_a \left( \frac{\sigma_b}{P_a} \right)^{k_2} \left( \frac{\tau_{oct}}{P_a} + 1 \right)^{k_3} \quad (4.1)$$

where:

$M_r$  = resilient modulus

$P_a$  = atmospheric pressure (101.325 kPa)

$\sigma_b$  = bulk stress =  $\sigma_1 + \sigma_2 + \sigma_3$

$\sigma_1$  = major principal stress

$\sigma_2$  = intermediate principal stress =  $\sigma_3$  in axisymmetric condition (triaxial test)

$\sigma_3$  = minor principal stress or confining pressure in the repeated load triaxial test

$\tau_{oct}$  = octahedral shear stress

$k_1, k_2$  and  $k_3$  = material model parameters

The octahedral shear stress is defined in general as:

$$\tau_{oct} = \frac{1}{3} \sqrt{(\sigma_1 - \sigma_2)^2 + (\sigma_1 - \sigma_3)^2 + (\sigma_2 - \sigma_3)^2} \quad (4.2)$$

For axisymmetric stress condition (triaxial),  $\sigma_2 = \sigma_3$  and  $\sigma_1 - \sigma_3 = \sigma_d$  (deviator stress), therefore the octahedral shear stress is reduced to:

$$\tau_{oct} = \frac{\sqrt{2}}{3} (\sigma_d) \quad (4.3)$$

The resilient modulus, the bulk stress and the octahedral shear stress are normalized in this model by the atmospheric pressure. This will result in non-dimensional model parameters.

Statistical analysis based on multiple linear regressions was utilized to determine the resilient modulus model parameters  $k_1$ ,  $k_2$  and  $k_3$ . The statistical analysis software STATISTICA and MINITAB were used to perform the analysis. In order to determine  $k_1$ ,  $k_2$ , and  $k_3$  using the experimental test results, the resilient modulus model Equation 4.1 was transformed to:

$$\log\left(\frac{M_r}{P_a}\right) = \log k_1 + k_2 \log\left(\frac{\sigma_b}{P_a}\right) + k_3 \log\left(\frac{\tau_{oct}}{P_a} + 1\right) \quad (4.4)$$

The resilient modulus is treated as the dependent variable, while bulk and octahedral shear stresses are used as the independent variables. The analysis was conducted to evaluate the model parameters ( $k_1$ ,  $k_2$  and  $k_3$ ) from the results of the 15 load sequences applied during repeated load triaxial test. A total of 130 repeated load tests were used in the analysis. Results of this analysis are summarized in Table 4.9.

**Table 4.9: Statistical data for estimated model parameters  $k_i$  from repeated load triaxial test results**

Parameter	Mean	Minimum	Maximum	Standard Deviation
$k_1$	939.7	201.1	1423.4	245.9
$k_2$	0.258483	0.059646	0.813049	0.147933
$k_3$	-1.7616	-5.98415	-0.01284	1.528041

The analysis showed that  $k_1$  ranges from 201.1 to 1423.4 with a mean value of 939.7. The magnitude of  $k_1$  was always  $> 0$  since the resilient modulus should always be greater than zero. The parameter  $k_2$ , which is related to the bulk stress, varies between 0.059 and 0.813 with mean value of 0.258. The values of  $k_2$  were also greater than zero since the resilient modulus increases with the increase in the bulk stress (confinement). Since the resilient modulus decreases with the increase in the deviator stress, the parameter  $k_3$  ranges from -5.984 to -0.01284 with a mean value of -1.7616.

#### 4.3.2 Correlations of Model Parameters with Soil Properties

The resilient modulus model parameters  $k_1$ ,  $k_2$ , and  $k_3$  were determined for all soil types. These parameters are then correlated to fundamental soil properties using regression analysis. The values of resilient modulus model parameters ( $k_1$ ,  $k_2$ , and  $k_3$ ) were alternatively used as dependent variables while various fundamental soil properties were treated as independent variables. Various combinations of soil properties (independent variables) were used in the regression analysis.

Before proceeding with the regression analysis for the resilient modulus material model parameters ( $k_1$ ,  $k_2$ ,  $k_3$ ), it is important to confirm that the distribution of the parameters' values follow the requirement of linear regression. These requirements include a normal distribution. Figures 4.9 to 4.11 illustrate the effort conducted to assure normal distribution of the model parameters. Normal distribution is confirmed using the “normal probability plots.” These plots include the value of the parameter on the x-axis, and the accumulated percent probability of occurrence for a value on the y-axis. The result graph is a straight line in the case of normal distribution. In this section, the model parameters are examined and transformation is applied when needed to achieve normal distribution of the data. For the first model parameter  $k_1$ , the normal probability plot indicates a normal distribution. The other two parameters  $k_2$  and  $k_3$  clearly show deviation from the normal distribution.

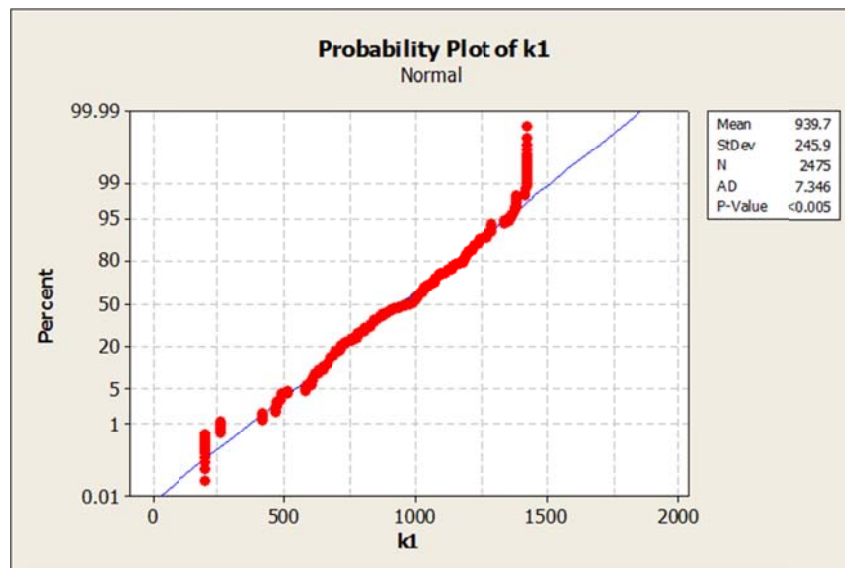


**Figure 4.9: Normal probability plot of  $k_1$**

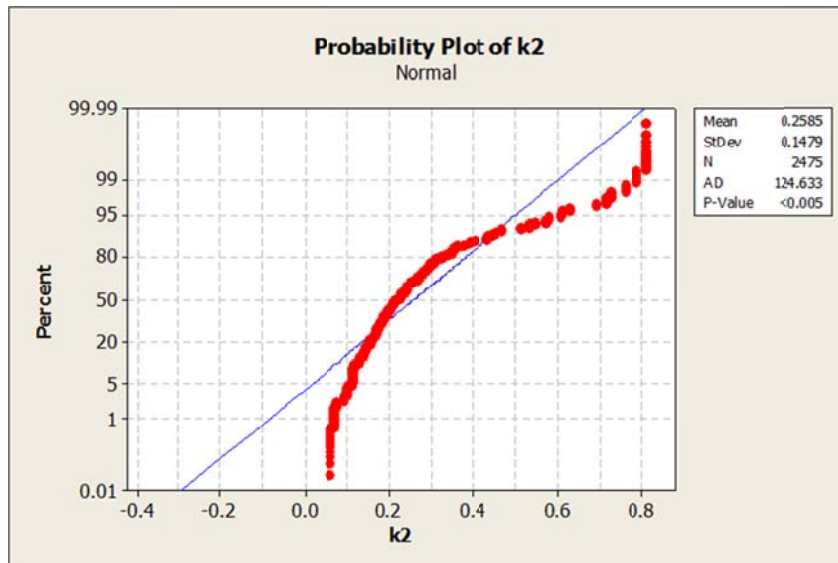


**Figure 4.10: Lack of normal distribution for  $k_2$**

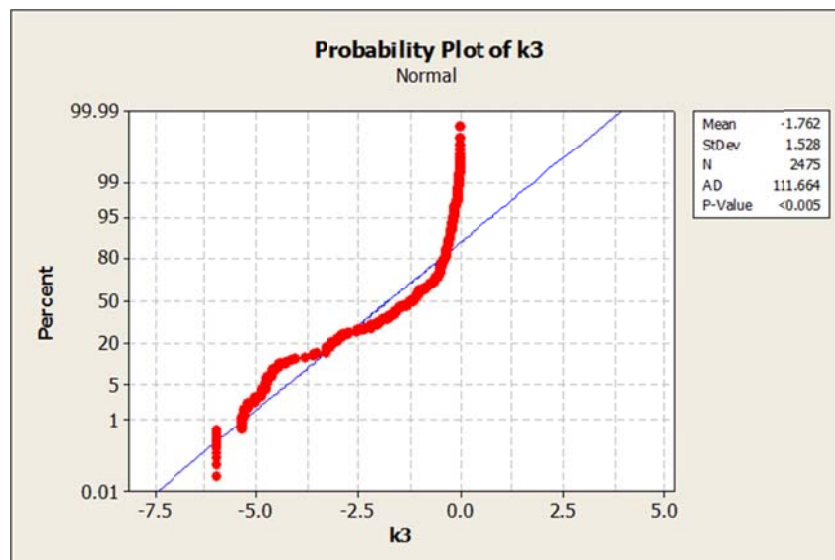
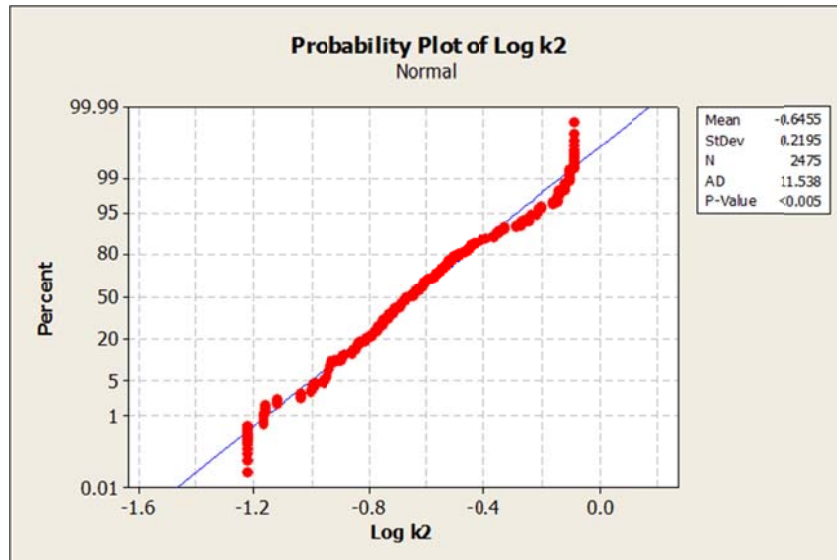


**Figure 4.11: Lack of normal distribution for  $k_3$**

Figures 4.10 and 4.11 show that parameters  $k_2$  and  $k_3$  are not normally distributed.

Therefore, it is necessary to apply transformation operations to normalize the data. The process also includes the identification of any outliers. For  $k_2$ , applying logarithmic operation achieved the desired effect. Figure 4.12 shows the normal probability plot for

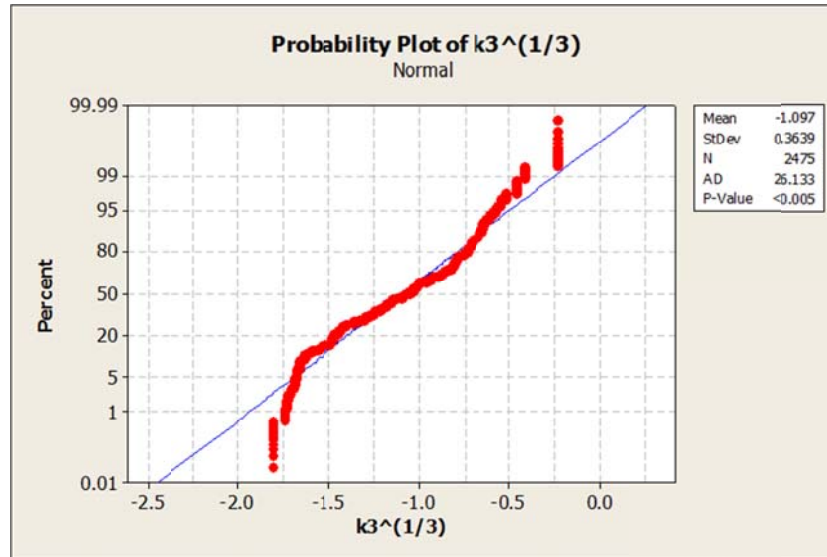
the transformed  $k_2$  values. It is important to note that the appropriate transformation operator is achieved using trial and error.



**Figure 4.12: Normal probability plot for transformed  $k_2$  values**

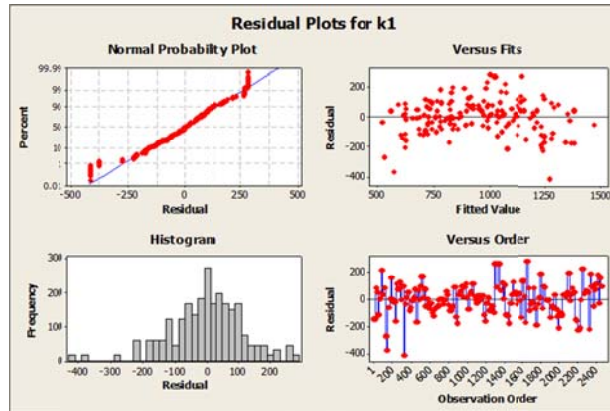
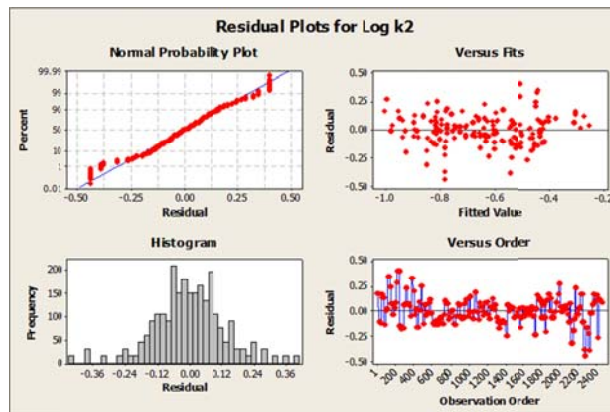
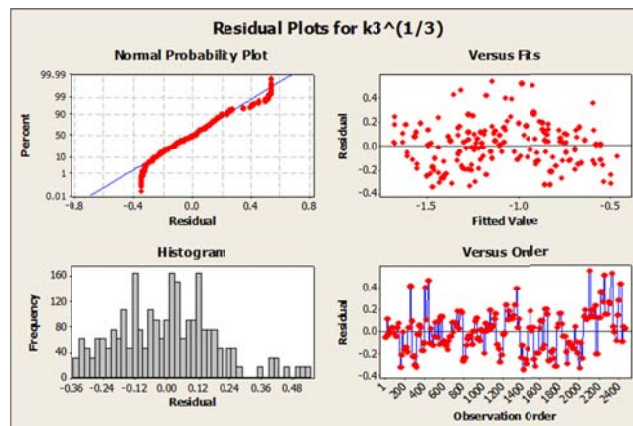
For  $k_3$  the situation was more complex. The most appropriate transformation was a power operator. In this case the  $k_3$  values are raised to a power of  $(1/3)$ . However, the normal probability plot still shows deviation from the normal distribution. Figure 4.13 shows that a group of data points deviate from the expected trend.

The data shown in Figure 4.13 indicate that the  $k_3$  values deviating from the linear trend are those of values greater than zero. This violates the resilient modulus model requirements. These data points were considered outliers.



**Figure 4.13: Normal probability plot for transformed  $k_3$  values**

Based on the data preparation discussed above, the model parameters used in the regression model are  $k_1$ ,  $\log(k_2)$ , and  $k_3^{(1/3)}$ . These parameters will be used in the regression analysis to find the soil characteristics that influence the numerical value of each model parameter. In addition, the residual plots for  $k_1$ ,  $\log(k_2)$ , and  $k_3^{(1/3)}$  shown in Figures 4.14 to 4.16 demonstrate that the data followed the normal probability distribution, and the model residuals are randomly distributed.

Figure 4.14: Residual plot for  $k_1$ Figure 4.15: Residual plot for  $\log k_2$ Figure 4.16: Residual plot for  $(k_3)^{1/3}$

The regression analysis is conducted using the statistical analysis software Minitab®. This software is used to find the best subset of soil properties that may correlate with the model parameters.

The general multiple linear regression model is expressed as:

$$k_i = \beta_0 + \beta_1 x_1 + \beta_2 x_2 + \dots + \beta_k x_k + \epsilon \quad (4.5)$$

where:

$k_i$  = the dependent variable for the regression, (model parameters  $k_1$ ,  $k_2$  or  $k_3$ )

$\beta_0$  = intercept of the regression plane

$\beta_i$  = regression coefficient

$x_i$  = the independent or regressor variable, (in this study, soil property or a combination of soil properties)

$\epsilon$  = random error

### ***Selection of Soil Properties***

The resilient modulus is used to evaluate the stiffness of bound/unbound materials.

Factors that affect resilient modulus are stress state, soil type and the environmental conditions of the soil that influence the soil physical state (unit weight and moisture content). Stress state is expressed in the resilient modulus model by including bulk and octahedral stresses. The soil type and the current soil physical condition should be included in attempted correlations in order to obtain valid estimation/prediction of the resilient modulus.

Sets of independent variables are specified to reflect soil type and current soil physical condition. Independent variables available from basic soil testing that represent soil type

and current soil physical condition are: percent passing sieve #4 ( $P_{No.4}$ ), percent passing sieve #40 ( $P_{No.40}$ ), percent passing sieve #200 ( $P_{No.200}$ ), liquid limit ( $LL$ ), plastic limit ( $PL$ ), Plasticity Index ( $PI$ ), Liquidity Index ( $LI$ ), amount of sand ( $\%Sand$ ), amount of silt ( $\%Silt$ ), amount of clay ( $\%Clay$ ), water content ( $w$ ) and dry unit weight ( $\gamma_d$ ). The optimum water content ( $w_{opt.}$ ) and maximum dry unit weight ( $\gamma_{dmax}$ ) and combinations of variables were also included.

The goal of the regression analysis is to identify the best subset of independent variables that results in accurate correlation between resilient modulus model parameters  $k_i$  and basic soil properties. Several combinations of regression equations were attempted and evaluated based on the criteria of the coefficient of multiple determination ( $R^2$ ), the significance of the model and the significance of the individual regression coefficients.

In this study, a correlation matrix was used as a preliminary method for selecting material properties used in the regression analysis models. The magnitude of each element in the correlation matrix indicates how strongly two variables (whether independent or dependent) are correlated. The degree of correlation is expressed by a number that has a maximum value of one for highly correlated variables, and zero if no correlation exists. This was used to evaluate the importance of each independent variable (soil property) among other independent variables to the dependent variable (model parameters  $k_i$ ).

### ***Measure of Model Adequacy***

The coefficient of multiple determination was used as a primary measure to select the best correlation. However, a high  $R^2$  does not necessarily imply that the regression model is a good one. Adding a variable to the model may increase  $R^2$  (at least slightly) whether the variable is statistically significant or not. This may result in poor predictions of new

observations. The significance of the model and individual regression coefficients were tested for each proposed model. In addition, the independent variables were checked for multicollinearity to insure the adequacy of the proposed models.

The model adequacy is also measured using the Mallows  $C_p$  values. Mallows's  $CP$  is used in General Regression Models (GRM) as the criterion for choosing the best subset of predictor effects when a best subset regression analysis is being performed. This measure of the quality of fit for a model tends to be less dependent (than the  $R^2$ ) on the number of effects in the model, and hence, it tends to find the best subset that includes only the important predictors of the respective dependent variable. As a general rule, the  $C_p$  value is preferred to be less than the number of variables in the model.

#### ***Test for Significance of the Model***

The significance of the model is tested using the  $F$ -test to insure a linear relationship between  $k_i$  and the estimated regression coefficients (independent variables).

For testing hypotheses on the model:

$$H_0: \beta_1 = \beta_2 = \dots = \beta_k = 0$$

$$H_a: \beta_i \neq 0 \text{ for at least one } i$$

where:  $H_0$  is the null hypothesis, and  $H_a$  is the alternative hypothesis.

The test statistic is:

$$F_0 = \frac{SS_R / p}{SS_E / (n - p - 1)} \quad (4.6)$$

where:  $SS_R$  is the sum of squares due to regression,  $SS_E$  is the sum of squares due to errors,  $n$  is the number of observations and  $p$  is the number of independent variables.

$H_0$  is rejected if  $F_0 > F_{\alpha, p, n-p-1}$

where:  $\alpha$  is the significance level (used as 0.05 for all purposes in this study).

### ***Test for Significance of Individual Regression Coefficients***

The hypotheses for testing the significance of individual regression coefficient  $\beta_i$  is based on the t-test and is given by:

$$H_0: \beta_i = 0$$

$$H_a: \beta_i \neq 0$$

The test statistic is:

$$t_0 = \frac{\hat{\beta}_i}{\sqrt{\hat{\sigma}^2 C_{ii}}} \quad (4.7)$$

where:  $C_{ii}$  is the diagonal element of  $(X'X)^{-1}$  corresponding to  $\hat{\beta}_i$  (estimator of  $\beta_i$ ) and  $\hat{\sigma}$  is estimator for the standard deviation of errors,  $X (n,p)$  is matrix of all levels of the independent variables,  $X'$  is the diagonal X matrix,  $n$  is the number of observations, and  $p$  is the number of independent variables.

$H_0$  is rejected if  $|t_0| > t_{\alpha/2, n-p-1}$

### **4.3.3 Statistical Analysis Results**

Regression analysis was conducted on the results of tests conducted on Wisconsin fine-grained soils. Different basic soil properties were included to obtain correlations with the resilient modulus model parameters  $k_1$ ,  $k_2$ , and  $k_3$ . Many attempts were made in which basic soil properties were included. Tables 4.10 to 4.12 present summaries of the regression analysis results in which models to estimate  $k_1$ ,  $k_2$ , and  $k_3$  from basic soil properties were obtained.

The tables show the number of variables incorporated in the models, the  $R^2$  Values and the adjusted  $R^2$ . The adjusted values represent a solid indicator of goodness of fit as they are adjusted to account for the number of variables in the model. The tables also include the  $C_p$  values, and the standard error (S). The variables included in the model all indicated by an “x” in the cells below them in the table.

**Table 4.10: Correlation of model parameter  $k_I$  to soil properties**

Response is  $k_I$

Vars	R-Sq	R-Sq(adj)	Mallows Cp	S	Y d m a x  ( k N w / m ( 3 % C C s % p L ) ) u c ) ) t L	w L w o I / p ( w t ( o / p L
1	65.4	65.4	1601.4	144.65		X
1	46.1	46.1	3874.0	180.56	X	
2	70.7	70.7	980.2	133.15	X	X
2	69.9	69.8	1079.2	135.05		X X
3	74.2	74.2	565.7	124.88	X	X X
3	73.6	73.5	646.7	126.54	X	X X
4	77.7	77.7	158.7	116.18	X	X X
4	76.9	76.8	259.0	118.38	X X	X X
5	79.0	78.9	15.2	112.93	X X	X X X
5	78.0	78.0	127.1	115.46	X X	X X X
6	79.0	79.0	9.4	112.78	X X	X X X X
6	79.0	78.9	14.9	112.91	X X X	X X X
7	79.1	79.0	7.8	112.72	X X X	X X X X
7	79.0	79.0	11.3	112.80	X X X	X X X X
8	79.1	79.0	9.0	112.72	X X X X	X X X X

Predictor	Coef	SE Coef	T	P
Constant	1373.57	35.23	38.99	0.000
$\gamma_{dmax}$ (kN/m <sup>3</sup> )	56.224	2.393	23.50	0.000
Cu	0.157012	0.007320	21.45	0.000
LI (%)	100.823	8.374	12.04	0.000
w/wopt	-953.86	13.61	-70.06	0.000
wopt/LL	-959.25	37.68	-25.46	0.000

S = 112.934    R-Sq = 79.0%    R-Sq(adj) = 78.9%

**Table 4.11: Correlation of model parameter  $k_2$  to soil properties**

Response is Log k2

Vars	R-Sq	R-Sq(adj)	Mallows Cp	S	Y d m a x  ( k N w / m ( 3 ) )	w L w o I / p w t ( o / % C C s % p L u c ) ) t L
1	31.8	31.7	2201.1	0.18136	X	
1	20.0	19.9	3008.8	0.19642		X
2	52.9	52.9	755.6	0.15070	X	X
2	42.3	42.3	1480.2	0.16678	X	X
3	57.5	57.4	444.8	0.14324	X	X X
3	56.8	56.7	494.3	0.14445	X	X X
4	61.1	61.0	201.5	0.13710	X	X X X
4	59.7	59.6	297.1	0.13953	X X	X X
5	62.4	62.3	113.3	0.13479	X	X X X X
5	62.2	62.1	123.9	0.13506	X X	X X X
<b>6</b>	<b>63.9</b>	<b>63.8</b>	<b>10.7</b>	<b>0.13205</b>	<b>X X</b>	<b>X X X X</b>
6	62.5	62.4	105.5	0.13456	X	X X X X X
7	64.0	63.9	8.6	0.13196	X X	X X X X X
7	63.9	63.8	11.4	0.13204	X X X	X X X X
8	64.0	63.9	9.0	0.13195	X X X	X X X X X

Predictor	Coef	SE Coef	T	P
Constant	1.2245	0.1234	9.92	0.000
γdmax (kN/m3)	-0.065086	0.006368	-10.22	0.000
w (%)	-0.053794	0.001932	-27.84	0.000
Cc	0.0093513	0.0008622	10.85	0.000
(Gs)	-0.43221	0.03159	-13.68	0.000
w/wopt	1.11648	0.03555	31.41	0.000
wopt/LL	0.48319	0.04505	10.73	0.000

S = 0.132047    R-Sq = 63.9%    R-Sq(adj) = 63.8%

**Table 4.12: Correlation of model parameter  $k_3$  to soil properties**Response is  $k_3^{(1/3)}$ 

Vars	R-Sq	R-Sq(adj)	Mallows Cp	S	Y d m a x  ( k N w / m ( 3 ) ) u c )	w L w o I / p ( w t G ( o / % C C s % p L ) t L
1	60.6	60.6	1426.5	0.22837		X
1	21.1	21.1	5342.0	0.32333	X	
2	71.0	70.9	406.8	0.19621		X X
2	65.1	65.1	981.5	0.21492	X	X
3	73.3	73.2	181.3	0.18832		X X X
3	72.3	72.3	273.2	0.19156	X	X X
4	74.1	74.0	103.6	0.18550	X	X X X
4	73.7	73.6	141.6	0.18687		X X X X
5	74.5	74.5	58.3	0.18383	X	X X X X
5	74.3	74.3	77.2	0.18451	X X	X X X
6	74.9	74.8	23.3	0.18251	X X	X X X X
6	74.7	74.7	41.4	0.18317	X X	X X X X
7	75.0	74.9	18.4	0.18229	X X X	X X X X
7	75.0	74.9	19.5	0.18233	X X X	X X X X
8	75.1	75.0	9.0	0.18191	X X X X	X X X X

Predictor	Coef	SE Coef	T	P
Constant	1.01699	0.03371	30.17	0.000
Cu	0.00010513	0.00001201	8.75	0.000
LI (%)	0.17388	0.01198	14.51	0.000
w/wopt	-1.37966	0.02086	-66.13	0.000
wopt/LL	-1.61745	0.05966	-27.11	0.000

S = 0.185505    R-Sq = 74.1%    R-Sq(adj) = 74.0%

Examining the above tables, the best models are highlighted in yellow. These models are selected based on the criteria mentioned above ( $R^2$ ,  $C_p$ , and Standard Error). The next step is to investigate the adequacy for each variable within the models. This is conducted the t-test for each variable, and the F-test for the overall model. The results of the analysis are shown also in Tables 4.10 to 4.12.

The output of the regression models show the results of the t-test and the F-test for the individual variable and the overall model efficiency. Figures 4.17 to 4.19 depict comparisons between  $k_i$  values obtained from analysis of the results of the repeated load triaxial test (considered herein as measured values) and  $k_i$  values estimated from basic soil properties using the proposed correlations (Tables 4.10 to 4.12).

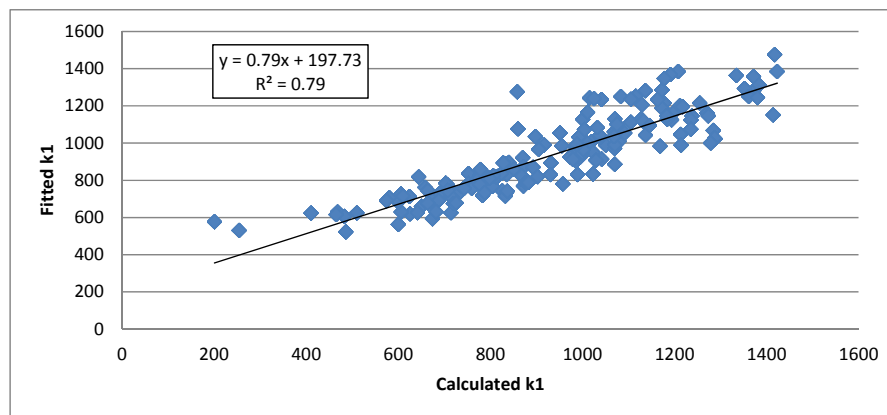


**Figure 4.17: Comparison of model parameter  $k_1$  for the values estimated from repeated load triaxial test results and  $k_1$  estimated from soil properties**

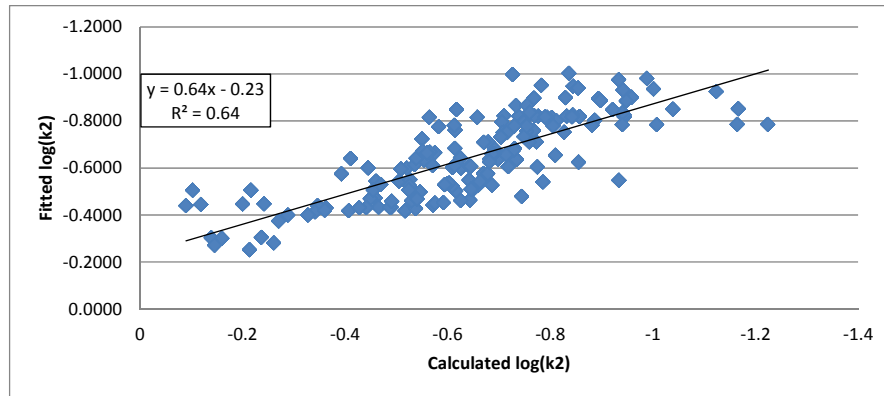


**Figure 4.18: Comparison of model parameter  $k_2$  for the values estimated from repeated load triaxial test results and  $k_2$  estimated from soil properties**

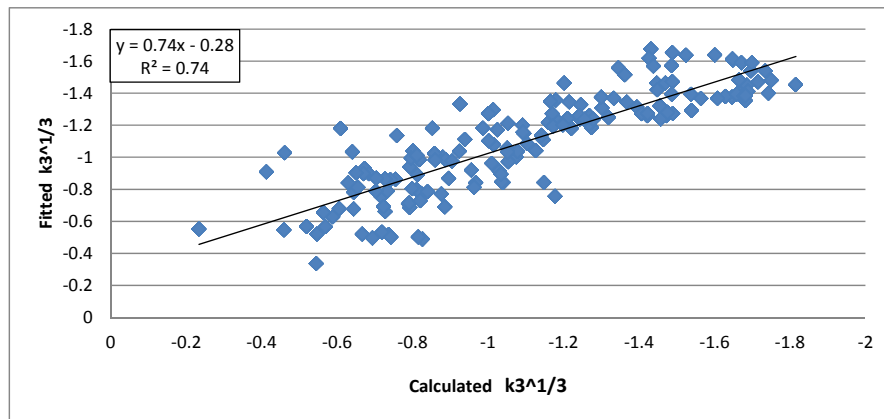


**Figure 4.19: Comparison of model parameter  $k_3$  for the values estimated from repeated load triaxial test results and  $k_3$  estimated from soil properties**

The magnitudes of  $R^2$  for  $k_1$  correlations range between 0.639 and 0.79, which is considered acceptable. Lower  $R^2$  values were obtained for  $k_2$  and  $k_3$ .

Based on the statistical analysis on the results of all investigated Wisconsin fine-grained soils, the resilient modulus model parameters ( $k_i$ ) can be estimated from basic soil properties using the following equations:

$$k_1 = 1374 + 56.2 \gamma_{dmax} + 0.157 C_u + 101 LI - 954 \frac{w}{w_{opt}} - 959 \frac{w_{opt}}{LL} \quad (4.8)$$

$$\begin{aligned} \text{Log } k_2 = & 1.22 - 0.0651 \gamma_{dmax} - 0.0538 w + 0.00935 C_c - 0.432 G_s + 1.12 \frac{w}{w_{opt}} + \\ & 0.483 \frac{w_{opt}}{LL} \end{aligned} \quad (4.9)$$

$$k_3^{\frac{1}{3}} = 1.02 + 0.000105 C_u + 0.174 LI - 1.38 \frac{w}{w_{opt}} - 1.62 \frac{w_{opt}}{LL} \quad (4.10)$$

where  $LL$  is the liquid limit,  $LI$  is the liquidity index,  $w$  is the moisture content of the soil,  $w_{opt}$  is the optimum moisture content,  $\gamma_{dmax}$  is the maximum dry unit weight,  $G_s$  is the specific gravity,  $C_u$  is the coefficient of uniformity, and  $C_c$  is the coefficient of curvature.

Equations 4.8 to 4.10 were used in the resilient modulus constitutive Equation (4.1) to estimate the resilient modulus of the investigated Wisconsin fine-grained soils. The results are presented in Figure 4.20, which depicts the predicted versus the measured resilient modulus values. Inspection of Figure 4.20 indicates that the resilient modulus of compacted fine-grained soils can be estimated from Equation 4.1 and the correlations proposed by Equations 4.8 to 4.10 with reasonable accuracy.

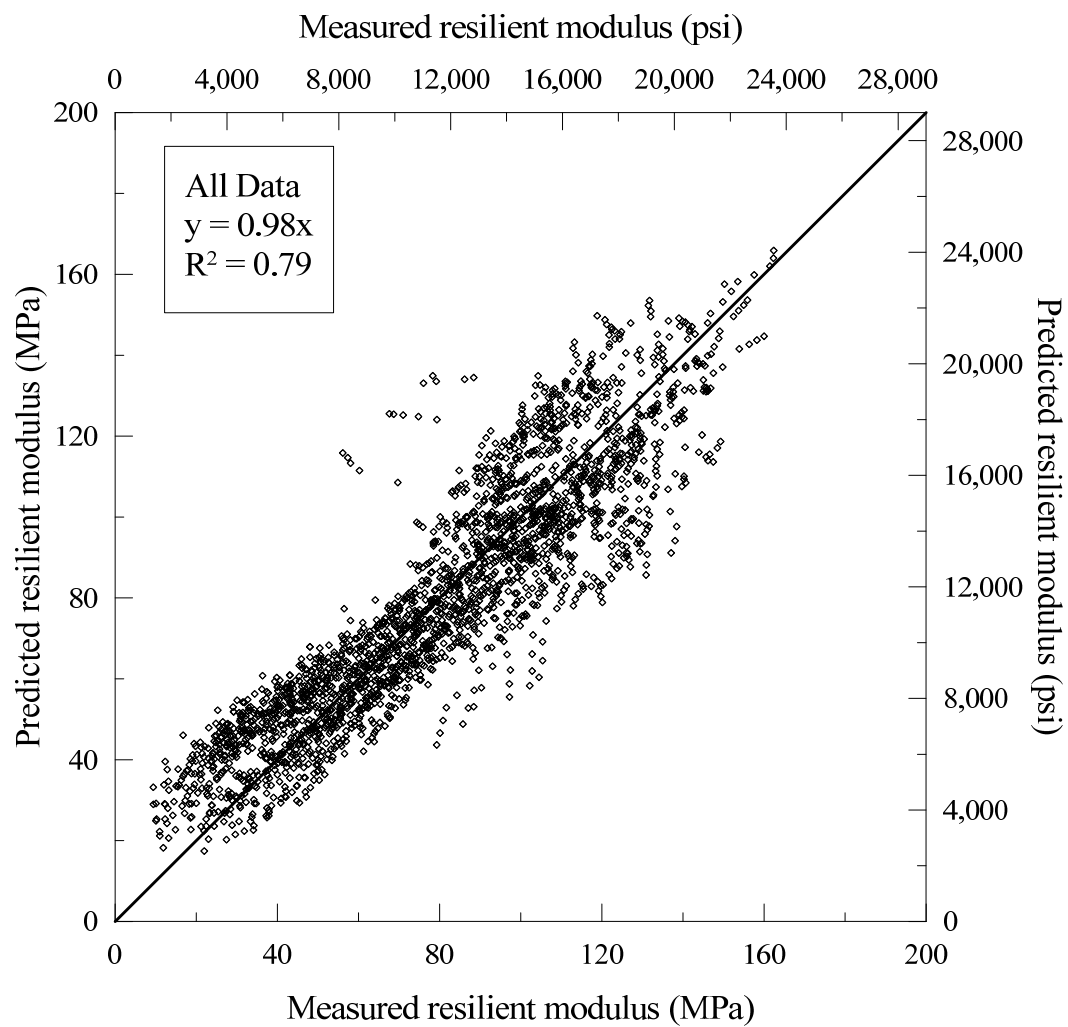


**Figure 4.20: Predicted versus measured resilient modulus of compacted fine-grained soils**

The ANOVA shows that soil classification has a significant influence on the observed values for the resilient modulus and the parameters  $k_i$ . However, the  $R^2$  values indicate that soil classification is not the sole factor influencing the measured resilient modulus values or their corresponding  $k_i$ . The ANOVA for  $k_2$  shows the most dependency on the soil classification.

Based on the statistical analysis on the results of investigated A-4 Wisconsin fine-grained soils, the resilient modulus model parameters ( $k_i$ ) can be estimated from basic soil properties using the following equations:

$$k_1 = 1556 + 0.844 C_u + 48.3 LI - 784 \frac{w}{w_{opt}} \quad (4.11)$$

$$\text{Log } k_2 = -0.389 + 0.00167 C_u - 0.00785 C_c + 0.321 LI \quad (4.12)$$

$$k_3^{\frac{1}{3}} = 8.58 - 0.662 \gamma_{dmax} + 0.00357 C_u + 0.370 C_c - 0.441 LI \quad (4.13)$$

Equations 4.11 to 4.13 were used in the resilient modulus constitutive Equation (4.1) to estimate the resilient modulus of the investigated Wisconsin fine-grained soils. The results are presented in Figure 4.21, which depicts the predicted versus the measured resilient modulus values.

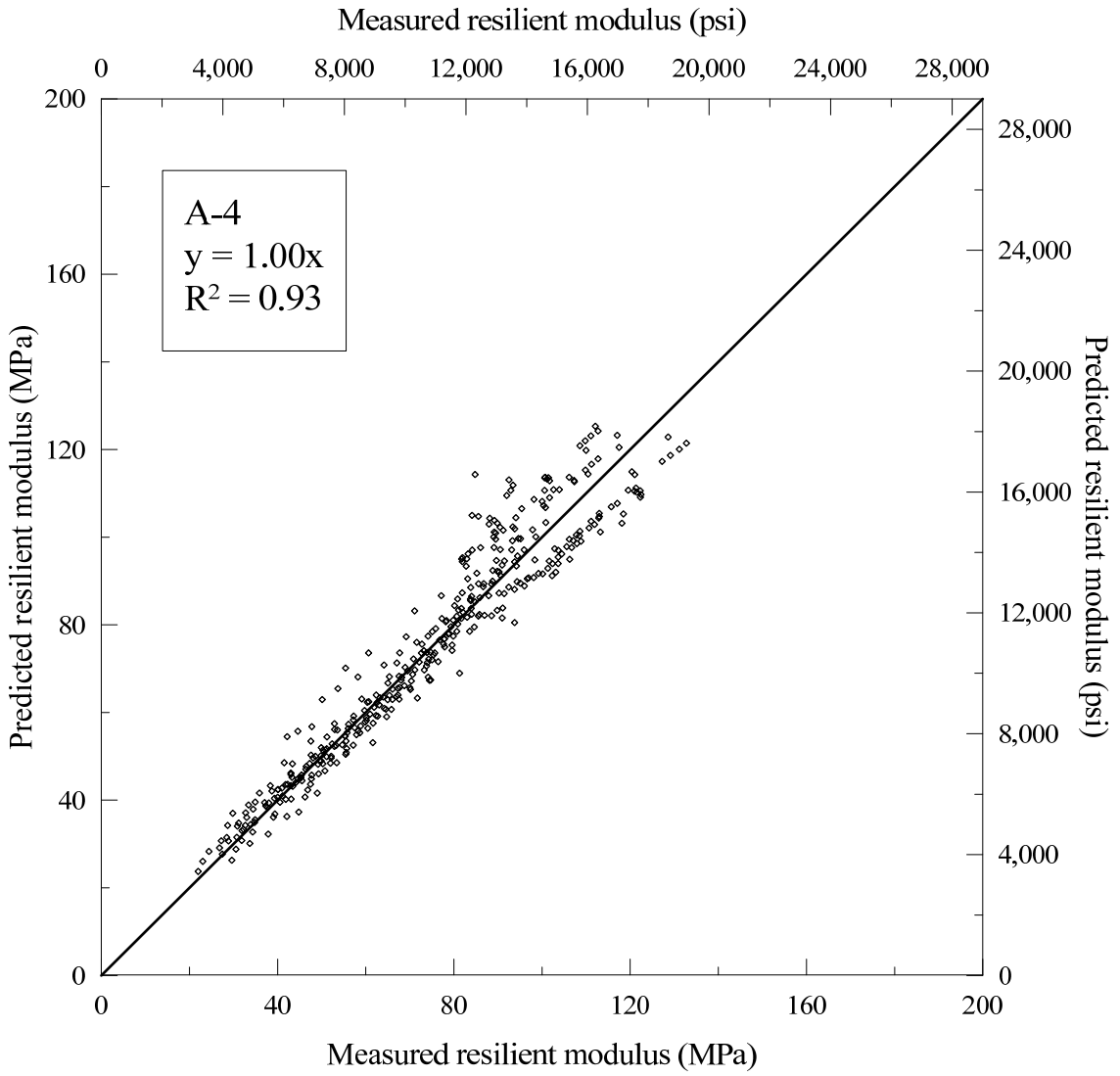


**Figure 4.21: Predicted versus measured resilient modulus of compacted A-4 fine-grained soils**

The results of statistical analysis for the investigated A-6 Wisconsin fine-grained soils were conducted and the resilient modulus model parameters ( $k_i$ ) can be estimated from basic soil properties using the following equations:

$$k_1 = 9593 - 58.2 \gamma_{dmax} + 0.204 C_u - 2173 G_s - 4311 \frac{w_{opt}}{LL} \quad (4.14)$$

$$\text{Log } k_2 = -7.05 - 0.175 \gamma_{dmax} - 0.000273 C_u + 2.87 G_s + 0.345 LI + 4.71 \frac{w_{opt}}{LL} \quad (4.15)$$

$$k_3^{\frac{1}{3}} = -1.48 + 0.0845 \gamma_{dmax} + 0.000167 C_u + 0.0159 C_c - 1.32 \frac{w}{w_{opt}} \quad (4.16)$$

Equations 4.14 to 4.16 were used in the resilient modulus constitutive Equation (4.1) to estimate the resilient modulus of the A-6 investigated Wisconsin fine-grained soils. The results are presented in Figure 4.22, which depicts the predicted versus the measured resilient modulus values.

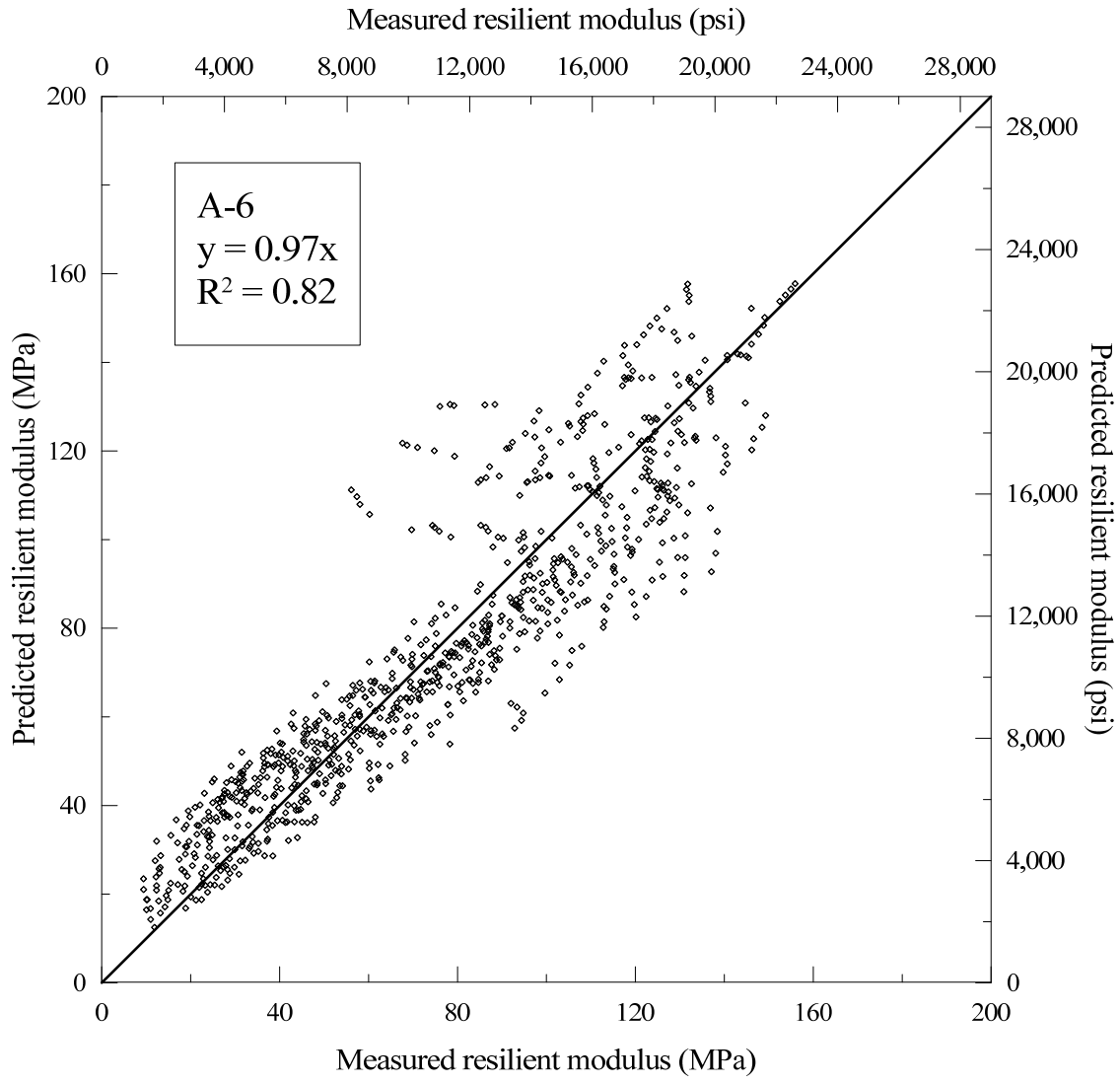


**Figure 4.22: Predicted versus measured resilient modulus of compacted A-6 fine-grained soils**

Analysis for soil A-7 was conducted for the main group and also for soil A-7-6. The number of data points was not enough to allow for analysis of soil A-7-5. Based on the statistical analysis on the results of investigated A-7 Wisconsin fine-grained soils, the resilient modulus model parameters ( $k_i$ ) can be estimated from basic soil properties using the following equations:

$$k_1 = 1492 + 28.4\gamma_{dmax} - 15.1 w - 482 \frac{w}{w_{opt}} + 0.239 C_u - 620 \frac{w_{opt}}{LL} \quad (4.17)$$

$$\text{Log } k_2 = -1.25 + 0.0716 \gamma_{dmax} - 0.185 \frac{w}{w_{opt}} + 0.000078 C_u - 0.196 G_s \quad (4.18)$$

$$k_3^{\frac{1}{3}} = -0.504 - 0.203\gamma_{dmax} - 0.0587 w + 2.01 G_s + 0.000594 C_u - 3.69 \frac{w_{opt}}{LL} \quad (4.19)$$

Equations 4.17 to 4.19 were used in the resilient modulus constitutive Equation (4.1) to estimate the resilient modulus of the A-7 investigated Wisconsin fine-grained soils. The results are presented in Figure 4.23, which depicts the predicted versus the measured resilient modulus values.

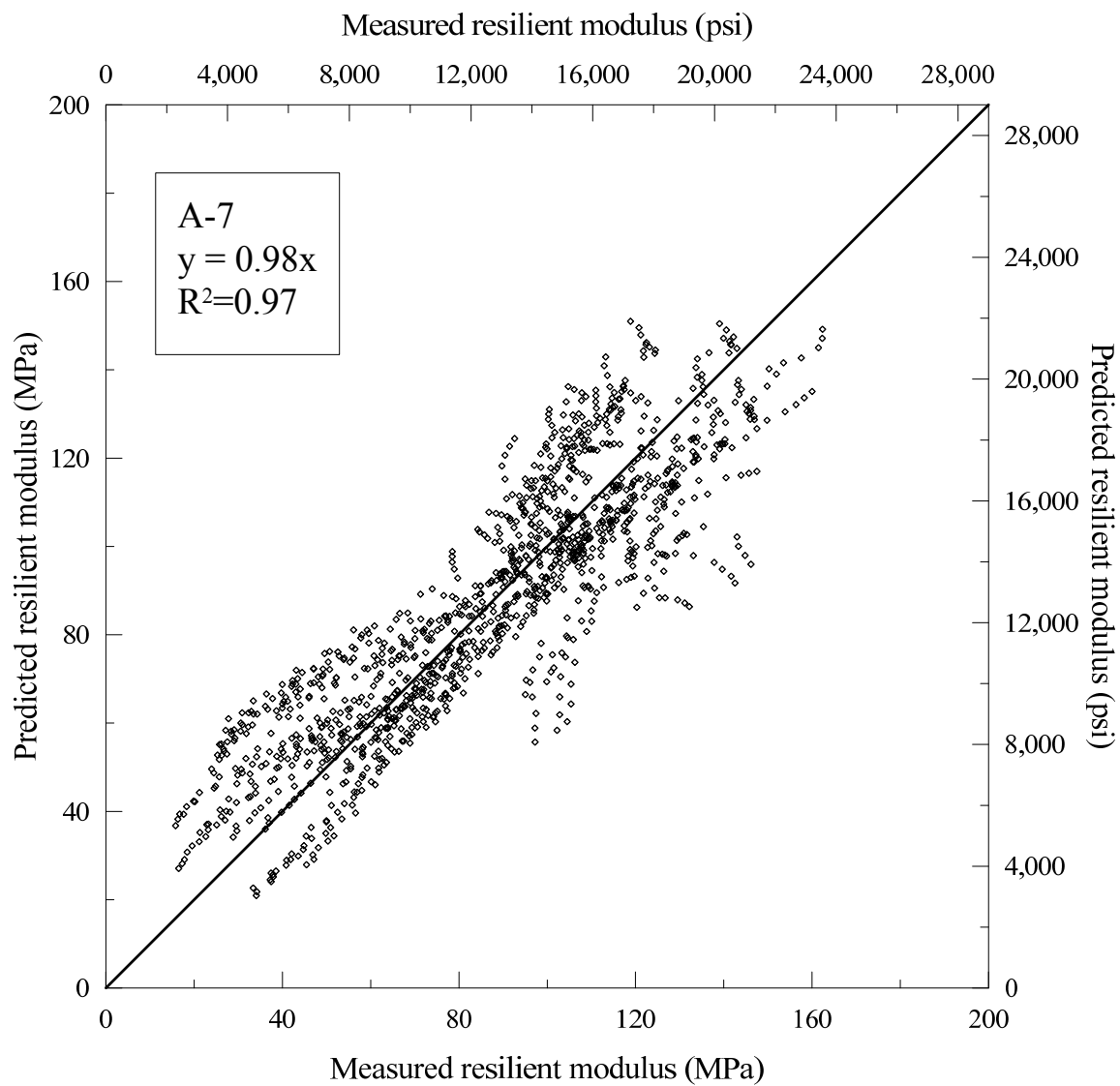


**Figure 4.23: Predicted versus measured resilient modulus of compacted A-7 fine-grained soils**

For A-7-6 soil, the resilient modulus model parameters ( $k_i$ ) can be estimated from basic soil properties using the following equations:

$$k_1 = 3965 - 4.55 \gamma_{dmax} - 360 w - 26.0 P_{40} + 0.203 C_u + 10.5 PI \quad (4.20)$$

$$\begin{aligned} \text{Log } k_2 = & 1.24 + 0.0762 \gamma_{dmax} - 0.0103 w - 0.0335 P_{40} + 0.000155 C_u + \\ & 0.00506 PI \end{aligned} \quad (4.21)$$

$$\begin{aligned} k_3^{1/3} = & -2.78 - 0.225 \gamma_{dmax} - 0.0588 w + 0.0640 P_{40} + 0.000357 C_u + 1.14 C_c + \\ & 0.017 PI \end{aligned} \quad (4.22)$$

Equations 4.20 to 4.22 were used in the resilient modulus constitutive Equation (4.1) to estimate the resilient modulus of the A-7-6 investigated Wisconsin fine-grained soils. The results are presented in Figure 4.24, which depicts the predicted versus the measured resilient modulus values.

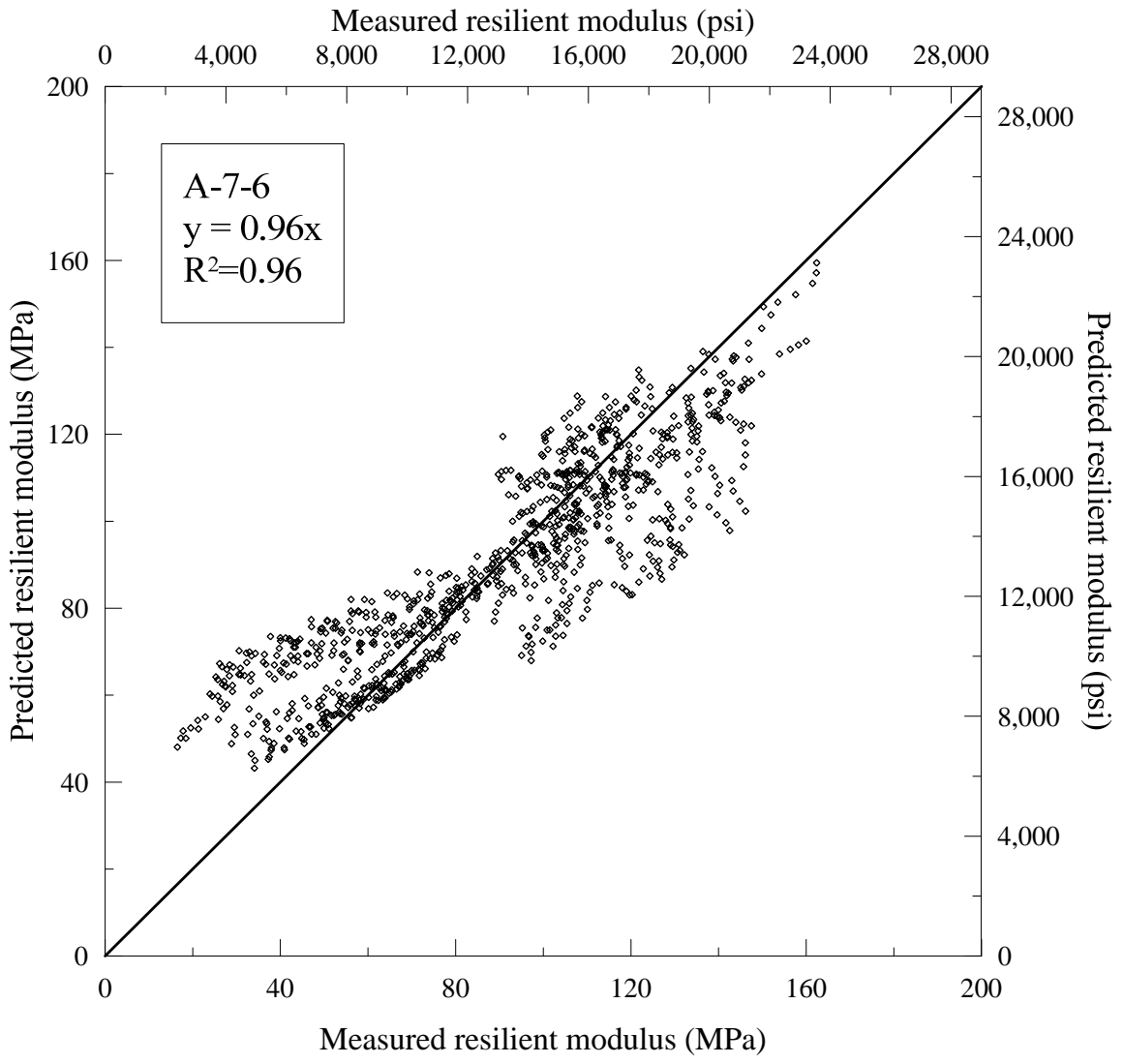


**Figure 4.24: Predicted versus measured resilient modulus of compacted A-7-6 fine-grained soils**

Further statistical analysis was conducted on the resilient modulus test results to establish input parameters for the ME pavement design utilizing level III. The analysis was conducted for all soils together and for each of the soil categories according to the AASHTO soil classification A-4, A-6, and A-7 (A-7-5 and A-7-6). The graphical representation of the data is presented in Appendix C. Tables 4.13 to 18 present the details of the analysis, which include the average resilient modulus for all soils as well as soil categories. The variation of the average resilient modulus is also given for three unit weight and moisture content combinations as well as three confining pressures. The resilient modulus values corresponding to the average minus one and two standard deviations ( $\mu-\sigma$  and  $\mu-2\sigma$ ) are calculated and presented in the tables. For the resilient modulus values of  $\mu-\sigma$ , 84.1% of the total area under the normal distribution curve is located to the right of  $\mu-\sigma$ . Selecting the resilient modulus from the  $\mu-\sigma$  values provides 84.1% probability that the selection is within with the measured values for the soil type. For the resilient modulus values of  $\mu-\sigma$ , 97.7% of the total area under the normal distribution curve is located to the right of  $\mu-2\sigma$ . Selecting the resilient modulus from the  $\mu-2\sigma$  values provides 97.7% probability that the selection is within the measured values for the soil type.

**Table 4.13: Results of the statistical analysis for the measured resilient modulus of all soils**

State of Compactness	Resilient Modulus, $M_r$ (psi)				
	Confining Pressure (psi)	Average All	6 psi	4 psi	2 psi
All	Mean, $\mu$	11,969	12,957	12,058	10,891
	Standard Deviation, $\sigma$	5,060	5,188	5,081	4,689
	Mean – Standard Deviation, $\mu - \sigma$	6,909	7,769	6,977	6,202
	Mean – 2 Standard Deviation, $\mu - 2 \sigma$	1,849	2,582	1,896	1,513
	Maximum	25,440	25,440	24,303	22,081
	Minimum	1,363	1,883	1,742	1,363
	Count	2683	895	895	893
Dry side of Optimum	Mean	16,422	17,596	16,615	15,054
	Standard Deviation	2,934	2,893	2,770	2,559
	Mean – Standard Deviation, $\mu - \sigma$	13,487	14,703	13,846	12,495
	Mean – 2 Standard Deviation, $\mu - 2 \sigma$	10,553	11,810	11,076	9,937
	Maximum	25,440	25,440	24,303	22,081
	Minimum	8,139	11,026	9,808	8,139
	Count	1035	345	345	345
Maximum Dry Unit Weight and Optimum Moisture Content	Mean	12,542	13,627	12,647	11,352
	Standard Deviation	3,209	3,124	3,123	2,975
	Mean – Standard Deviation, $\mu - \sigma$	9,333	10,502	9,524	8,377
	Mean – 2 Standard Deviation, $\mu - 2 \sigma$	6,125	7,378	6,400	5,401
	Maximum	21,392	21,392	20,674	19,172
	Minimum	5,699	7,182	6,566	5,699
	Count	255	85	85	85
Wet side of Optimum	Mean	7,007	7,749	6,986	6,281
	Standard Deviation	2,773	2,728	2,732	2,669
	Mean – Standard Deviation, $\mu - \sigma$	4,234	5,021	4,254	3,612
	Mean – 2 Standard Deviation, $\mu - 2 \sigma$	1,461	2,294	1,522	942
	Maximum	17,680	17,680	17,223	15,603
	Minimum	1,363	1,883	1,742	1,363
	Count	1003	335	335	333

**Table 4.14: Results of the statistical analysis for the measured resilient modulus of A-4 soils**

State of Compactness	Resilient Modulus, $M_r$ (psi)				
	Confining Pressure (psi)	Average All	6 psi	4 psi	2 psi
All	Mean, $\mu$	10,355	11,600	10,412	9,035
	Standard Deviation, $\sigma$	3,657	3,548	3,552	3,433
	Mean – Standard Deviation, $\mu - \sigma$	6,697	8,053	6,860	5,601
	Mean – 2 Standard Deviation, $\mu - 2 \sigma$	3,040	4,505	3,307	2,168
	Maximum	19,255	19,255	17,763	15,785
	Minimum	3,187	4,619	3,980	3,187
	Count	448	150	150	148
Dry side of Optimum	Mean	13,909	15,122	14,048	12,558
	Standard Deviation	2,130	2,106	1,877	1,559
	Mean – Standard Deviation, $\mu - \sigma$	11,779	13,016	12,170	10,999
	Mean – 2 Standard Deviation, $\mu - 2 \sigma$	9,650	10,910	10,293	9,440
	Maximum	19,255	19,255	17,763	15,785
	Minimum	9,584	11,298	10,702	9,584
	Count	180	60	60	60
Maximum Dry Unit Weight and Optimum Moisture Content	Mean	9,446	10,741	9,500	8,098
	Standard Deviation	1,985	1,754	1,642	1,633
	Mean – Standard Deviation, $\mu - \sigma$	7,461	8,987	7,858	6,466
	Mean – 2 Standard Deviation, $\mu - 2 \sigma$	5,476	7,234	6,215	4,833
	Maximum	14,265	14,265	13,211	11,791
	Minimum	5,699	7,182	6,566	5,699
	Count	120	40	40	40
Wet side of Optimum	Mean	6,769	8,062	6,779	5,411
	Standard Deviation	1,695	1,387	1,285	1,263
	Mean – Standard Deviation, $\mu - \sigma$	5,074	6,675	5,494	4,147
	Mean – 2 Standard Deviation, $\mu - 2 \sigma$	3,379	5,287	4,210	2,884
	Maximum	10,726	10,726	9,715	8,934
	Minimum	3,187	4,619	3,980	3,187
	Count	148	50	50	48

**Table 4.15: Results of the statistical analysis for the measured resilient modulus of A-6 soils**

State of Compactness	Resilient Modulus, $M_r$ (psi)				
	Confining Pressure (psi)	Average All	6 psi	4 psi	2 psi
All	Mean, $\mu$	11,805	12,990	11,874	10,551
	Standard Deviation, $\sigma$	5,865	5,993	5,896	5,456
	Mean – Standard Deviation, $\mu - \sigma$	5,939	6,998	5,978	5,095
	Mean – 2 Standard Deviation, $\mu - 2\sigma$	74	1,005	83	-361
	Maximum	25,440	25,440	24,303	22,081
	Minimum	1,363	1,883	1,742	1,363
	Count	960	320	320	320
Dry side of Optimum	Mean	17,719	19,121	17,935	16,100
	Standard Deviation	3,195	2,963	2,964	2,925
	Mean – Standard Deviation, $\mu - \sigma$	14,524	16,159	14,971	13,175
	Mean – 2 Standard Deviation, $\mu - 2\sigma$	11,330	13,196	12,007	10,250
	Maximum	25,440	25,440	24,303	22,081
	Minimum	8,139	11,026	9,808	8,139
	Count	345	115	115	115
Maximum Dry Unit Weight and Optimum Moisture Content	Mean	12,286	13,495	12,343	11,021
	Standard Deviation	2,704	2,620	2,556	2,367
	Mean – Standard Deviation, $\mu - \sigma$	9,582	10,875	9,788	8,654
	Mean – 2 Standard Deviation, $\mu - 2\sigma$	6,878	8,254	7,232	6,287
	Maximum	18,771	18,771	17,134	15,390
	Minimum	5,852	7,596	6,873	5,852
	Count	270	90	90	90
Wet side of Optimum	Mean	5,514	6,465	5,445	4,633
	Standard Deviation	2,245	2,297	2,108	1,946
	Mean – Standard Deviation, $\mu - \sigma$	3,269	4,168	3,337	2,687
	Mean – 2 Standard Deviation, $\mu - 2\sigma$	1,025	1,871	1,229	742
	Maximum	11,228	11,228	10,134	9,510
	Minimum	1,363	1,883	1,742	1,363
	Count	345	115	115	115

**Table 4.16: Results of the statistical analysis for the measured resilient modulus of A-7 soils**

State of Compactness	Resilient Modulus, $M_r$ (psi)				
	Confining Pressure (psi)	Average All	6 psi	4 psi	2 psi
All	Mean, $\mu$	12,661	13,410	12,777	11,794
	Standard Deviation, $\sigma$	4,679	4,944	4,727	4,204
	Mean – Standard Deviation, $\mu - \sigma$	7,981	8,466	8,050	7,590
	Mean – 2 Standard Deviation, $\mu - 2\sigma$	3,302	3,523	3,324	3,387
	Maximum	23,552	23,552	22,267	19,787
	Minimum	2,290	2,426	2,365	2,290
	Count	1275	425	425	425
Dry side of Optimum	Mean	17,719	19,121	17,935	16,100
	Standard Deviation	3,195	2,963	2,964	2,925
	Mean – Standard Deviation, $\mu - \sigma$	14,524	16,159	14,971	13,175
	Mean – 2 Standard Deviation, $\mu - 2\sigma$	11,330	13,196	12,007	10,250
	Maximum	25,440	25,440	24,303	22,081
	Minimum	8,139	11,026	9,808	8,139
	Count	345	115	115	115
Maximum Dry Unit Weight and Optimum Moisture Content	Mean	14,269	15,124	14,449	13,234
	Standard Deviation	2,987	3,148	2,929	2,576
	Mean – Standard Deviation, $\mu - \sigma$	11,282	11,976	11,521	10,658
	Mean – 2 Standard Deviation, $\mu - 2\sigma$	8,295	8,829	8,592	8,082
	Maximum	21,392	21,392	20,674	19,172
	Minimum	8,607	9,152	9,074	8,607
	Count	255	85	85	85
Wet side of Optimum	Mean	8,086	8,526	8,089	7,641
	Standard Deviation	2,865	2,971	2,902	2,660
	Mean – Standard Deviation, $\mu - \sigma$	5,221	5,555	5,188	4,982
	Mean – 2 Standard Deviation, $\mu - 2\sigma$	2,356	2,583	2,286	2,322
	Maximum	17,680	17,680	17,223	15,603
	Minimum	2,290	2,426	2,365	2,290
	Count	510	170	170	170

**Table 4.17: Results of the statistical analysis for the measured resilient modulus of A-7-5 soils**

State of Compactness	Resilient Modulus, $M_r$ (psi)				
	Confining Pressure (psi)	Average All	6 psi	4 psi	2 psi
All	Mean, $\mu$	11,290	11,981	11,374	10,626
	Standard Deviation, $\sigma$	4,086	4,194	4,141	3,775
	Mean – Standard Deviation, $\mu - \sigma$	7,204	7,787	7,233	6,851
	Mean – 2 Standard Deviation, $\mu - 2 \sigma$	3,117	3,593	3,092	3,075
	Maximum	18,234	18,234	17,424	15,936
	Minimum	2,290	2,880	2,365	2,290
	Count	300	100	100	100
Dry side of Optimum	Mean	14,827	15,609	14,993	13,877
	Standard Deviation	1,695	1,692	1,544	1,391
	Mean – Standard Deviation, $\mu - \sigma$	13,132	13,918	13,450	12,486
	Mean – 2 Standard Deviation, $\mu - 2 \sigma$	11,438	12,226	11,906	11,095
	Maximum	18,234	18,234	17,424	15,936
	Minimum	11,380	12,587	12,221	11,380
	Count	120	40	40	40
Maximum Dry Unit Weight and Optimum Moisture Content	Mean	12,331	12,876	12,463	11,655
	Standard Deviation	1,727	1,785	1,688	1,688
	Mean – Standard Deviation, $\mu - \sigma$	10,604	11,091	10,775	9,968
	Mean – 2 Standard Deviation, $\mu - 2 \sigma$	8,877	9,306	9,087	8,280
	Maximum	14,999	14,999	14,472	14,472
	Minimum	8,607	9,152	9,074	9,074
	Count	60	20	20	20
Wet side of Optimum	Mean	7,233	7,667	7,210	6,823
	Standard Deviation	2,803	3,021	2,817	2,557
	Mean – Standard Deviation, $\mu - \sigma$	4,431	4,645	4,393	4,267
	Mean – 2 Standard Deviation, $\mu - 2 \sigma$	1,628	1,624	1,575	1,710
	Maximum	13,136	13,136	11,930	10,901
	Minimum	2,290	2,426	2,365	2,290
	Count	120	40	40	40

**Table 4.18: Results of the statistical analysis for the measured resilient modulus of A-7-6 soils**

State of Compactness	Resilient Modulus, $M_r$ (psi)				
	Confining Pressure (psi)	Average All	6 psi	4 psi	2 psi
All	Mean, $\mu$	13,082	13,879	13,214	12,158
	Standard Deviation, $\sigma$	4,770	5,044	4,814	4,271
	Mean – Standard Deviation, $\mu - \sigma$	8,312	8,835	8,400	7,887
	Mean – 2 Standard Deviation, $\mu - 2 \sigma$	3,542	3,790	3,586	3,616
	Maximum	23,552	23,552	22,267	19,787
	Minimum	2,393	2,584	2,507	2,393
	Count	975	325	325	325
Dry side of Optimum	Mean	16,925	18,000	17,132	15,642
	Standard Deviation	2,334	2,314	2,158	1,883
	Mean – Standard Deviation, $\mu - \sigma$	14,591	15,685	14,974	13,759
	Mean – 2 Standard Deviation, $\mu - 2 \sigma$	12,257	13,371	12,816	11,876
	Maximum	23,552	23,552	22,267	19,787
	Minimum	12,823	14,658	13,952	12,823
	Count	390	130	130	130
Maximum Dry Unit Weight and Optimum Moisture Content	Mean	14,866	15,816	15,061	13,720
	Standard Deviation	3,042	3,161	2,967	2,641
	Mean – Standard Deviation, $\mu - \sigma$	11,823	12,655	12,094	11,079
	Mean – 2 Standard Deviation, $\mu - 2 \sigma$	8,781	9,493	9,128	8,439
	Maximum	21,392	21,392	20,674	19,172
	Minimum	8,828	9,335	9,265	8,828
	Count	195	65	65	65
Wet side of Optimum	Mean	8,348	8,791	8,360	7,893
	Standard Deviation	2,836	2,917	2,884	2,650
	Mean – Standard Deviation, $\mu - \sigma$	5,512	5,874	5,476	5,243
	Mean – 2 Standard Deviation, $\mu - 2 \sigma$	2,676	2,957	2,592	2,594
	Maximum	17,680	17,680	17,223	15,603
	Minimum	2,393	2,584	2,507	2,393
	Count	390	130	130	130

## Chapter 5

### Conclusions and Recommendations

This research presented the results of a comprehensive study conducted to evaluate the resilient modulus of common Wisconsin fine grained soils. The primary objective of this research project was to develop a methodology for estimating the resilient modulus of Wisconsin fine-grained soils from basic soil properties. This was achieved by carrying out laboratory-testing program on Wisconsin fine-grained soils. The program included tests to evaluate basic soil properties and repeated load triaxial tests to determine the resilient modulus. High quality test results were obtained in this study by insuring the repeatability of results and also by performing two tests on each soil replicate specimens at the specified physical condition.

The resilient modulus model given by Equation 4.1 is the constitutive equation developed by NCHRP project 1-28A and adopted by the NCHRP project 1-37A for the “Guide for Mechanistic-Empirical Design of New and Rehabilitated Pavement Structures.” This study focused on developing correlations between basic soil properties and the parameters  $k_1$ ,  $k_2$ , and  $k_3$  (Equation 4.1).

The laboratory-testing program provided the research team with high quality database that was utilized to develop and validate correlations between resilient modulus model parameters and basic soil properties. Comprehensive statistical analysis including multiple linear regression was performed to develop these correlations. Statistical analysis conducted on all test results produced good correlations between model parameters and basic soil properties.

Based on the results of this research, the following conclusions are reached:

1. The repeated load triaxial test (which is specified by AASHTO to determine the resilient modulus of subgrade soils for pavement design) is complicated, time consuming, expensive, and requires advanced machine and skilled operators.
2. The results of the repeated load triaxial test on the investigated Wisconsin fine grained soils provide resilient modulus database that can be utilized to estimate values for mechanistic-empirical pavement design in the absence of basic soils testing (level III input parameters). Tables 4.13 to 4.18 can be used to provide resilient modulus input for Level III. The average values minus one standard deviation ( $\mu - \sigma$ ) on the wet category and confining pressure of 4 psi can be used as a representative value for the specific soil type.
3. The equations that correlate resilient modulus model parameters ( $k_1$ ,  $k_2$ , and  $k_3$ ) to basic soil properties for fine grained soils can be utilized to estimate level II resilient modulus input for the mechanistic-empirical pavement design. These equations are:
  - a. Equations 4.8 to 4.10 for all soil types
  - b. Equations 4.11 to 4.13 for A-4 soil
  - c. Equations 4.14 to 4.16 for A-6 soil
  - d. Equations 4.17 to 4.19 for A-7 soil
  - e. Equations 4.20 to 4.22 for A-7-6 soil
4. The equations (models) developed in this research were based on statistical analysis of laboratory test results that were limited to the soil physical conditions

specified. Estimation of resilient modulus of subgrade soils beyond these conditions was not validated.

Based on the results of this research, the following recommendations are reached:

1. The use of the resilient modulus test database (Tables 4.13 to 4.18) in the absence of any basic soil testing when designing low volume roads as indicated by AASHTO.
2. The use of the equations provided in Chapter 4 (Equations 4.8 to 4.22) to estimate the resilient modulus of subgrade soils from basic soil properties. These equations can be used based on available basic soil test results.
3. Further research is needed to explore newly developed field devices such as light drop weight (LWD). This can provide Wisconsin DOT and contractors with field tools to assure quality of compacted subgrade soils in terms of stiffness.
4. Further research is needed to explore the effect of freeze-thaw cycles on the resilient modulus of Wisconsin subgrade soils. This is essential since the resilient modulus is highly influenced by the seasonal variations in moisture and extreme temperatures.

## References

Achampong, Francis, Mumtaz Usmen, and Takaaki Kagawa. "Evaluation of Resilient Modulus for Lime- and Cement-Stabilized Synthetic Cohesive Soils." *Transportation Research Record 1589.*, pp. 70-75. Print.

AASHTO 2002 Guide for Mechanistic-Empirical Design of New and Rehabilitated Pavement Structures. NCHRP Project 1-37A Final Report by ERES Consultants, March 2004.

Barksdale, R.D., Rix, G. J., Itani, S., Khosla, P.N., Kim, R., Lambe, D., and Rahman, M.S., (1990). "Laboratory Determination of Resilient Modulus for Flexible Pavement Design," NCHRP, Transportation Research Board, Interim Report No. 1-28, Georgia Institute of Technology, Georgia.

Carmichael, R.F., III and E. Stuart, "Predicting Resilient Modulus: A Study to Determine the Mechanical Properties of Subgrade Soils," *Transportation Research Record 1043*, Transportation Research Board, National Research Council, Washington, D.C., 1985, pp. 145-148

Elias, M.B., and Titi, H.H., (2006). "Evaluation of Resilient Modulus Model Parameters for Mechanistic Empirical Pavement Design," *Journal of the Transportation Research Board, No. 1967*, Geology and Properties of Earth Materials 2006, Transportation Research Board, Washington, D.C., pp.89-100.

Hall, Kevin D., and Marshall R. Thompson. "Soil-Property-Based Subgrade Resilient Modulus Estimation for Flexible Pavement Design." *Transportation Research Record 1449.*, pp. 30-38.

Jin, Myung S., and William D. Kovacs. (July/August 1994) "Seasonal Variation of Resilient Modulus of Subgrade Soils." *Journal of Transportation Engineering 120.4* pp. 603-617.

Khoury, C., and N. Khoury. (2009) "The Effect of Moisture Hysteresis on Resilient Modulus of Subgrade Soils." *Bearing Capacity of Roads, Railways and Airfields.*, pp. 71-78.

Lekarp, Fredrick, Ulf Isacsson, and Andrew Dawson. (Jan/Feb 2000) "State of The Art. I: Resilient Response of Unbound Aggregates." *Journal of Transportation Engineering.*, pp. 66-75.

Lekarp, Fredrick, Ulf Isacsson, and Andrew Dawson. (Jan/Feb 2000) "State of the Art. II: Permanent Strain Response of Unbound Aggregates." *Journal of Transportation Engineering.*, pp. 76-83.

- Li, Dingqing, and Ernest T. Selig. (June 1994) "Resilient Modulus for Fine-Grained Subgrade Soils." *Journal of Geotechnical Engineering* 120.6 pp. 939-57.
- Malla R.B. and Joshi, S. (Sept. 2007) "Resilient Modulus Prediction Models Based on Analysis of LTPP Data for Subgrade Soils and Experimental Verification." *Journal of Transportation Engineering*, ASCE. pp. 491-504.
- May, R. W., and M. W. Witczak. (1981) "Effective Granular Modulus to Model Pavement Responses." *Transportation Research Record No. 810*, Transportation Research Board, pp. 1-9.
- Moghaddas-Nejad, Fereidoon. (2003) "Resilient and Permanent Characteristics of Reinforced Granular Materials by Repeated Load Triaxial Tests." *Geotechnical Testing Journal* 26.2, pp. 1-15.
- Montgomery, Douglas C., and George C. Runger. Applied Statistics and Probability for Engineers. 4th ed. John Wiley & Sons, 2007.
- NCHRP Project 1-37A Summary of the 2000, 2001, and 2002 AASHTO Guide for The Design of New and Rehabilitated Pavement Structures, NCHRP, Washington D.C.
- NCHRP Synthesis 382, Estimating Stiffness of Subgrade and Unbound Materials for Pavement Design. Transportation Research Board, 2008.
- Pezo, Rafael, and W. Ronald Hudson. (Sept 1994) "Prediction Models of Resilient Modulus for Nongranular Materials." *Geotechnical Testing Journal* 17.3 pp. 349-55.
- Santha, B. L. (1994) "Resilient Modulus of Subgrade Soils: Comparison of Two Constitutive Equations." *Transportation Research Record* 1462, Transportation Research Board, National Research Council, Washington, D.C., pp. 79-90.
- Seed, H., C. Chan, and C. Lee. (1962) "Resilient Modulus of Subgrade Soils and Their Relation to Fatigue Failures in Asphalt Pavements." *Proceedings, International Conference on the Structural Design of Asphalt Pavements*, University of Michigan, Ann Arbor, Michigan., pp. 611-36.
- Seed, H.B., F.G. Mitry, C.L. Monismith, and C.K. Chan, *NCHRP Report 35: Prediction of Flexible Pavement Deflections from Laboratory Repeated-Load Tests*, Highway Research Board, National Research council, Washington, D.C., 1967.
- Ooi, Philip S. K., Archilla A. R, and Sandefur K.G. (2004). "Resilient Modulus Models for Compacted Cohesive Soils," *Transportation Research Record No. 1874*, Transportation Research Board, National Research Council, Washington, D.C., 2004, pp.115-124.

Titi, H., B Elias, and S. Helwany, *Determination of Typical Resilient Modulus Values for Selected Soils in Wisconsin*, SPR 0092-03-11, Wisconsin Department of Transportation, University of Wisconsin, Milwaukee, May 2006

Uzan, J. (1985) "Characterization of Granular Material." *Transportation Research Record No. 1022*, pp. 52-59.

Witczak, M. W., and J. Uzan. The Universal Airport Pavement Design System. Report 1 of 4, Granular Material Characterization, University of Maryland, College Park, 1988.

Yand, Shu-Rong, Wei-Hsing Huang, and Chi-Chou Liao. (2008) "Correlation Between Resilient Modulus and Plastic Deformation for Cohesive Subgrade Soil Under Repeated Loading." *Journal of the Transportation Research Board 2053rd ser.* pp. 72-79.

Yau, A., and Von Quintus (2004). "Predicting Elastic Response Characteristics of Unbound Materials and Soils," *Transportation Research Record No. 1874*, Transportation Research Board, National Research Council, Washington, D.C., pp.47-56.

## Appendix A

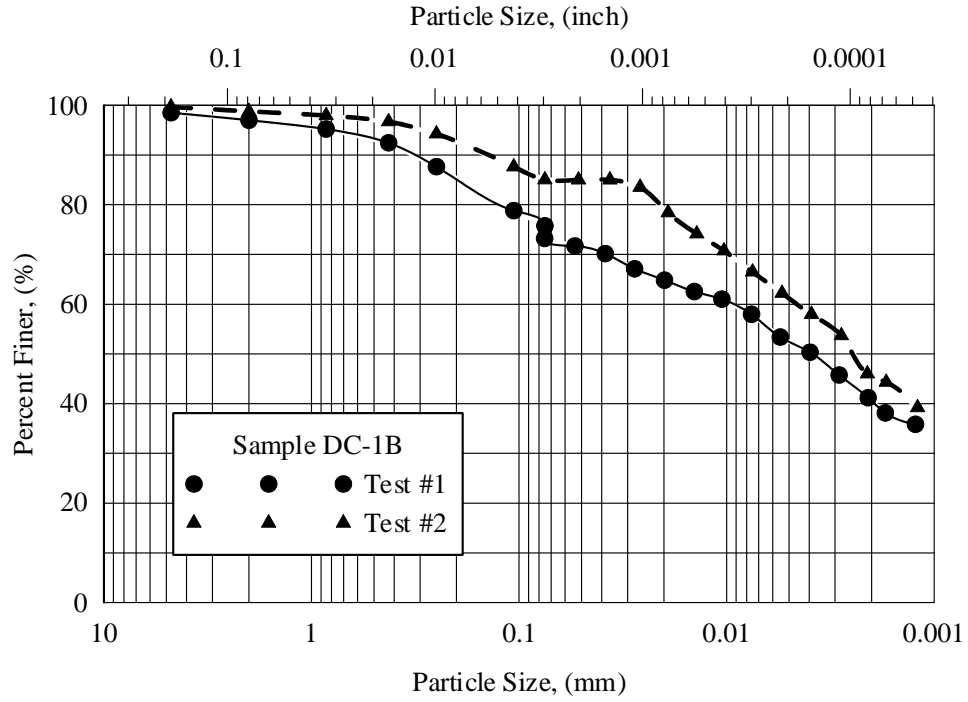


Figure A.1: Grain size distribution curve for soil Deer Creek-1B

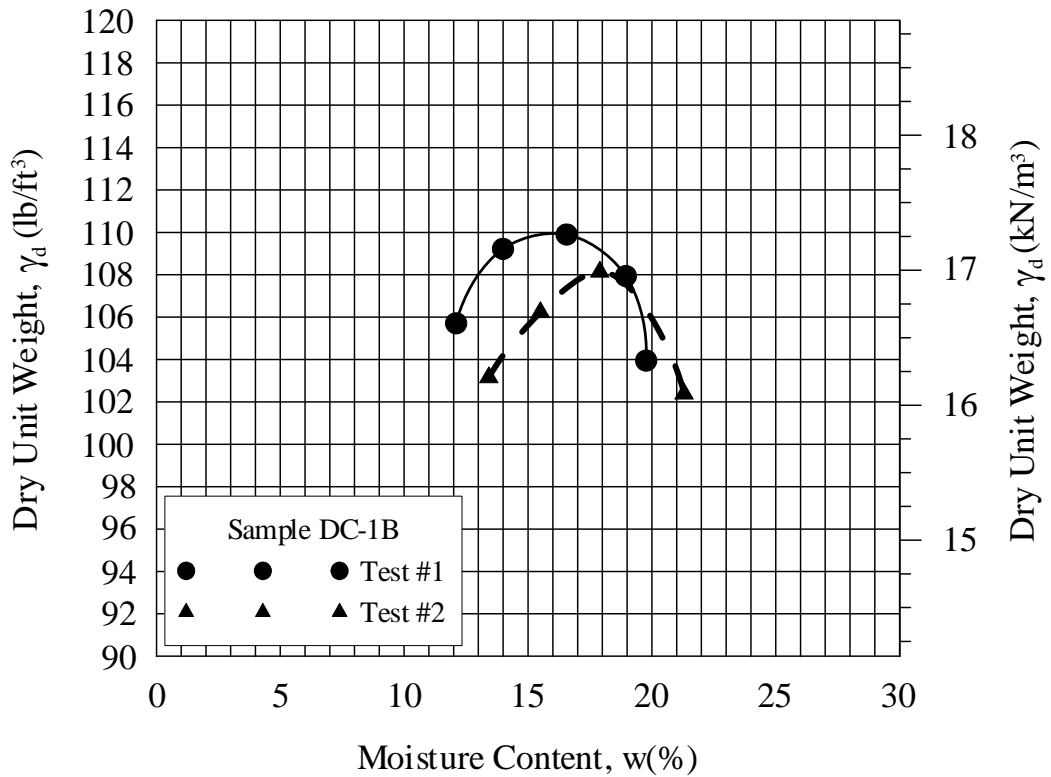


Figure A.2: Moisture - unit weight relationship for soil Deer Creek-1B

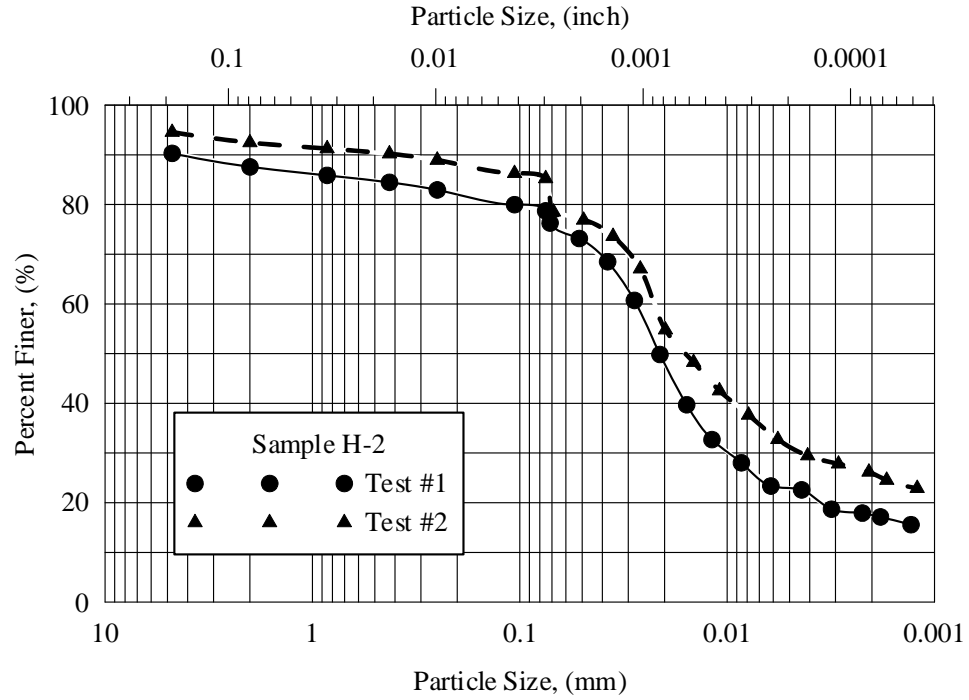


Figure A.3: Grain size distribution curve for soil Highland-2

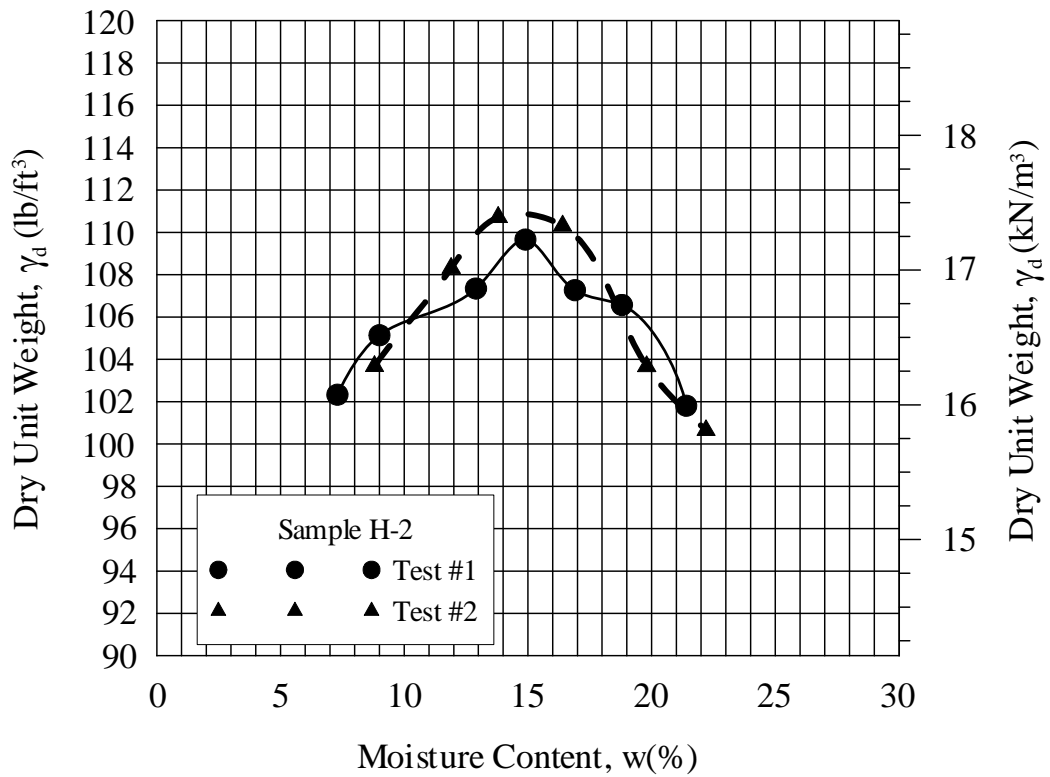


Figure A.4: Moisture – unit weight relationship for soil Highland-2

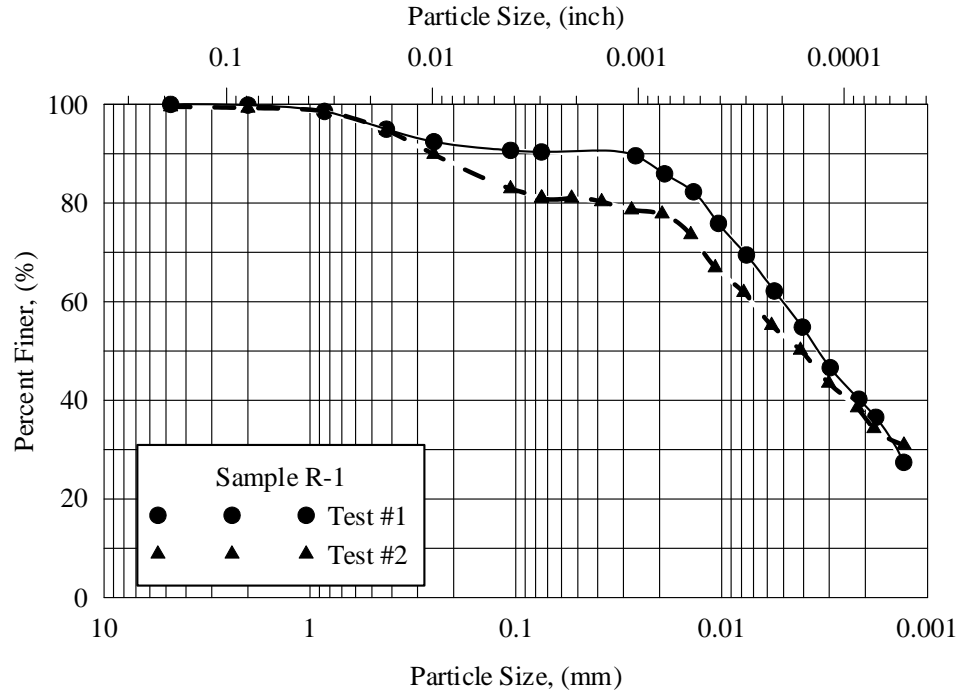


Figure A.5: Grain size distribution curve for soil Racine-1

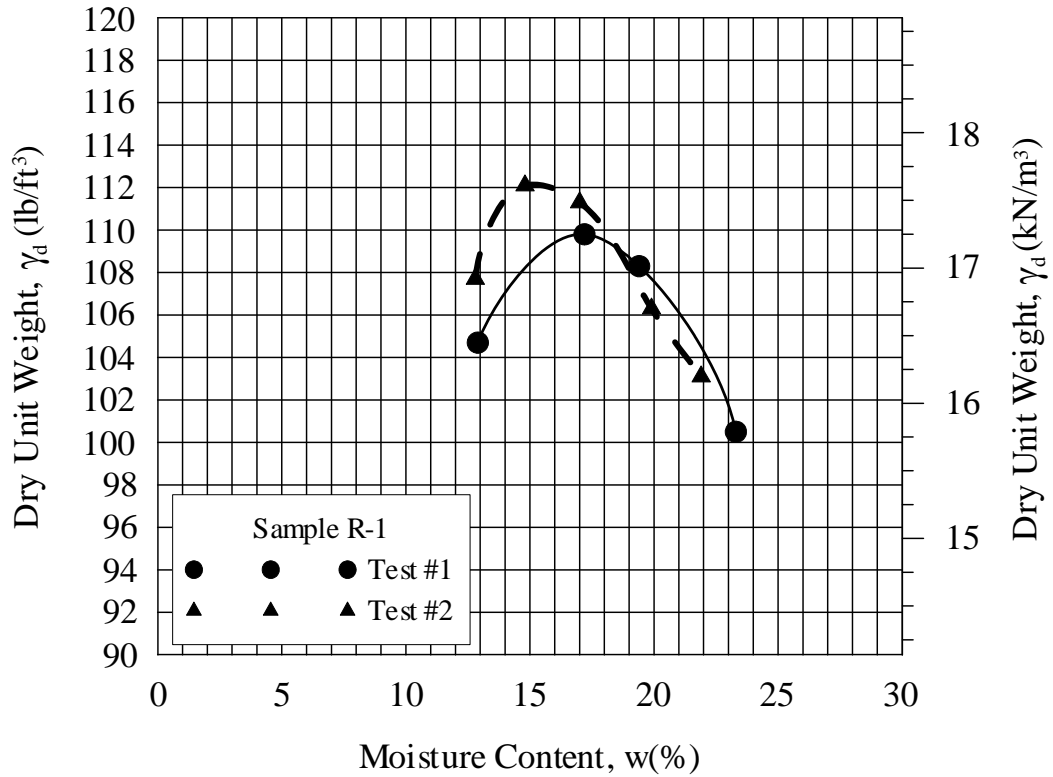
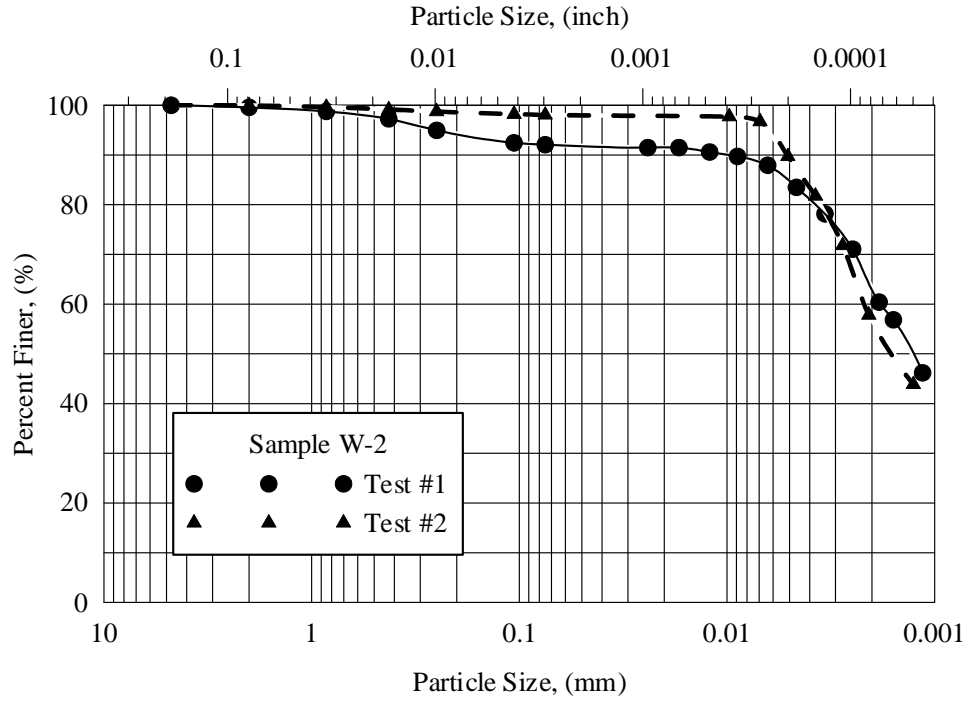
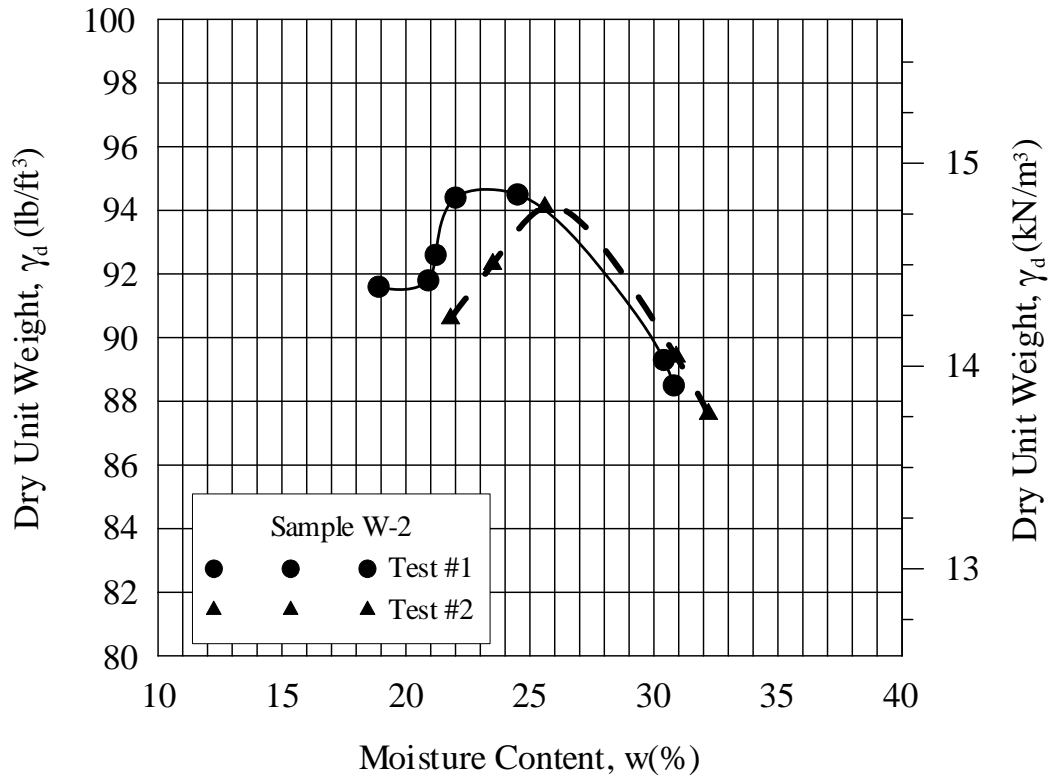


Figure A.6: Moisture – unit weight relationship for soil Racine-1



**Figure A.7: Grain size distribution curve for soil Winnebago-2**



**Figure A.8: Moisture - unit weight relationship for Winnebago-2**

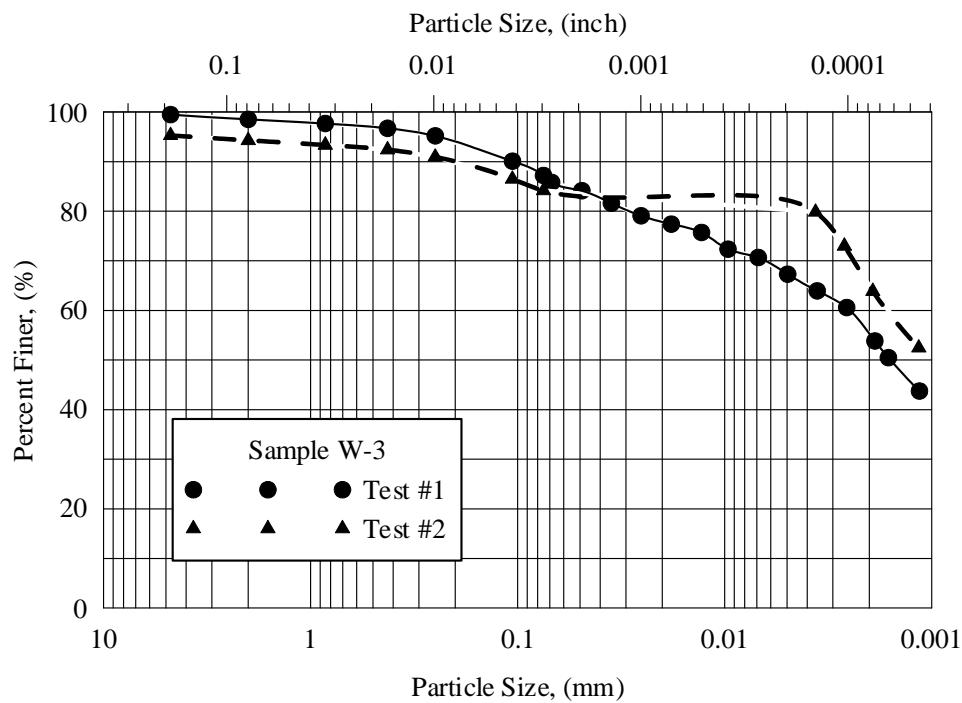


Figure A.9: Grain size distribution curve for soil Winnebago-3

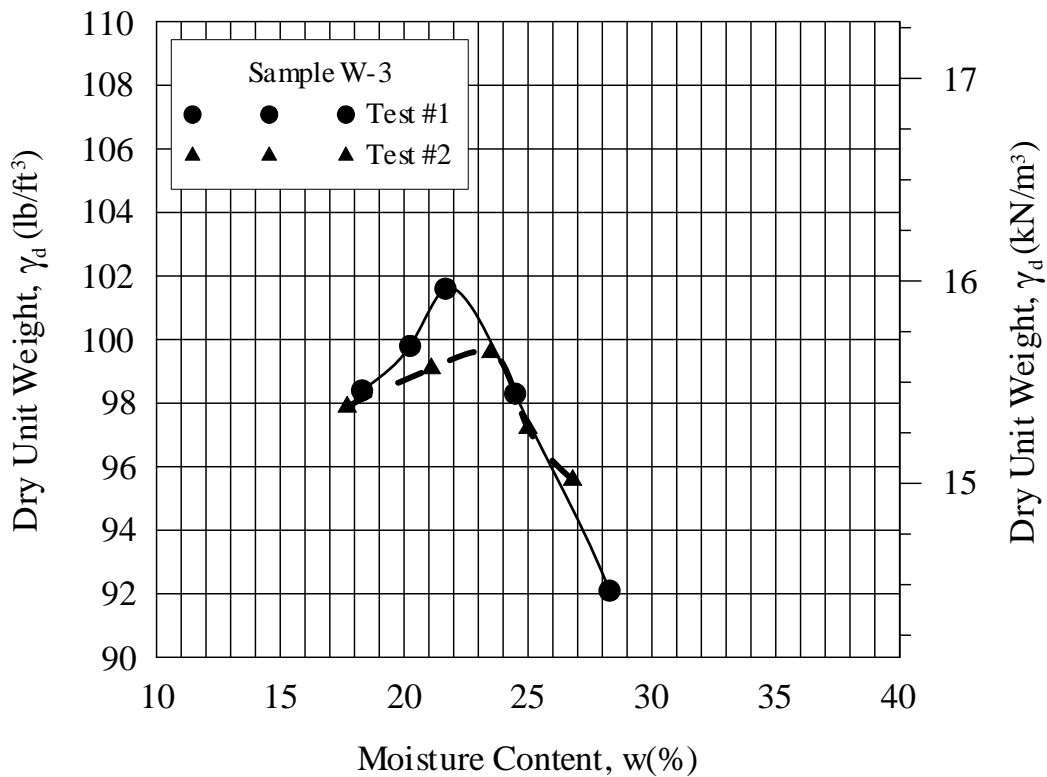


Figure A.10: Moisture - unit weight relationship for soil Winnebago-3

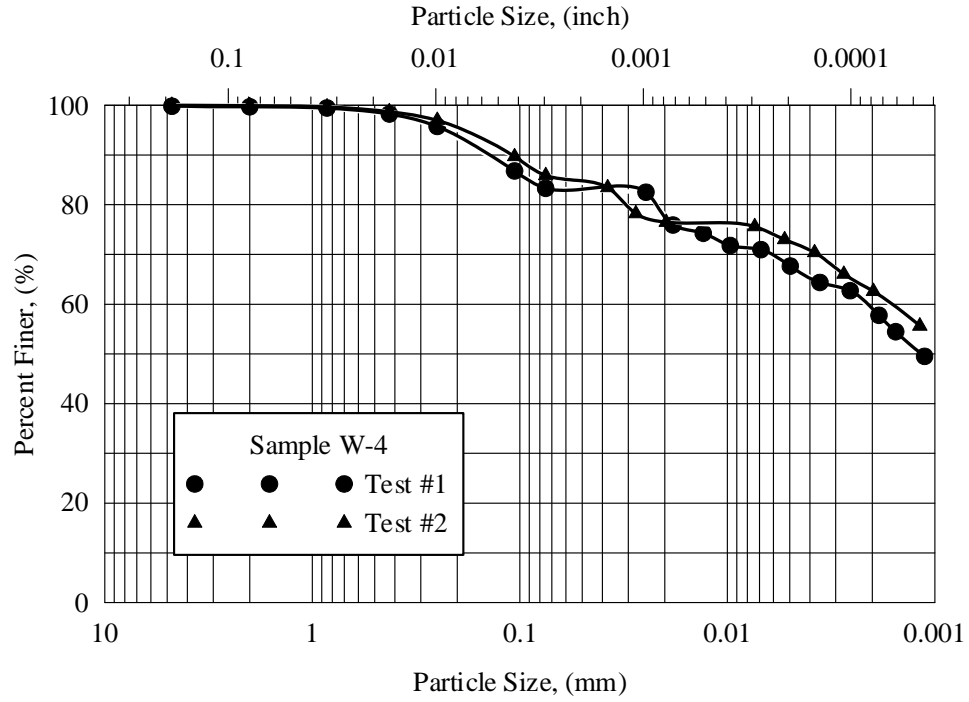


Figure A.11: Grain size distribution curve for soil Winnebago-4

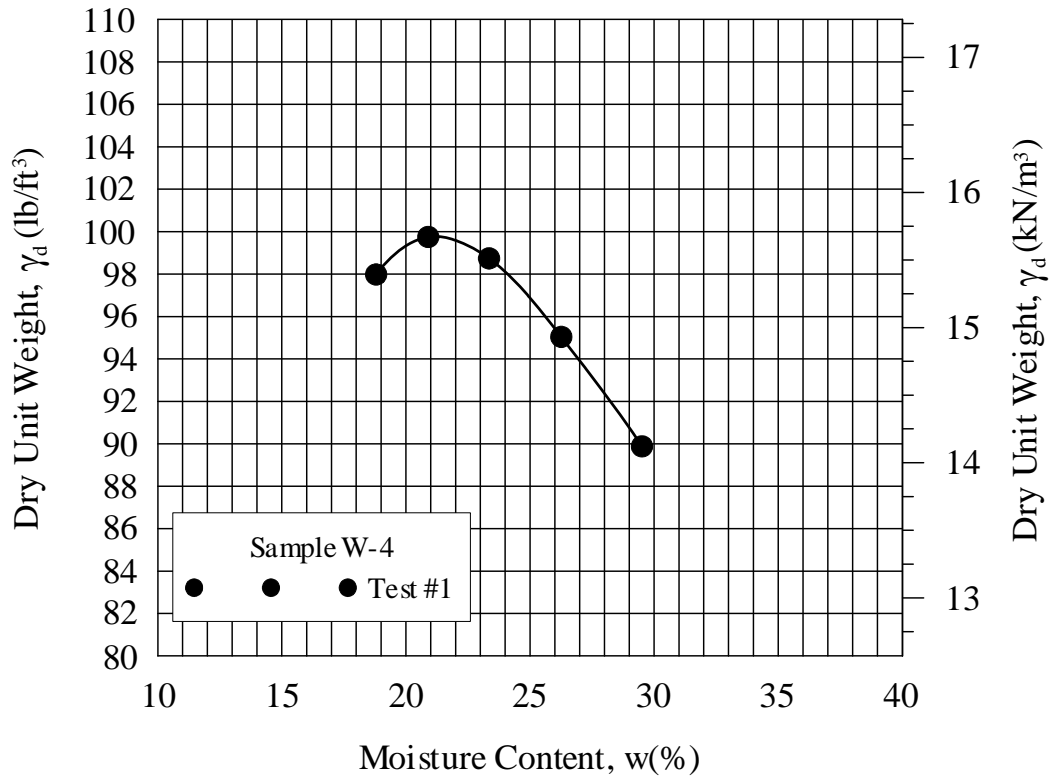


Figure A.12: Moisture - unit weight relationship for soil Winnebago-4

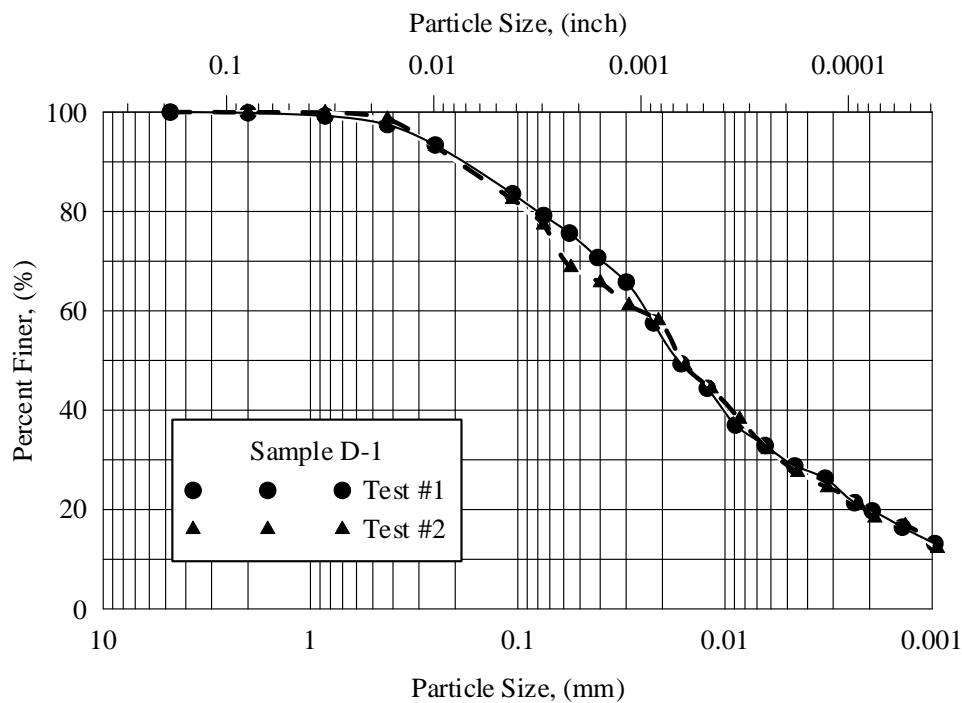


Figure A.13: Grain size distribution curve for soil Dodge-1

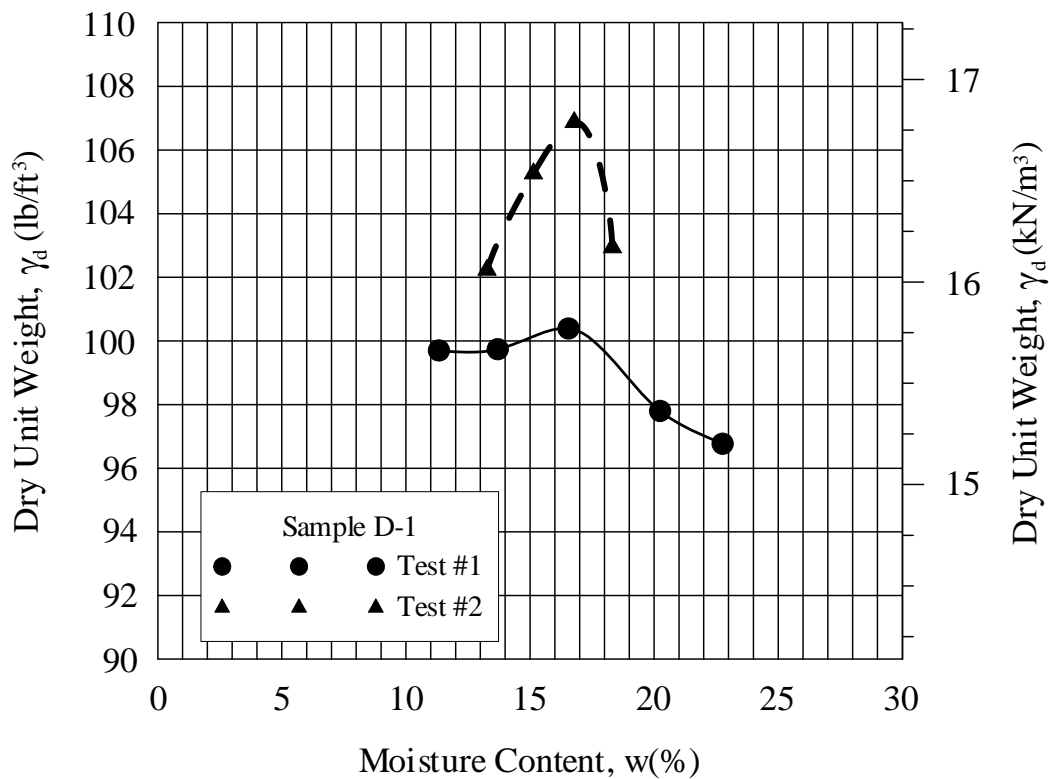


Figure A.14: Moisture - unit weight relationship for soil Dodge-1

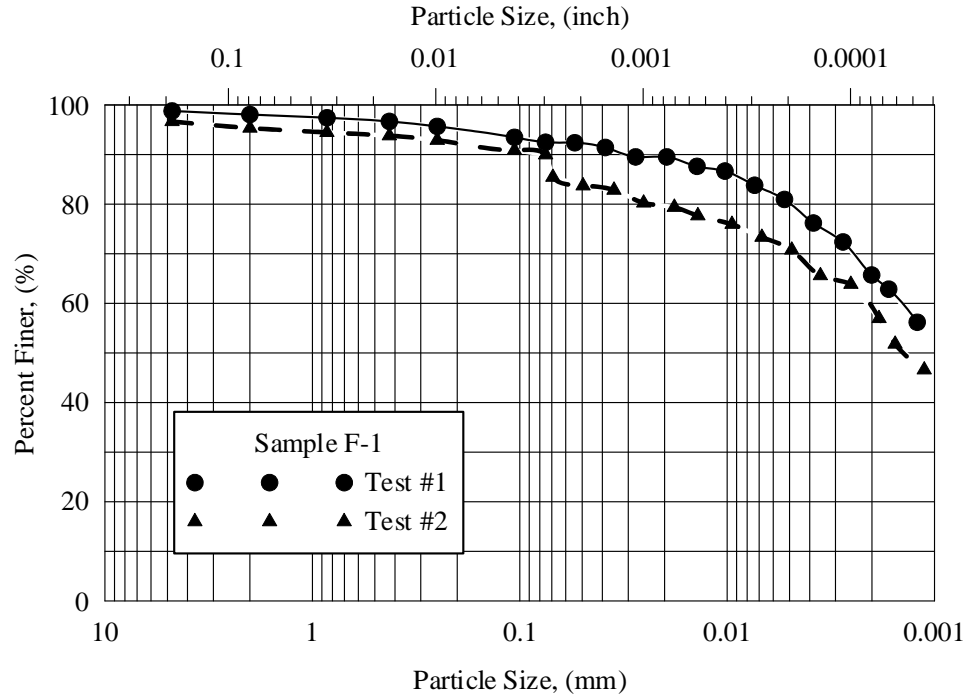


Figure A.15: Grain size distribution curve for soil Fond du Lac-1

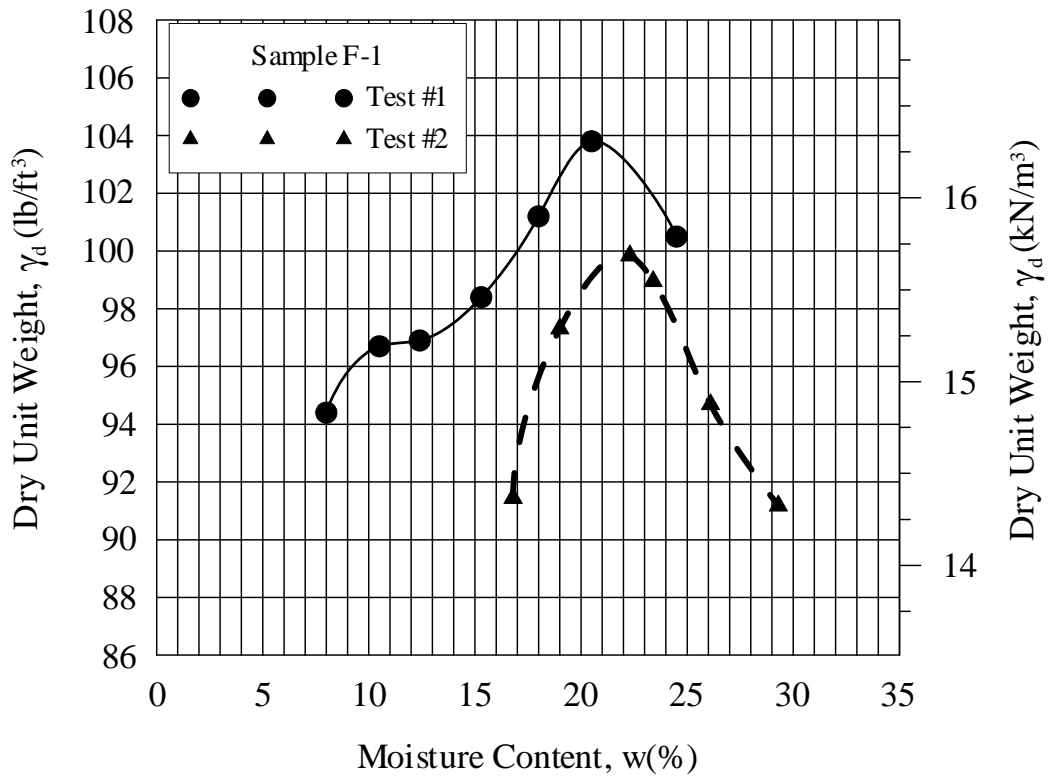


Figure A.16: Moisture - unit weight relationship for soil Fond du Lac-1

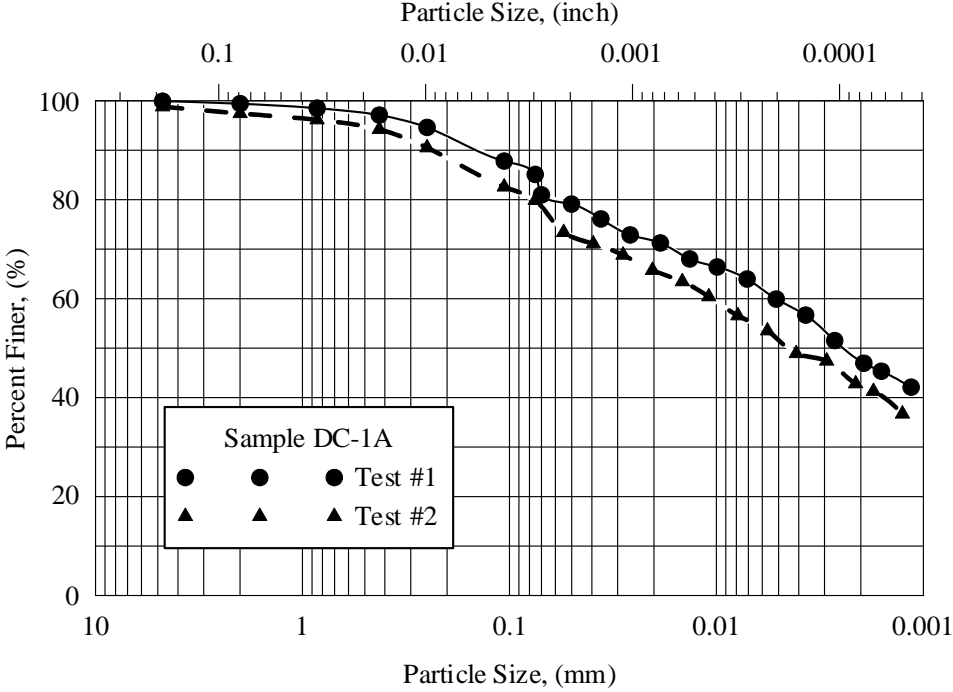


Figure A.17: Grain size distribution curve for soil Deer Creek-1A

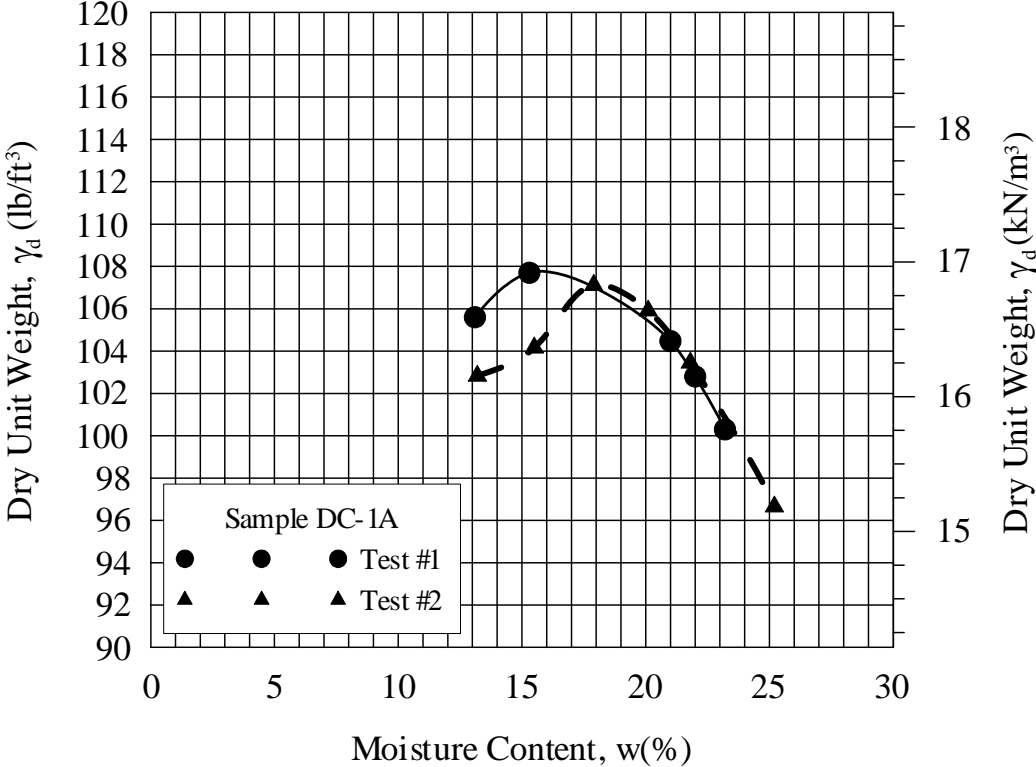
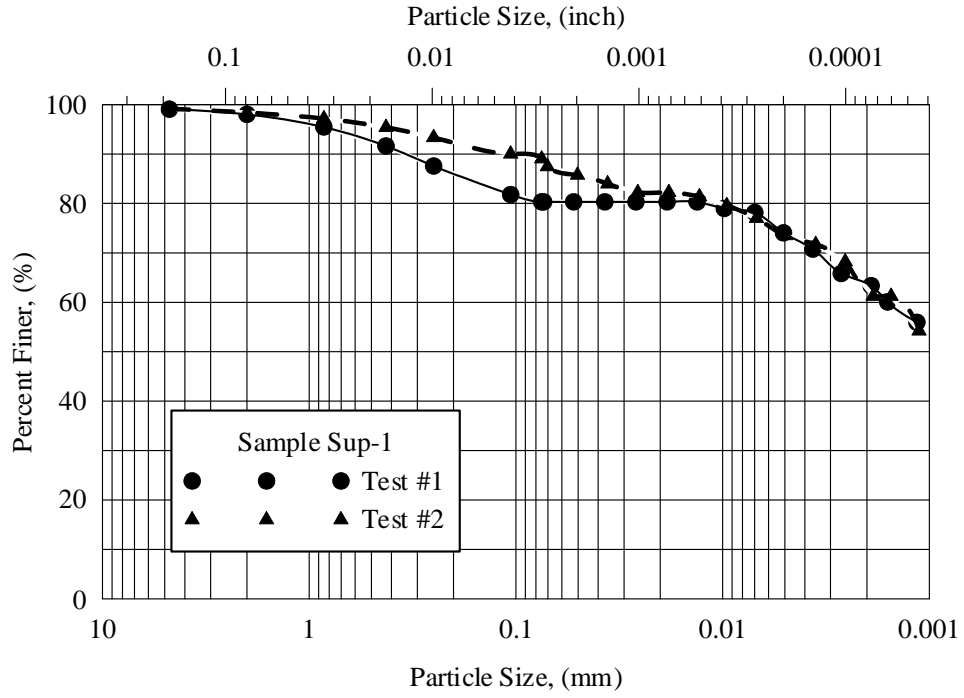
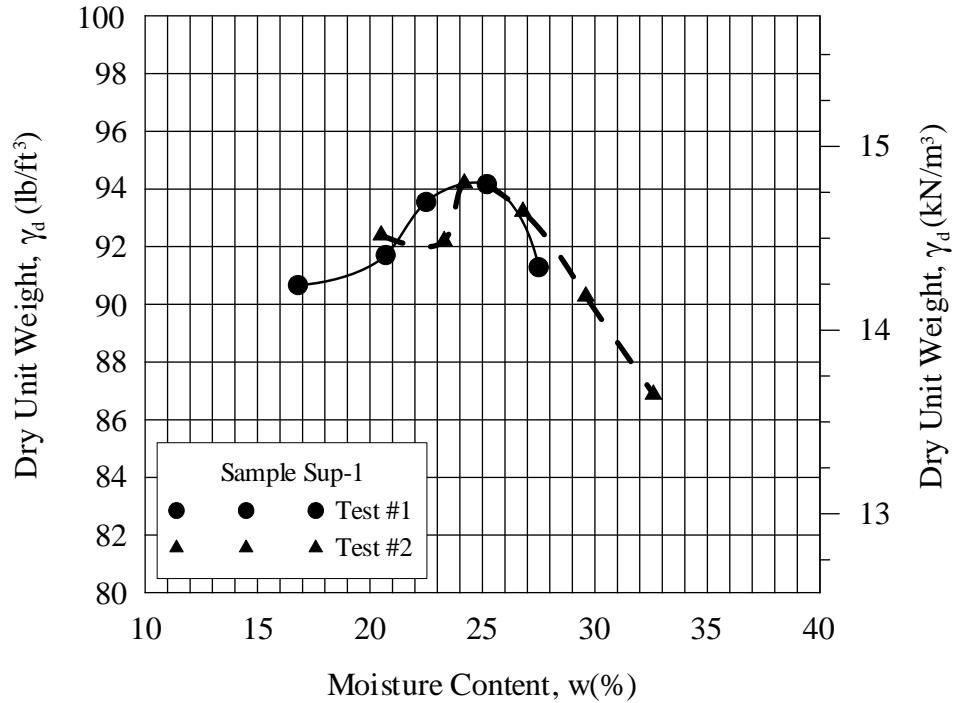


Figure A.18: Moisture - unit weight relationship for soil Deer Creek-1A



**Figure A.19: Grain size distribution curve for soil Superior-1**



**Figure A.20: Moisture – unit weight relationship for soil Superior-1**

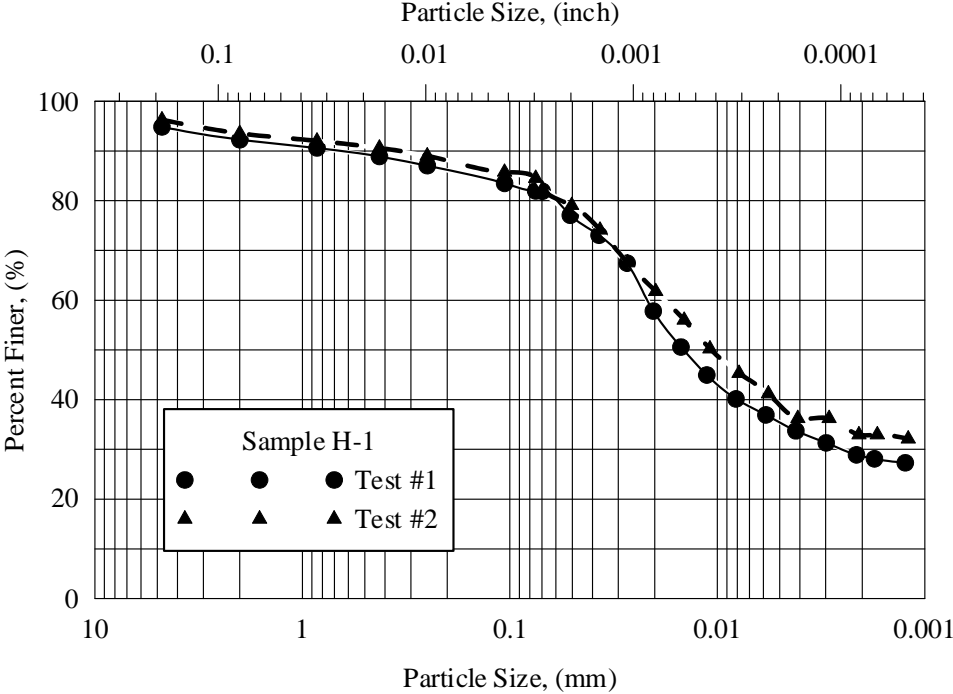


Figure A.21: Grain size distribution curve for soil Highland-1

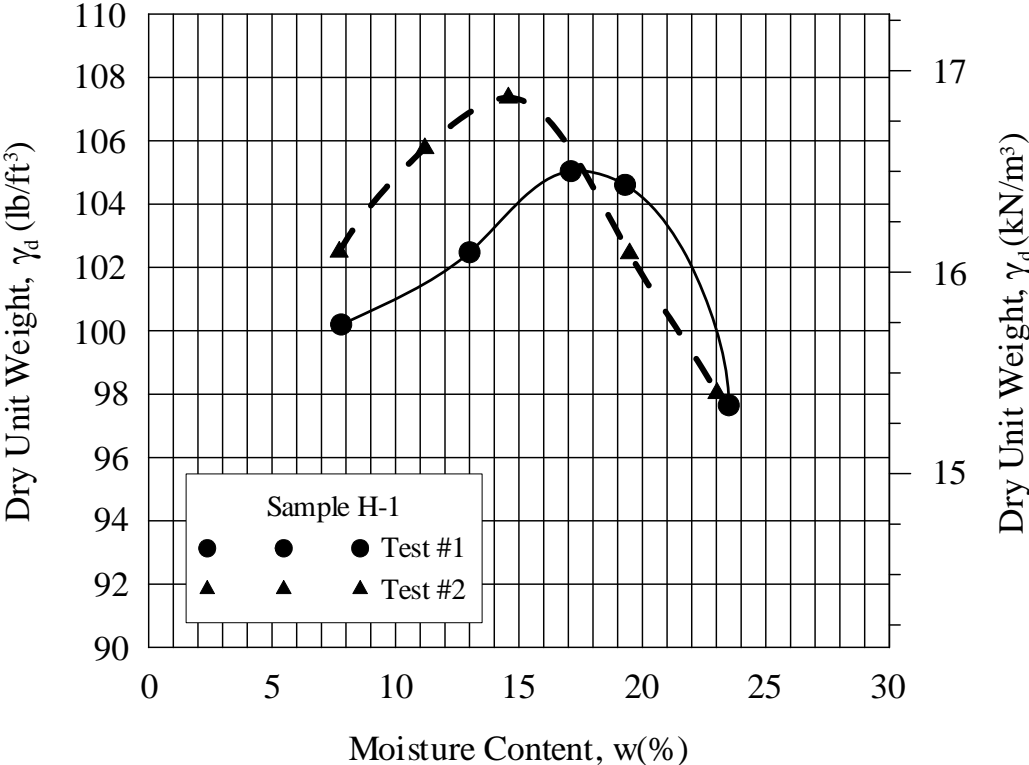


Figure A.22: Moisture - unit weight relationship for soil Highland-1

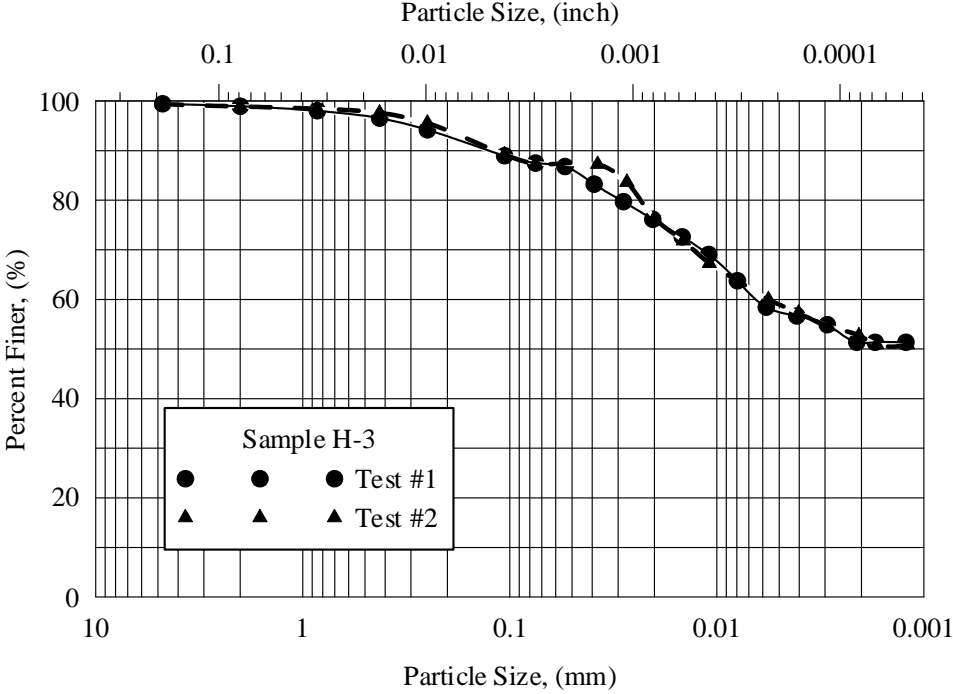


Figure A.23: Grain size distribution curve for soil Highland-3

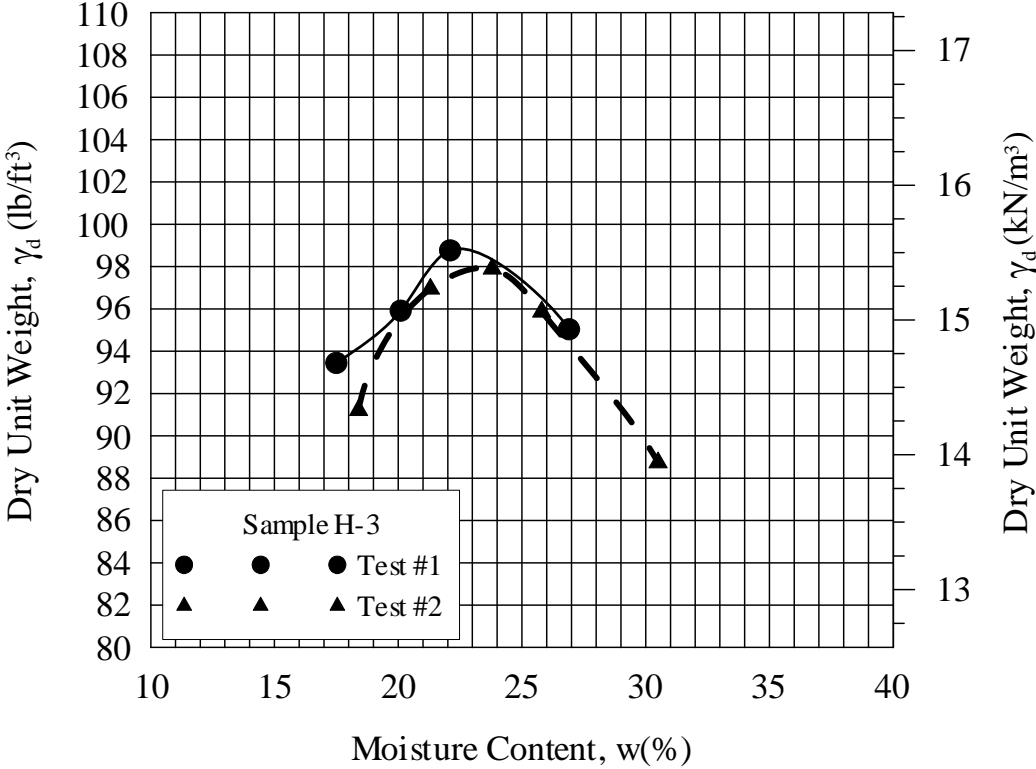


Figure A.24: Moisture - unit weight relationship for soil Highland-3



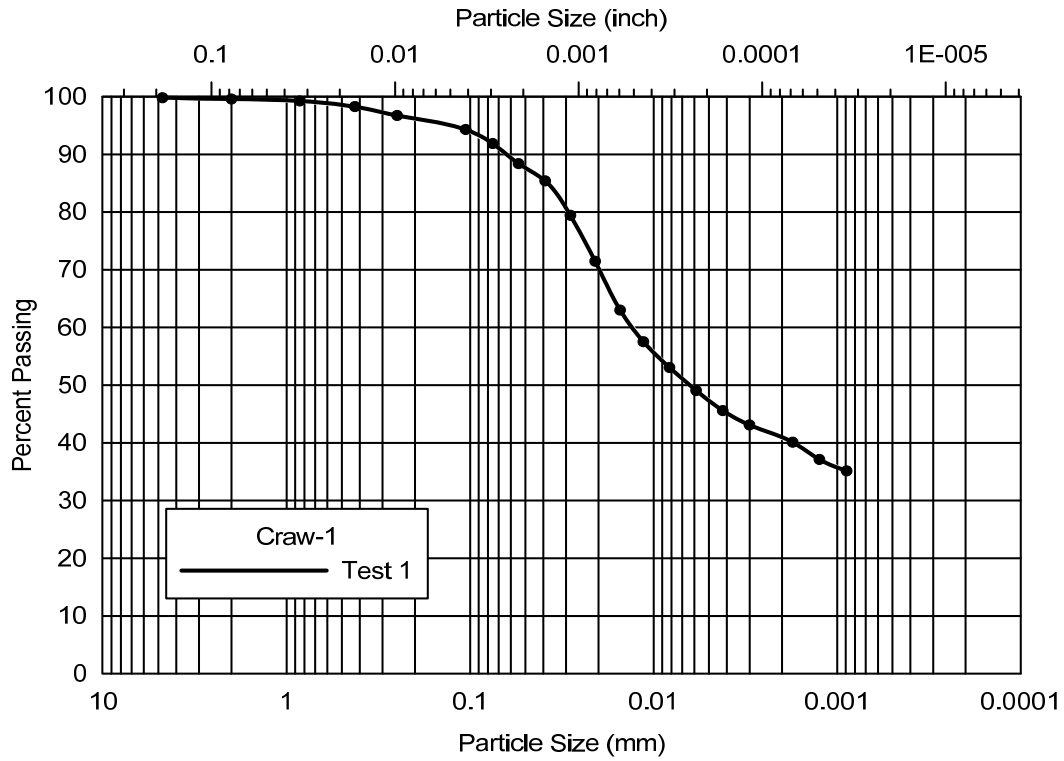


Figure A.26: Grain size distribution curve for soil Craw-1

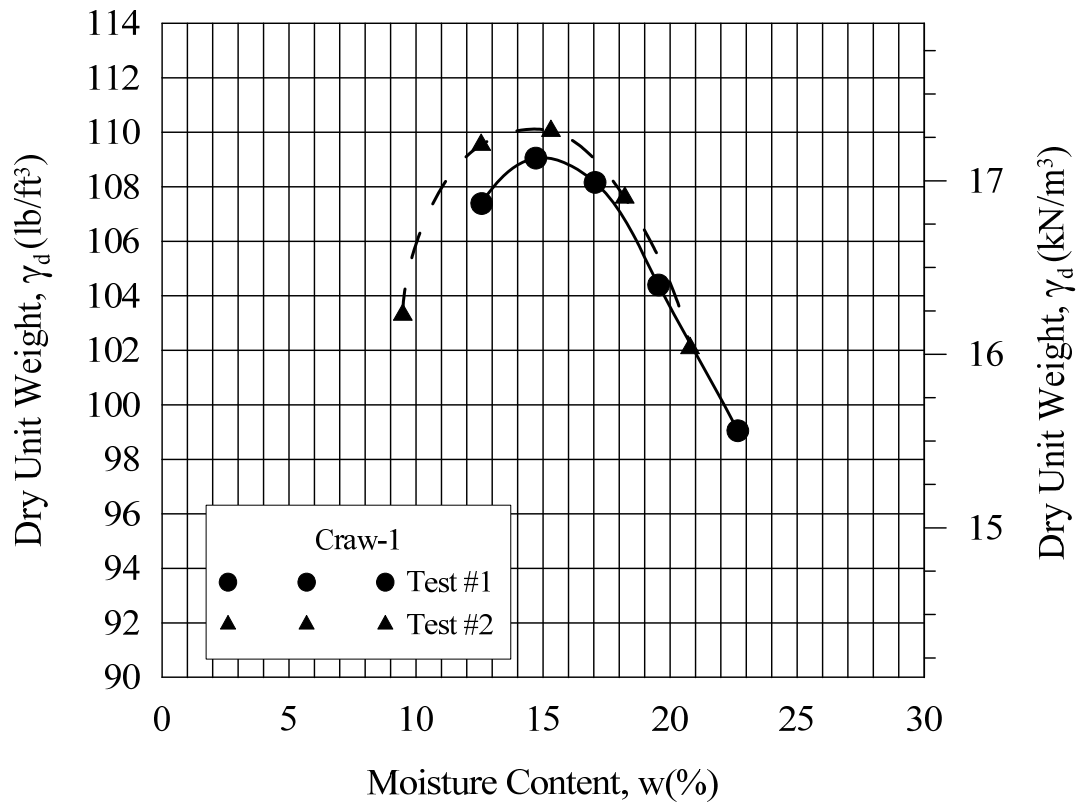
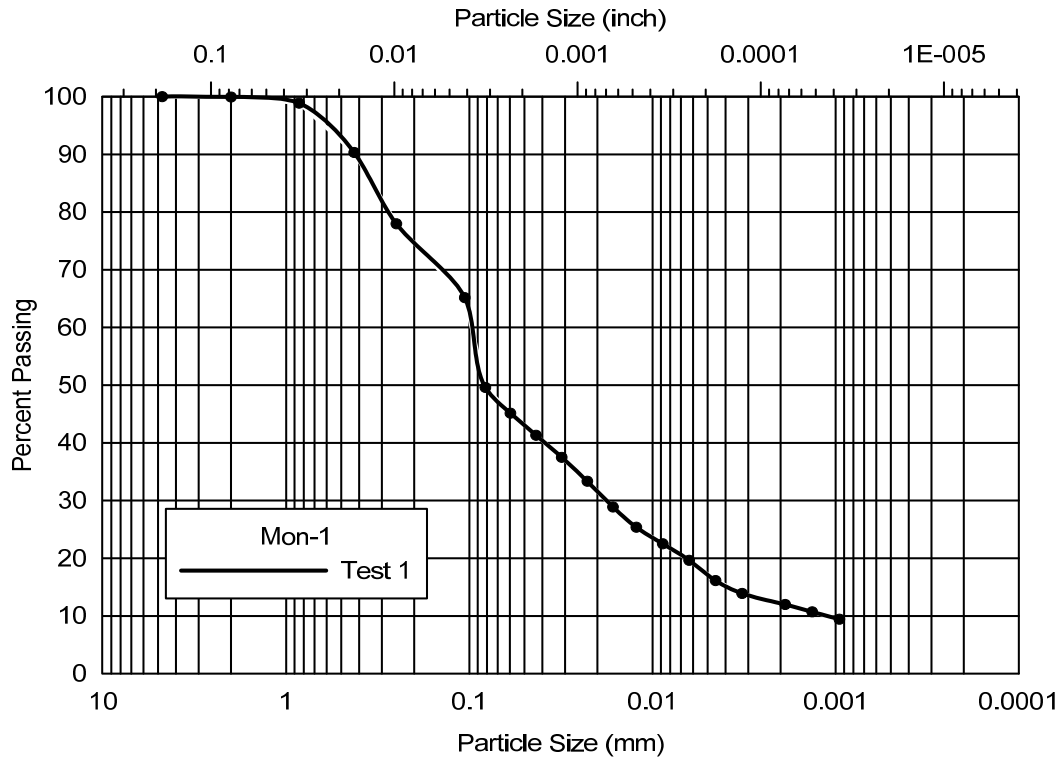


Figure A.27: Moisture – unit weight relationship for soil Craw-1



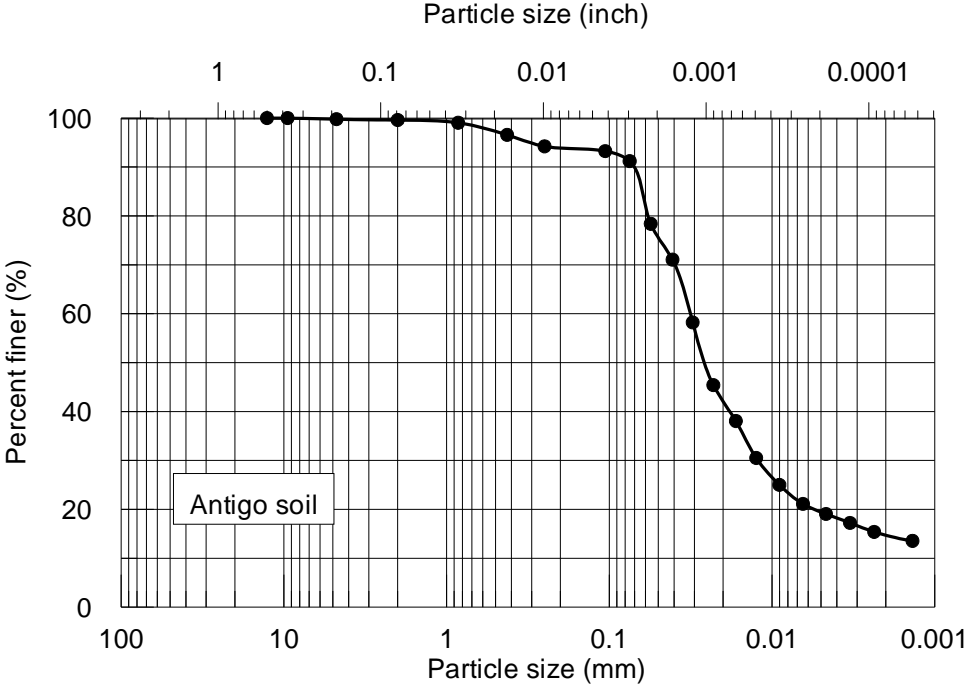


Figure A.30: Grain size distribution curve for Antigo soil

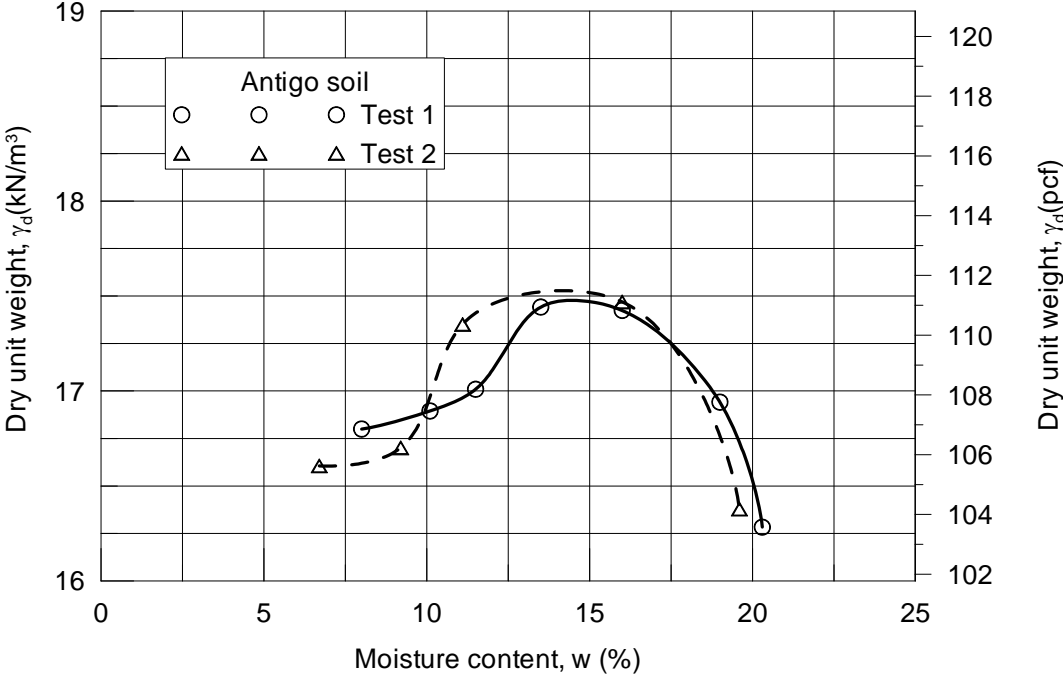
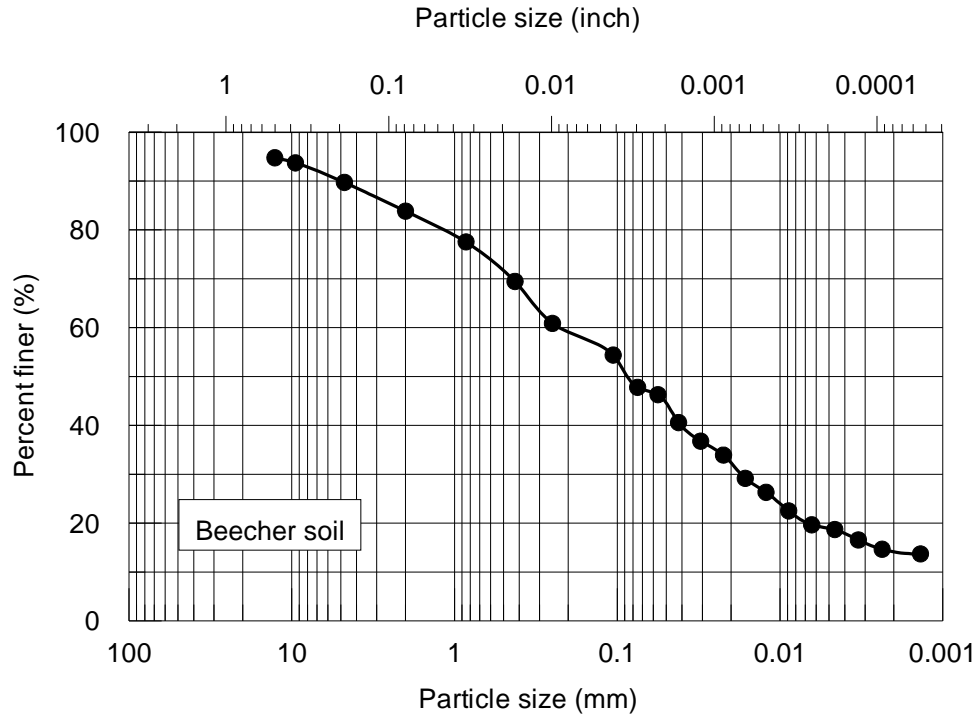
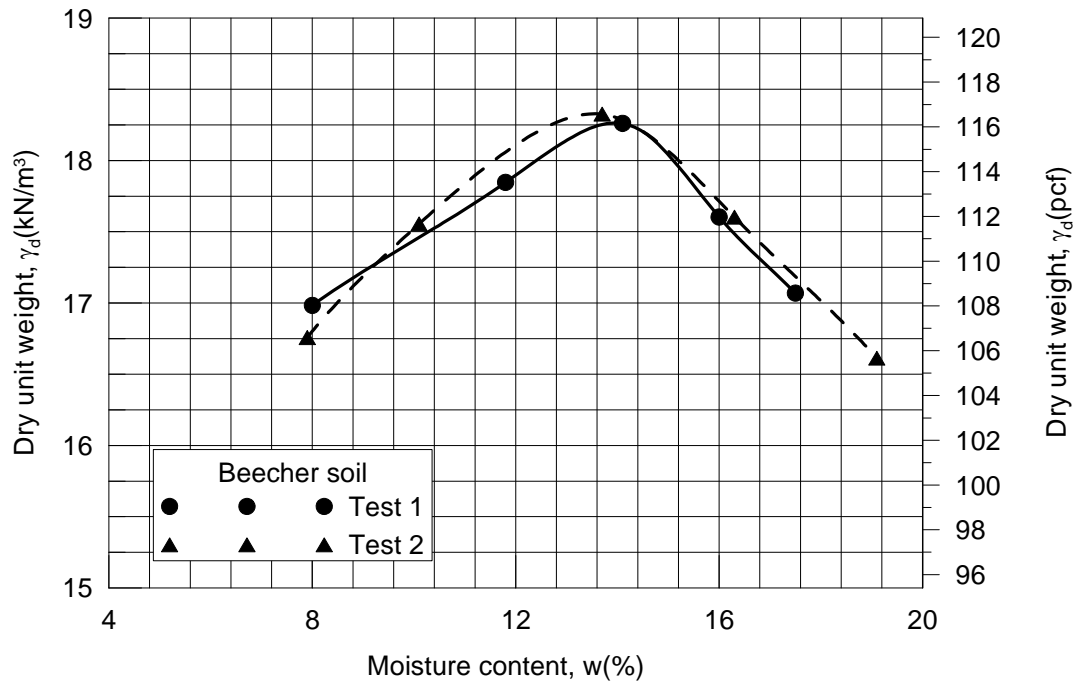


Figure A.31: Moisture – unit weight relationship for Antigo soil



**Figure A.32: Grain size distribution curve for Beecher soil**



**Figure A.33: Moisture - unit weight relationship for Beecher soil**

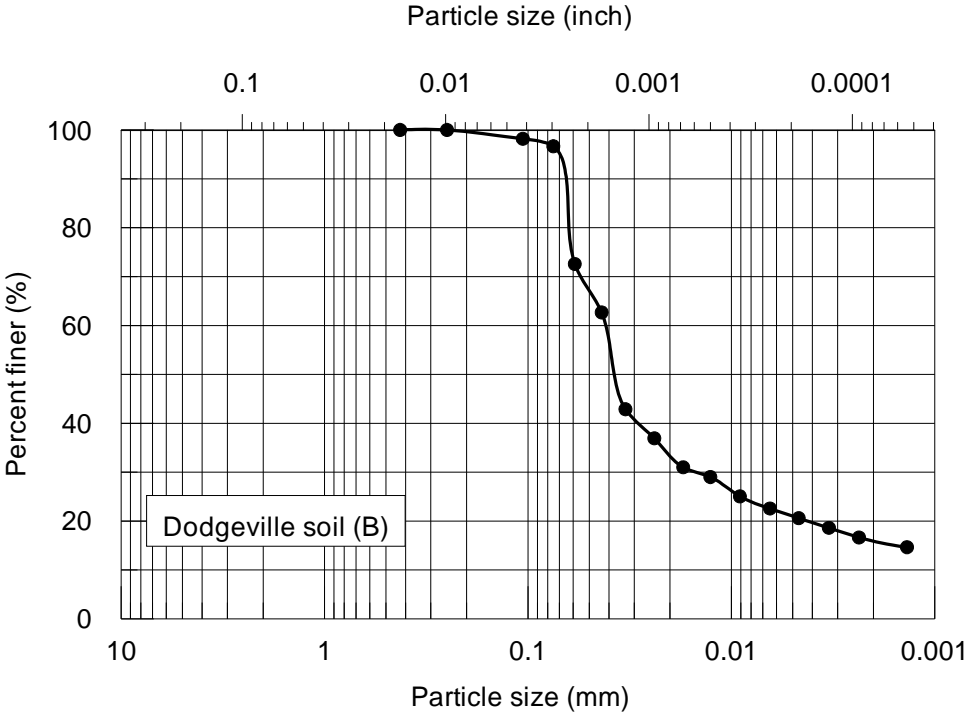


Figure A.34: Grain size distribution curve for Dodgeville soil

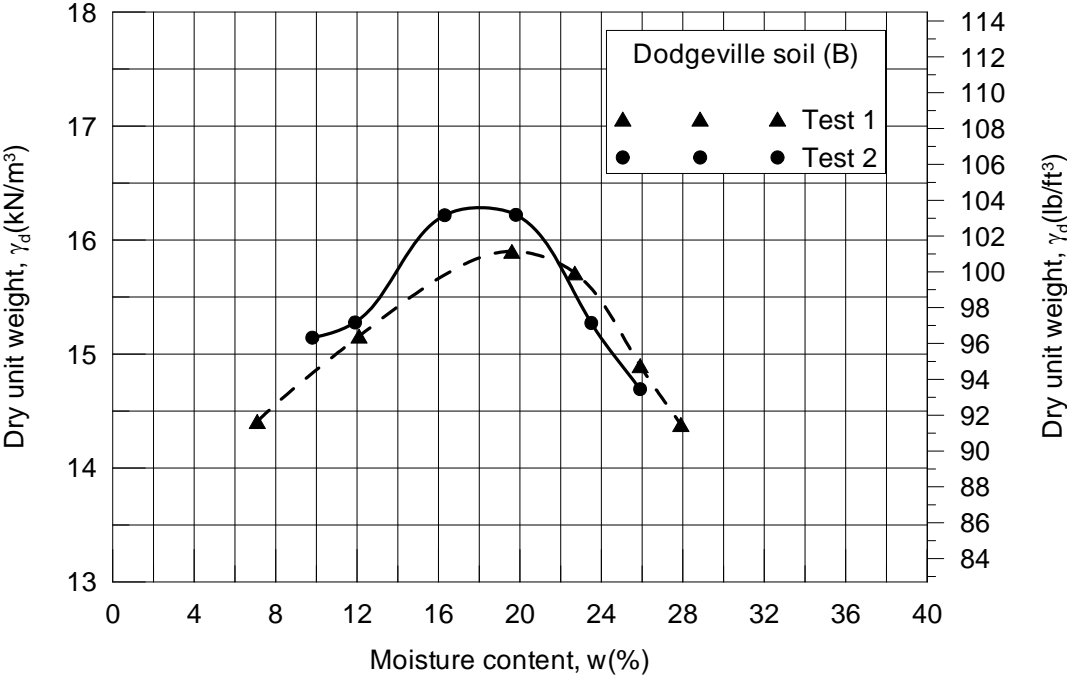


Figure A.35: Moisture - unit weight relationship for Dodgeville soil

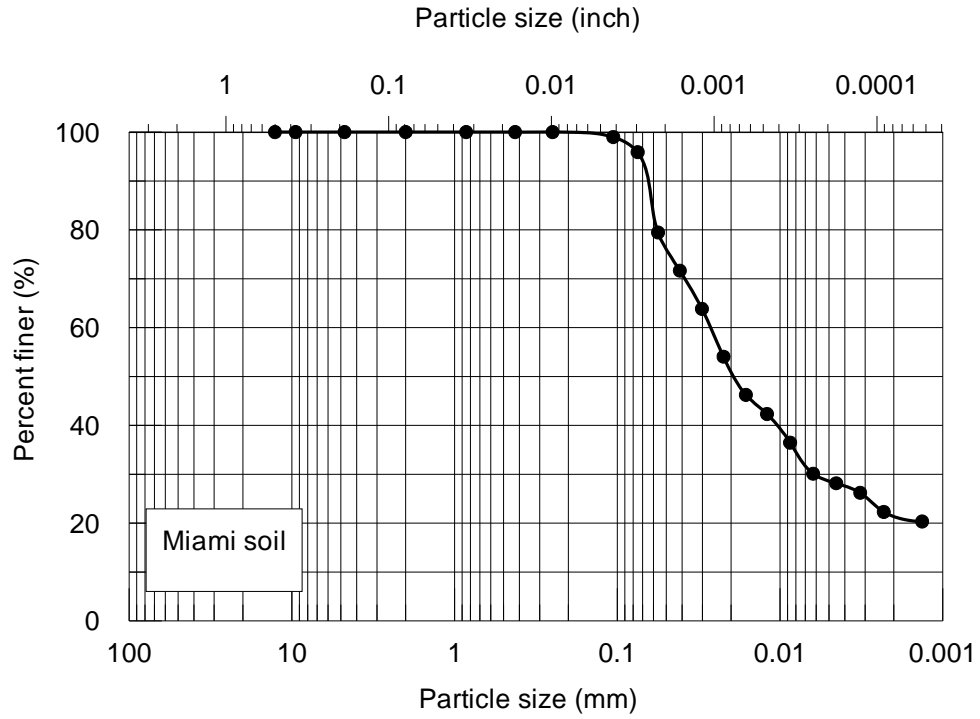


Figure A.36: Grain size distribution curve for Miami soil

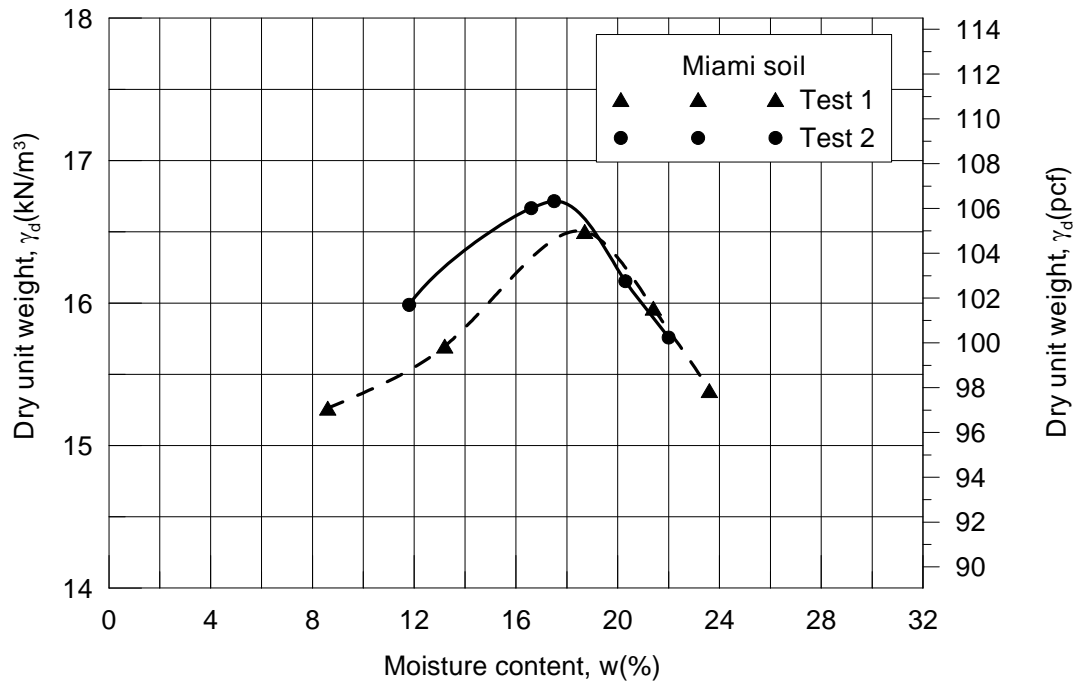
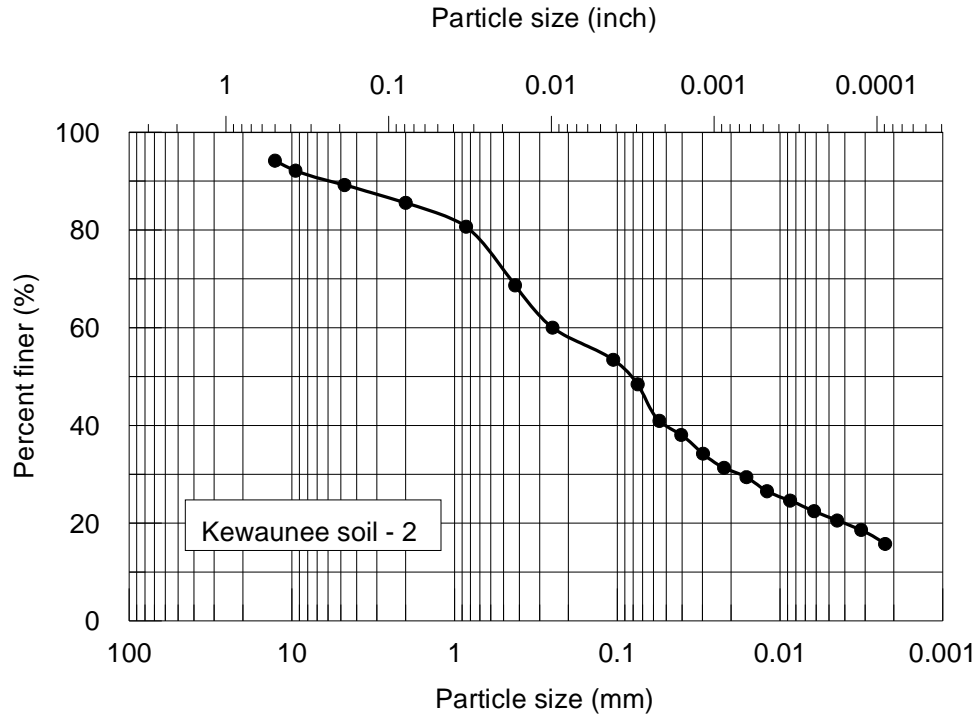
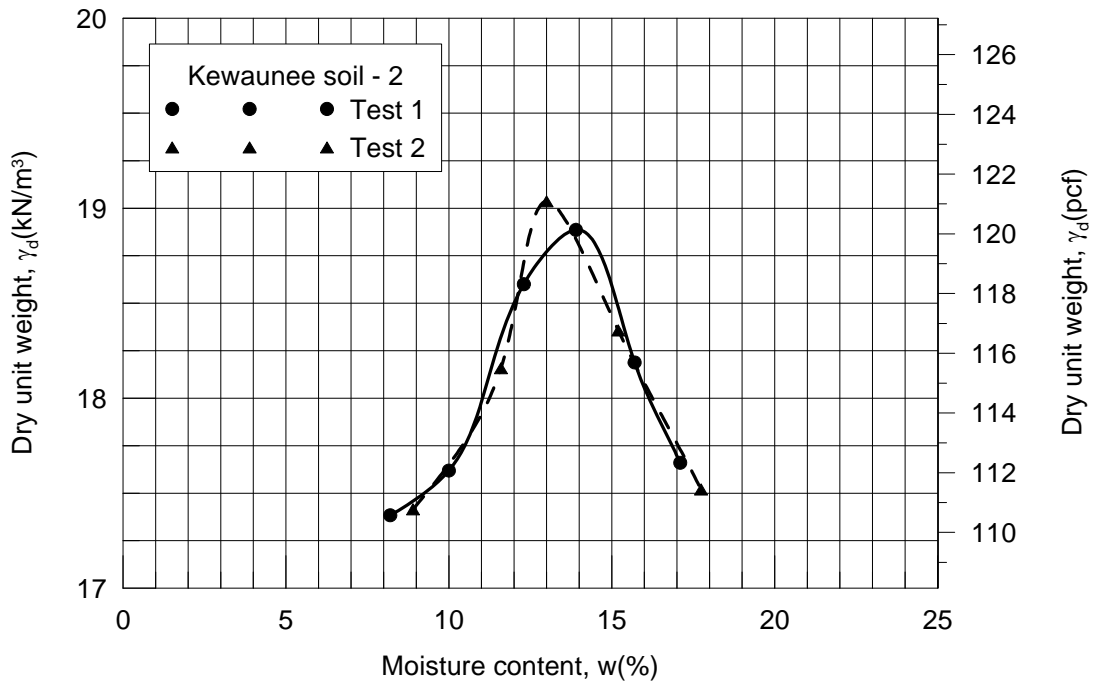


Figure A.37: Moisture - unit weight relationship for Miami soil



**Figure A.38: Grain size distribution curve for Kewaunee soil - 2**



**Figure A.39: Moisture - unit weight relationship for Kewaunee soil - 2**

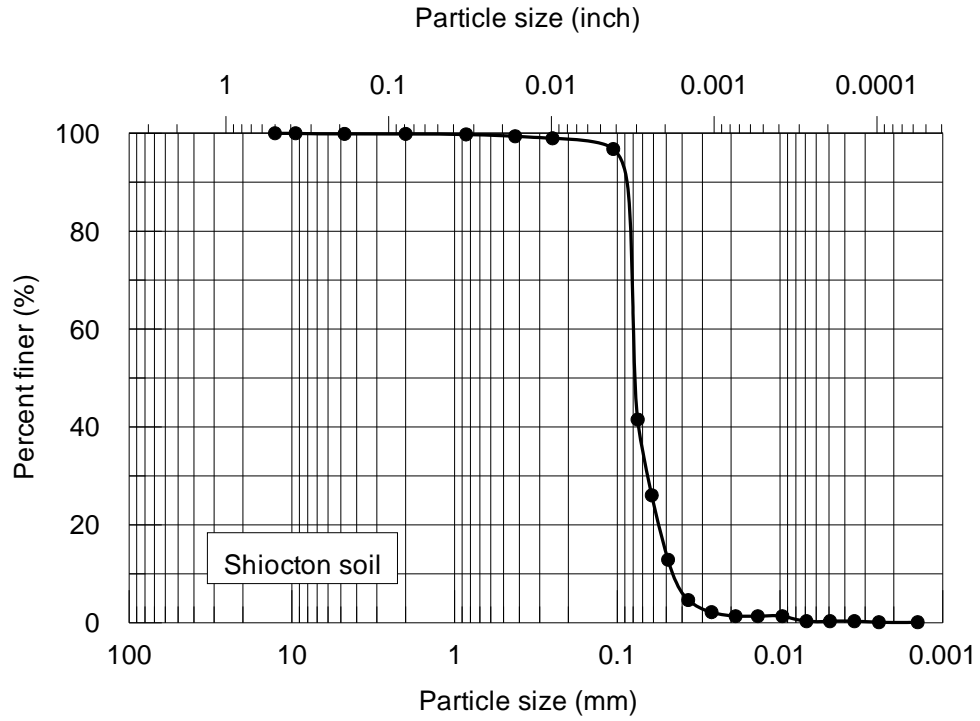


Figure A.40: Grain size distribution curve for Shiocton soil

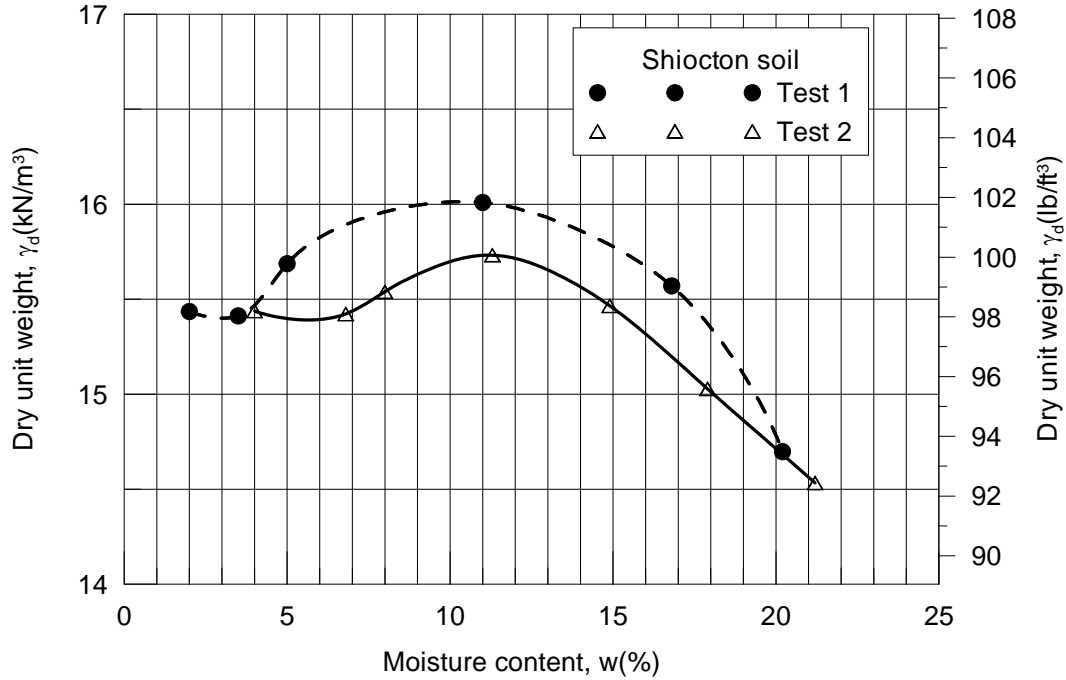
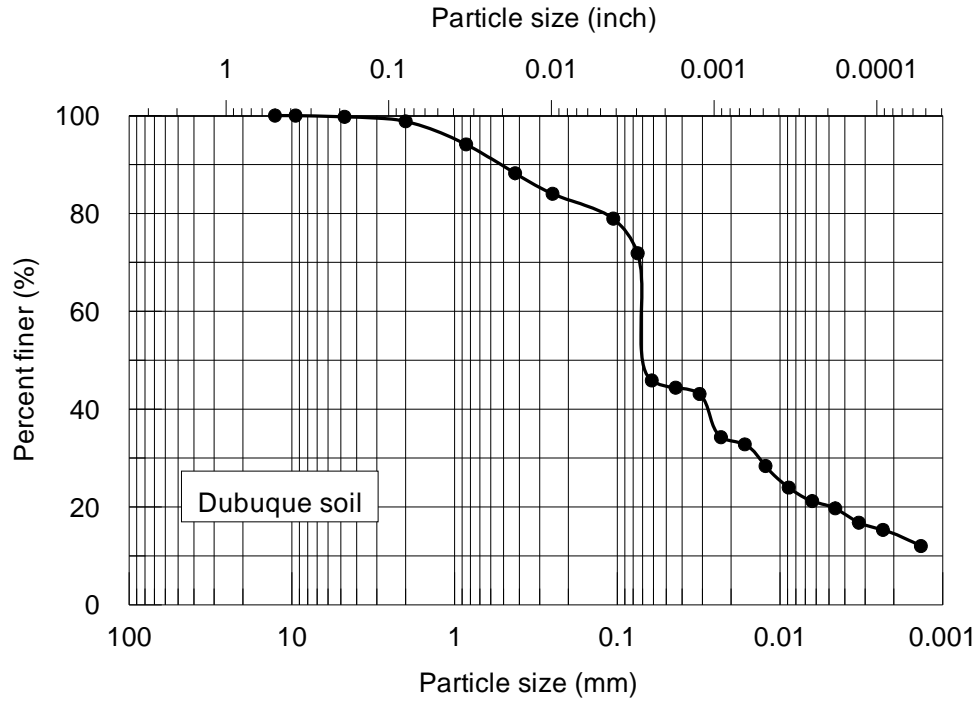
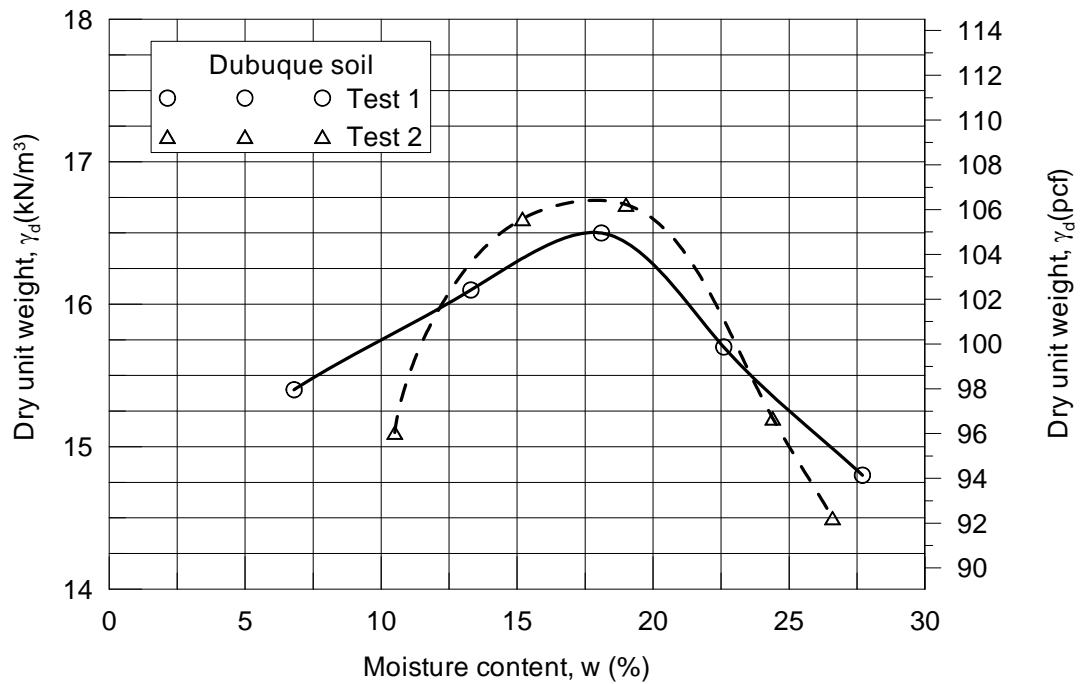


Figure A.41: Moisture - unit weight relationship for Shiocton soil

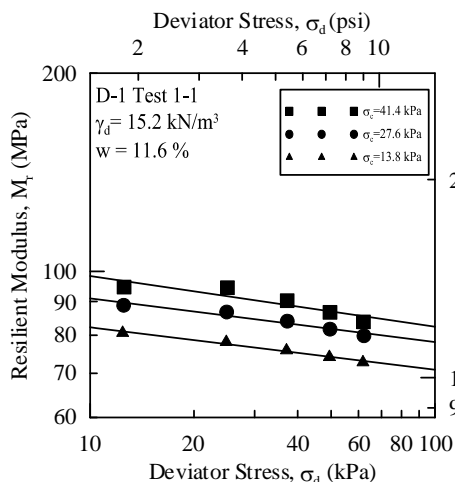


**Figure A.42: Grain size distribution curve for Dubuque soil**

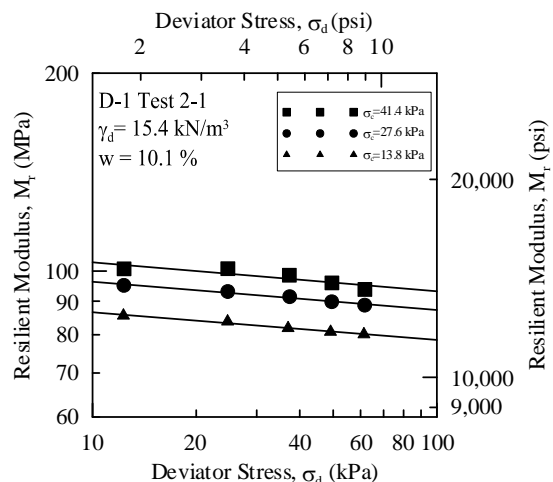


**Figure A.43: Moisture - unit weight relationship for Dubuque soil**

## Appendix B

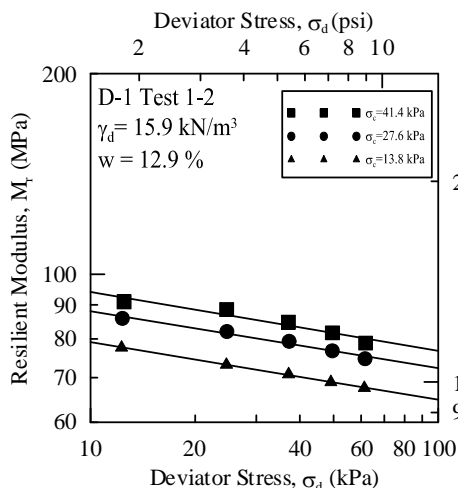


(a) Test D1\_Set1\_1d

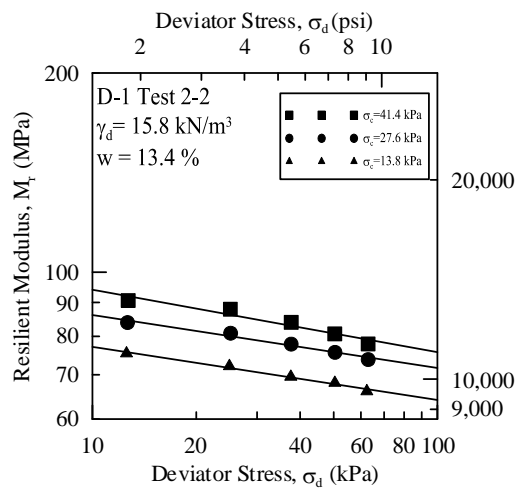


(b) Test D1\_Set2\_1d

**Figure B.1: Results of repeated load triaxial test for soil Dodge-1 compacted at 95% of  $\gamma_{dmax}$  and dry of  $w_{opt}$ , target compaction value of  $\gamma_d = 15.5 \text{ kN/m}^3$  and  $w = 10.0\%$**

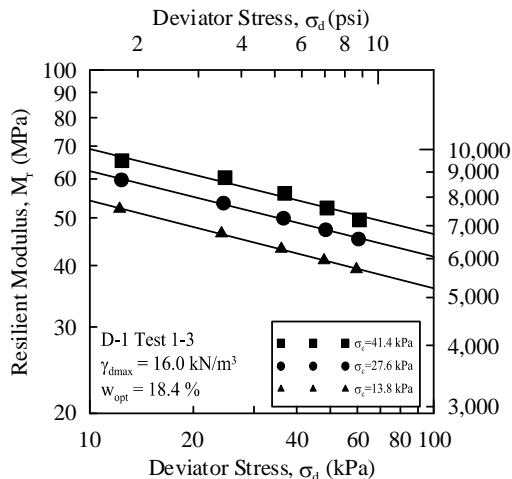


(a) Test D1\_Set1\_2d

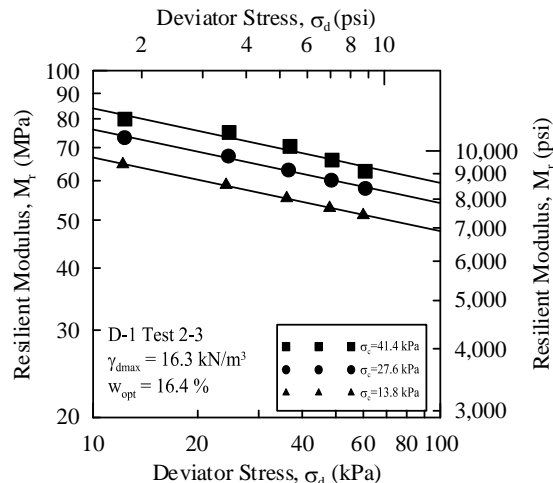


(b) Test D1\_Set2\_2d

**Figure B.2: Results of repeated load triaxial test for soil Dodge-1 compacted at 97% of  $\gamma_{dmax}$  and dry of  $w_{opt}$ , target compaction value of  $\gamma_d = 15.9 \text{ kN/m}^3$  and  $w = 13.3\%$**

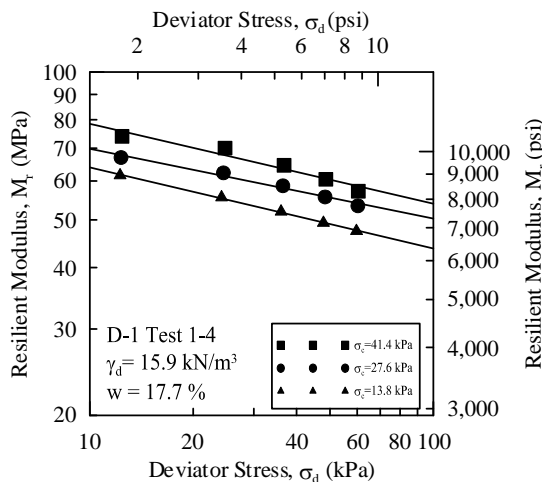


(c) Test D1\_Set1\_3o

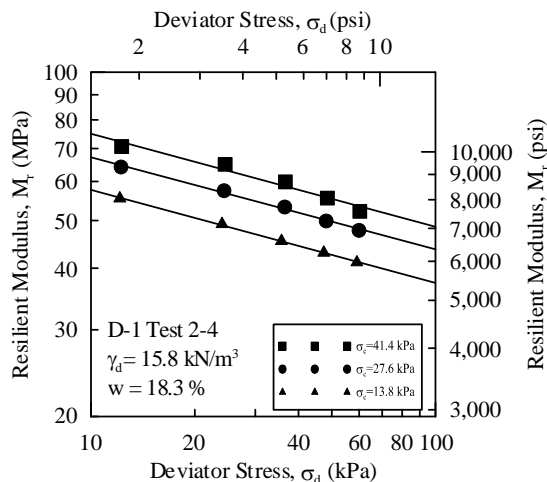


(d) Test D1\_Set2\_3o

**Figure B.3: Results of repeated load triaxial test for soil Dodge-1 compacted at  $\gamma_{dmax}$  and  $w_{opt}$ , target compaction value of  $\gamma_d = 16.3 \text{ kN/m}^3$  and  $w = 16.5\%$**



(c) Test D1\_Set1\_4w



(d) Test D1\_Set2\_4w

**Figure B.4: Results of repeated load triaxial test for soil Dodge-1 compacted at 97% of  $\gamma_{dmax}$  and wet of  $w_{opt}$ , target compaction value of  $\gamma_d = 15.9 \text{ kN/m}^3$  and  $w = 18.3\%$**

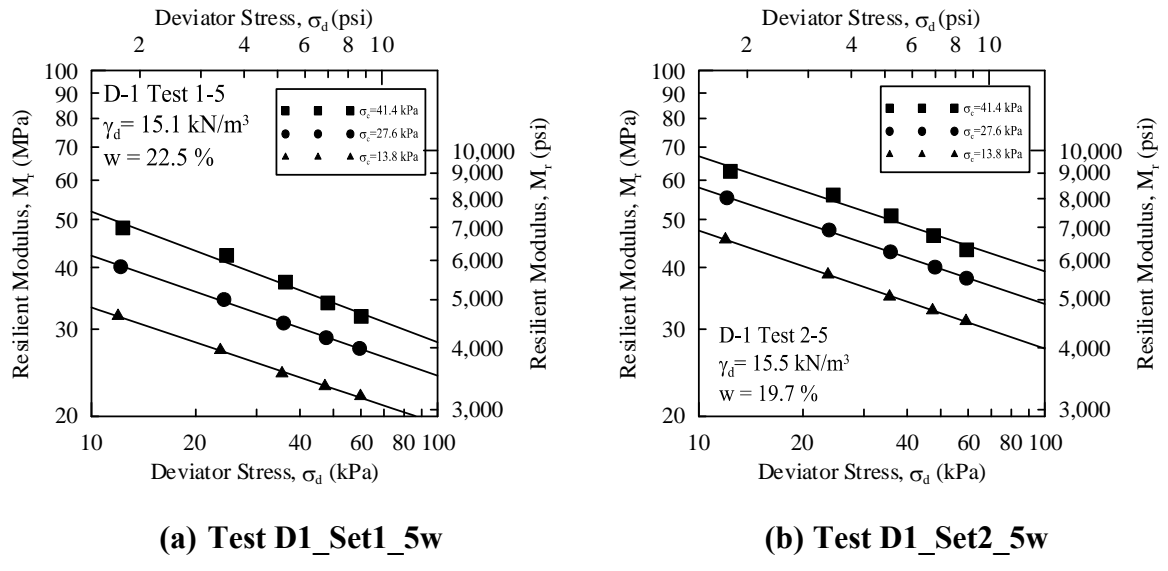


**Figure B.5: Results of repeated load triaxial test for soil Dodge-1 compacted at 95% of  $\gamma_{dmax}$  and wet of  $w_{opt}$ , target compaction value of  $\gamma_d = 15.5 \text{ kN/m}^3$  and  $w = 19.8\%$**

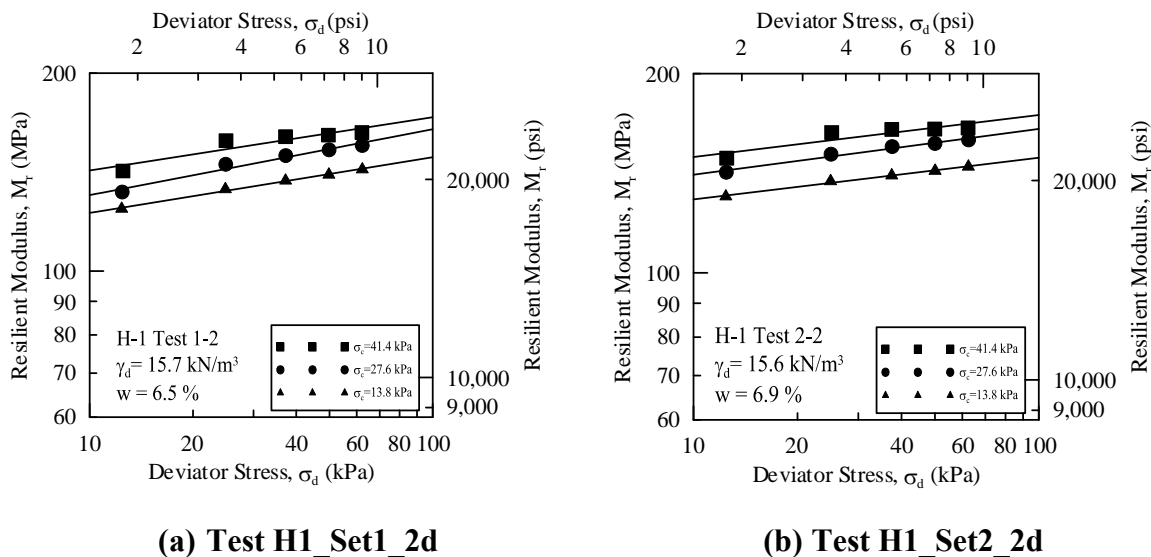


**Figure B.6: Results of repeated load triaxial test for soil Highland-1 compacted at 93% of  $\gamma_{dmax}$  and dry of  $w_{opt}$ , target compaction value of  $\gamma_d = 15.6 \text{ kN/m}^3$  and  $w = 7.0\%$**

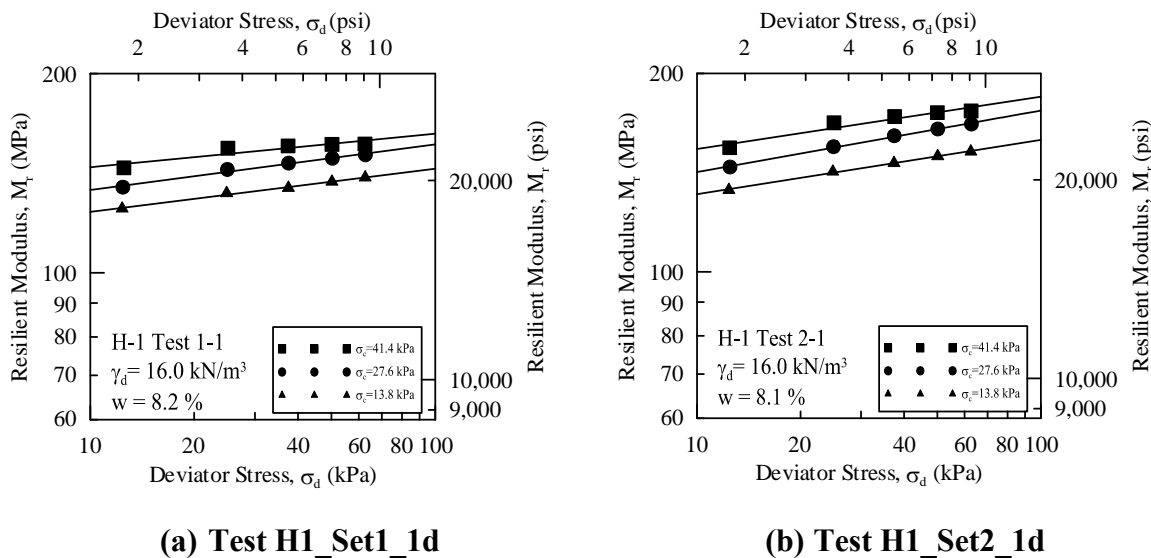


**Figure B.7: Results of repeated load triaxial test for soil Highland-1 compacted at 95% of  $\gamma_{dmax}$  and dry of  $w_{opt}$ , target compaction value of  $\gamma_d = 16.0 \text{ kN/m}^3$  and  $w = 8.5\%$**

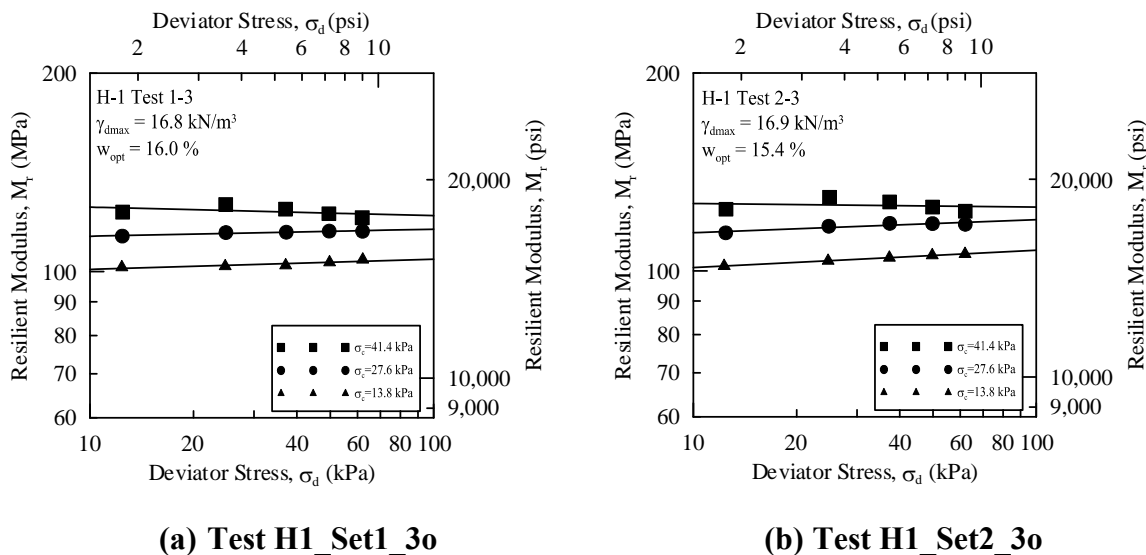


**Figure B.8: Results of repeated load triaxial test for soil Highland-1 compacted at  $\gamma_{dmax}$  and  $w_{opt}$ , target compaction value of  $\gamma_d = 16.8 \text{ kN/m}^3$  and  $w = 16.0\%$**

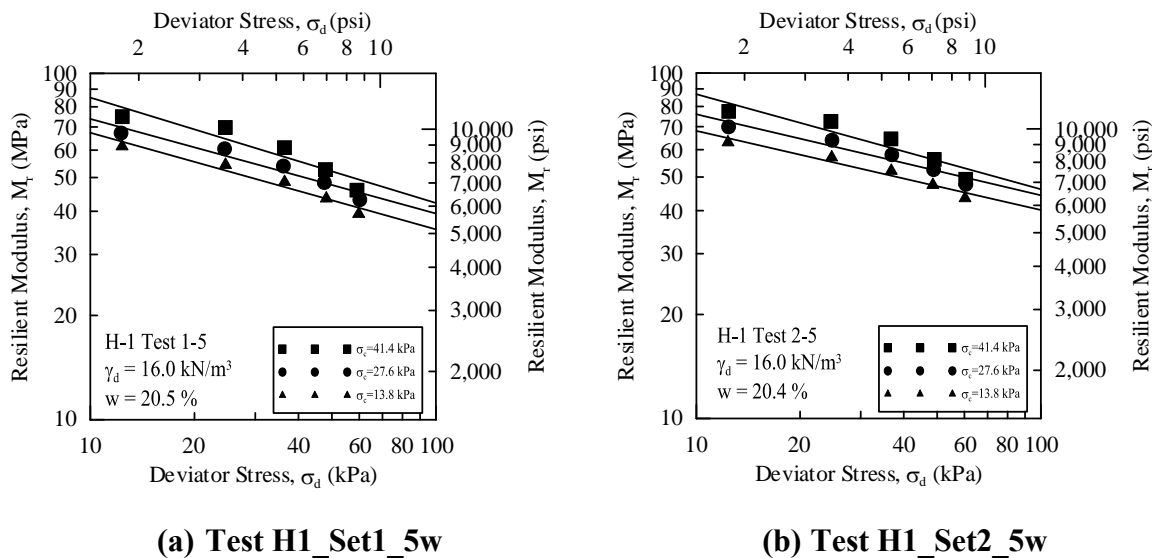


**Figure B.9: Results of repeated load triaxial test for soil Highland-1 compacted at 95% of  $\gamma_{dmax}$  and wet of  $w_{opt}$ , target compaction value of  $\gamma_d = 16.0 \text{ kN/m}^3$  and  $w = 21.0\%$**

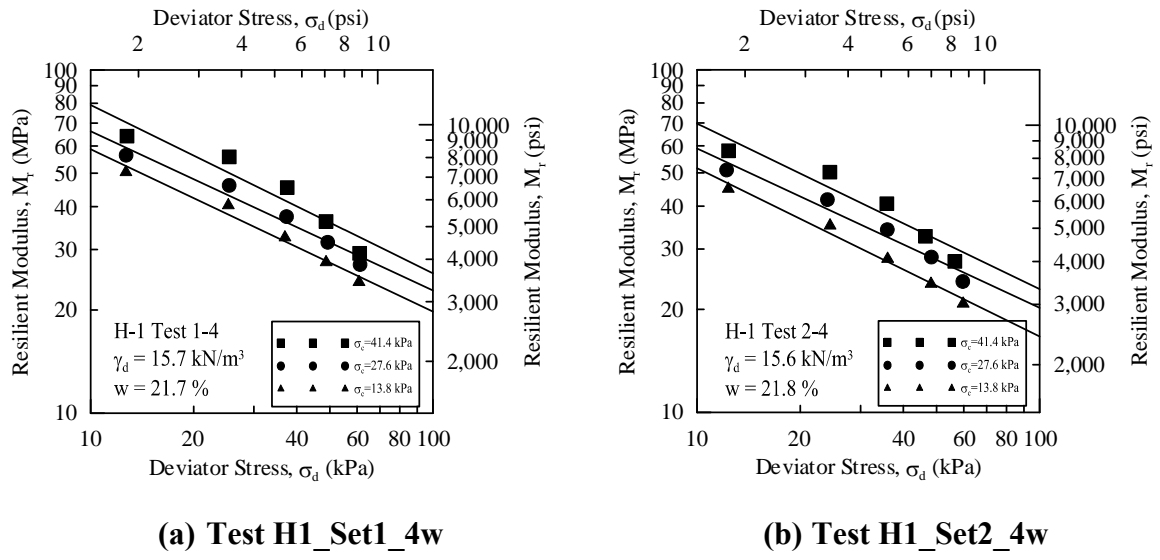


**Figure B.10: Results of repeated load triaxial test for soil Highland-1 compacted at 93% of  $\gamma_{dmax}$  and wet of  $w_{opt}$ , target compaction value of  $\gamma_d = 15.6 \text{ kN/m}^3$  and  $w = 22.5\%$**

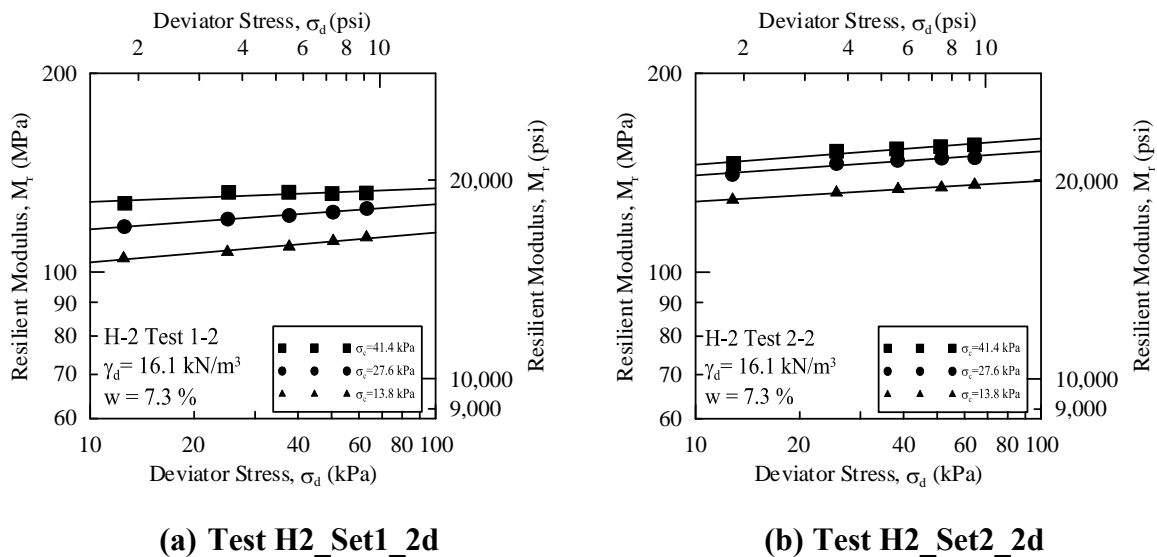


**Figure B.11: Results of repeated load triaxial test for soil Highland-2 compacted at 93% of  $\gamma_{dmax}$  and dry of  $w_{opt}$ , target compaction value of  $\gamma_d = 16.1 \text{ kN/m}^3$  and  $w = 7.5\%$**

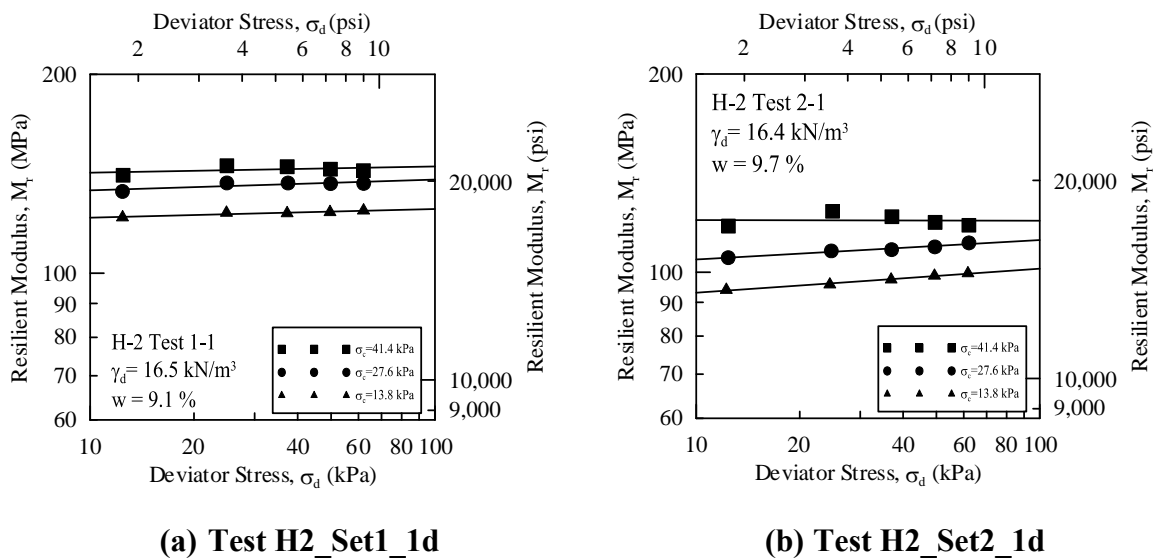


**Figure B.12: Results of repeated load triaxial test for soil Highland-2 compacted at 95% of  $\gamma_{dmax}$  and dry of  $w_{opt}$ , target compaction value of  $\gamma_d = 16.5 \text{ kN/m}^3$  and  $w = 9.5\%$**

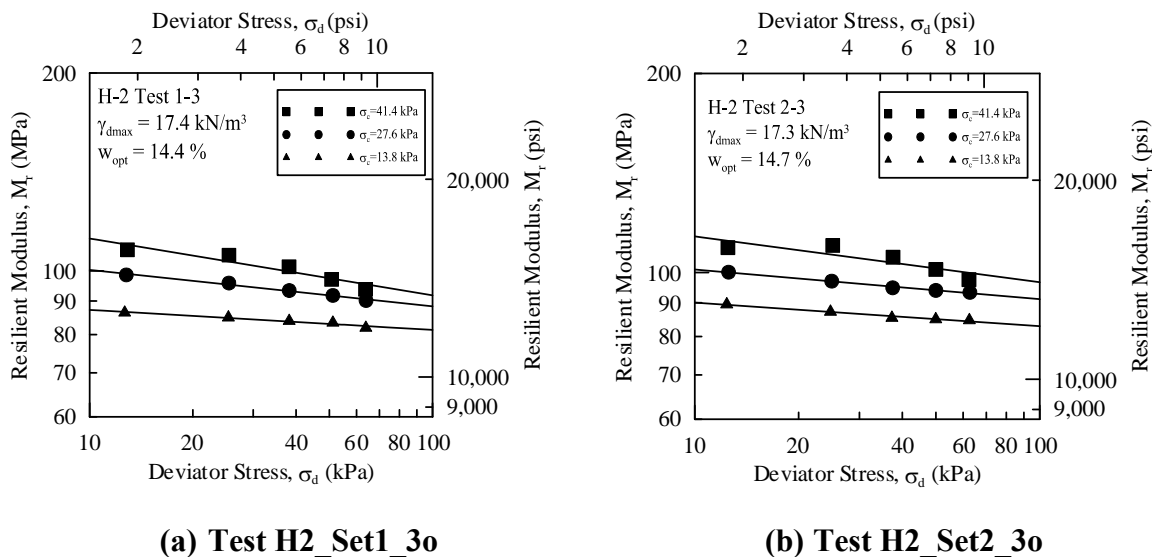


**Figure B.13: Results of repeated load triaxial test for soil Highland-2 compacted at  $\gamma_{dmax}$  and  $w_{opt}$ , target compaction value of  $\gamma_d = 17.3 \text{ kN/m}^3$  and  $w = 15.0\%$**

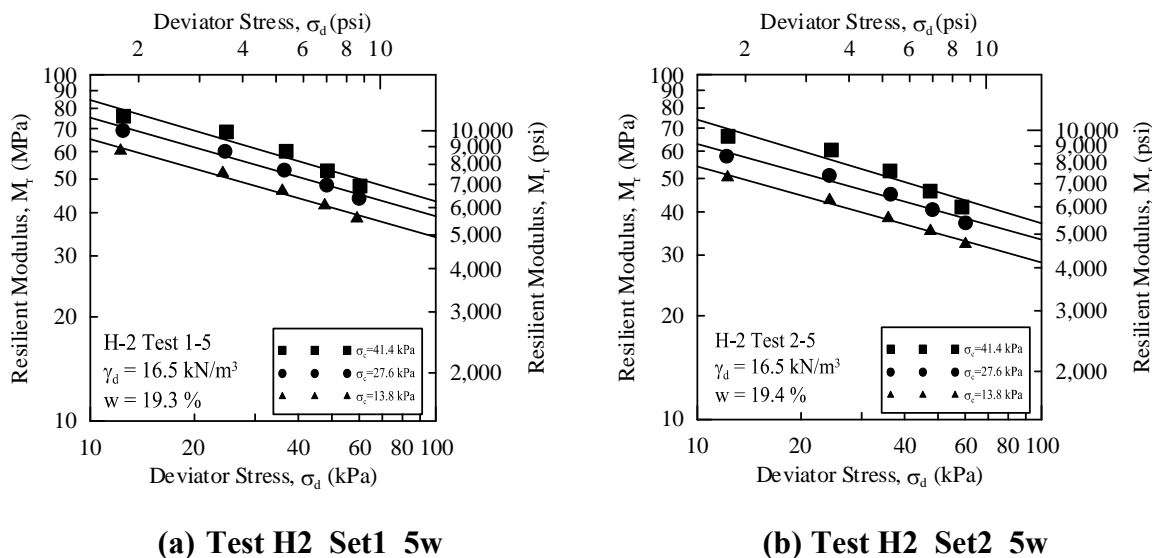
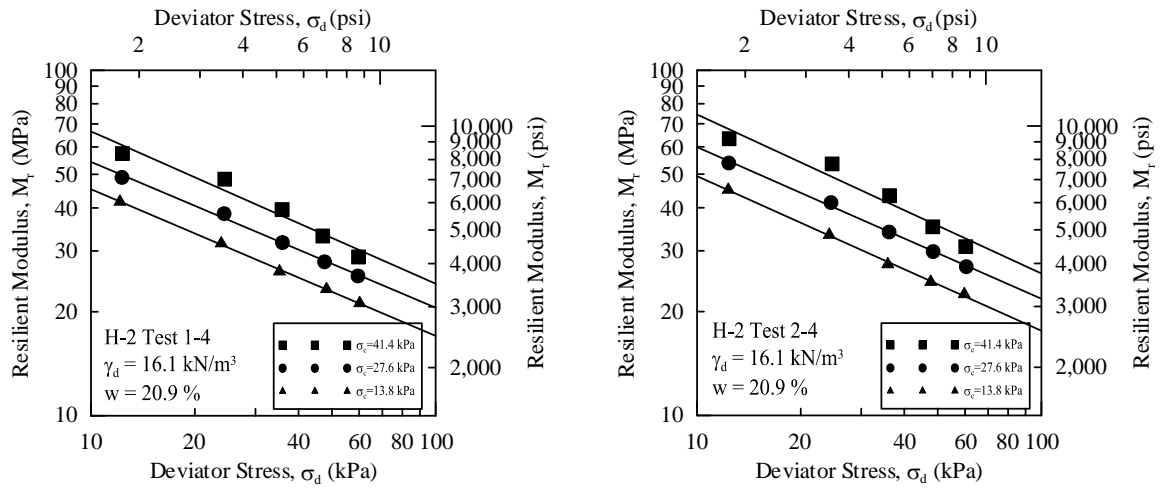


**Figure B.14: Results of repeated load triaxial test for soil Highland-2 compacted at 95% of  $\gamma_{dmax}$  and wet of  $w_{opt}$ , target compaction value of  $\gamma_d = 16.5 \text{ kN/m}^3$  and  $w = 19.5\%$**



(a) Test H2\_Set1\_4w

(b) Test H2\_Set2\_4w

**Figure B.15: Results of repeated load triaxial test for soil Highland-2 compacted at 93% of  $\gamma_{dmax}$  and wet of  $w_{opt}$ , target compaction value of  $\gamma_d = 16.1 \text{ kN/m}^3$  and  $w = 21.0\%$**

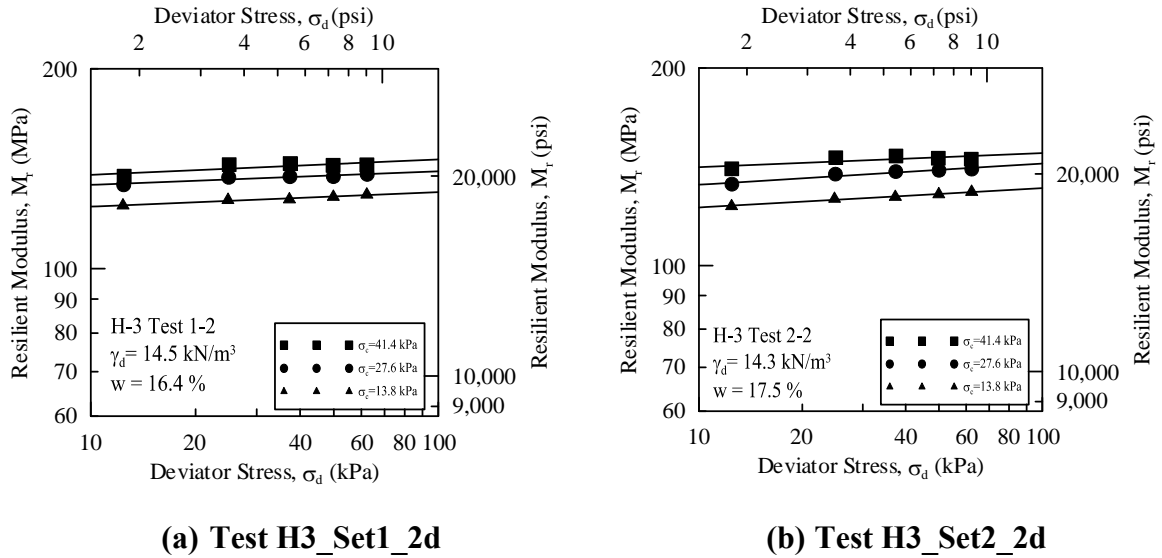


**Figure B.16: Results of repeated load triaxial test for soil Highland-3 compacted at 93% of  $\gamma_{dmax}$  and dry of  $w_{opt}$ , target compaction value of  $\gamma_d = 14.4 \text{ kN/m}^3$  and  $w = 17.5\%$**

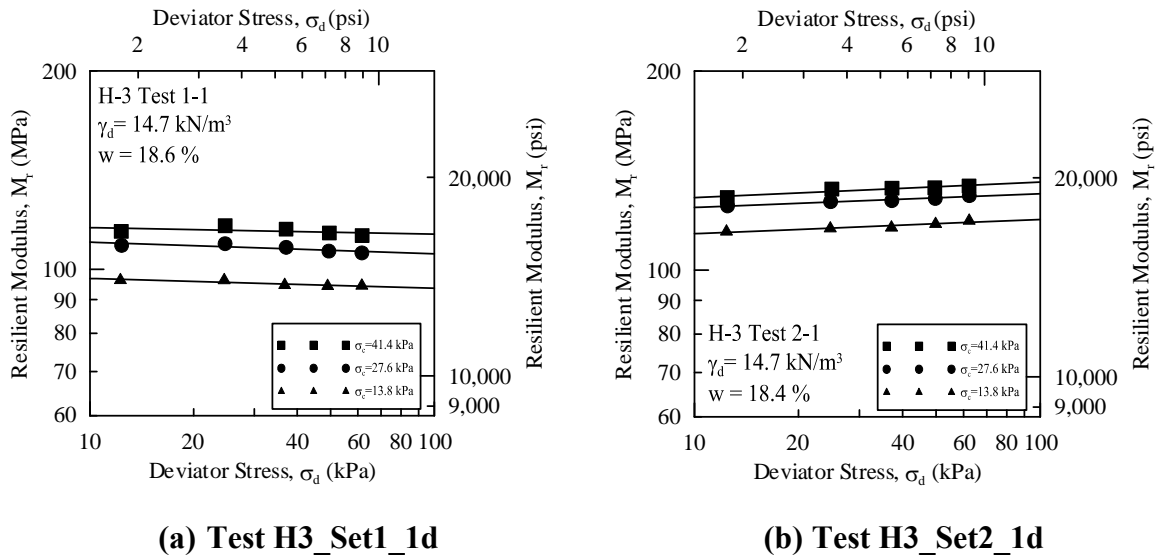


**Figure B.17: Results of repeated load triaxial test for soil Highland-3 compacted at 95% of  $\gamma_{dmax}$  and dry of  $w_{opt}$ , target compaction value of  $\gamma_d = 14.7 \text{ kN/m}^3$  and  $w = 19.0\%$**

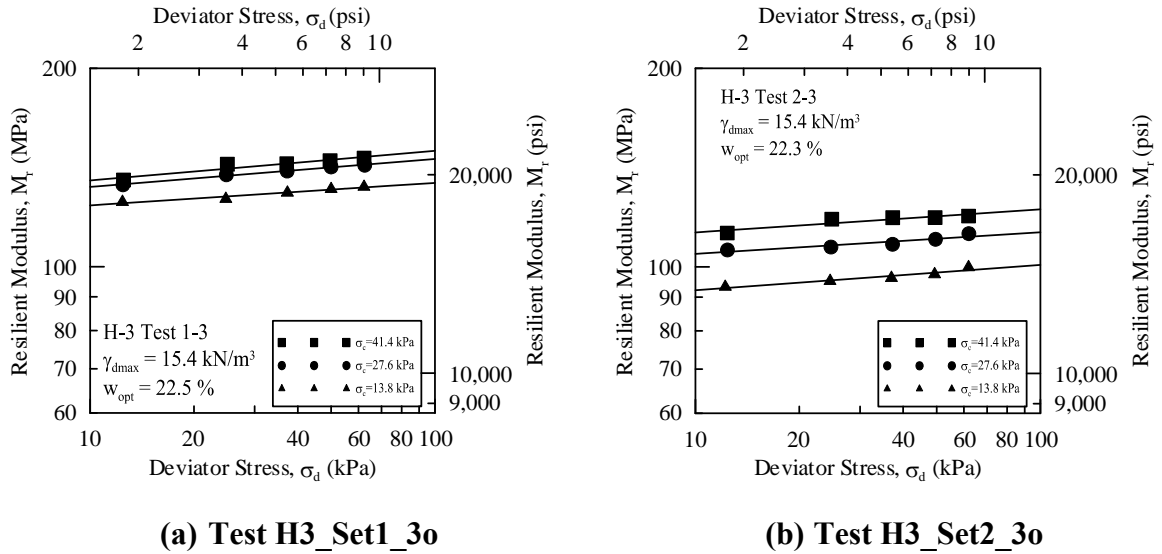


**Figure B.18: Results of repeated load triaxial test for soil Highland-3 compacted at  $\gamma_{dmax}$  and  $w_{opt}$ , target compaction value of  $\gamma_d = 15.4 \text{ kN/m}^3$  and  $w = 22.5\%$**

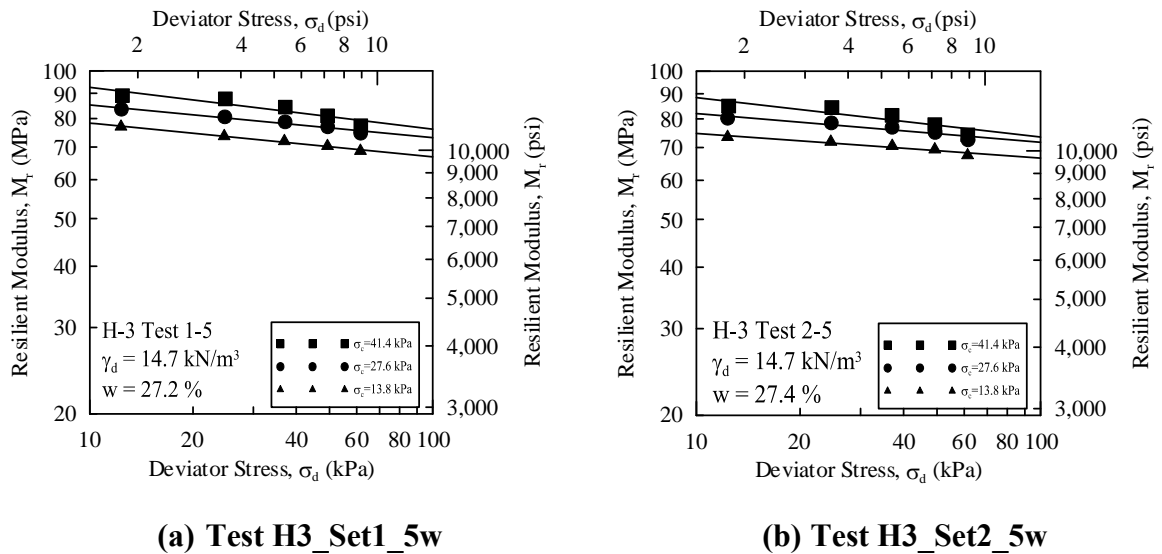
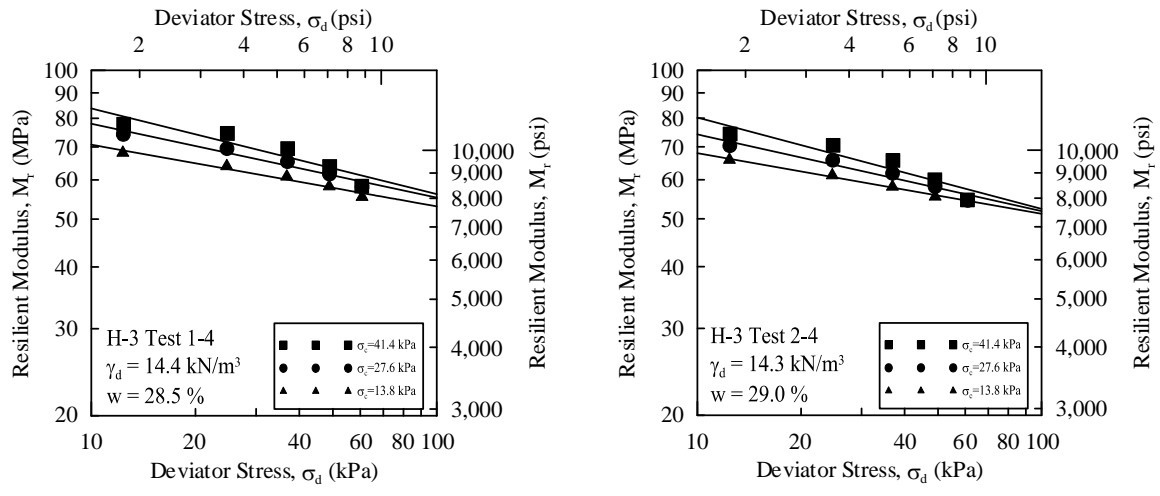


**Figure B.19: Results of repeated load triaxial test for soil Highland-3 compacted at 95% of  $\gamma_{dmax}$  and wet of  $w_{opt}$ , target compaction value of  $\gamma_d = 14.7 \text{ kN/m}^3$  and  $w = 27.8\%$**



(a) Test H3\_Set1\_4w

(b) Test H3\_Set2\_4w

**Figure B.20: Results of repeated load triaxial test for soil Highland-3 compacted at 93% of  $\gamma_{dmax}$  and wet of  $w_{opt}$ , target compaction value of  $\gamma_d = 14.4 \text{ kN/m}^3$  and  $w = 29.0\%$**

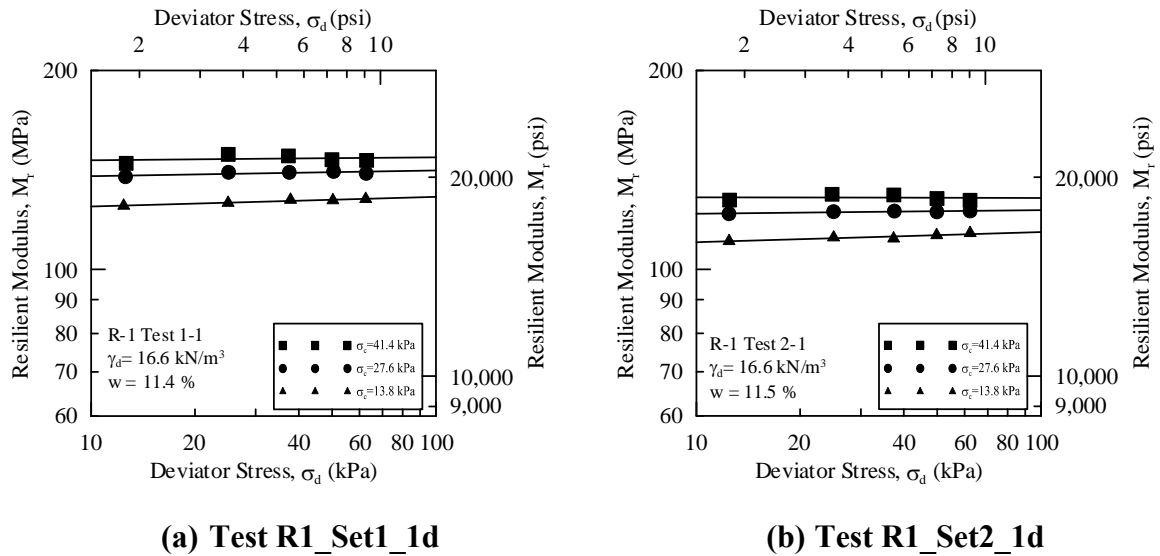


**Figure B.21: Results of repeated load triaxial test for soil Racine-1 compacted at 95% of  $\gamma_{dmax}$  and dry of  $w_{opt}$ , target compaction value of  $\gamma_d = 16.5 \text{ kN/m}^3$  and  $w = 12.0\%$**

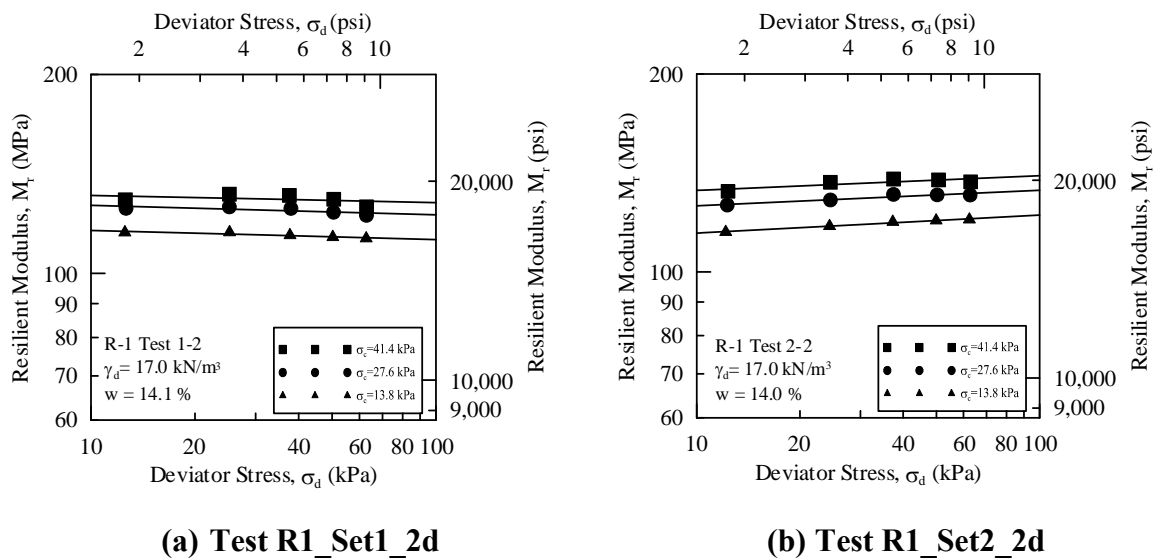


**Figure B.22: Results of repeated load triaxial test for soil Racine-1 compacted at 98% of  $\gamma_{dmax}$  and dry of  $w_{opt}$ , target compaction value of  $\gamma_d = 17.0 \text{ kN/m}^3$  and  $w = 14.3\%$**

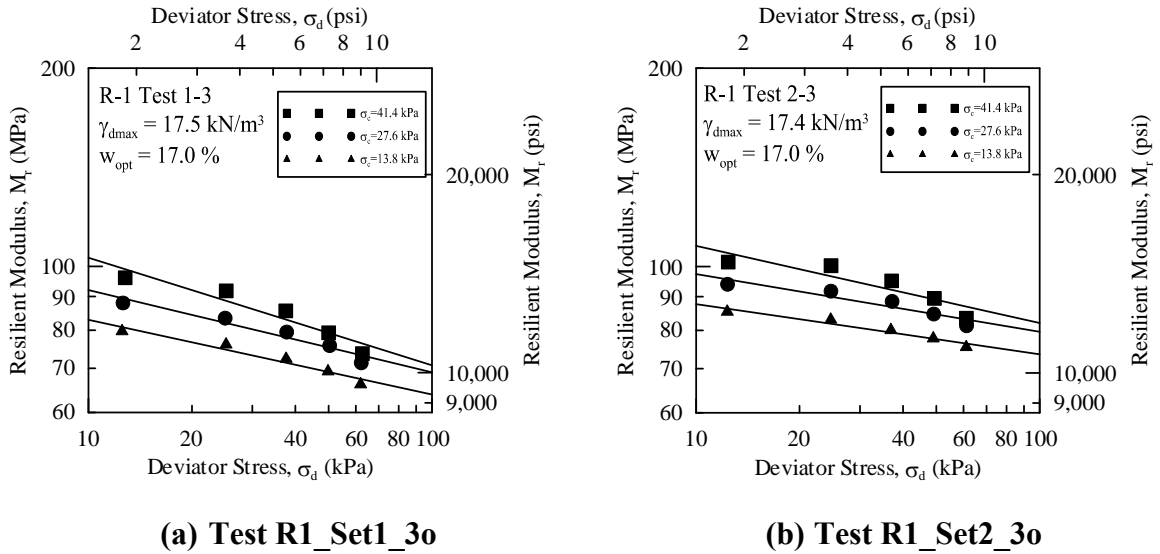


**Figure B.23: Results of repeated load triaxial test for soil Racine-1 compacted at  $\gamma_{dmax}$  and  $w_{opt}$ , target compaction value of  $\gamma_d = 17.4 \text{ kN/m}^3$  and  $w = 17.0\%$**

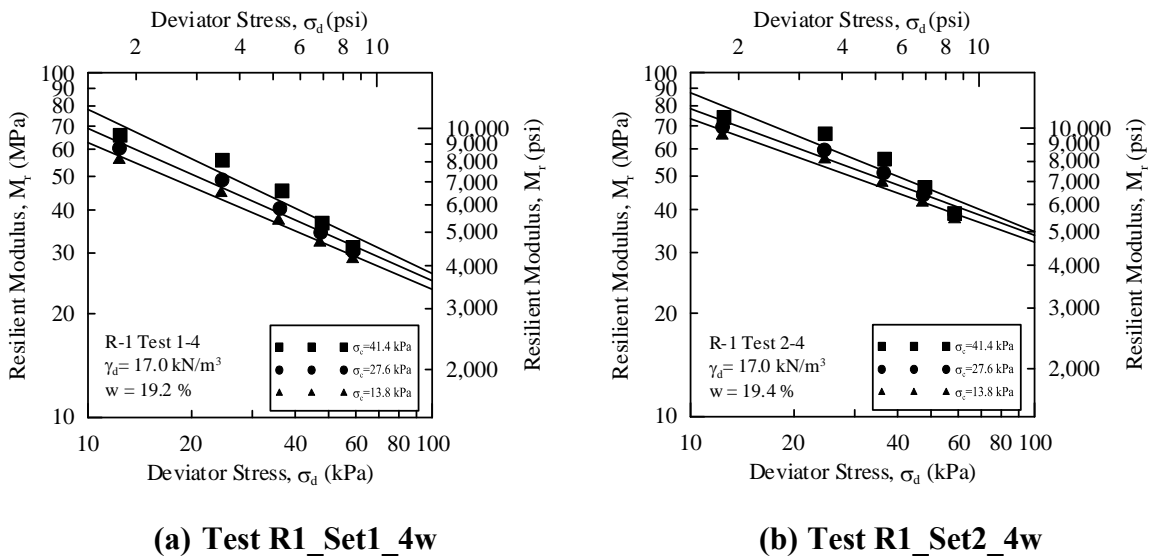


**Figure B.24: Results of repeated load triaxial test for soil Racine-1 compacted at 98% of  $\gamma_{dmax}$  and wet of  $w_{opt}$ , target compaction value of  $\gamma_d = 17.0 \text{ kN/m}^3$  and  $w = 19.3\%$**

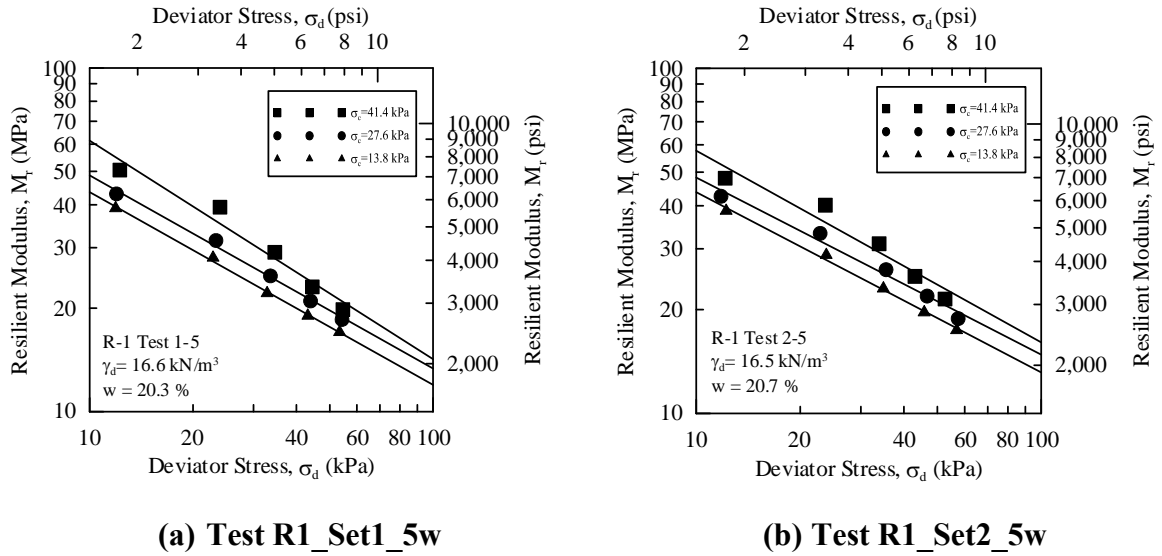
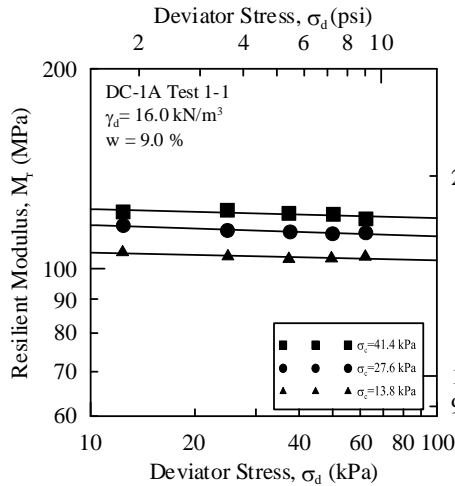
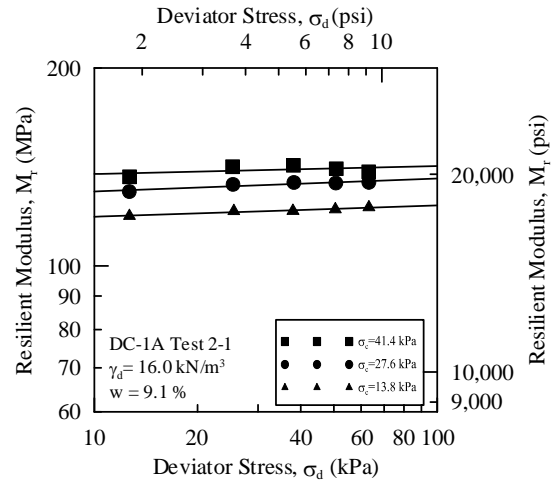


**Figure B.25: Results of repeated load triaxial test for soil Racine-1 compacted at 95% of  $\gamma_{dmax}$  and wet of  $w_{opt}$ , target compaction value of  $\gamma_d = 16.5 \text{ kN/m}^3$  and  $w = 21.0\%$**

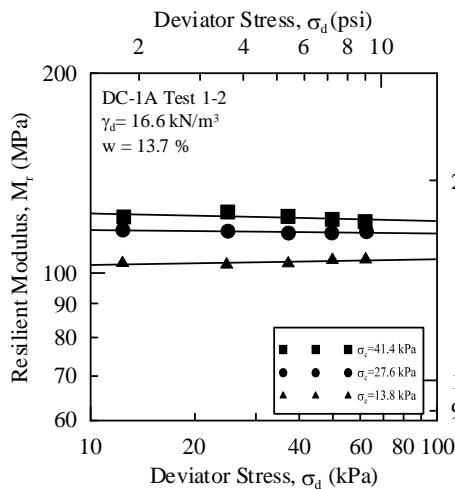


(a) Test DC-1A\_Set1\_1d

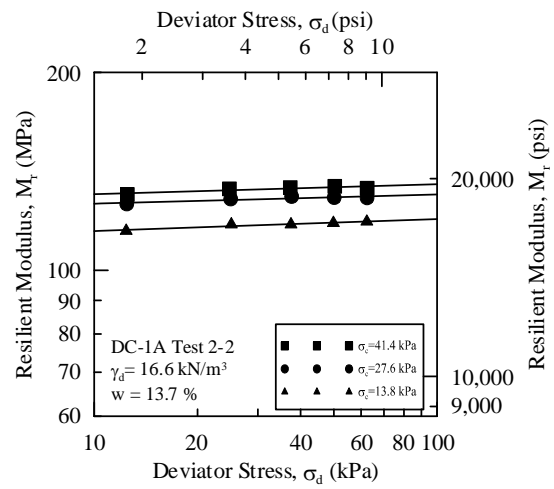


(b) Test DC-1A\_Set2\_1d

**Figure B.26: Results of repeated load triaxial test for soil Deer Creek-1A compacted at 95% of  $\gamma_{dmax}$  and dry of  $w_{opt}$ , target compaction value of  $\gamma_d = 16.0 \text{ kN/m}^3$  and  $w = 9.5\%$**



(a) Test DC-1A\_Set1\_2d



(b) Test DC-1A\_Set2\_2d

**Figure B.27: Results of repeated load triaxial test for soil Deer Creek-1A compacted at 98% of  $\gamma_{dmax}$  and dry of  $w_{opt}$ , target compaction value of  $\gamma_d = 16.5 \text{ kN/m}^3$  and  $w = 14.0\%$**

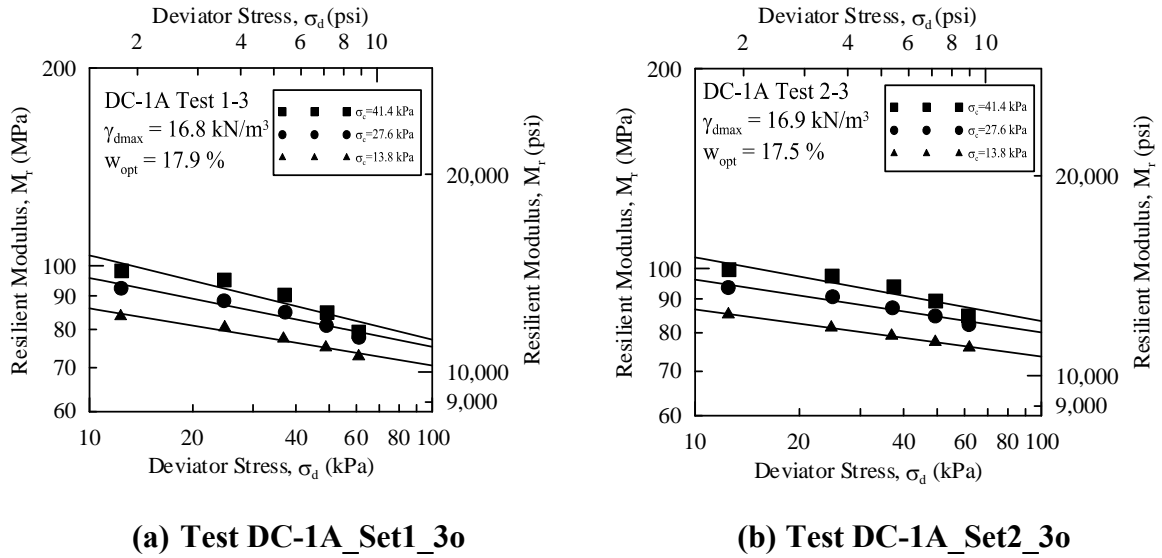


**Figure B.28: Results of repeated load triaxial test for soil Deer Creek-1A compacted at  $\gamma_{dmax}$  and  $w_{opt}$ , target compaction value of  $\gamma_d = 16.8 \text{ kN/m}^3$  and  $w = 18.0\%$**

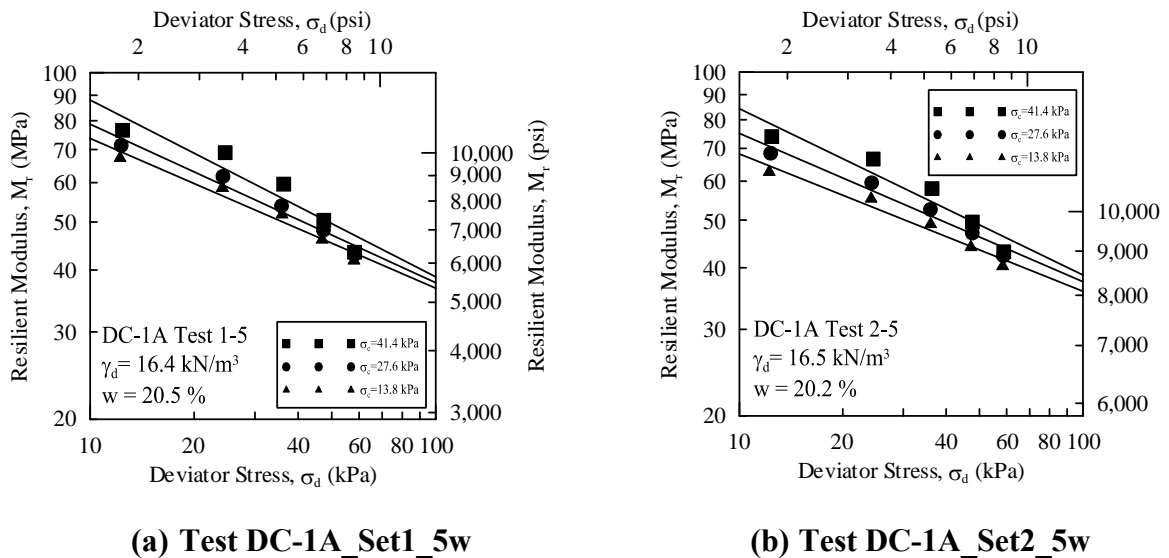
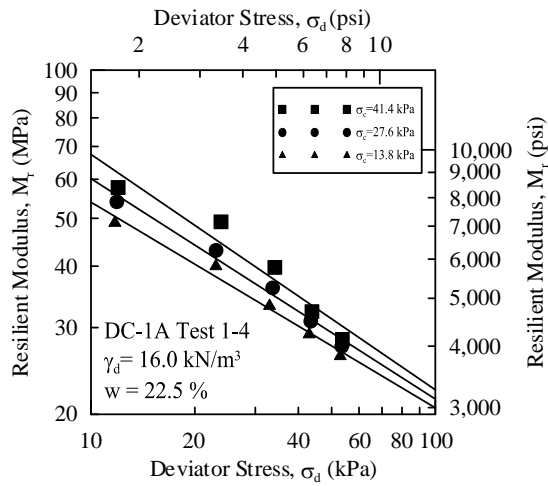
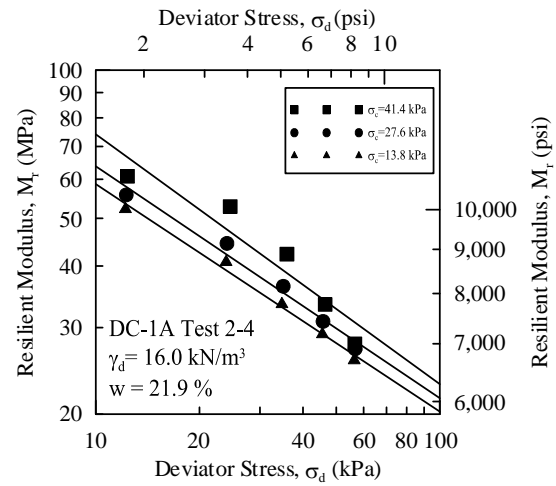


**Figure B.29: Results of repeated load triaxial test for soil Deer Creek-1A compacted at 98% of  $\gamma_{dmax}$  and wet of  $w_{opt}$ , target compaction value of  $\gamma_d = 16.5 \text{ kN/m}^3$  and  $w = 20.5\%$**

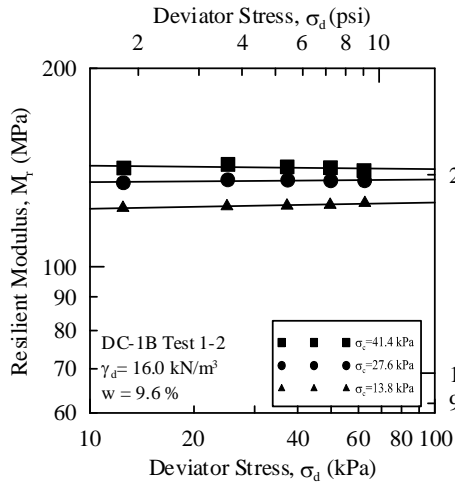


(a) Test DC-1A\_Set1\_4w

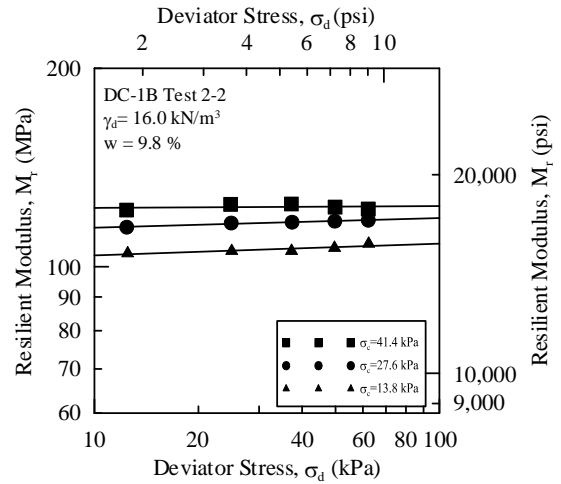


(b) Test DC-1A\_Set2\_4w

**Figure B.30: Results of repeated load triaxial test for soil Deer Creek-1A compacted at 95% of  $\gamma_{dmax}$  and wet of  $w_{opt}$ , target compaction value of  $\gamma_d = 16.0 \text{ kN/m}^3$  and  $w = 22.5\%$**

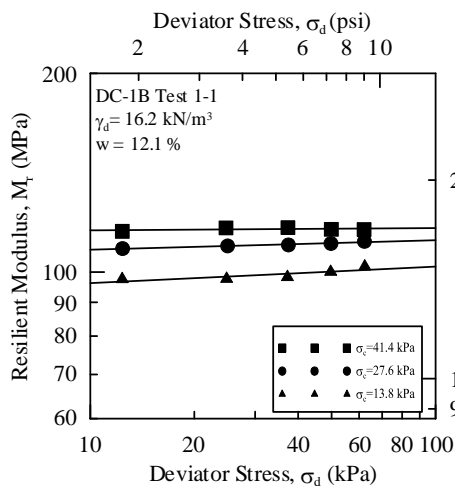


(a) Test DC-1B\_Set1\_2d

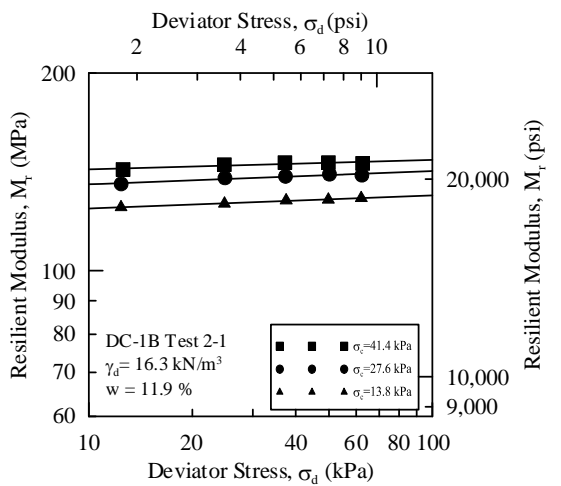


(b) Test DC-1B\_Set2\_2d

**Figure B.31: Results of repeated load triaxial test for soil Deer Creek-1B compacted at 93% of  $\gamma_{dmax}$  and dry of  $w_{opt}$ , target compaction value of  $\gamma_d = 15.9 \text{ kN/m}^3$  and  $w = 10.0\%$**



(a) Test DC-1B\_Set1\_1d



(b) Test DC-1B\_Set2\_1d

**Figure B.32: Results of repeated load triaxial test for soil Deer Creek-1B compacted at 95% of  $\gamma_{dmax}$  and dry of  $w_{opt}$ , target compaction value of  $\gamma_d = 16.3 \text{ kN/m}^3$  and  $w = 12.0\%$**

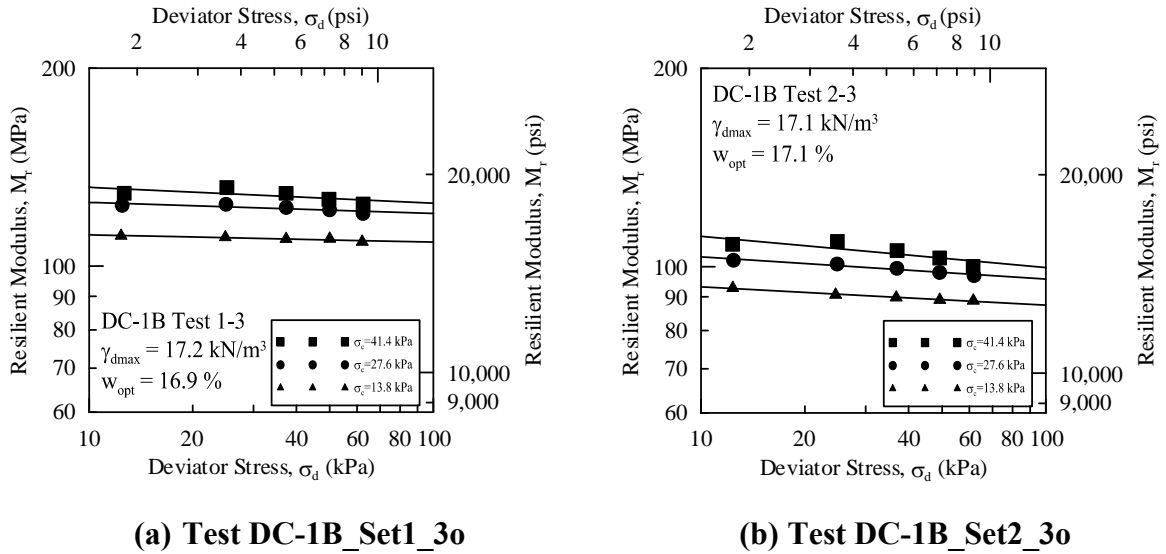


**Figure B.33: Results of repeated load triaxial test for soil Deer Creek-1B compacted at  $\gamma_{dmax}$  and  $w_{opt}$ , target compaction value of  $\gamma_d = 17.1 \text{ kN/m}^3$  and  $w = 17.6\%$**

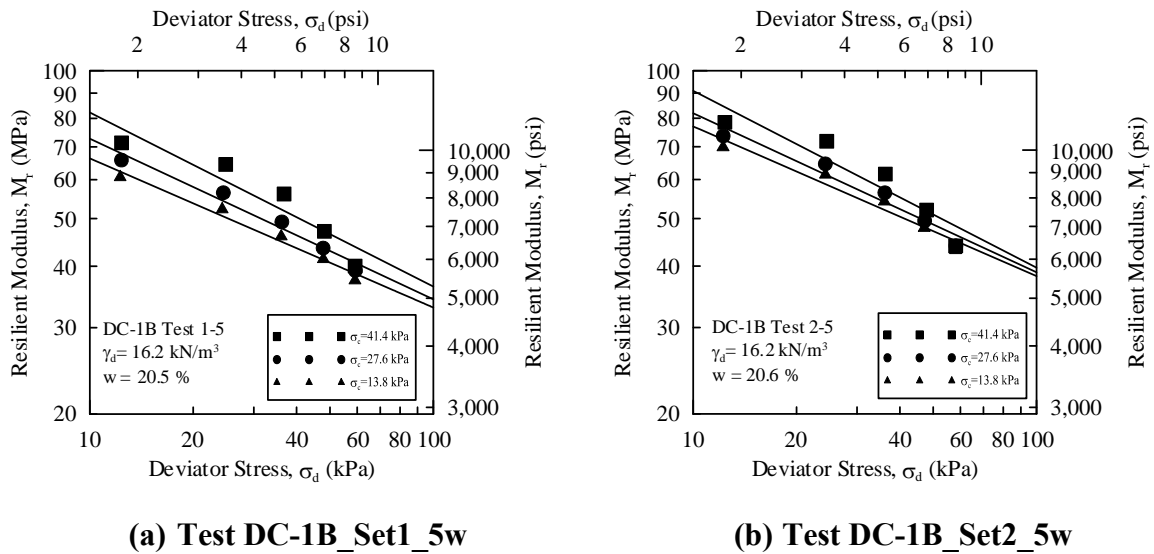
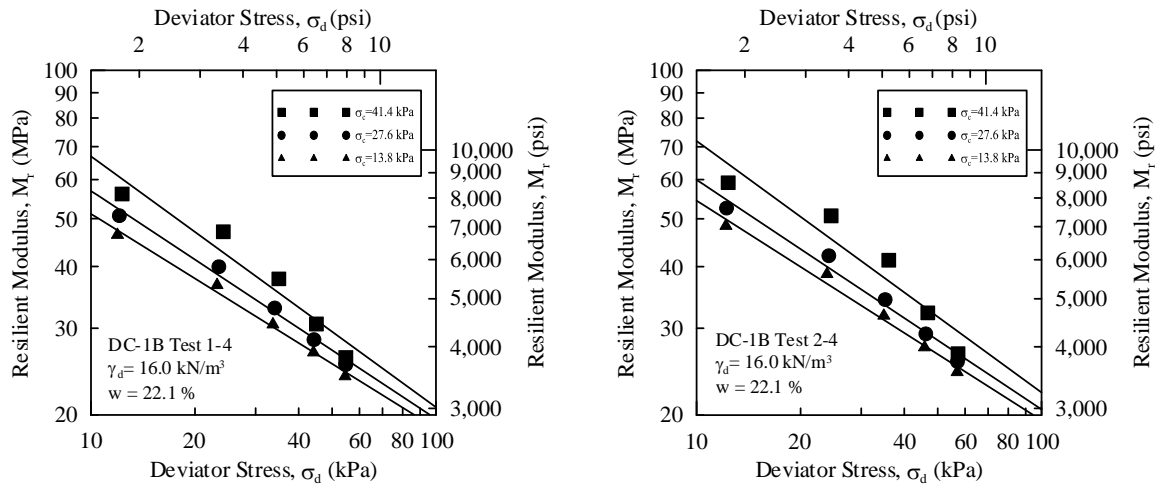


**Figure B.34: Results of repeated load triaxial test for soil Deer Creek-1B compacted at 95% of  $\gamma_{dmax}$  and wet of  $w_{opt}$ , target compaction value of  $\gamma_d = 16.3 \text{ kN/m}^3$  and  $w = 20.5\%$**



(a) Test DC-1B\_Set1\_4w

(b) Test DC-1B\_Set2\_4w

**Figure B.35: Results of repeated load triaxial test for soil Deer Creek-1B compacted at 93% of  $\gamma_{dmax}$  and wet of  $w_{opt}$ , target compaction value of  $\gamma_d = 15.9$  kN/m<sup>3</sup> and  $w = 22.5\%$**

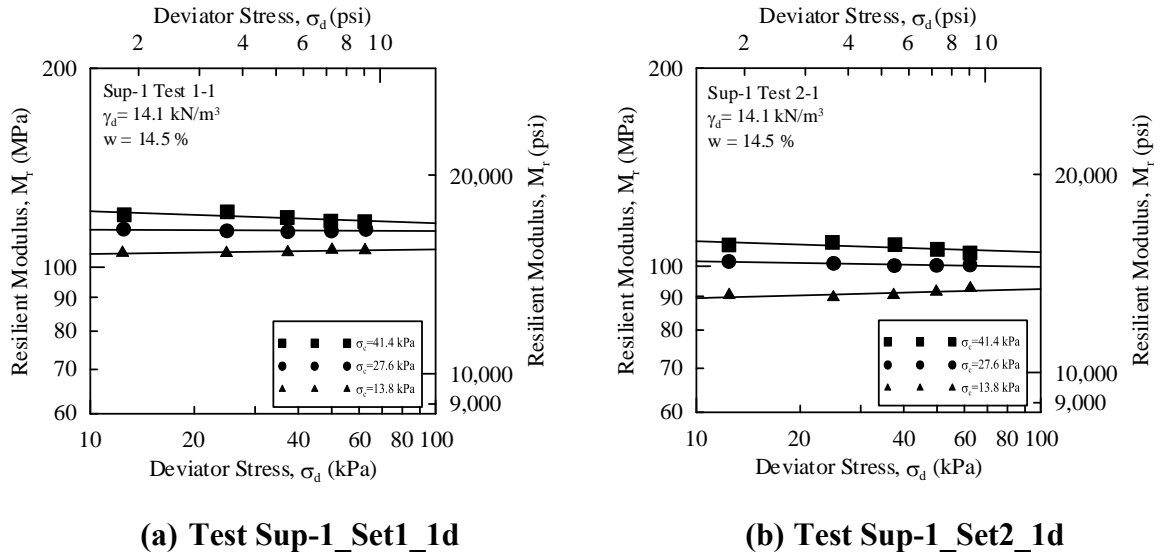


**Figure B.36: Results of repeated load triaxial test for soil Superior-1 compacted at 95% of  $\gamma_{dmax}$  and dry of  $w_{opt}$ , target compaction value of  $\gamma_d = 14.1 \text{ kN/m}^3$  and  $w = 15.0\%$**

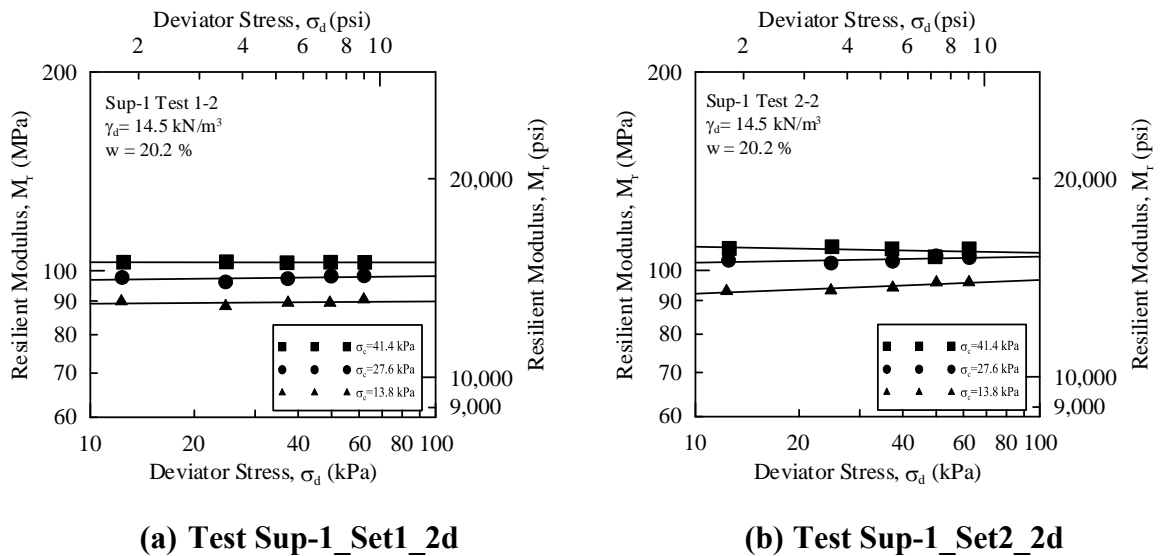


**Figure B.37: Results of repeated load triaxial test for soil Superior-1 compacted at 98% of  $\gamma_{dmax}$  and dry of  $w_{opt}$ , target compaction value of  $\gamma_d = 14.5 \text{ kN/m}^3$  and  $w = 20.5\%$**

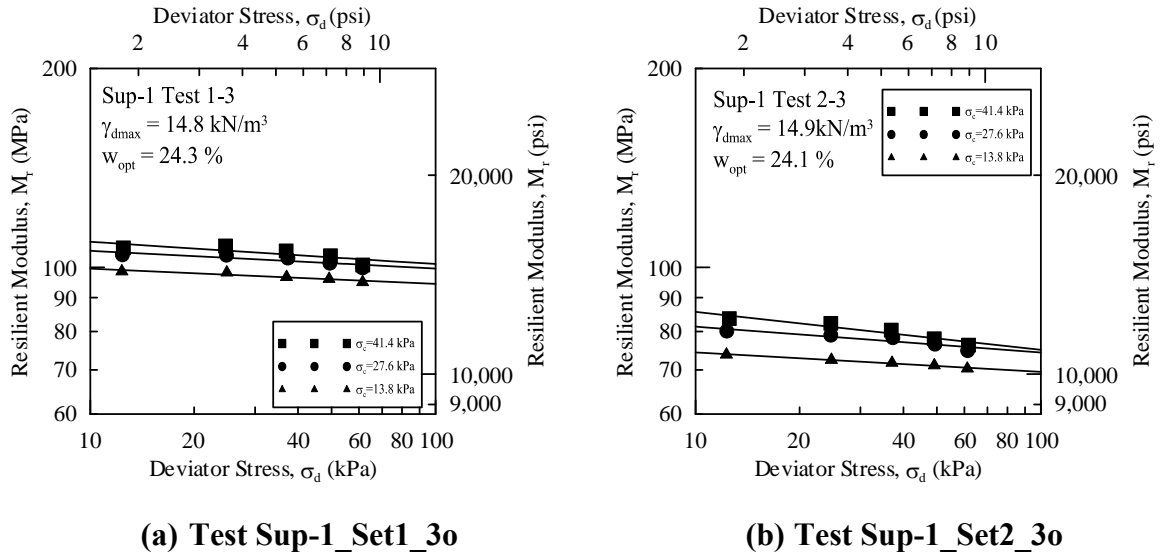


**Figure B.38: Results of repeated load triaxial test for soil Superior-1 compacted at  $\gamma_{dmax}$  and  $w_{opt}$ , target compaction value of  $\gamma_d = 14.8 \text{ kN/m}^3$  and  $w = 24.8\%$**

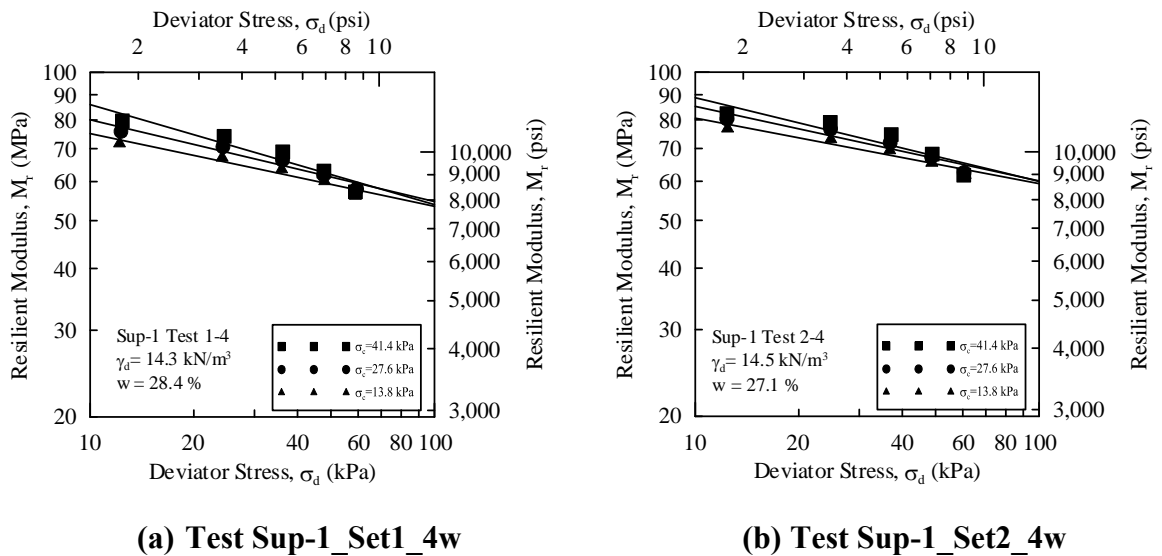
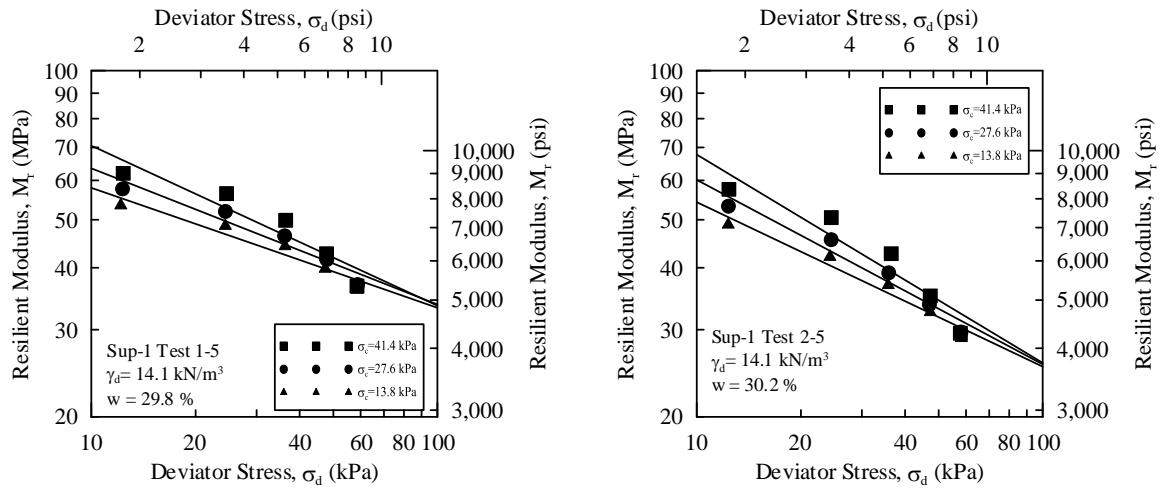


**Figure B.39: Results of repeated load triaxial test for soil Superior-1 compacted at 98% of  $\gamma_{dmax}$  and wet of  $w_{opt}$ , target compaction value of  $\gamma_d = 14.5 \text{ kN/m}^3$  and  $w = 27.5\%$**



(a) Test Sup-1\_Set1\_5w

(b) Test Sup-1\_Set2\_5w

**Figure B.40: Results of repeated load triaxial test for soil Superior-1 compacted at 95% of  $\gamma_{dmax}$  and wet of  $w_{opt}$ , target compaction value of  $\gamma_d = 14.1 \text{ kN/m}^3$  and  $w = 30.5\%$**

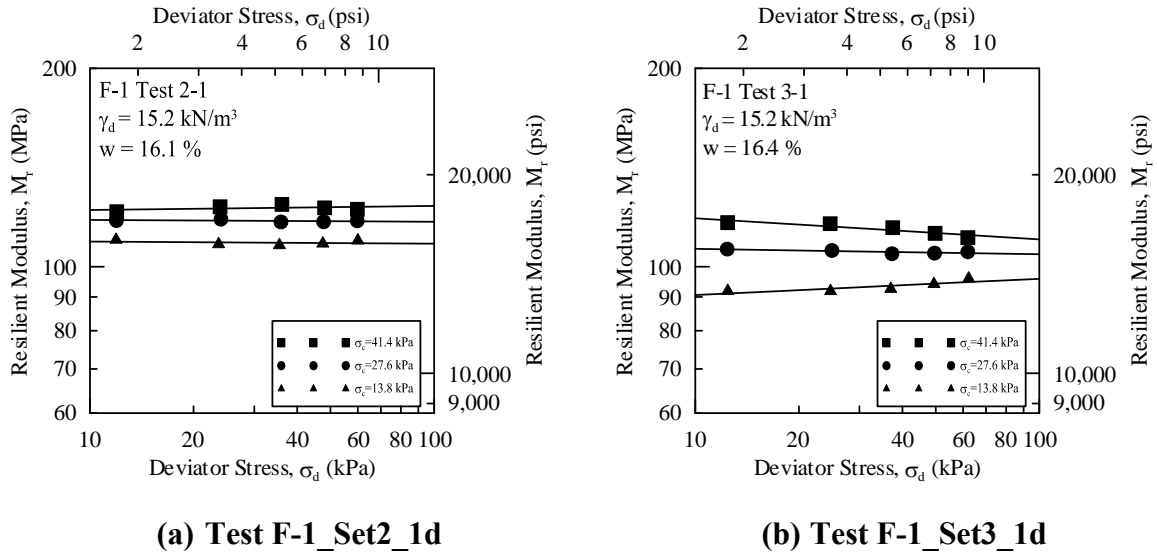


**Figure B.41: Results of repeated load triaxial test for soil Fond du Lac-1 compacted at 94% of  $\gamma_{dmax}$  and dry of  $w_{opt}$ , target compaction value of  $\gamma_d = 15.1 \text{ kN/m}^3$  and  $w = 17.0\%$**

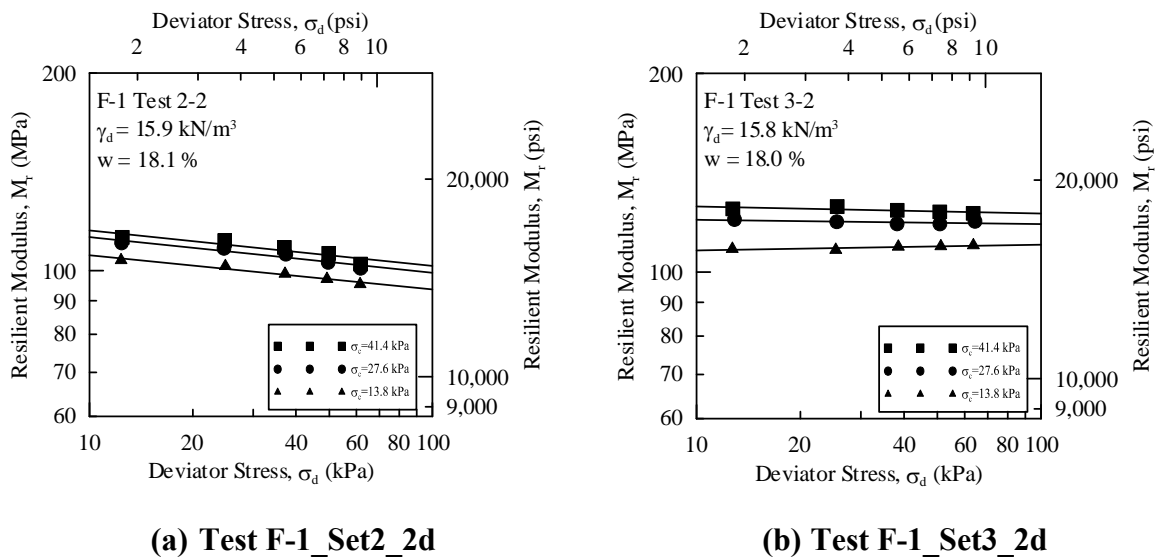


**Figure B.42: Results of repeated load triaxial test for soil Fond du Lac-1 compacted at 98% of  $\gamma_{dmax}$  and dry of  $w_{opt}$ , target compaction value of  $\gamma_d = 15.7 \text{ kN/m}^3$  and  $w = 19.0\%$**

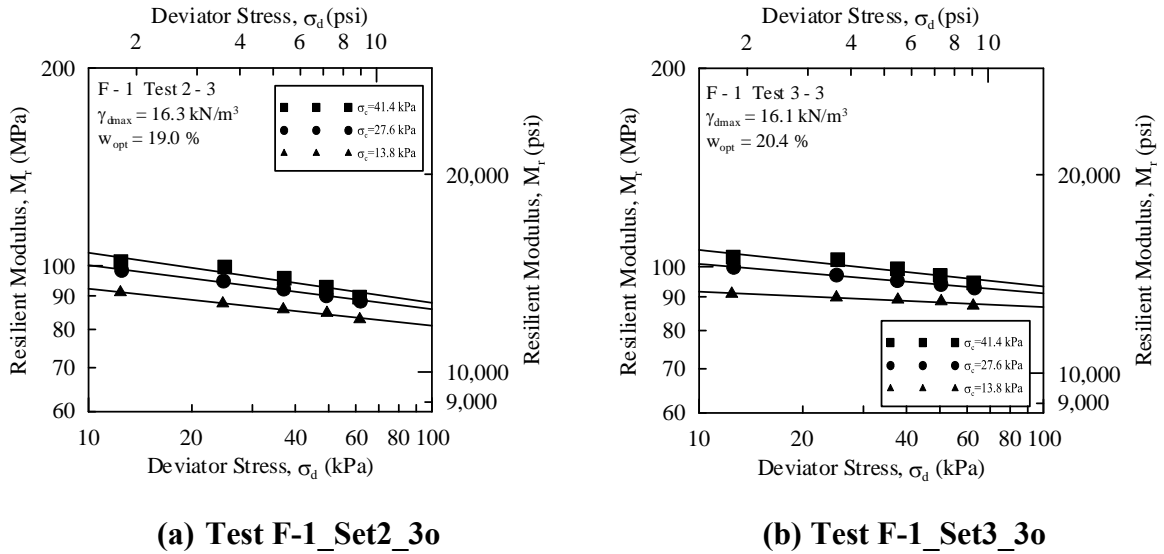


**Figure B.43: Results of repeated load triaxial test for soil Fond du Lac-1 compacted at  $\gamma_{dmax}$  and  $w_{opt}$ , target compaction value of  $\gamma_d = 16.0 \text{ kN/m}^3$  and  $w = 21.0\%$**

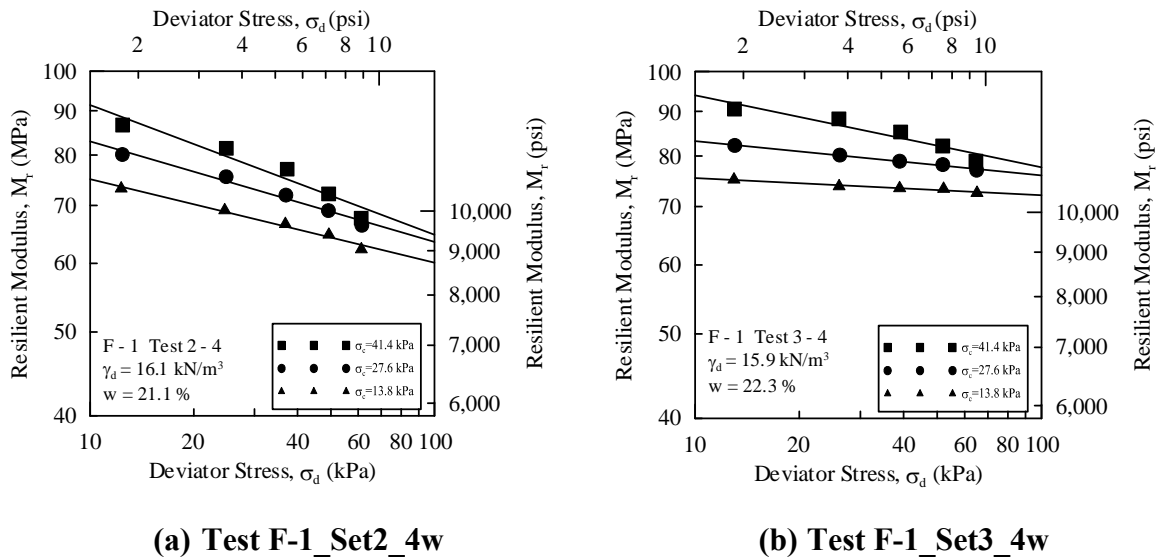


**Figure B.44: Results of repeated load triaxial test for soil Fond du Lac-1 compacted at 99% of  $\gamma_{dmax}$  and wet of  $w_{opt}$ , target compaction value of  $\gamma_d = 15.9 \text{ kN/m}^3$  and  $w = 23.0\%$**

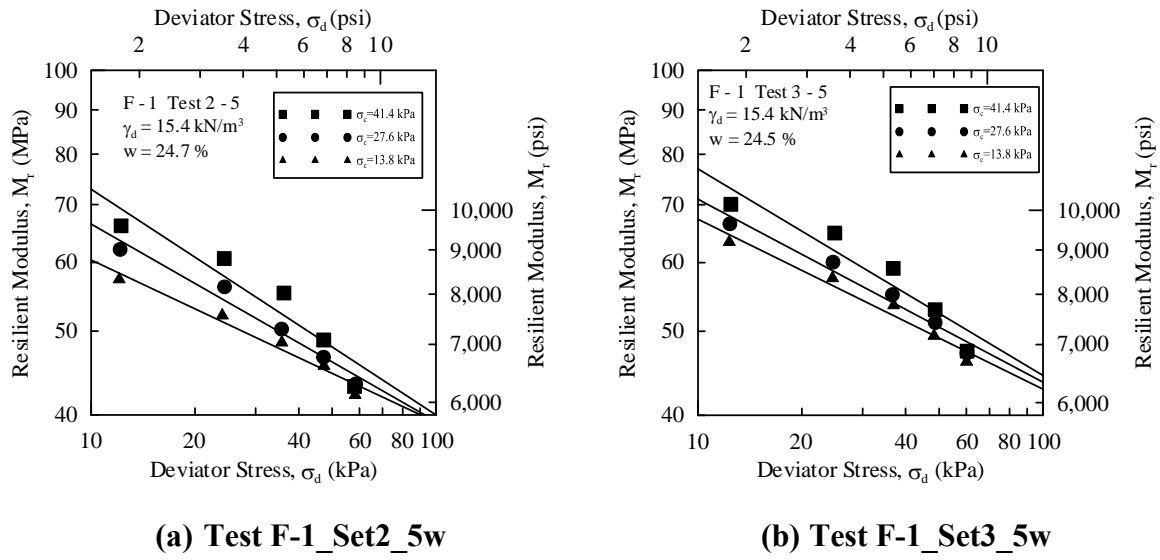


**Figure B.45: Results of repeated load triaxial test for soil Fond du Lac-1 compacted at 96% of  $\gamma_{dmax}$  and wet of  $w_{opt}$ , target compaction value of  $\gamma_d = 15.4 \text{ kN/m}^3$  and  $w = 25.0\%$**

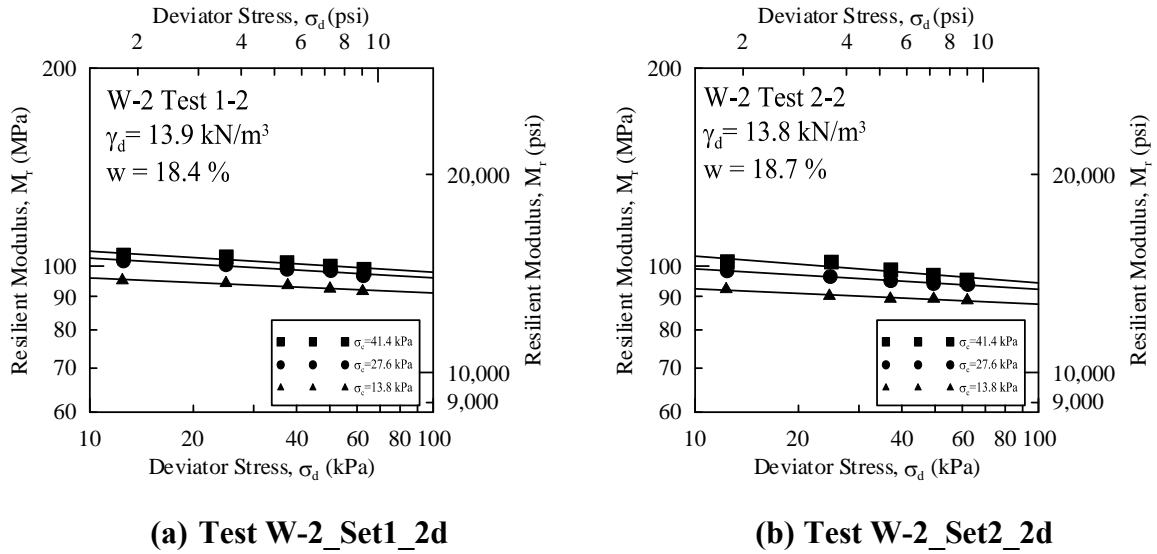


**Figure B.46: Results of repeated load triaxial test for soil Winnebago-2 compacted at 93% of  $\gamma_{dmax}$  and dry of  $w_{opt}$ , target compaction value of  $\gamma_d = 13.8$  kN/m<sup>3</sup> and  $w = 19.0\%$**

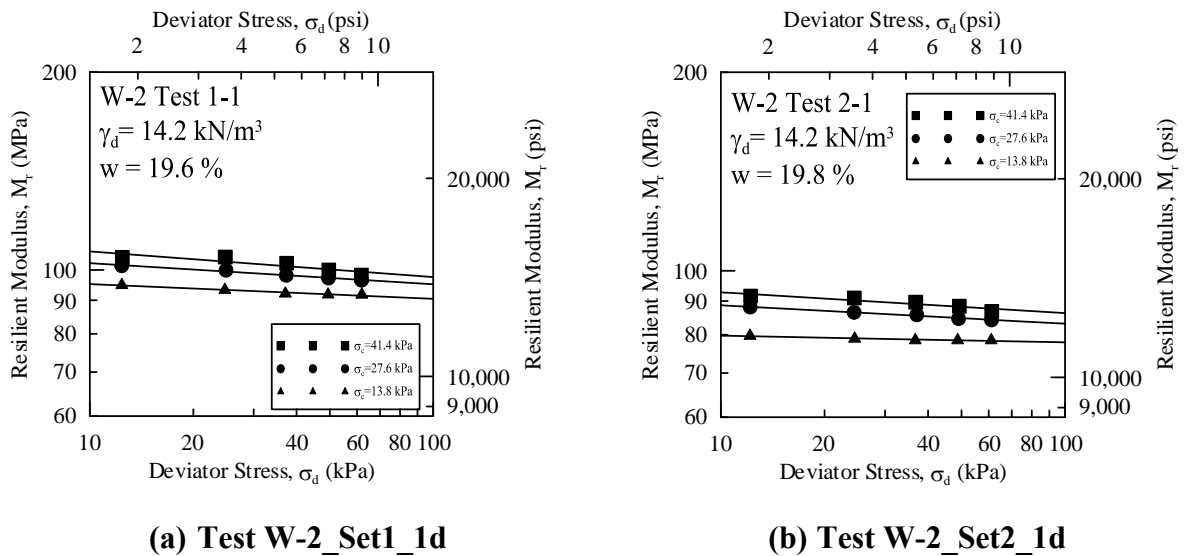
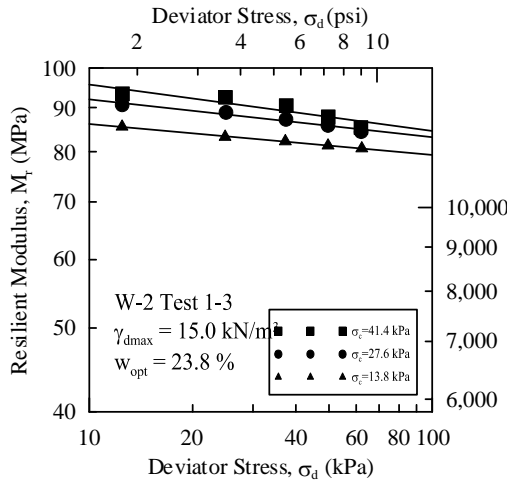
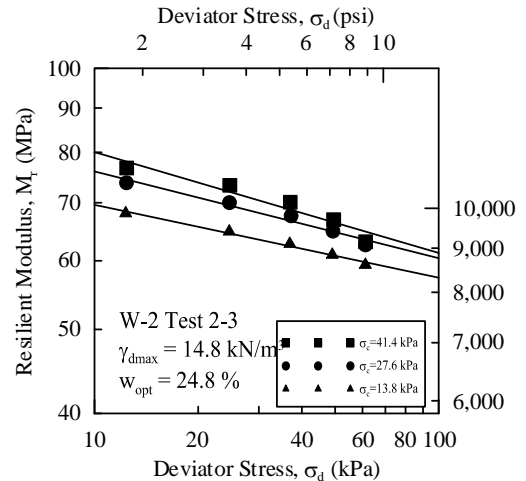


**Figure B.47: Results of repeated load triaxial test for soil Winnebago-2 compacted at 95% of  $\gamma_{dmax}$  and dry of  $w_{opt}$ , target compaction value of  $\gamma_d = 14.1$  kN/m<sup>3</sup> and  $w = 20.5\%$**

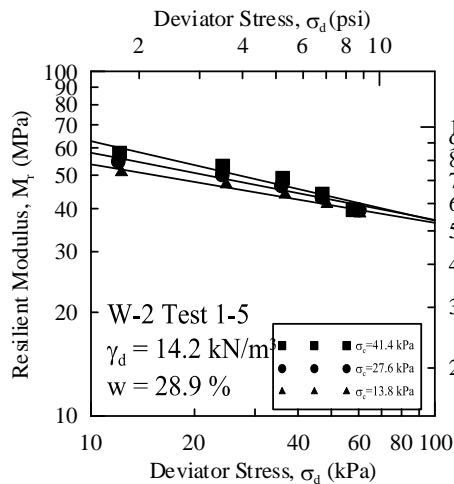


(a) Test W-2\_Set1\_3o

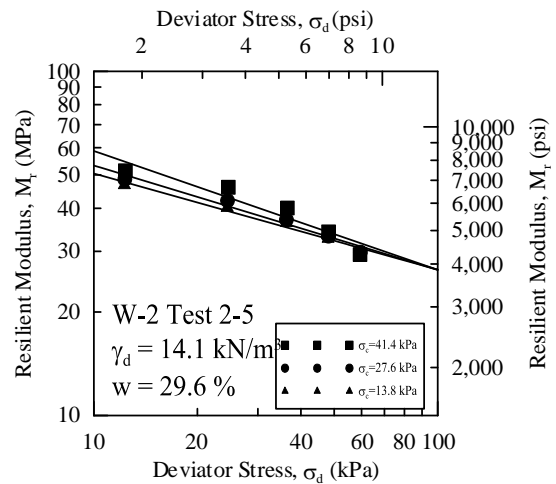


(b) Test W-2\_Set2\_3o

Figure B.48: Results of repeated load triaxial test for soil Winnebago-2 compacted at  $\gamma_{dmax}$  and  $w_{opt}$ , target compaction value of  $\gamma_d = 14.8 \text{ kN/m}^3$  and  $w = 24.8\%$

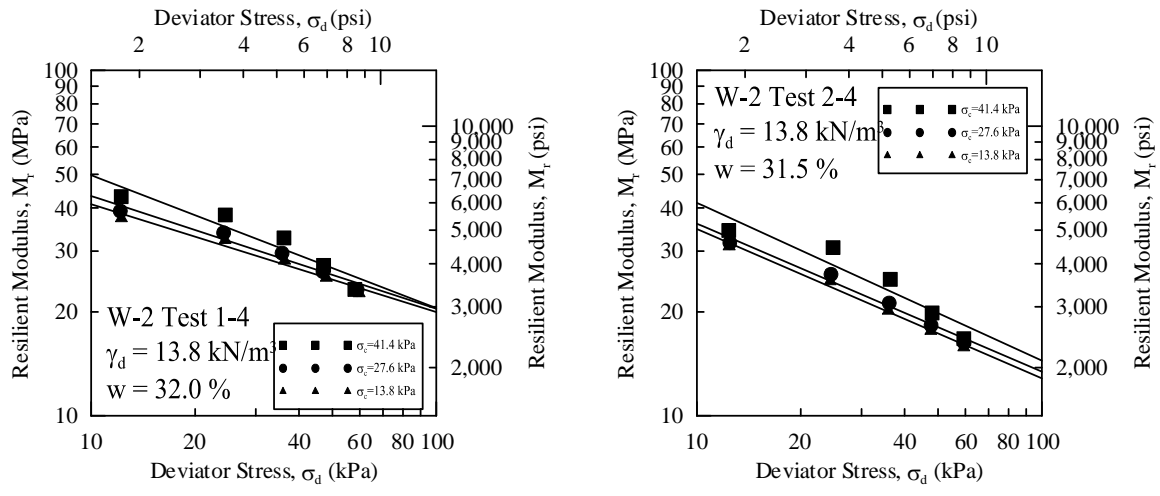


(a) Test W-2\_Set1\_5w



(b) Test W-2\_Set2\_5w

Figure B.49: Results of repeated load triaxial test for soil Winnebago-2 compacted at 95% of  $\gamma_{dmax}$  and wet of  $w_{opt}$ , target compaction value of  $\gamma_d = 14.1 \text{ kN/m}^3$  and  $w = 29.8\%$



(a) Test W-2\_Set1\_4w

(b) Test W-2\_Set2\_4w

**Figure B.50: Results of repeated load triaxial test for soil Winnebago-2 compacted at 93% of  $\gamma_{dmax}$  and wet of  $w_{opt}$ , target compaction value of  $\gamma_d = 13.8 \text{ kN/m}^3$  and  $w = 32.0\%$**

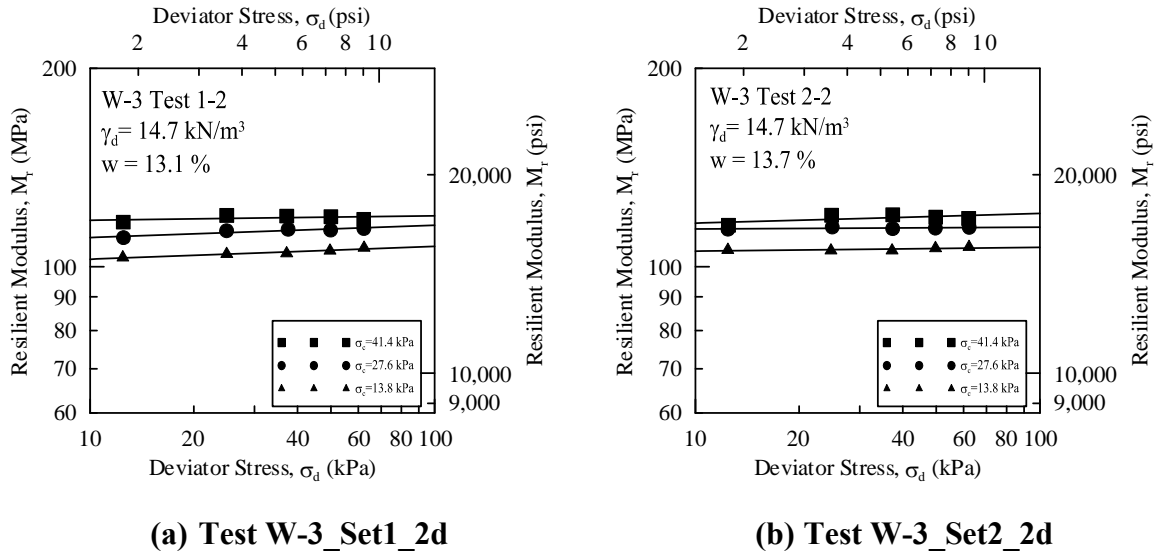


**Figure B.51: Results of repeated load triaxial test for soil Winnebago-3 compacted at 93% of  $\gamma_{dmax}$  and dry of  $w_{opt}$ , target compaction value of  $\gamma_d = 14.7 \text{ kN/m}^3$  and  $w = 13.5\%$**

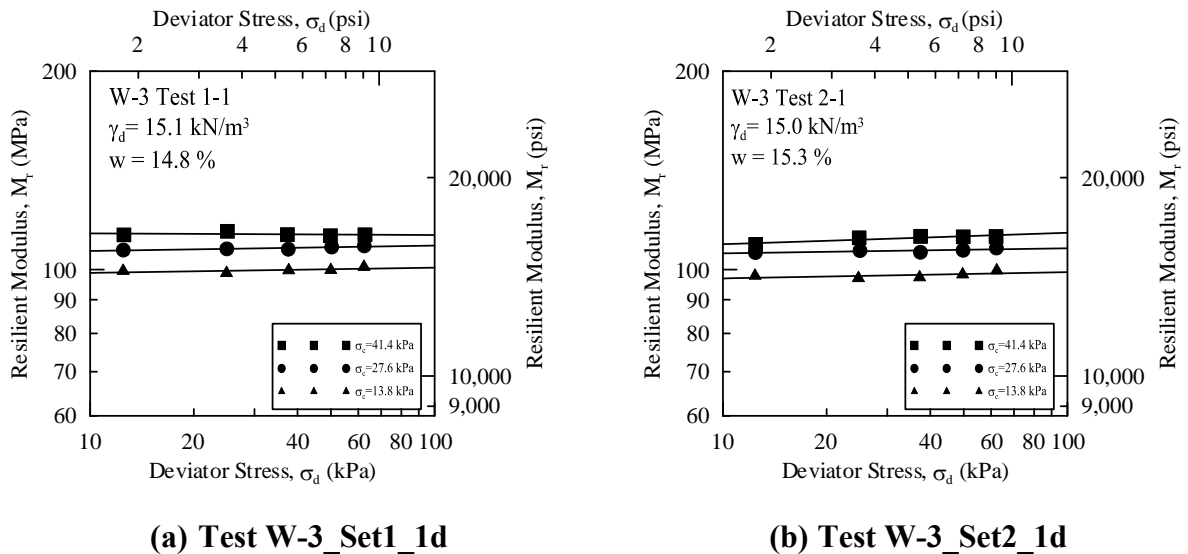
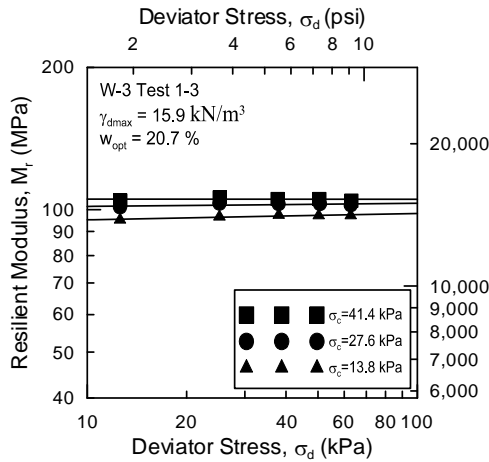
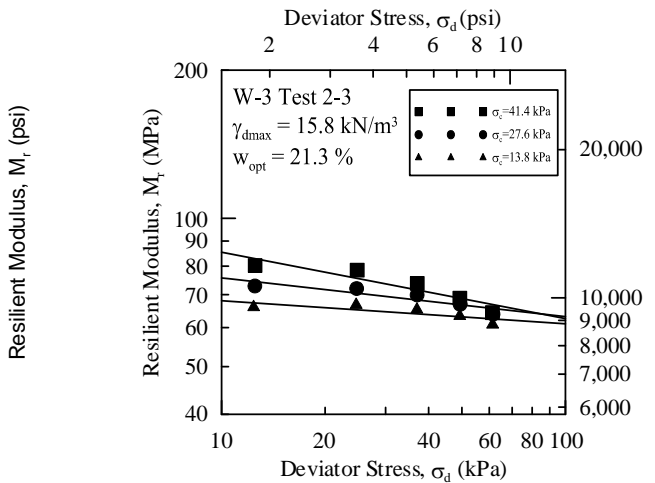


**Figure B.52: Results of repeated load triaxial test for soil Winnebago-3 compacted at 95% of  $\gamma_{dmax}$  and dry of  $w_{opt}$ , target compaction value of  $\gamma_d = 15.0 \text{ kN/m}^3$  and  $w = 15.5\%$**

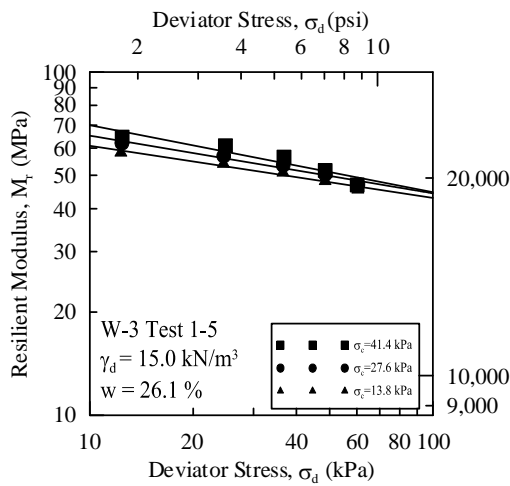


(a) Test W-3\_Set1\_3o

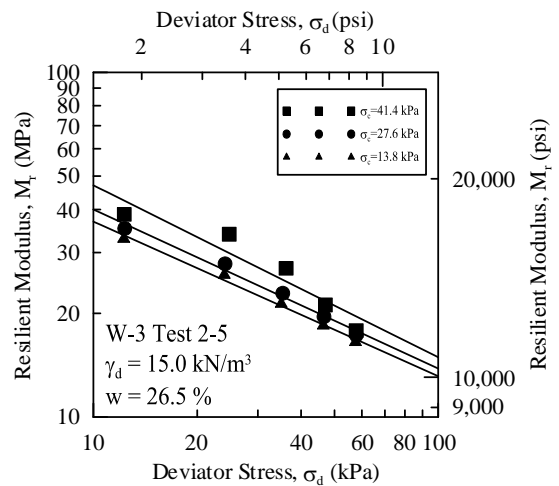


(b) Test W-3\_Set2\_3o

Figure B.53: Results of repeated load triaxial test for soil Winnebago-3 compacted at  $\gamma_{dmax}$  and  $w_{opt}$ , target compaction value of  $\gamma_d = 15.8 \text{ kN/m}^3$  and  $w = 21.8\%$

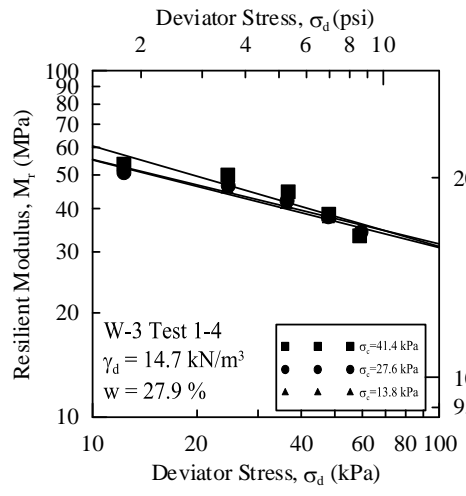


(a) Test W-3\_Set1\_5w

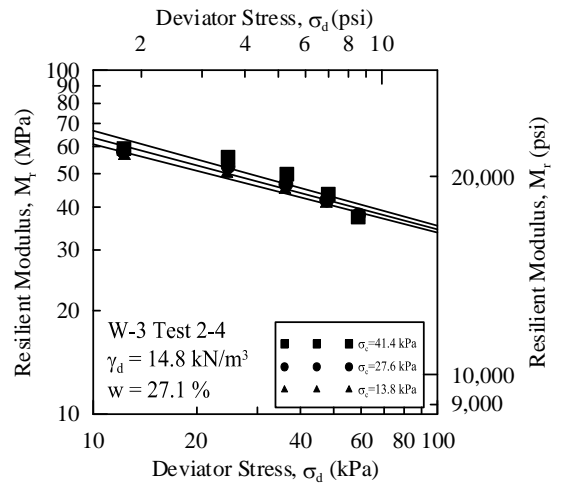


(b) Test W-3\_Set2\_5w

Figure B.54: Results of repeated load triaxial test for soil Winnebago-3 compacted at 95% of  $\gamma_{dmax}$  and wet of  $w_{opt}$ , target compaction value of  $\gamma_d = 15.0 \text{ kN/m}^3$  and  $w = 26.5\%$

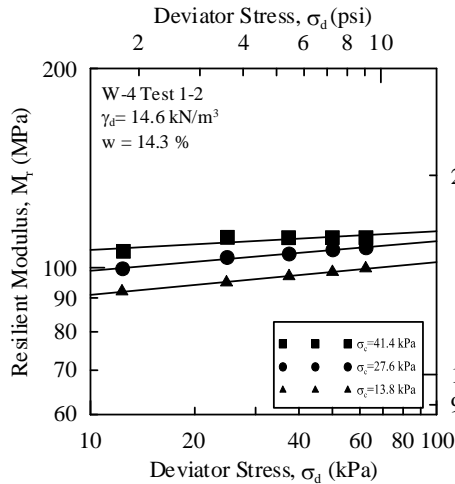


(a) Test W-3\_Set1\_4w

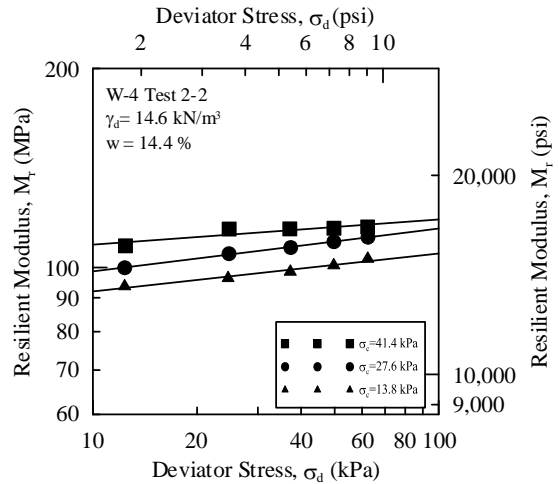


(b) Test W-3\_Set2\_4w

**Figure B.55: Results of repeated load triaxial test for soil Winnebago-3 compacted at 93% of  $\gamma_{dmax}$  and wet of  $w_{opt}$ , target compaction value of  $\gamma_d = 14.7 \text{ kN/m}^3$  and  $w = 28.0\%$**

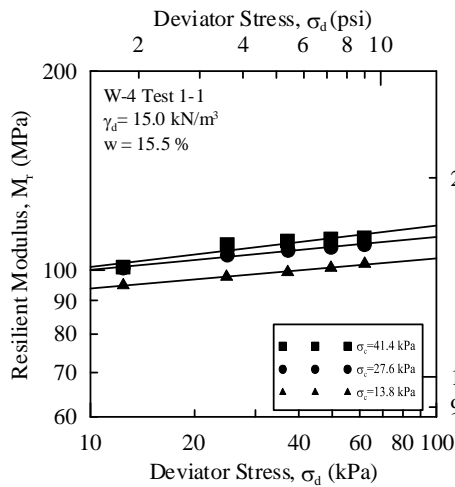


(a) Test W-4\_Set1\_2d

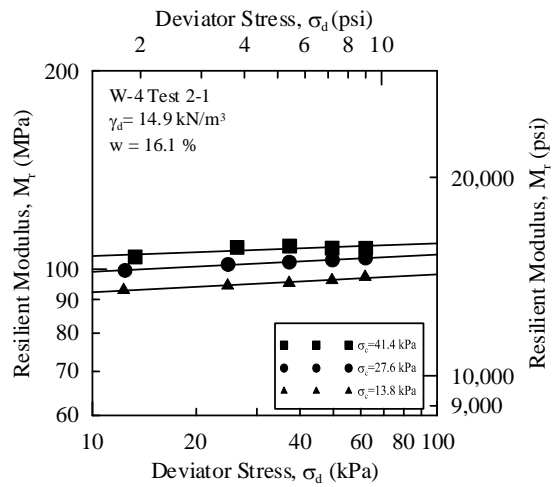


(b) Test W-4\_Set2\_2d

**Figure B.56: Results of repeated load triaxial test for soil Winnebago-4 compacted at 93% of  $\gamma_{dmax}$  and dry of  $w_{opt}$ , target compaction value of  $\gamma_d = 14.6 \text{ kN/m}^3$  and  $w = 14.5\%$**



(a) Test W-4\_Set1\_1d



(b) Test W-4\_Set2\_1d

**Figure B.57: Results of repeated load triaxial test for soil Winnebago-4 compacted at 95% of  $\gamma_{dmax}$  and dry of  $w_{opt}$ , target compaction value of  $\gamma_d = 14.9 \text{ kN/m}^3$  and  $w = 16.0\%$**

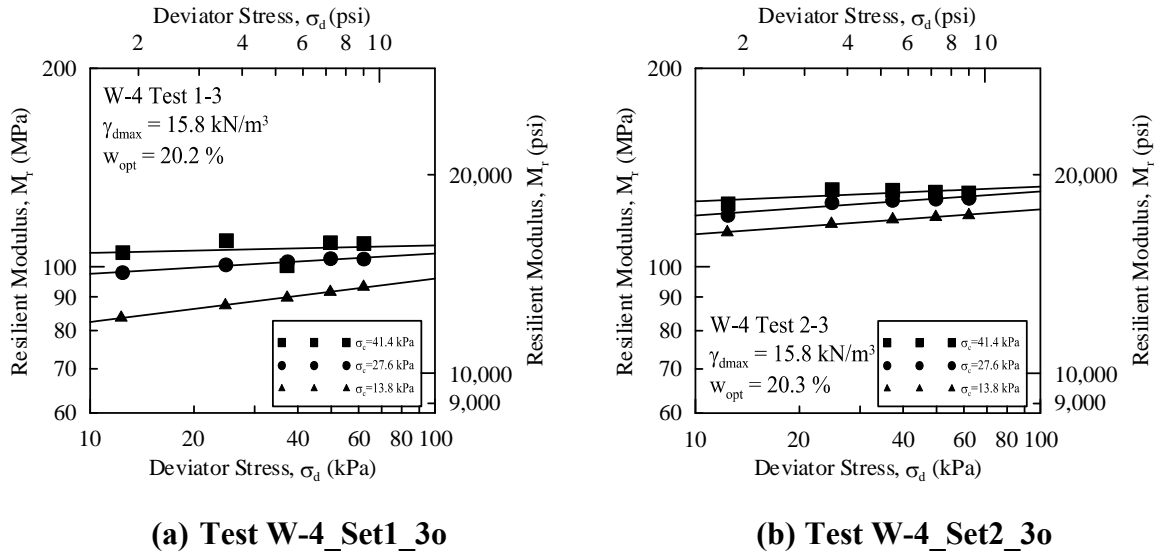


**Figure B.58: Results of repeated load triaxial test for soil Winnebago-4 compacted at  $\gamma_{dmax}$  and  $w_{opt}$ , target compaction value of  $\gamma_d = 15.7 \text{ kN/m}^3$  and  $w = 21.0\%$**

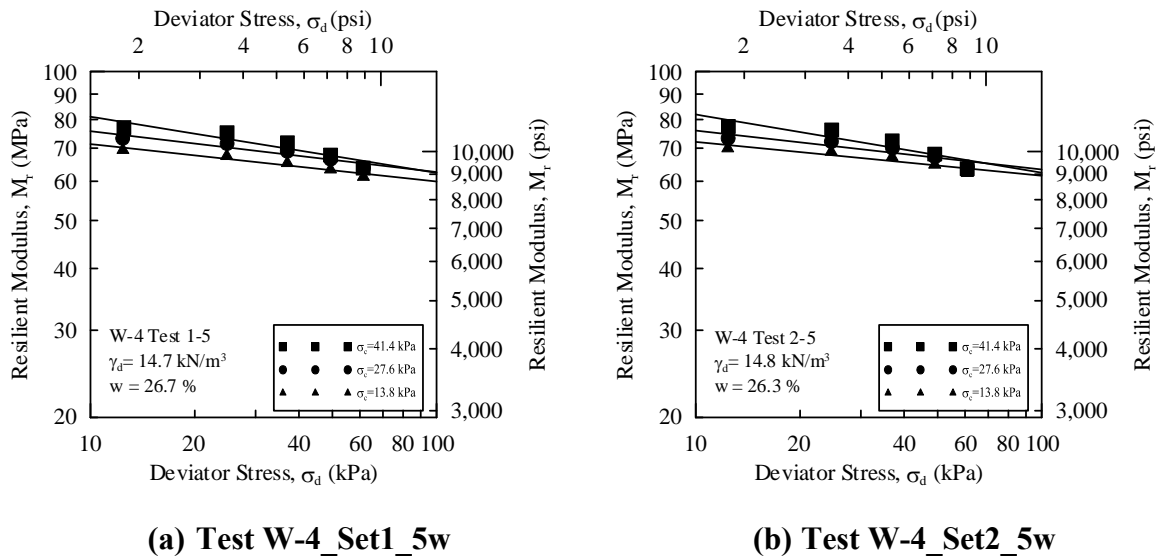
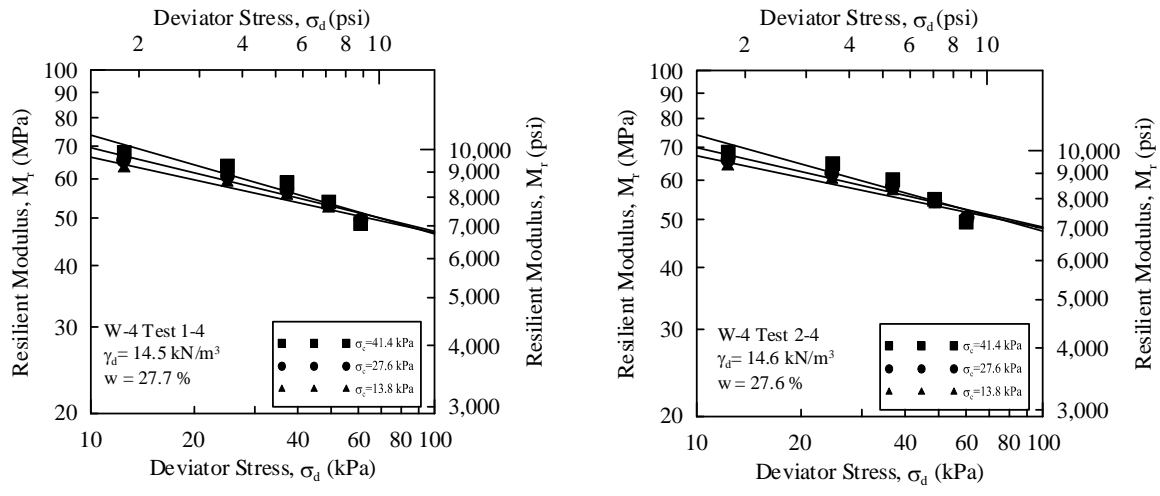


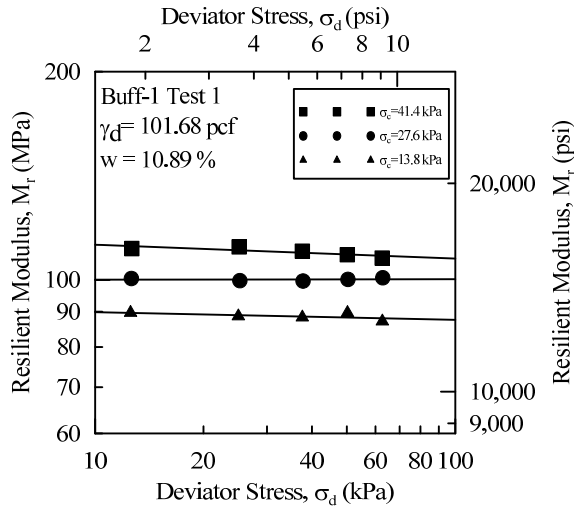
**Figure B.59: Results of repeated load triaxial test for soil Winnebago-4 compacted at 95% of  $\gamma_{dmax}$  and wet of  $w_{opt}$ , target compaction value of  $\gamma_d = 14.9 \text{ kN/m}^3$  and  $w = 26.0\%$**



(a) Test W-4\_Set1\_4w

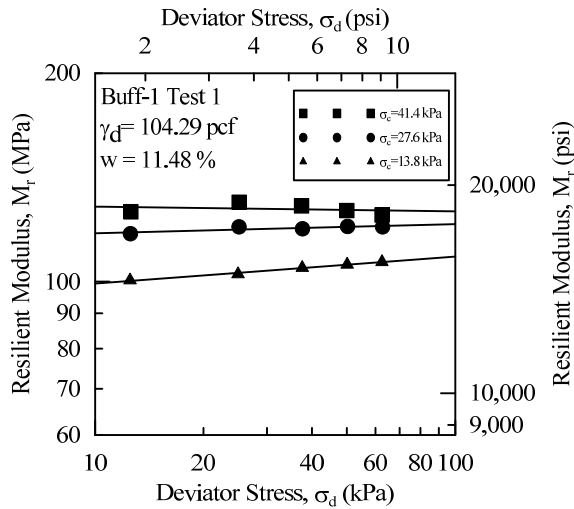
(b) Test W-4\_Set2\_4w

**Figure B.60: Results of repeated load triaxial test for soil Winnebago-4 compacted at 93% of  $\gamma_{dmax}$  and wet of  $w_{opt}$ , target compaction value of  $\gamma_d = 14.6$  kN/m<sup>3</sup> and  $w = 27.5\%$**



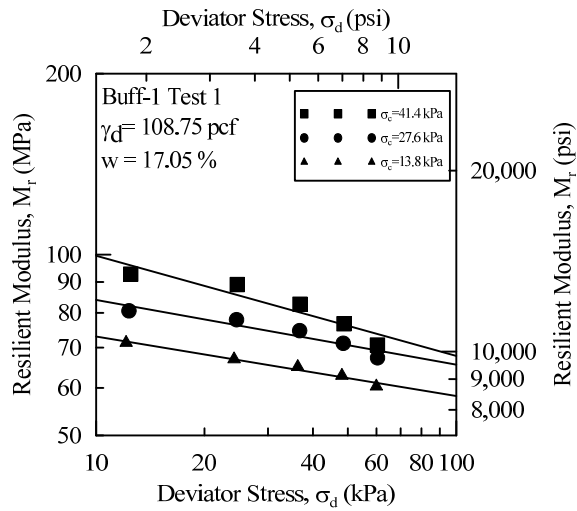
(c) Test Buff-1\_1d

Figure B.61: Results of repeated load triaxial test for soil Buff-1 compacted at 93%  $\gamma_{dmax}$  and dry of  $w_{opt}$ , target compaction value of  $\gamma_d = 15.98$  kN/m<sup>3</sup> and  $w = 10.7\%$



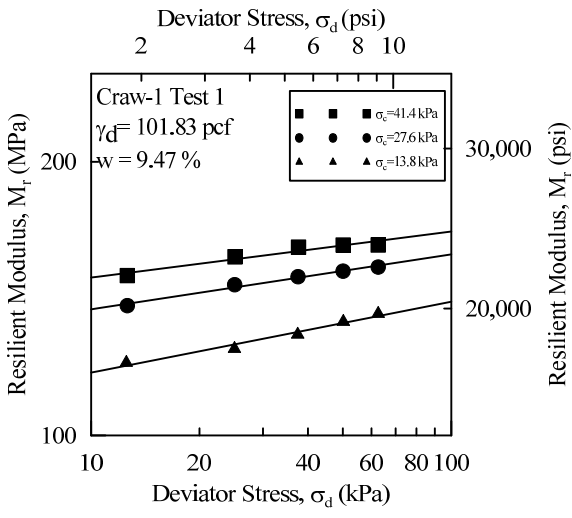
(c) Test Buff-1\_2d

Figure B.62: Results of repeated load triaxial test for soil Buff-1 compacted at 95%  $\gamma_{dmax}$  and dry of  $w_{opt}$ , target compaction value of  $\gamma_d = 16.4$  kN/m<sup>3</sup> and  $w = 11.73\%$



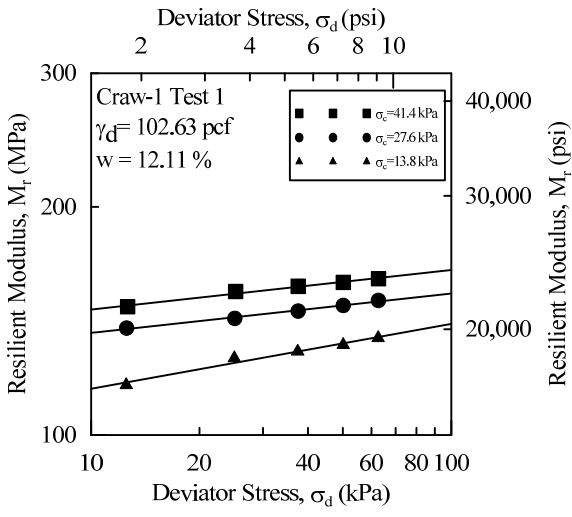
(a) Test Buff-1\_Opt

Figure B.63: Results of repeated load triaxial test for soil Buff-1 compacted at  $\gamma_{dmax}$  and  $w_{opt}$ , target compaction value of  $\gamma_d = 17.2$  kN/m<sup>3</sup> and  $w = 16.9\%$



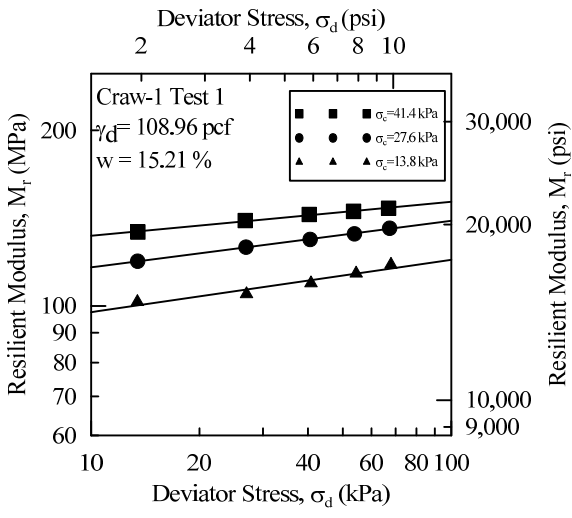
(d) Test Craw-1\_1d

Figure B.64: Results of repeated load triaxial test for soil Craw-1 compacted at 93%  $\gamma_{dmax}$  and dry of  $w_{opt}$ , target compaction value of  $\gamma_d = 15.96$  kN/m<sup>3</sup> and  $w = 9.7\%$



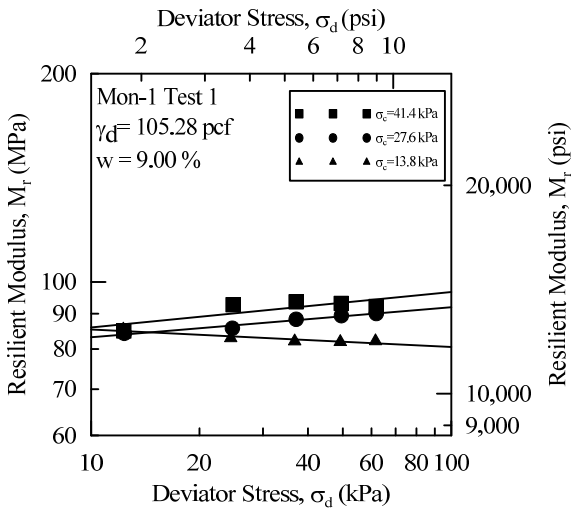
(d) Test Craw-1\_2d

Figure B.65: Results of repeated load triaxial test for soil Craw-1 compacted at 95%  $\gamma_{dmax}$  and dry of  $w_{opt}$ , target compaction value of  $\gamma_d = 16.4$  kN/m<sup>3</sup> and  $w = 10.6\%$



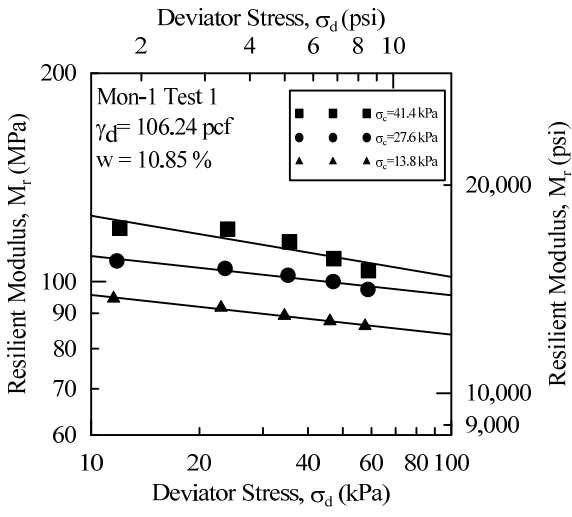
(b) Test Craw-1\_Opt

Figure B.66: Results of repeated load triaxial test for soil Craw-1 compacted at  $\gamma_{dmax}$  and  $w_{opt}$ , target compaction value of  $\gamma_d = 17.3$  kN/m<sup>3</sup> and  $w = 14.9$ %



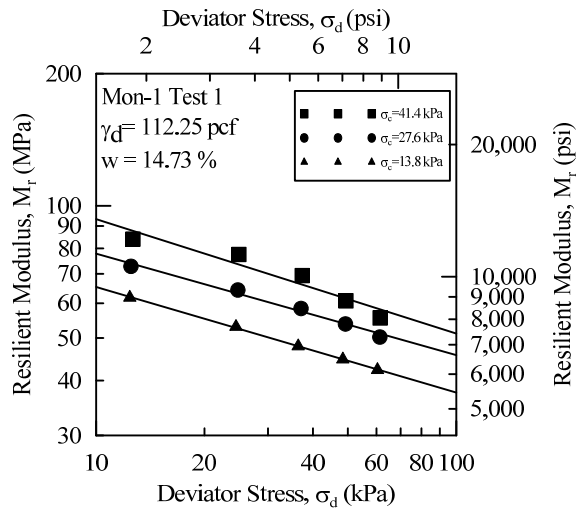
(e) Test Mon-1\_1d

Figure B.67: Results of repeated load triaxial test for soil Mon-1 compacted at 93%  $\gamma_{dmax}$  and dry of  $w_{opt}$ , target compaction value of  $\gamma_d = 16.3$  kN/m<sup>3</sup> and  $w = 9.75\%$



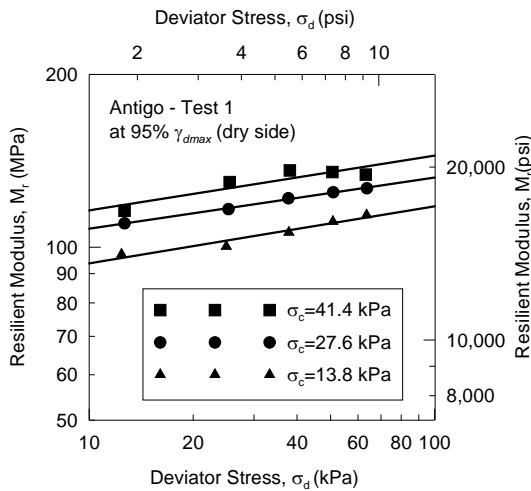
(e) Test Mon-1\_2d

Figure B.68: Results of repeated load triaxial test for soil Mon-1 compacted at 95%  $\gamma_{dmax}$  and dry of  $w_{opt}$ , target compaction value of  $\gamma_d = 16.7$  kN/m<sup>3</sup> and  $w = 10.7\%$

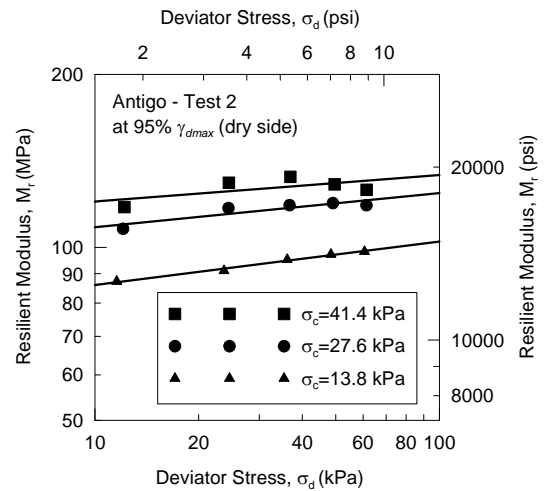


(c) Test Mon-1\_Opt

**Figure B.69: Results of repeated load triaxial test for soil Mon-1 compacted at  $\gamma_{dmax}$  and  $w_{opt}$ , target compaction value of  $\gamma_d = 17.6 \text{ kN/m}^3$  and  $w = 14.75\%$**

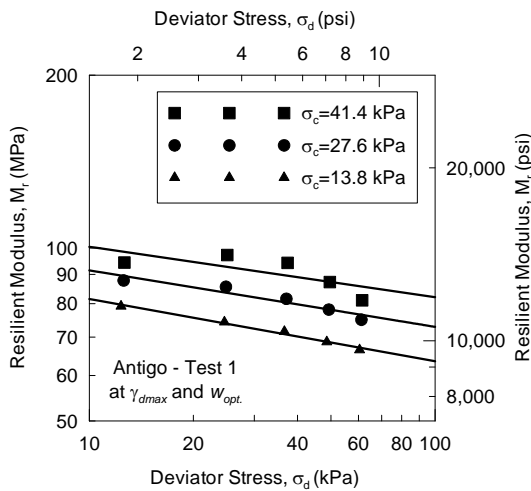


(a) Test on soil specimen #1

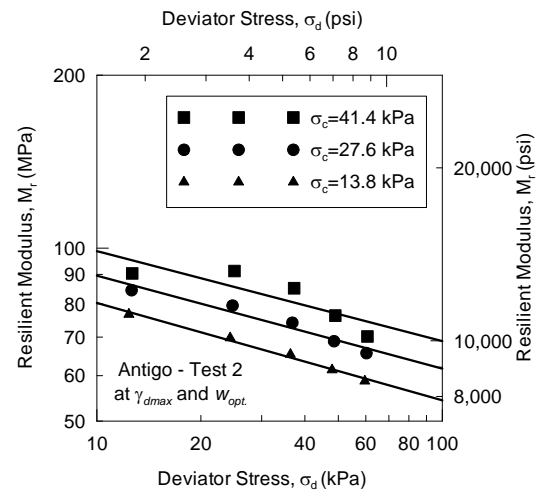


(b) Test on soil specimen #2

**Figure B.70: Results of repeated load triaxial test on Antigo soil compacted at 95% of maximum dry unit weight ( $\gamma_{dmax}$ ) and moisture content less than wopt. (dry side)**

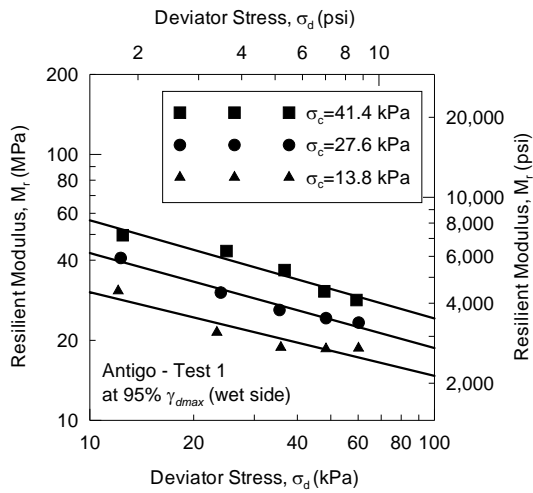


(a) Test on soil specimen #1

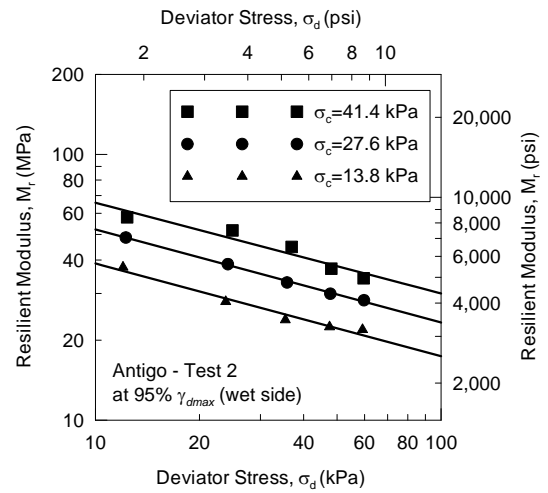


(b) Test on soil specimen #2

**Figure B.71: Results of repeated load triaxial test on Antigo soil compacted at maximum dry unit weight ( $\gamma_{dmax}$ ) and optimum moisture content ( $w_{opt}$ )**

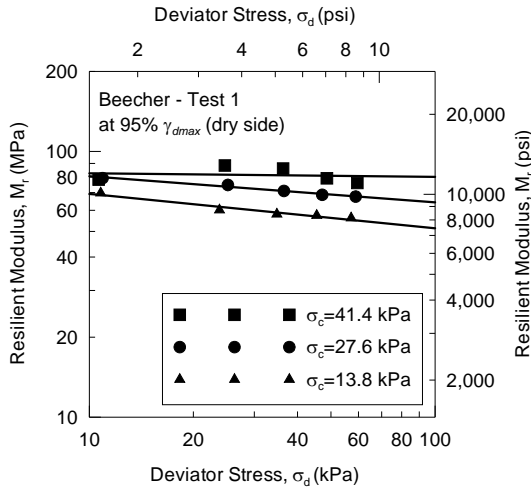


(c) Test on soil specimen #1

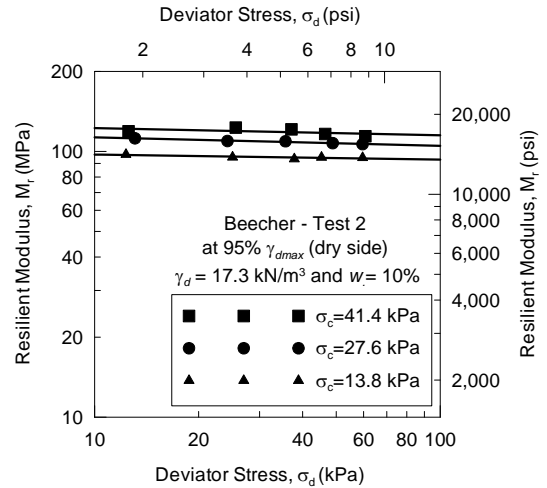


(d) Test on soil specimen #2

**Figure B.72: Results of repeated load triaxial test on Antigo soil compacted at 95% of maximum dry unit weight ( $\gamma_{dmax}$ ) and moisture content more than  $w_{opt}$ . (wet side)**

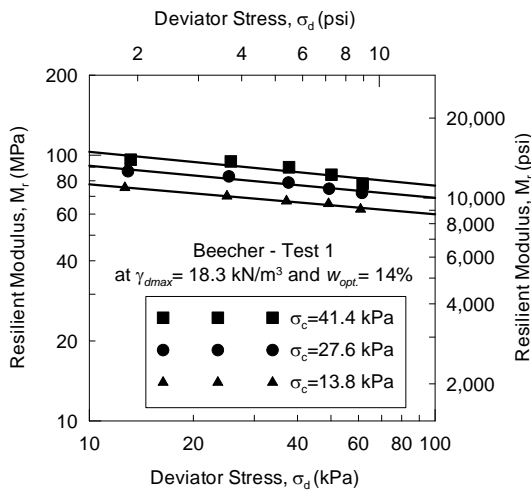


(e) Test on soil specimen #1

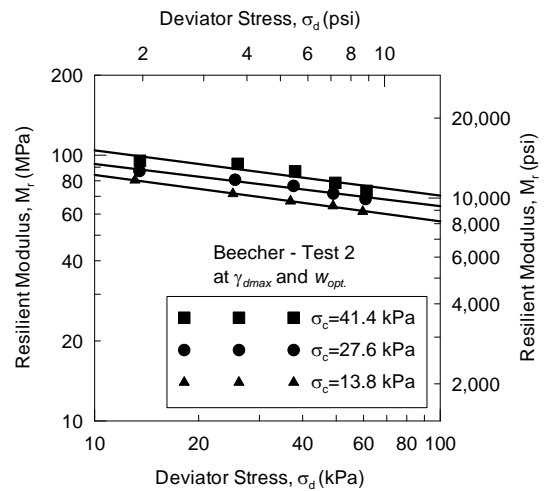


(f) Test on soil specimen #2

**Figure B.73: Results of repeated load triaxial test on Beecher soil compacted at 95% of maximum dry unit weight ( $\gamma_{dmax}$ ) and moisture content less than  $w_{opt}$  (dry side)**

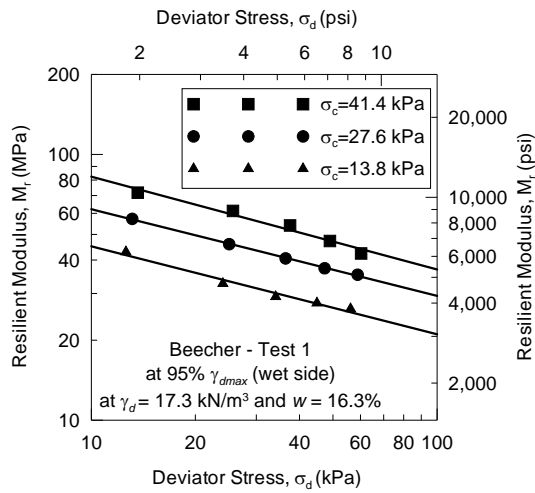


(c) Test on soil specimen #1

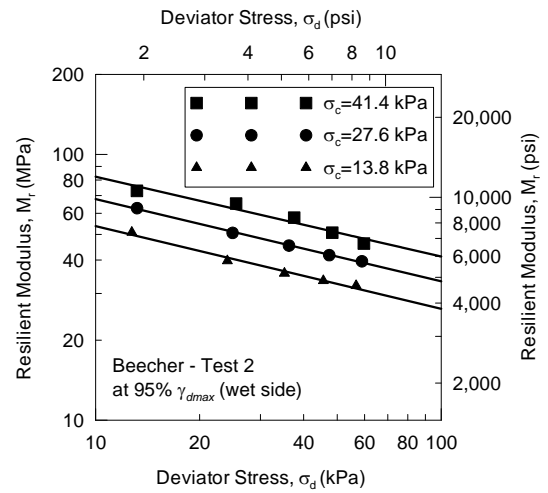


(d) Test on soil specimen #2

**Figure B.74: Results of repeated load triaxial test on Beecher soil compacted at maximum dry unit weight ( $\gamma_{dmax}$ ) and optimum moisture content ( $w_{opt}$ )**

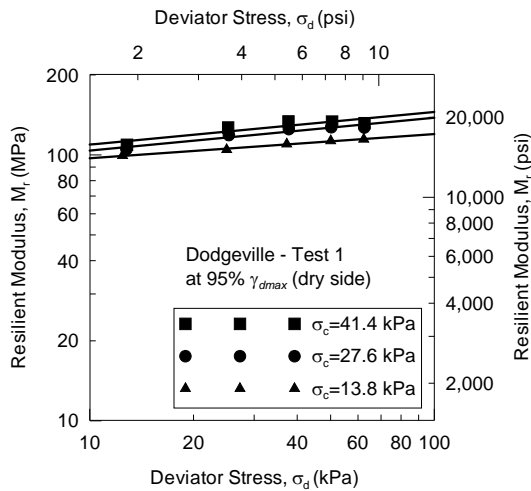


(a) Test on soil specimen #1

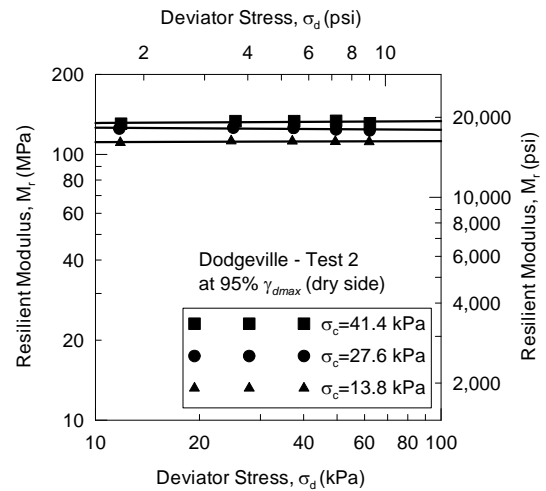


(b) Test on soil specimen #2

**Figure B.75: Results of repeated load triaxial test on Beecher soil compacted at 95% of maximum dry unit weight ( $\gamma_{dmax}$ ) and moisture content more than  $w_{opt}$ . (wet side)**

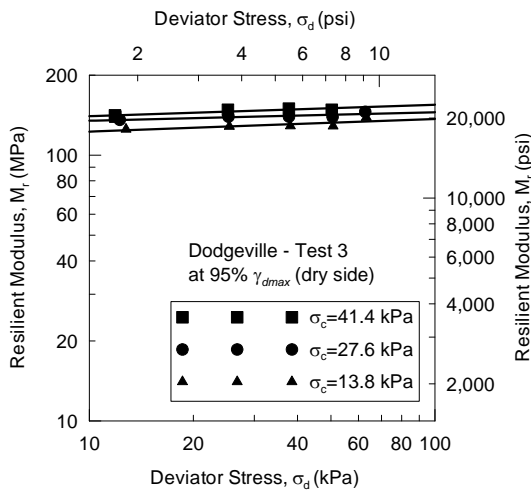


(g) Test on soil specimen #1

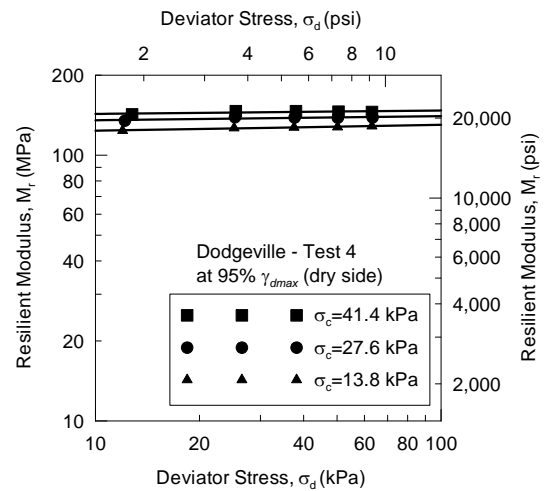


(h) Test on soil specimen #2

**Figure B.76: Results of repeated load triaxial test on Dodgeville soil compacted at 95% of maximum dry unit weight ( $\gamma_{dmax}$ ) and moisture content less than  $w_{opt}$ . (dry side)**

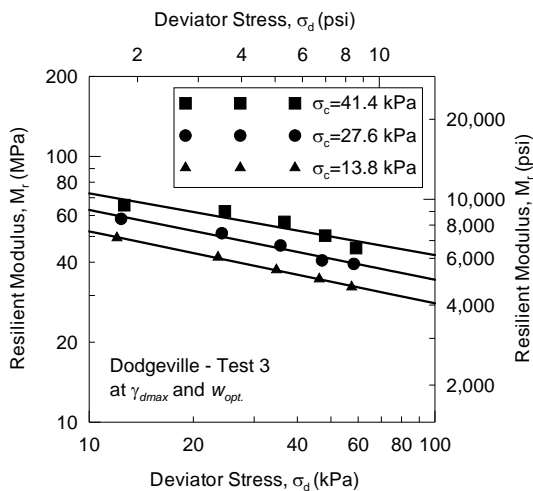


(e) Test on soil specimen #3

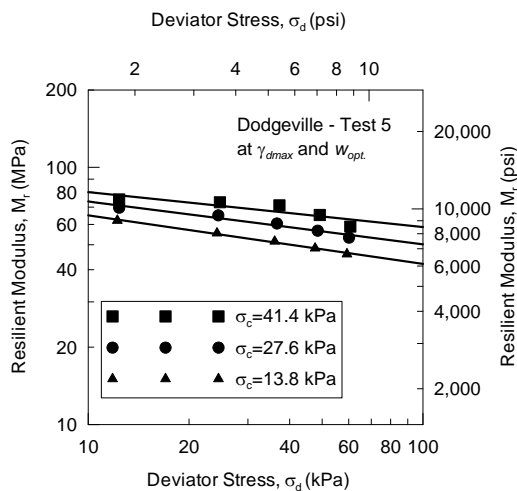


(f) Test on soil specimen #4

**Figure B.77: Results of repeated load triaxial test on Dodgeville soil compacted at 95% of maximum dry unit weight ( $\gamma_{dmax}$ ) and moisture content less than  $w_{opt}$ . (dry side)**

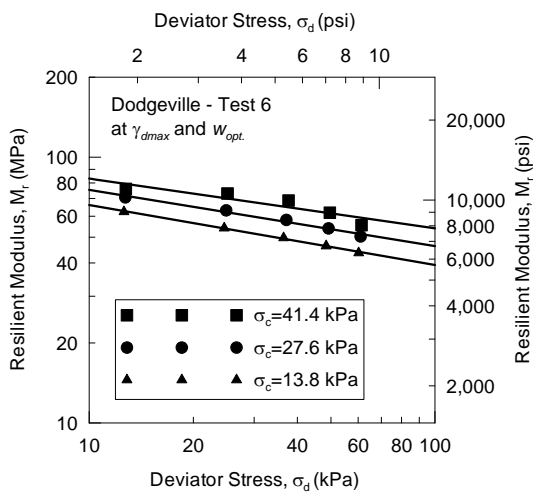


(c) Test on soil specimen #1

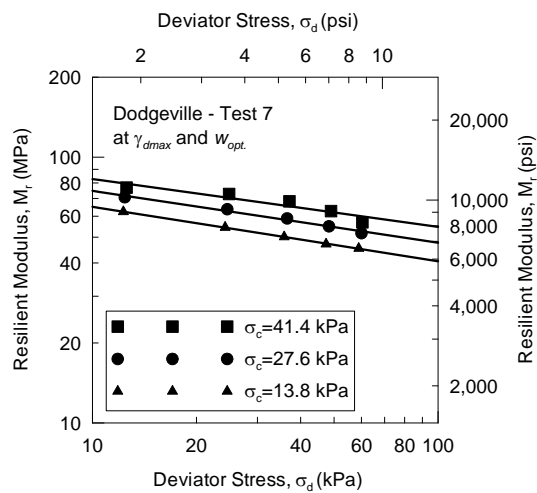


(d) Test on soil specimen #2

**Figure B.78: Results of repeated load triaxial test on Dodgeville soil compacted at maximum dry unit weight ( $\gamma_{dmax}$ ) and optimum moisture content ( $w_{opt}$ .)**

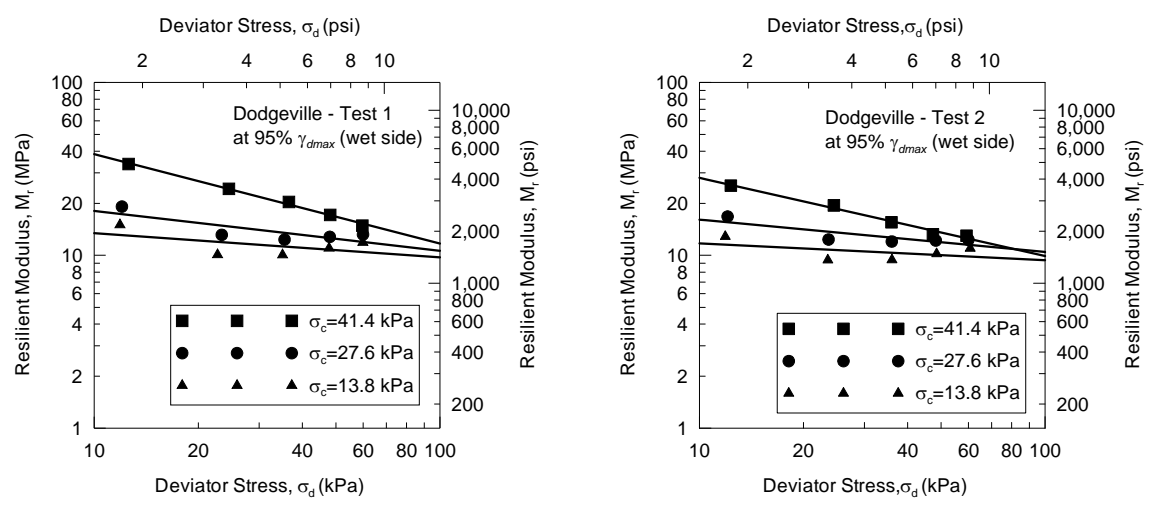


(a) Test on soil specimen #3



(b) Test on soil specimen #4

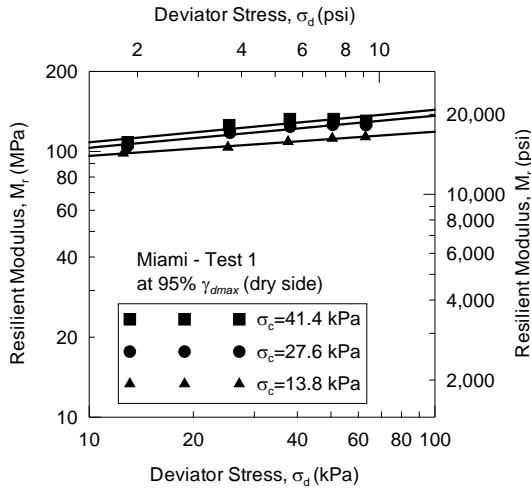
**Figure B.79: Results of repeated load triaxial test on Dodgeville soil compacted at maximum dry unit weight ( $\gamma_{dmax}$ ) and optimum moisture content ( $w_{opt}$ .)**



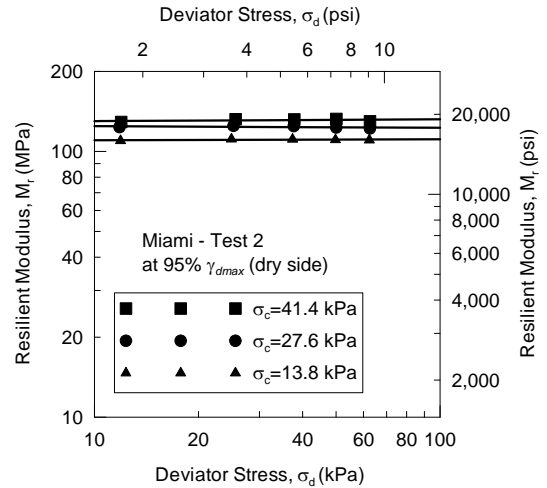
(a) Test on soil specimen #1

(b) Test on soil specimen #2

**Figure B.80: Results of repeated load triaxial test on Dodgeville soil compacted at 95% of maximum dry unit weight ( $\gamma_{dmax}$ ) and moisture content more than wopt. (wet side)**

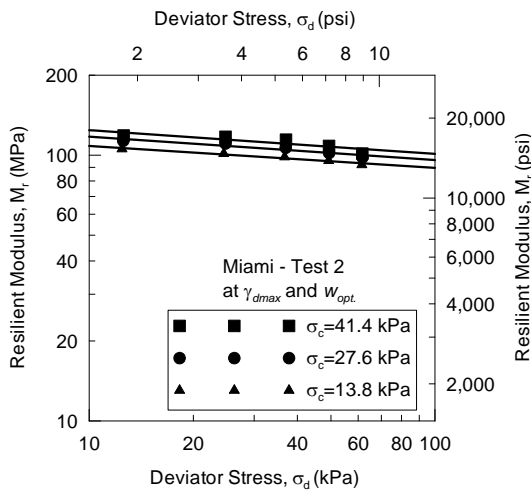


(i) Test on soil specimen #1

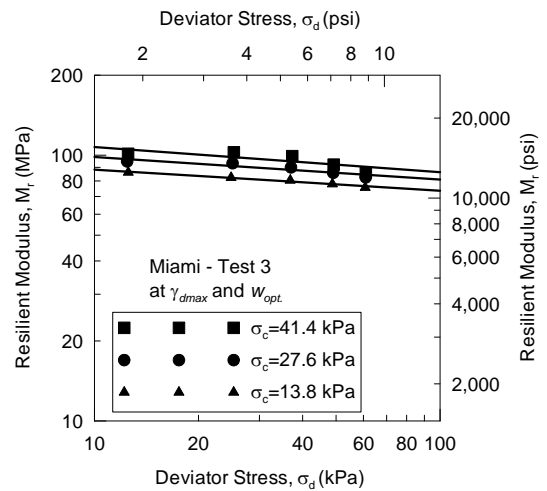


(j) Test on soil specimen #2

**Figure B.81: Results of repeated load triaxial test on Miami soil compacted at 95% of maximum dry unit weight ( $\gamma_{dmax}$ ) and moisture content less than  $w_{opt}$ . (dry side)**

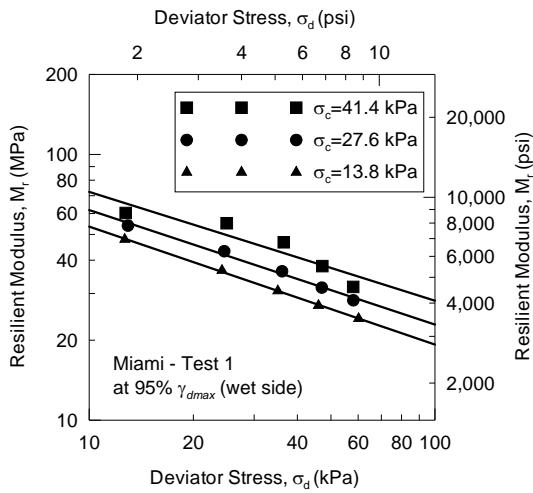


(g) Test on soil specimen #1

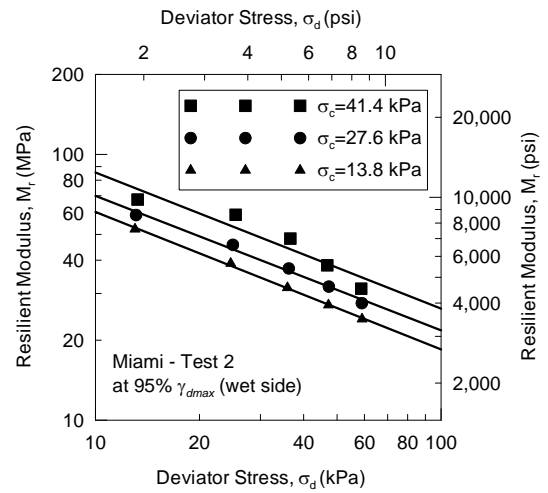


(h) Test on soil specimen #2

**Figure B.82: Results of repeated load triaxial test on Miami soil compacted at maximum dry unit weight ( $\gamma_{dmax}$ ) and optimum moisture content ( $w_{opt}$ )**

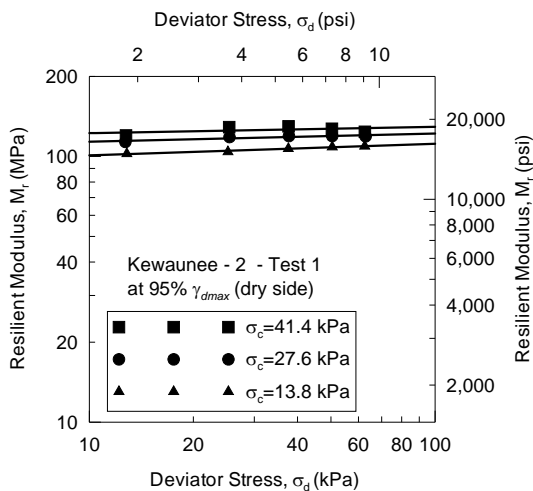


(e) Test on soil specimen #1



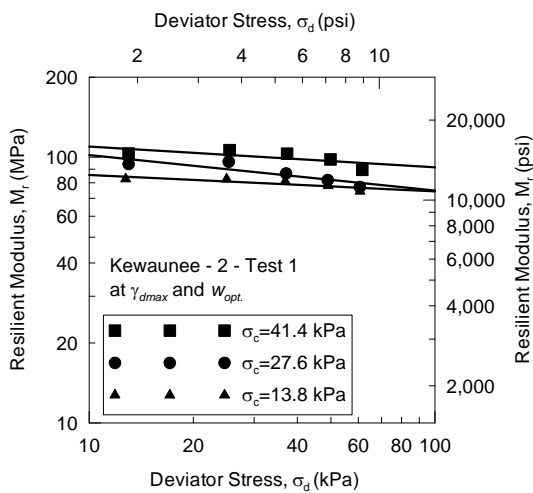
(f) Test on soil specimen #2

**Figure B.83: Results of repeated load triaxial test on Miami soil compacted at 95% of maximum dry unit weight ( $\gamma_{dmax}$ ) and moisture content more than  $w_{opt}$ . (wet side)**

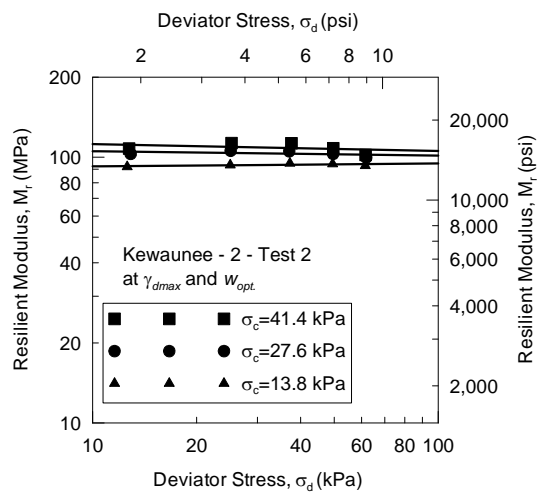


(a) Test on soil specimen #1

**Figure B.84: Results of repeated load triaxial test Kewaunee soil - 2 compacted at 95% of maximum dry unit weight ( $\gamma_{dmax}$ ) and moisture content less than  $w_{opt}$ . (dry side)**

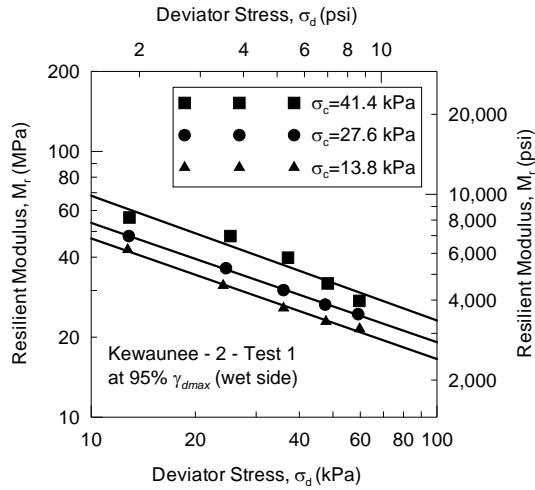


(a) Test on soil specimen #1



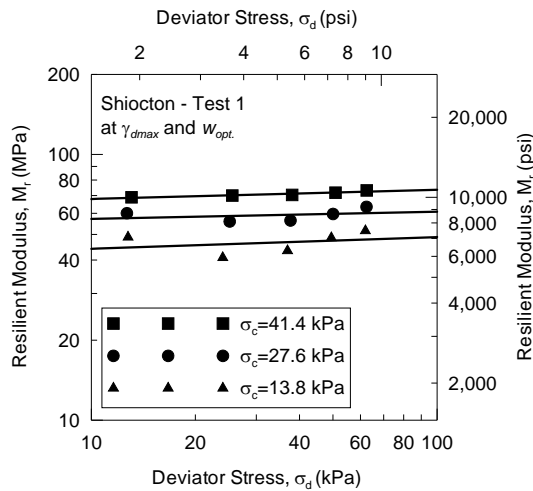
(b) Test on soil specimen #2

**Figure B.85: Results of repeated load triaxial test on Kewaunee soil - 2 compacted at maximum dry unit weight ( $\gamma_{dmax}$ ) and optimum moisture content ( $w_{opt}$ .)**

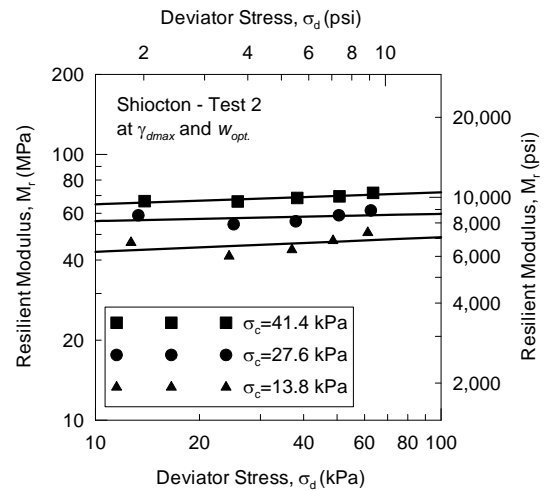


(a) Test on soil specimen #1

**Figure B.86: Results of repeated load triaxial test on Kewaunee soil - 2 compacted at 95% of maximum dry unit weight ( $\gamma_{dmax}$ ) and moisture content more than  $w_{opt}$ . (wet side)**

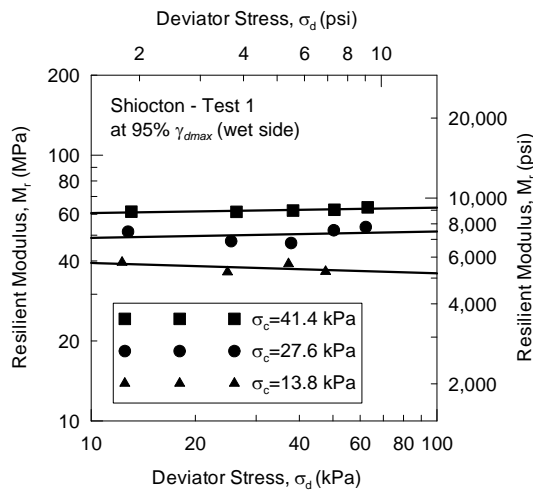


(k) Test on soil specimen #1

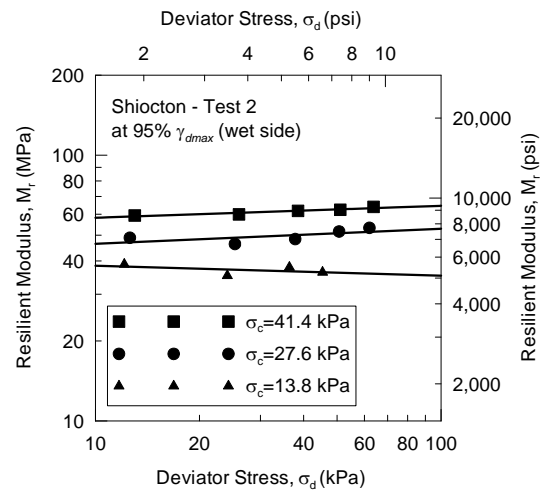


(l) Test on soil specimen #2

**Figure B.87: Results of repeated load triaxial test on Shiocton soil compacted at maximum dry unit weight ( $\gamma_{dmax}$ ) and optimum moisture content ( $w_{opt}$ )**

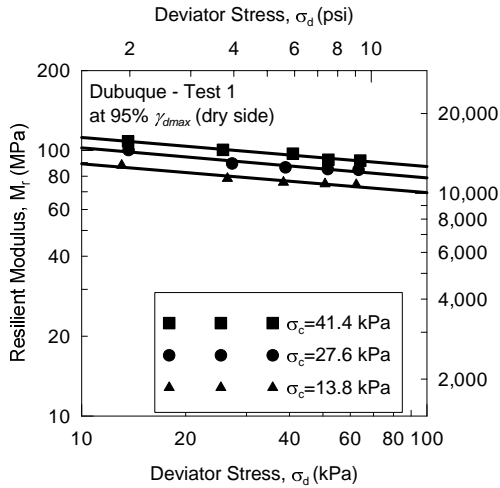


(i) Test on soil specimen #1

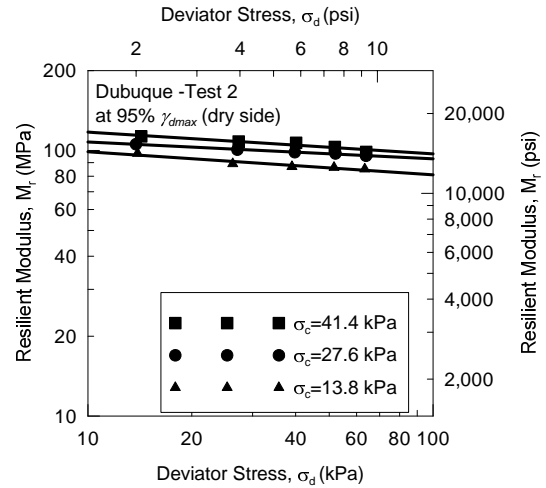


(j) Test on soil specimen #2

**Figure B.88: Results of repeated load triaxial test on Shiocton soil compacted at 95% of maximum dry unit weight ( $\gamma_{dmax}$ ) and moisture content more than  $w_{opt}$  (wet side)**

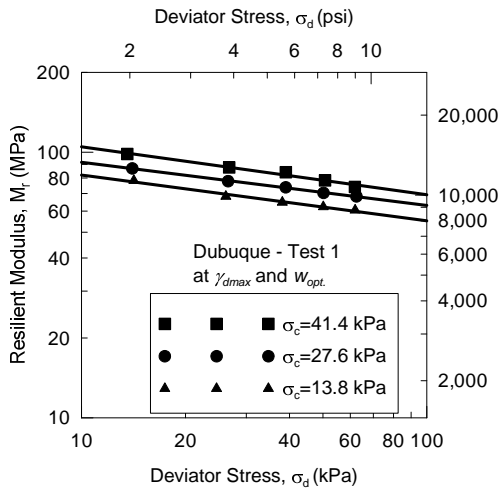


(m) Test on soil specimen #1

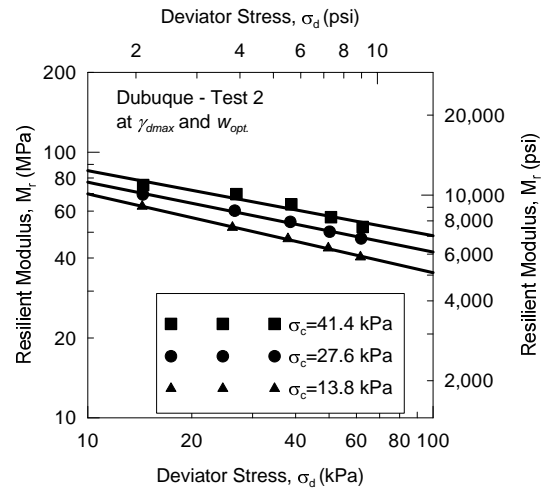


(n) Test on soil specimen #2

**Figure B.89: Results of repeated load triaxial test on Dubuque soil compacted at 95% of maximum dry unit weight ( $\gamma_{dmax}$ ) and moisture content less than  $w_{opt}$ . (dry side)**

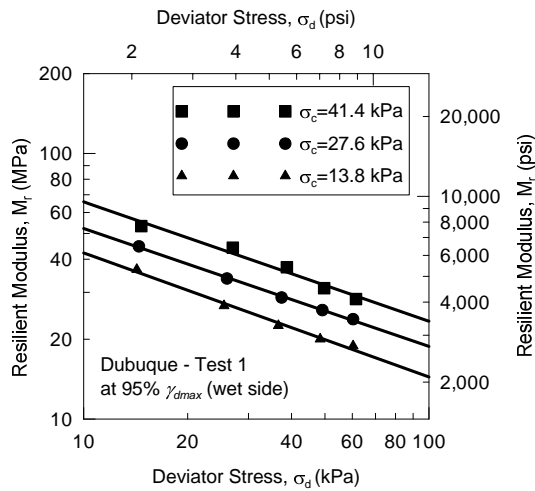


(k) Test on soil specimen #1

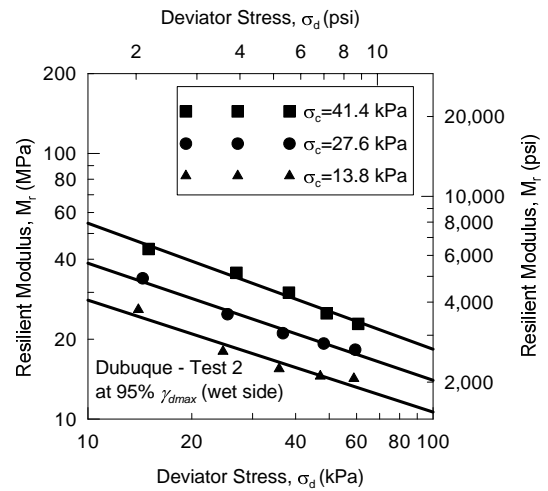


(l) Test on soil specimen #2

**Figure B.90: Results of repeated load triaxial test on Dubuque soil compacted at maximum dry unit weight ( $\gamma_{dmax}$ ) and moisture content at  $w_{opt}$ .**



(a) Test on soil specimen #1



(b) Test on soil specimen #2

**Figure B.91: Results of repeated load triaxial test on Dubuque soil compacted at 95% of maximum dry unit weight ( $\gamma_{dmax}$ ) and moisture content more than  $w_{opt}$ . (wet side)**

## Appendix C

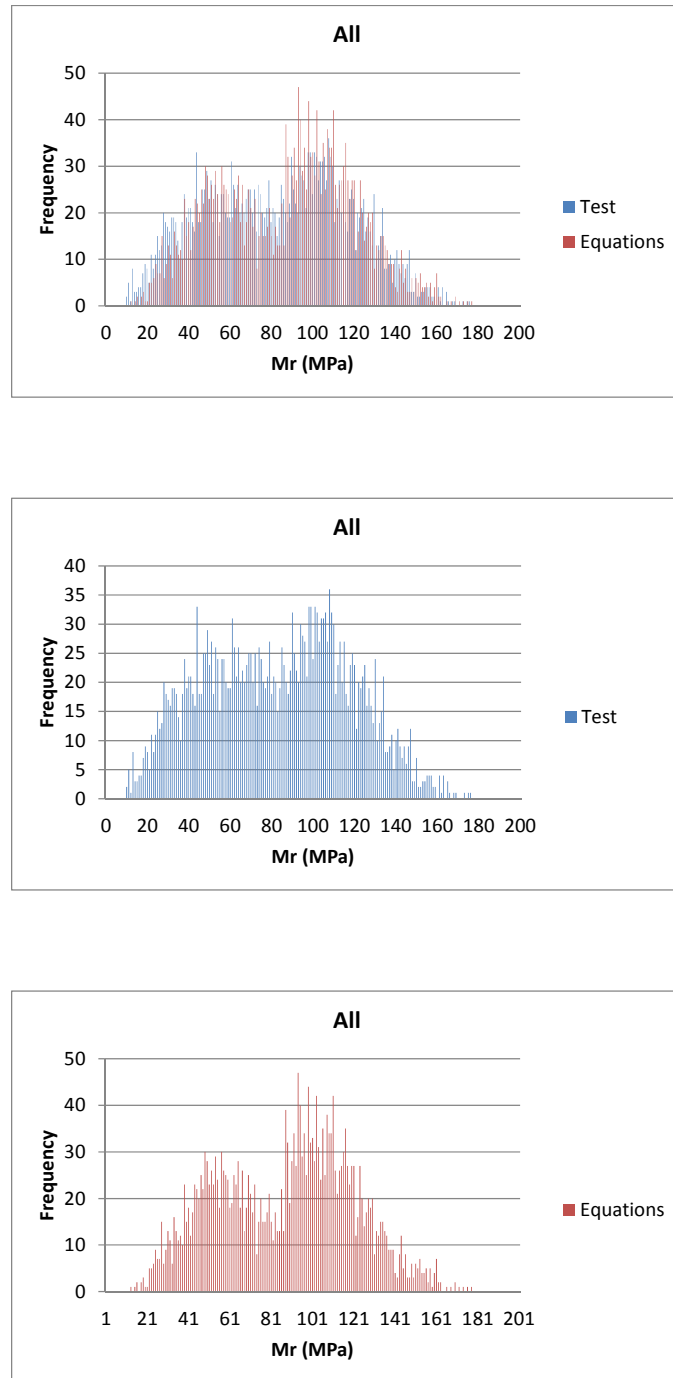


**Figure C.1: Distribution of resilient modulus from test data and statistical modeling for all soils.**

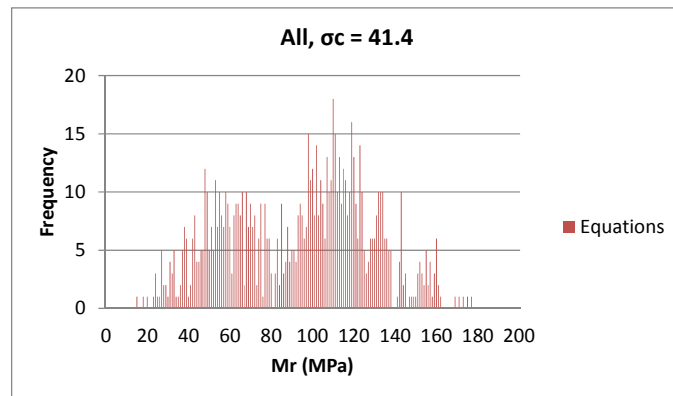
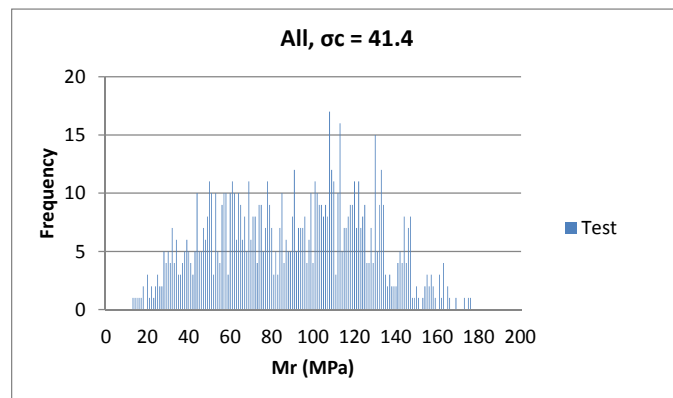
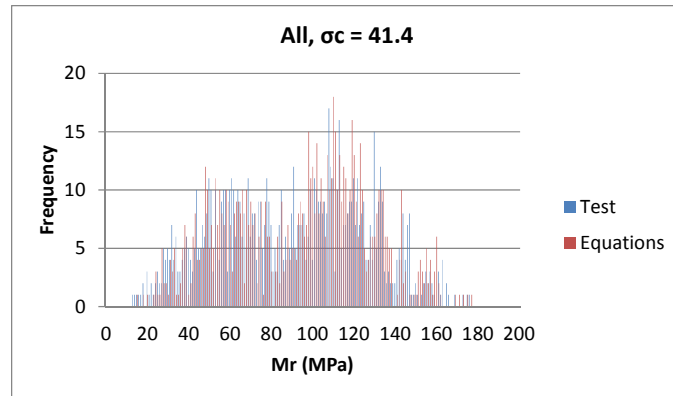


**Figure C.2: Distribution of resilient modulus from test data and statistical modeling for all soils under confining pressure  $\sigma_c = 41.4$  kPa.**

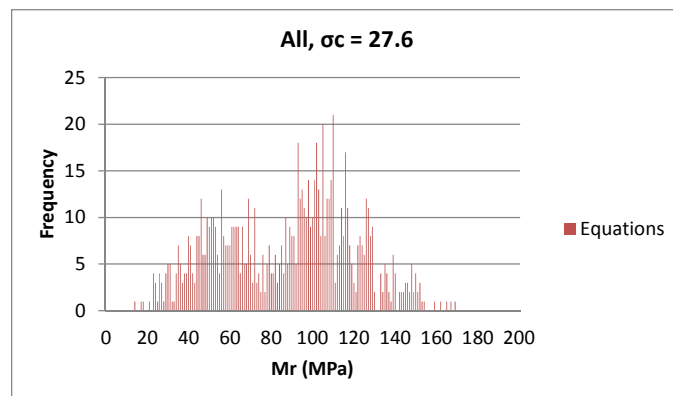
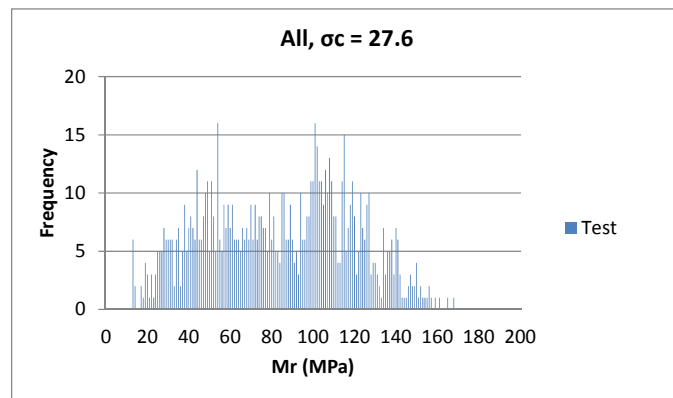
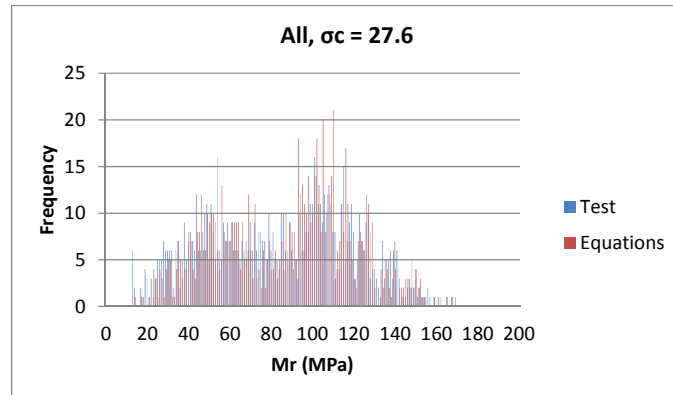


**Figure C.3: Distribution of resilient modulus from test data and statistical modeling for all soils under confining pressure  $\sigma_c = 27.6$  kPa.**

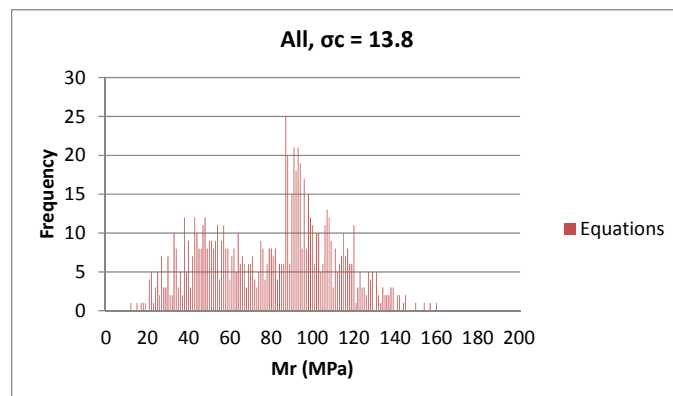
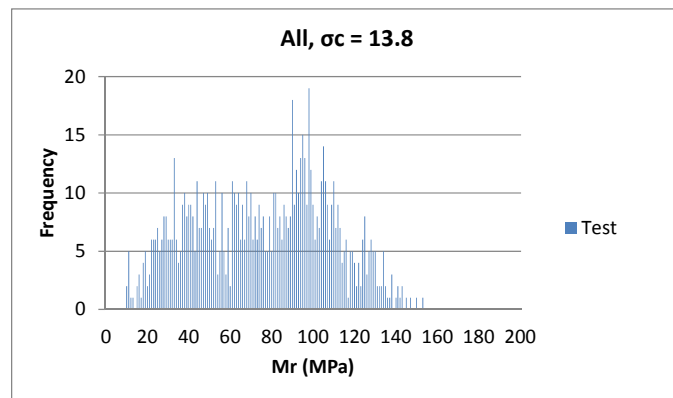
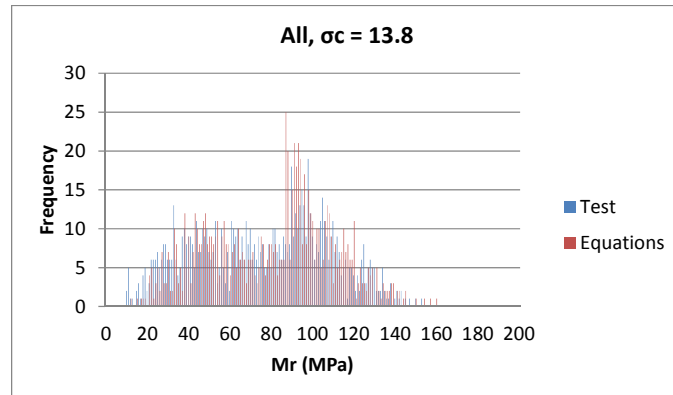


**Figure C.4: Distribution of resilient modulus from test data and statistical modeling for all soils under confining pressure  $\sigma_c = 13.8$  kPa.**

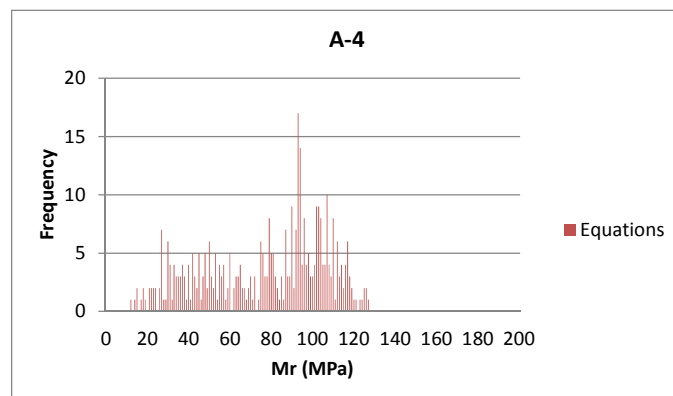
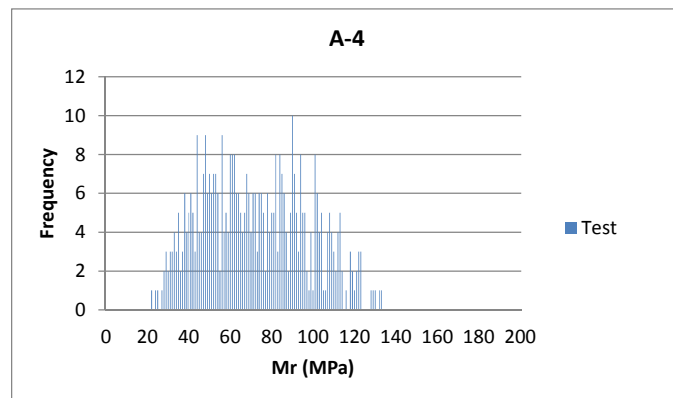
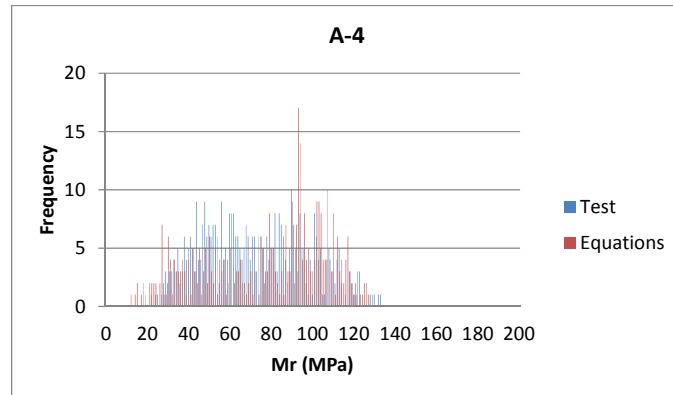


**Figure C.5: Distribution of resilient modulus from test data and statistical modeling for A-4 soil.**

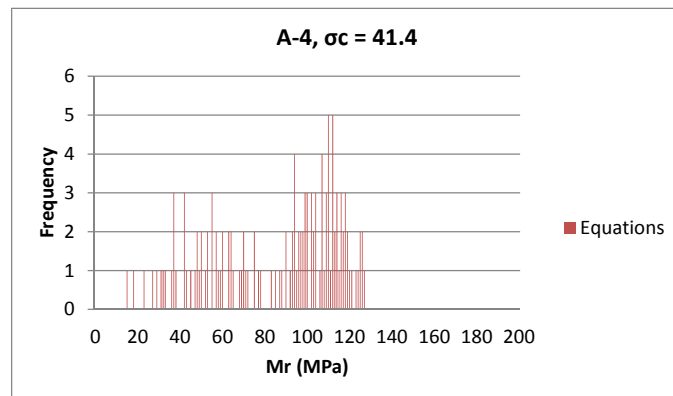
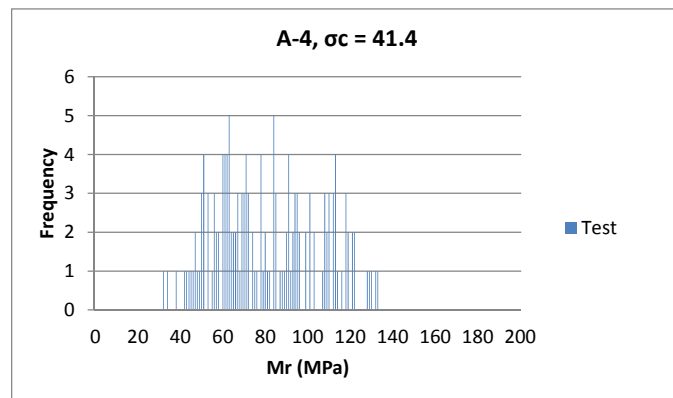
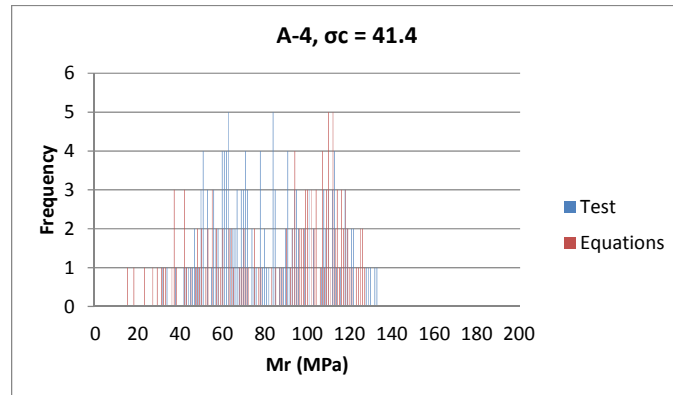


**Figure C.6: Distribution of resilient modulus from test data and statistical modeling for A-4 soil under confining pressure  $\sigma_c = 41.4$  kPa.**

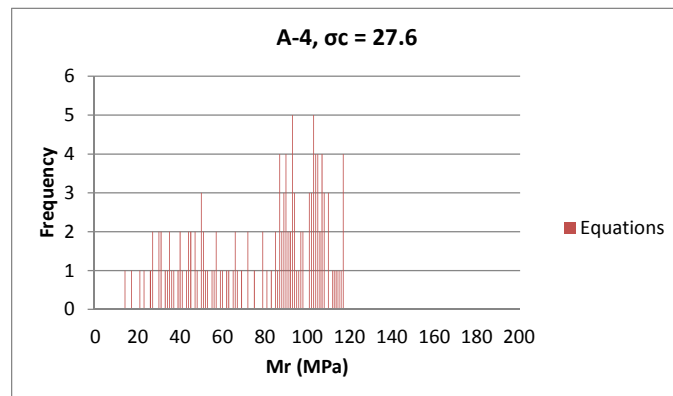
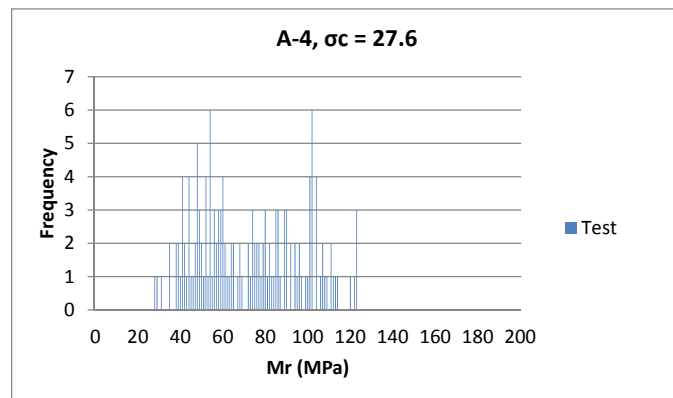
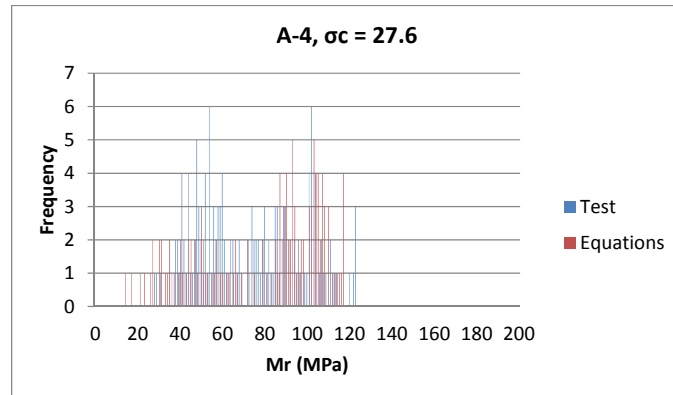


**Figure C.7: Distribution of resilient modulus from test data and statistical modeling for A-4 soil under confining pressure  $\sigma_c = 27.6$  kPa.**

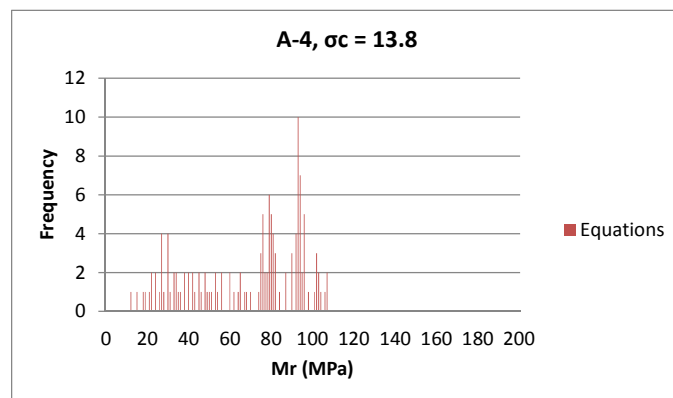
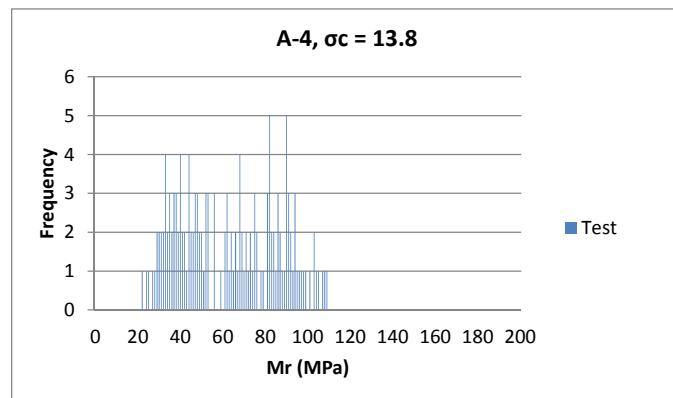
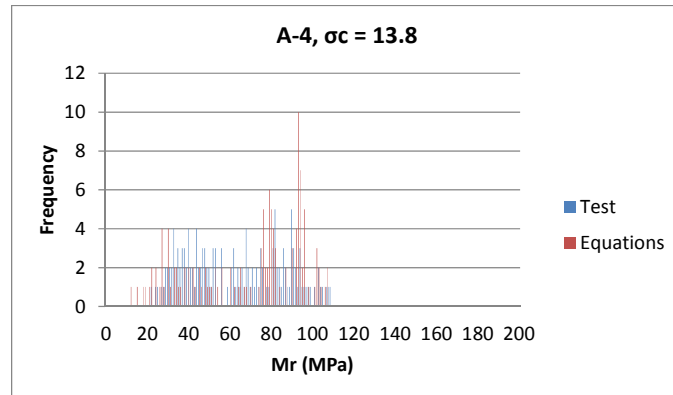


**Figure C.8: Distribution of resilient modulus from test data and statistical modeling for A-4 soil under confining pressure  $\sigma_c = 13.8$  kPa.**

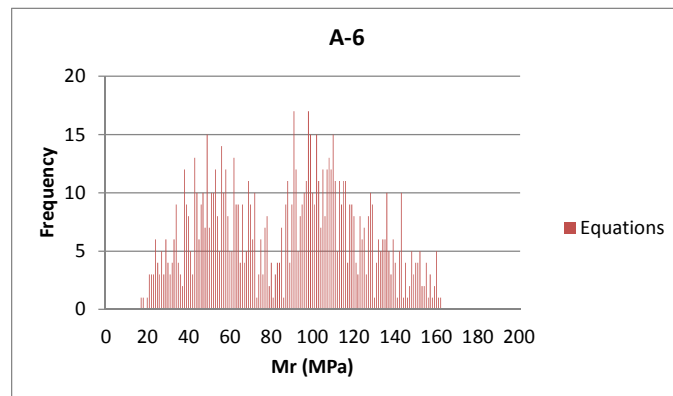
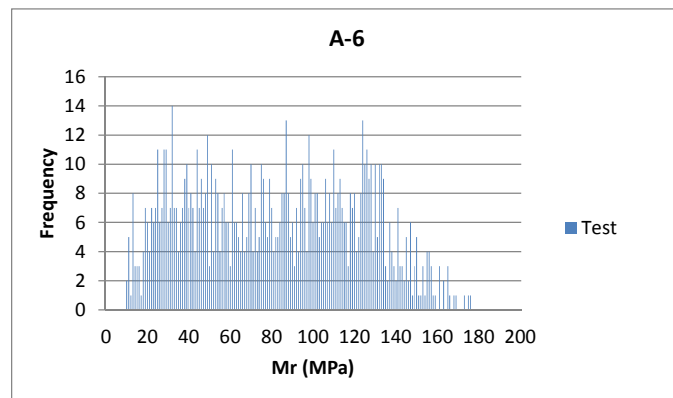
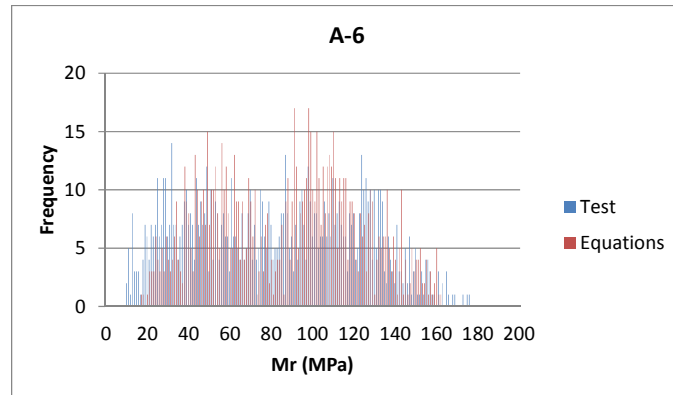


**Figure C.9: Distribution of resilient modulus from test data and statistical modeling for A-6 soil.**

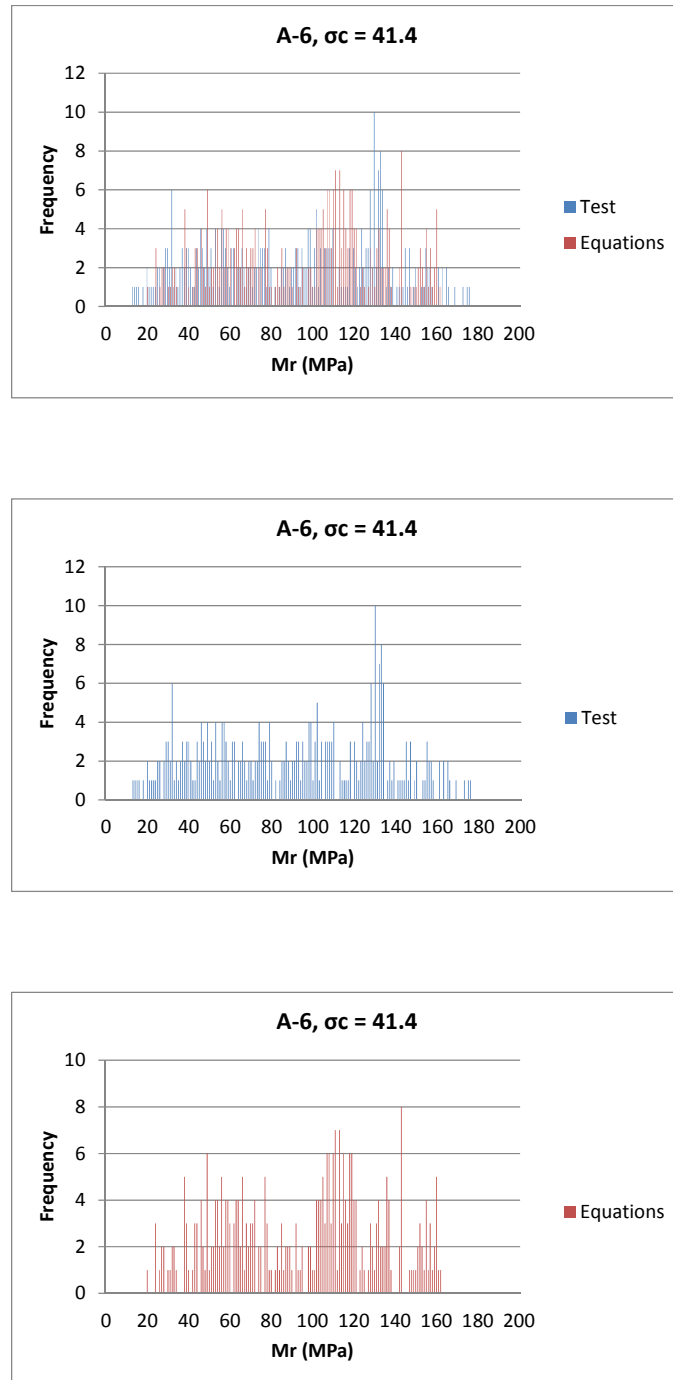


**Figure C.10: Distribution of resilient modulus from test data and statistical modeling for A-6 soil under confining pressure  $\sigma_c = 41.4$  kPa.**

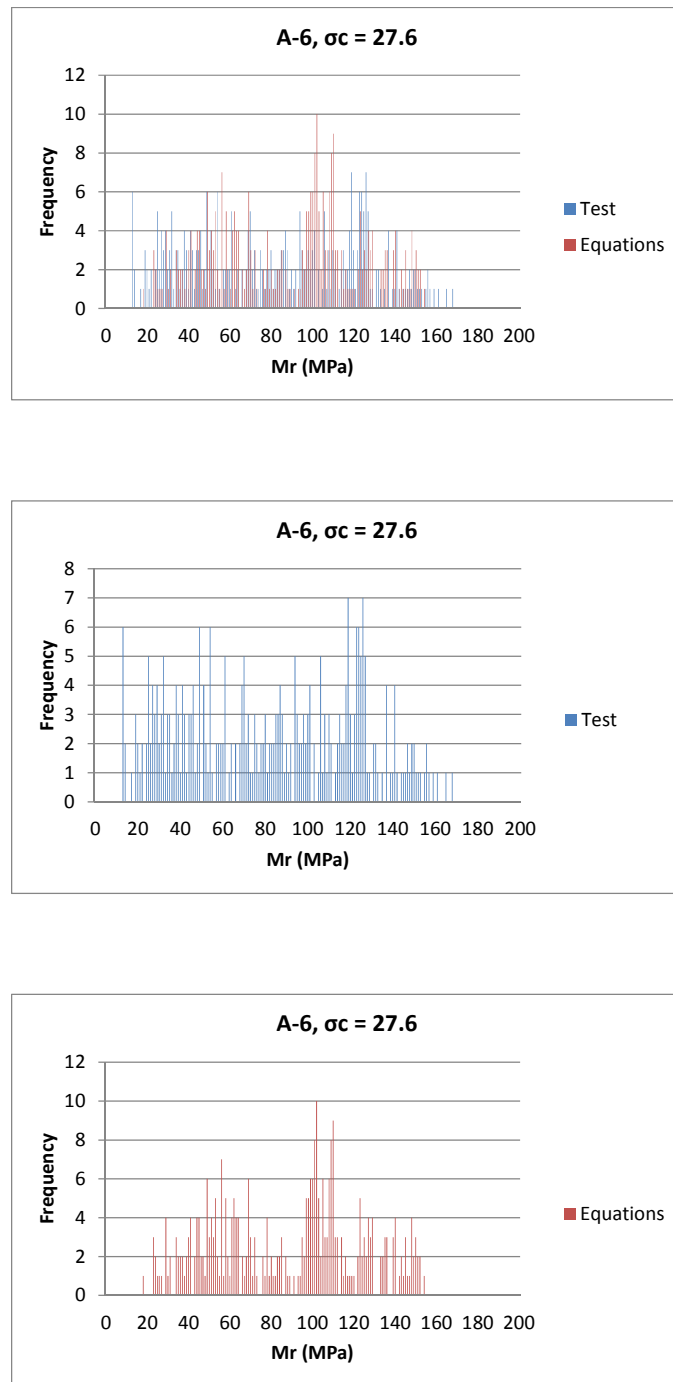


**Figure C.11: Distribution of resilient modulus from test data and statistical modeling for A-6 soil under confining pressure  $\sigma_c = 27.6$  kPa.**

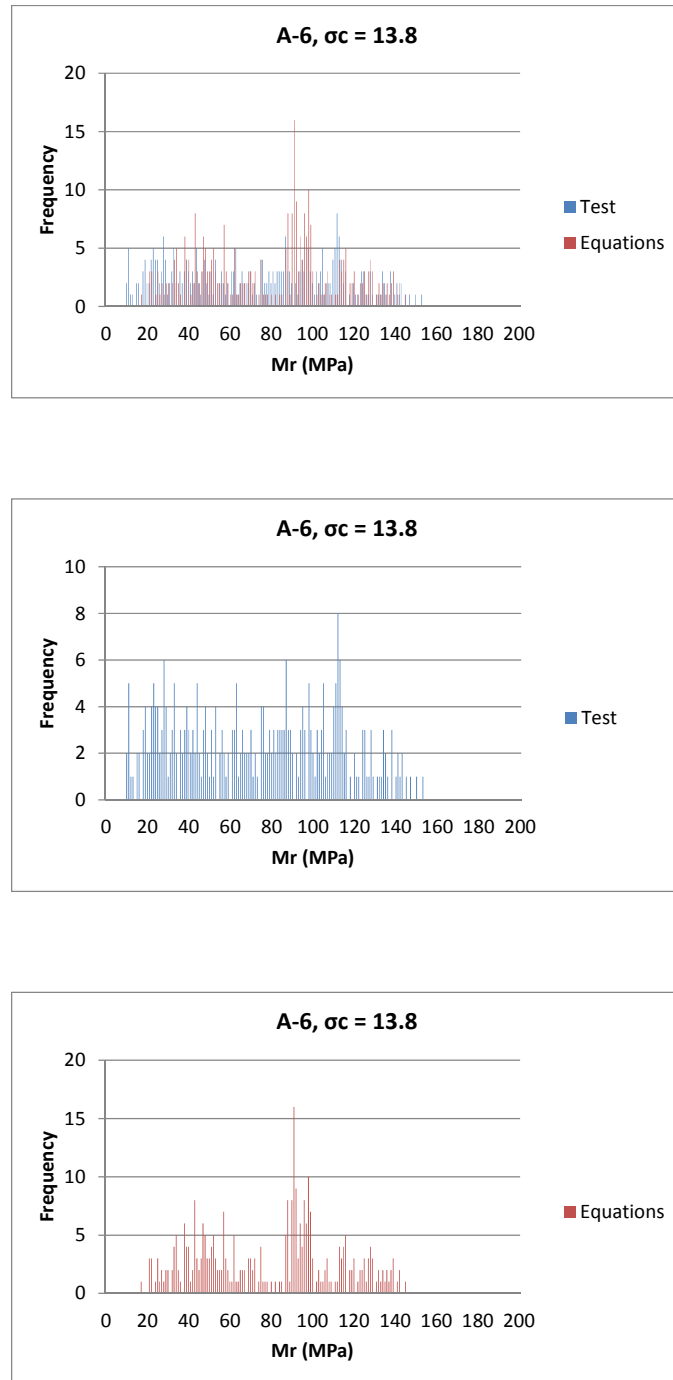


**Figure C.12: Distribution of resilient modulus from test data and statistical modeling for A-6 soil under confining pressure  $\sigma_c = 13.8$  kPa.**

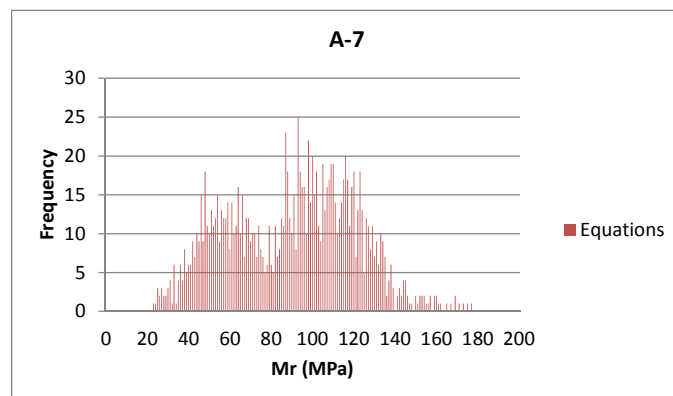
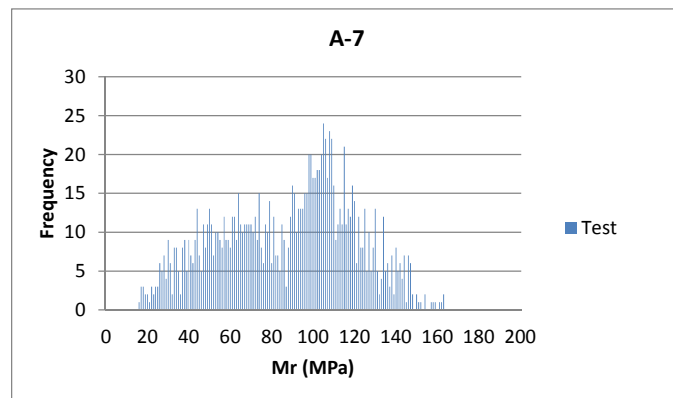
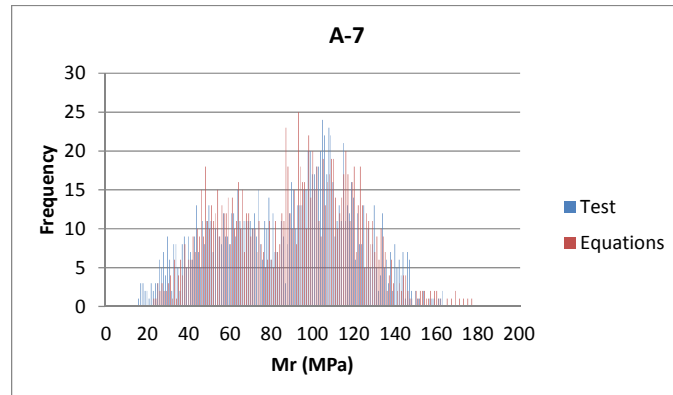


**Figure C.13: Distribution of resilient modulus from test data and statistical modeling for A-7 soil.**

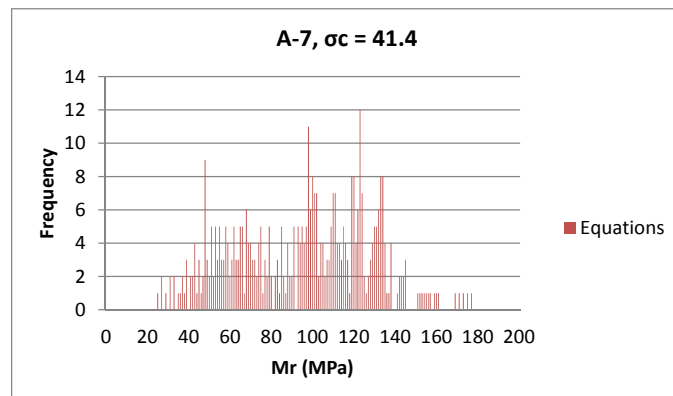
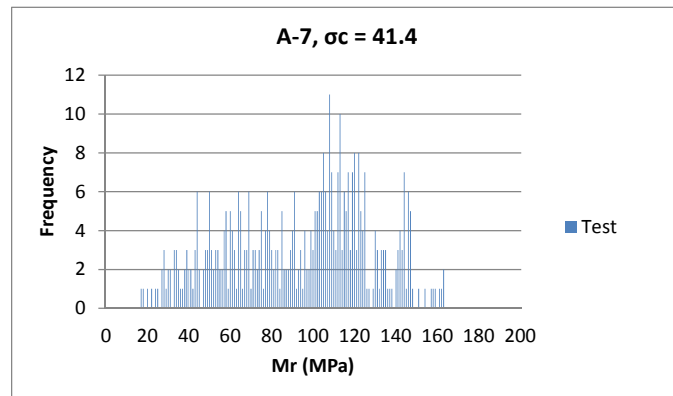
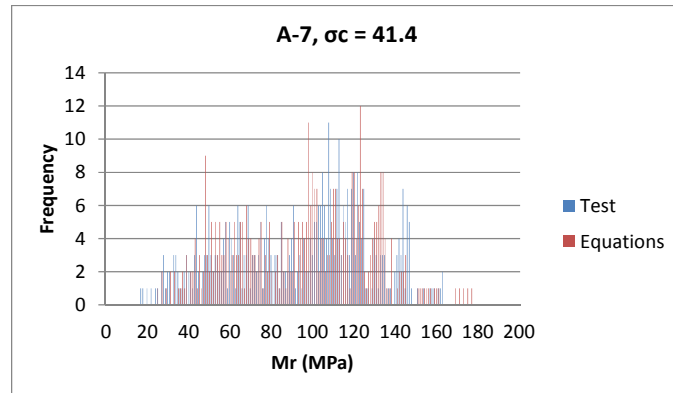


**Figure C.14: Distribution of resilient modulus from test data and statistical modeling for A-7 soil under confining pressure  $\sigma_c = 41.4$  kPa.**

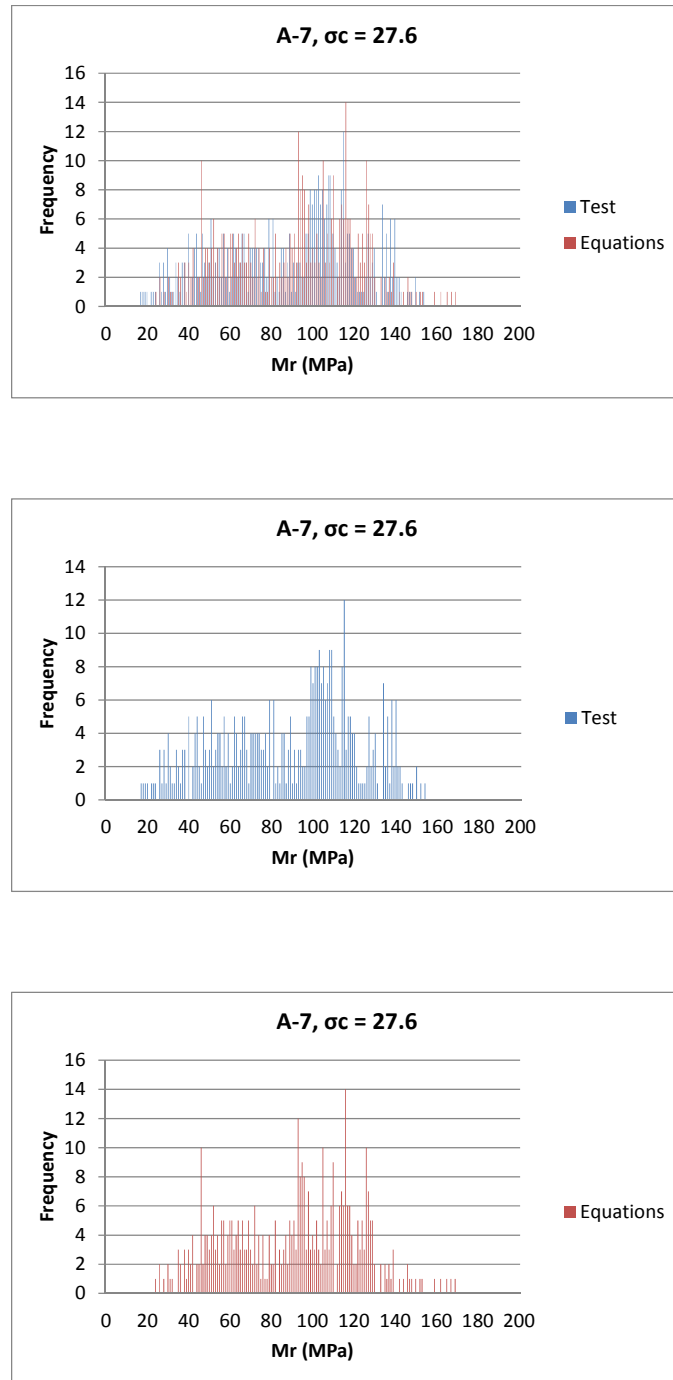


**Figure C.15: Distribution of resilient modulus from test data and statistical modeling for A-7 soil under confining pressure  $\sigma_c = 27.6$  kPa.**

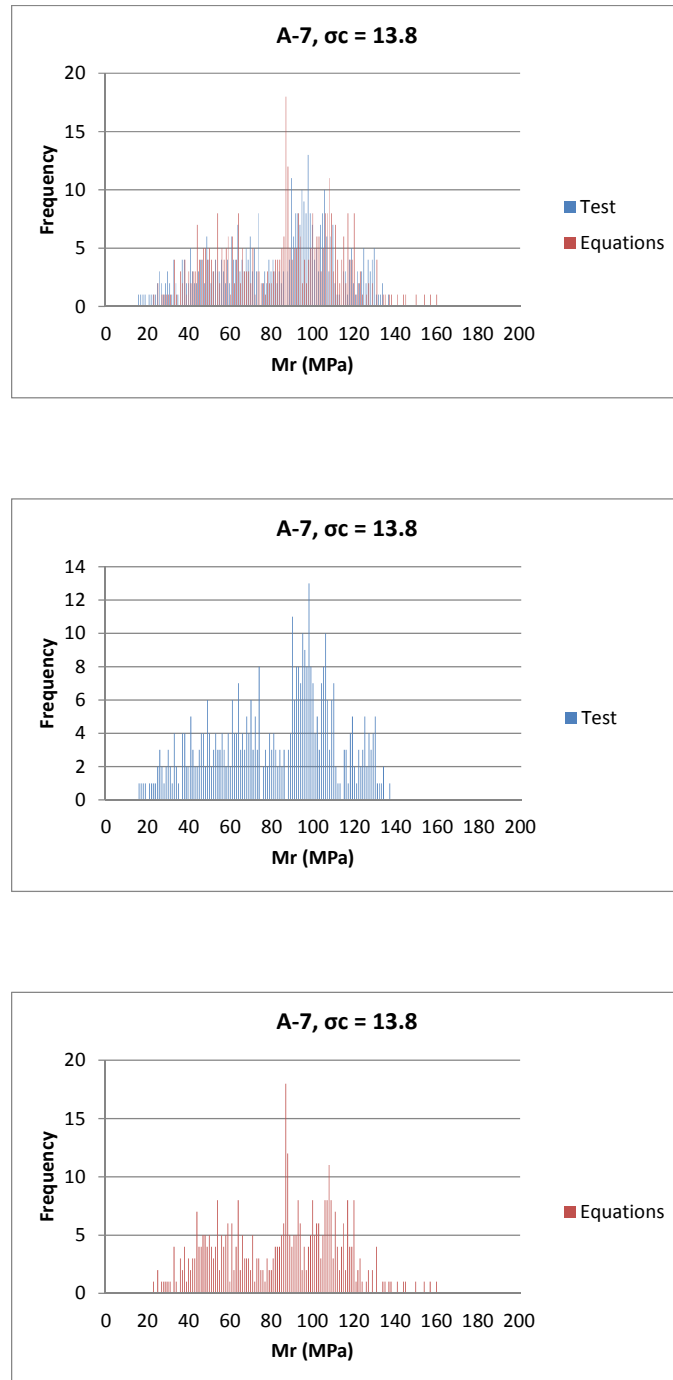


**Figure C.16: Distribution of resilient modulus from test data and statistical modeling for A-7 soil under confining pressure  $\sigma_c = 13.8$  kPa.**

---

Wisconsin Highway Research Program  
University of Wisconsin-Madison  
1415 Engineering Drive  
Madison, WI 53706  
608/262-2013  
[www.whrp.org](http://www.whrp.org)